Development of Formulated Canola Protein-based Ingredients for the Food Industry

Final Report

Prepared for:

SK ADF
(#2010-0044)
&
SaskCanola
(CUP-SCDC 2010-9)

Michael Nickerson, Ph.D., P.Ag.

Saskatchewan Ministry of Agricultural Research Chair
Department of Food and Bioproduct Sciences
University of Saskatchewan
51 Campus Dr., Saskatoon, SK, S7N 5A8
Tel: (306) 966-5030
Fax: (306) 966-8898
Email: Michael.Nickerson@usask.ca

TABLE OF CONTENTS

Part IV: Gelation properties of canola proteins

Part V: Value-added opportunity (Edible films)

Part VI: Other

Part VII: Appendices

-Chapter 1-

Executive summary

The overall goal of this research was to develop formulated canola protein-based ingredents that could then be tailored to specific food applications [e.g., baking, meats, beverages and/or dairy alternatives (i.e., coffee whiteners)]. Canola proteins represent an emerging plant-based alternative to animal proteins, expected to be soon commercially available to the food industry. However despite plant proteins experiencing greater market growth than animal-derived ingredients, their wide spread use has been hindered by their reduced functionality relative to animal-based products. Over the past number of decades, researchers have been trying to improve the functionality via improved processing practices, enzymatic hydrolysis or through chemical modification. The focus of this research was to explore an alternative non-invasive consumer-friendly approach by creating formulated canola protein ingredients comprised of minor amounts of polysaccharides using a process known as complex coacervation. This technology could have a positive, neutral or negative impact on functionality and food structure relative to the protein alone, and in principle, could be tailored for specific applications in the food industry. The project: identifies optimal solvent and biopolymer (i.e., proteins or polysaccharides) conditions for producing the formulated protein ingredients; develops in-house standardized methods for assessing ingredient functionality; and evaluates the functionality of the formulated protein ingredients relative to commonly used food proteins by the food industry, with emphasis on its use in emulsions and gels (or as a thickener). The project also explored the potential use of canola proteins as film forming agents in the development of edible and biodegradable packaging. The research will aid in developing a currently large untapped market (i.e., food industry) for canola producers, which will lead to high value applications for underutilized meal fractions and increased product demand.

The research was broken up into four parts, associated with the formation and functionality of protein-polysaccharide complexes; and the use of canola proteins as emulsifiers, gelling agents and in the development of edible biodegradable films/packages.

(a) Formation and functionality of protein-polysaccharide complexes: The formation of canola protein-polysaccharide interactions was studied as a function of pH, mixing ratio and polysaccharide-type in order to better understand mechanisms of interaction during coacervation.

And then, the functionality of insoluble and soluble complexes were evaluated. Canola proteins were found to follow a typical coacervation process, whereby initial interactions occur via electrostatic attraction, with secondary by hydrogen bonding and hydrophobic interactions. Protein-protein aggregation also plays an important role in complex formation. Initial interactions lead to the formation of a soluble complex, followed by an insoluble complex where macroscopic phase separation ensues. Depending on the polysaccharide present, the insoluble complex may remain as a coacervate or form a precipitate structure and fall out of solution. Protein interactions within the present study involving a weakly charged polysaccharide (e.g., gum Arabic) lead to the formation of a coacervate structure, whereas interactions with a highly charged polysaccharide (e.g., carrageenan) lead to the formation of a precipitate. Overall, the functionality of protein-polysaccharide complexes involving curciferin-rich (CPI) or napin-rich protein isolates had a neutral or negative effect on protein functionality. Solubility and foaming capacity were the greatest properties negatively affected in all cases. This trend was found for most systems with the exception of CPI and gum Arabic at pH 4.2 (near its isoelectric point), where a rise in solubility was observed. Despite rejecting our null hypothesis that the addition of the polysaccharide would improve protein functionality, findings arising from this work will aid the food industry in understanding complex ingredient interactions occurring in food and aid in formulation throughout the product development process when canola proteins are present. The ability to reduce solubility of protein in the presence of a polysaccharide may have implications in the development of new separation procedures for isolating proteins from canola meal or in clarification applications. Furthermore the protein produced performed much better than expected as a control material, and had very comparable functionality relative to commercial protein ingredients derived from egg and milk.

(b) Canola proteins as emulsifers: The effect of pH and NaCl concentration on the physciochemical and emulsifying properties of a crucferin-rich and napin-rich isolate was examined to better understand how solvent and properites of the proteins lead to either the stability or instability of emulsions. Overall, this research found that despite cruciferin-rich and napin-rich protein isolates having quite different surface characteristics (charge and hydrophobicity) and solubility, the emulsifying forming and stabilizing effects were similar. Suggesting that separation of the two proteins from the isolate ingredient may not be necessary if emulsification is the only functional role the proteins are being used for, from a commercial stand point. Emulsions were

found to be most stable when proteins were away from their isoelectric point where they exerted a net replusive charge into the solution. The addition of NaCl tends to screen charges on the protein's surface leading to a reduction in replusive forces within the system, causing emulsion instability (NaCl concentration dependent) due to first flocculation, followed by droplet coalescence and creaming.

(c) Canola proteins, as gelling agents: The gelation properties of a mixed canola protein isolate as a function of protein concentration, temperature, ionic strength and in the presence of network destabilizing agents were examined using rheological measurements, calarimetry and confocal scanning laser microscopy. The gelling properties were also studied in relation to the performance of a commercial soy protein isolate product for comparative purposes. Overall, CPI formed stronger gels than SPI, with less dependence on disulfide and hydrogen bonds relative to SPI. For both proteins, there was no significant difference (~77°C - ~90°C) in gelling temperature as the protein concentration increased. Fractal dimension and lacunarity was analyzed using CLSM images to show the microstructure of CPI gels became denser as the concentration increased from and followed a cluster-cluster aggregate growth model during the formation of the gel network.

(d) Canola proteins, as film forming agents: The film forming properties of a mixed CPI were also studied in response to plasticizer-type and concentration, and the presence of a non-toxic natural fixative. Specifically, the mechanical, water vapor and optical properties were assessed, and then related to literature values. Overall, CPI films were less flexible, had better water vapor barrier properties, and comparable film strength relative to other plant protein-based films. Plasticizer-type and concentration, and the presence of fixatives all had a significant impact on film performance. Based on this research, CPI shows promise as a potential material for the development of edible films/packaging in the future.

Part 1: Background

-Chapter 2-
Introduction

Protein ingredients represent a multi-billion dollar industry, presently dominated by animal proteins, such as gelatin, ovalbumin, casein and whey. In 2011, the US protein ingredient market for food was worth ~2.84 billion, with $1.17 (avg. annual growth rate, AAGR 6.4%) and ~1.67 (AAGR 1.7%) billion coming from plant and animal sources, respectively. With increased concerns over the safety of animal-derived products, rising costs of dairy-based ingredients; growing dietary preferences and consumer demand for healthier foods; market trends are shifting towards lower cost and abundant plant-based alternatives. Canola proteins represent an emerging plant-based alternative, expected to be soon commercially available in the market place. Ingredient manufacturers in Canada (e.g., BioExx Speciality Proteins Ltd. and Burcon NutraScience Corp.) have or are seeking GRAS (generally recognized as safe) status for a variety of their non-GMO (genetically modified organism) canola protein products. Similar to soy, canola proteins are of high nutritional value and have acceptable functional attributes required for many food applications. Plant proteins also have a significant price advantage over animal-based ingredients, for instance casein is sold for ~$4.90 (USD) a pound, compared to soy, which ranges between $0.42 to $2.08 (USD) per pound. Despite experiencing greater market growth than animal-derived protein ingredients, the wide spread use of plant proteins is hindered by their reduced solubility (and functionality) relative to animal-based products, and in the case of soy, its beany flavour, allergencity and tendency to cause flatulence.

Canola was originally bred from rapeseed varieties (e.g., *Brassica napus* L.*)* to have low levels of erucic acid (<2%) and glucosinolates (<30 µmol/g) for use as an edible healthy oil (Canola Council of Canada, 2011). Canola meal, the co-product of oil processing, is rich in protein (36- 39%) and crude fibre (~12%), and to- date is commonly used in low cost livestock feed for its nutritional value (Khattab and Arntfield, 2009; Newkirk, 2009). The meal also contains high levels of phenolic compounds and phytic acid which can lead to poor protein functionality depending on the extraction method used (Wu and Muir, 2008; Aider and Barbana, 2011). However, research surrounding adding value to the under-utilized and under-valued meal has intensified recently, particularly as it relates to the protein fraction. Despite its well-balanced amino acid profile (Ohlson and Anjou, 1979), the utilization of canola protein by the food industry

has been limited due to its poorer functionality compared to animal-derived protein ingredients. Depending on the canola variety used, processing practices and methods of extraction, protein functionality can vary considerably (Aluko and McIntosh, 2001; Khattab and Arntfield, 2009; Can Karaca et al., 2011). Successful processing innovations and product characterization could lead to the development of a new plant sourced protein food ingredient.

a) Development of formulated canola protein-based ingredients

This research project will focus on improving the functional properties of canola protein products through non-invasive and low cost means (i.e., not chemically or enzymatically treated) through the development of speciality formulated protein-based ingredients via a complex coacervation technology, and to demonstrate applicability of the developed ingredients to food manufacturers for a variety of food applications. Resulting coacervates (or complexes – defined as bound protein-polysaccharide macromolecules) could have a positive, neutral or negative impact on functionality and food structure relative to the protein alone, and in principle, could be tailored for specific applications in the food industry.

The behaviour of protein and polysaccharide mixtures is governed by biopolymer characteristics (*e.g. size, type and distribution of reactive groups and the charge density along the protein or polysaccharide surface*), mixing ratio and concentration, and solvent conditions (*e.g., pH, salt and temperature*). The coacervation process, in general, occurs when both the protein and polysaccharide carry opposing net charges, so that the two biopolymers are dominated by electrostatic attractive forces, leading to the separation into solvent-rich and biopolymer-rich (also known as the coacervate-rich) phases (Weinbreck et al., 2003). Although the mechanisms for complex formation are not fully elucidated, it is believed to follow two structure-forming events associated with the formation of 'soluble' and 'insoluble' complexes. Typically, structure formation is described by a turbidimetric analysis during a pH titration to identify conditions where the two biopolymers interact to form one complex (Liu et al., 2009). Soluble protein-polysaccharide complexes form near the protein's isoelectric point (pI), as evident by a slight rise in turbidity (denoted as pH_c); signifying the initial experimentally detectable interaction between the two biopolymers. As pH is lowered further, soluble complexes continue to grow in size and number until reaching a critical point at $pH_{\phi 1}$ where macroscopic phase separation occurs (and the bulk of the coacervates form). An optimal pH is observed once an overall neutral charge on the

complex is reached (i.e., charges on the protein and polysaccharide offset one another), and is typically accompanied by the highest complex yield. As pH is lowered further, complexes begin to disassociate as charges on the polysaccharide backbone (i.e., carboxylated) become protonated (denoted at $pH_{\phi 2}$). The formed complexes tend to rearrange to form liquid coacervates containing small amounts of entrapped solvent to give unique functional properties relative to protein alone (Liu et al., 2009). de Kruif et al. (2004) generalized polysaccharides involved with complexation as being weakly or strongly charged. In general, weakly charged polysaccharides, such as gum Arabic, pectin, xanthan gum, sodium carboxylmethyl and guar gum form a coacervate, whereas strongly charged polysaccharide, such as chitosan, carrageenan, and sulphated dextran form precipitates. Depending on the type of structure present, different functional attributes can be displayed (Liu et al., 2010). Research apart of this ADF project focuses on investigating for formation of soluble and insoluble complexes involving cruciferin-rich and napin-rich isolates with a range of food grade polysaccharides, and then the subsequent functionality of both the soluble and insoluble complexes relate to the canola proteins alone. Solubility, foaming and emulsification were considered. A range of commercial protein isolates were also tested using the same functionality tests for comparative purposes.

b) Canola proteins, as emulsifiers

Emulsions consist a mixture of two (or more) immiscible liquids formed after an input of mechanical energy (e.g., homogenization), where one liquid becomes dispersed as small droplets within a continuous phase of the other (Hill, 1996; McClements, 2005). The stability of protein-stabilized emulsions is dependent upon protein characteristics (e.g., globular vs. fibrous, conformational entropy, molecular weight), surface properties (e.g., hydrophobic and hydrophilic residues), processing (e.g., shear) and solvent properties (e.g., temperature, pH and salts). During emulsion formation, soluble proteins diffuse towards the interface, then re-arrange and re-organize at the interface to orient hydrophobic amino groups towards the non-polar oil phase and the hydrophilic amino groups toward the aqueous polar phase in order to reduce interfacial tension and form a viscoelastic film (Dalgleish, 1997). The viscoelastic film typically induces an electric charge on the emulsion droplet, which depending on the pH may lead to attractive or repulsive forces between neighboring droplets (Tcholakova et al., 2002; McClements, 2004). At solution pHs close to the pI of the protein, emulsion droplets would exert little to no repulsive charge

leading to flocculation and/or aggregation due to hydrophobic interaction, followed by partial or complete coalescence (Xu et al., 2005). In contrast, at pHs away from the pI, proteins in the interface may exert a repulsive force between neighboring droplets to keep the emulsions stable. The addition of NaCl or other salts can cause shielding of the repulsive charge on the droplets, inducing droplet flocculation even if the solution pH is away from the pI. To date, mixed information is found in the literature regarding the emulsifying properties of napin. Krause and Schwenke (2001) reported napin to be highly surface active and capable of forming emulsions, whereas Malabat et al. (2001) reported neither native nor chemically modified napin fraction (acylation and sulfamidation) can form stable emulsion even though the hydrophobicity of napin was increased in the process. The research within this ADF project focused on studying the emulsifying properties of cruciferin- and napin-rich protein isolates, in response to changes in solution pH and NaCl levels.

c) Canola proteins, as gelling agents

A gel is defined as a 3-dimensional network comprised of an 'infinitely branched polymer or aggregate' that spans the dimensions of the container. Gelation requires aggregation or association of protein particles, which is formed from the partial protein denaturation or change in conformation. However the exact mode of gel formation depends on the properties of the protein and the solvent conditions being used. The overall goal of part III of this research is to examine the gelation mechanism of canola protein isolates (CPI) for use in food applications, and to compare it to that of a commercial soy protein isolate (SPI). Canola proteins are dominated by two main proteins, a salt-soluble globulin protein (cruciferin) and a water-soluble albumin protein (napin). The two proteins differ in terms of size, amino acid composition and surface characteristics (e.g., charge and hydrophobicity), which can impact protein functionality in a considerable way. Gelation studies involving canola proteins have typically involved the use of cross-linking agents (Pinterits and Arntfield, 2007; Sun and Arntfield, 2011) alone or in combination with polysaccharides (Uruakpa and Arntfield 2004, 2006a, b; Klassen et al., 2010), or involve the use of chemically modified canola proteins (Paulson and Tung, 1988; Schwenke et al. 1998). In the present work, mechanisms of gelation will be elucidated for canola proteins as a function of temperature, protein concentration, NaCl and destabilizing agents (e.g., urea and mercaptoethanol) using rheology and calorimetry, and compared with that of soy.

d) Canola proteins, as film forming agents

Over the past decade, there has been an increased interest surrounding the use of biodegradable edible films by the food packaging industry as a way to reduce their environmental footprint (Vargas et al., 2008; Gomez-Estaca et al., 2009; Janjarasskul & Krochta, 2010). As such, researchers have been investigating the use of natural biopolymer-based materials (e.g., protein-, polysaccharide- and lipid-based) as an alternative to synthetic petroleum-based polymers as they are considered to be both economical and bio-friendly. Furthermore, depending on the composition, films may display excellent barrier properties to moisture, gases and aromas; have the ability to carry and deliver various additives (e.g., antimicrobial agents and antioxidants) for extended product shelf-life or improved quality; or help improve a product's structural integrity and handling characteristics (Psomiadou et al., 1996; Krochta & De Mulder-Johnston, 1997; Han & Gennadios, 2005). Protein- and polysaccharide-based materials tend to form films with excellent mechanical properties and gas barrier properties, but offer poor moisture control (Kester & Fennema, 1986; Baldwin et al., 1995; Vargas et al., 2008; Janjarasskul & Krochta, 2010). In contrast, lipid-based films tend to have excellent moisture barrier property, but have poor mechanical and gas barrier properties (Greener & Fennema, 1989; Janjarasskul & Krochta, 2010). The formation of edible films using proteins from plant sources has been limited, but may be advantageous to those from animal sources, because of their low cost, and perceived safety concerns (e.g., prions) by consumers or dietary restrictions over consuming animal-derived products (Uppstrom, 1995; Gennadios, 2002). Films have been prepared previously using proteins from plant sources, such as soy (Cho & Rhee, 2004), sunflower (Orliac et al., 2002), lentil (Bamdad et al., 2006), faba bean (Saremnezhad et al., 2011), pea (Kowalczyk & Baraniak, 2011), and rapeseed (Jang et al., 2011). The research presented as part of this project focuses on the design of canola protein isolate-based films, such that they offer excellent mechanical, optical and moisture barrier properties. Specifically, protein concentration, plasticizer-type and concentration, and the presence of genipin (natural crosslinking agent) were tested for their effects on film properties. Enhanced utilization of canola proteins may increase their integration into the vegetable protein ingredient market.

Reading this report

This final research report is broken down into four main research parts. In part II, the formation and functionality of mixed canola protein-polysaccharide complexes are discussed in relation to canola proteins alone (cruciferin- or napin-rich isolates) and to commercial protein ingredients available in the marketplace. Part II represents the original focus of this research grant, where SK ADF grant focused on the napin-rich isolates and the SaskCanola grant focused on the cruciferin-rich protein isolates. However, based on the student scholarship funds generated, additional work in the area of canola protein-stabilized emulsions (Part III), canola protein gelation (Part IV) and the use of canola proteins as film forming agents (Part V) were included. The latter provides an example of a potential value-added opportunity for canola proteins in food and/or non-food packaging. Each part comprises of a literature review on the topic, the main research studies written in manuscript format, followed by a summary section. *Note, the terms 'cruciferin-rich protein isolates' and 'canola protein isolates' are used interchangeably (also denoted as CPI) throughout this report. In contrast, the napin-rich isolate is always clearly identified as NPI.*

Part II: Formation and functionality of mixed canola protein-based ingredients

-Chapter 3-

Literature review

3.1 Introduction

Currently, the global protein ingredient market is dominated by animal-derived proteins such as casein, whey, ovalbumin and gelatin, with soy dominating the plant-based protein ingredient market. However, with increased perceived consumer fears of animal-based products (e.g., prion diseases), changing dietary preferences and diet restrictions because of religious or moral beliefs, the food industry is searching for plant-based alternatives (Liu et al., 2009). Furthermore, consumers are also concerned with soy-based products associated with allergies, flavor and flatulence. Potential alternatives could include proteins arising from legume or oilseed crops; however the functionality attributes tend to be poorer than those of the current proteins on the market. For many decades, researchers have been trying to enhance the functionality of plant proteins through chemical (Matsudomi et al., 1985; Ponall et al., 2010) or enzymatic (Hettiarachchy et al., 1985; Ortiz and Wagner, 2002) means with only some success. Alternatively, another approach could involve controlling protein-polysaccharide interactions to coat the surface of the protein to change its physicochemical properties and then ultimately its functional behavior. Proteins and polysaccharides are macromolecules commonly used by the food industry in a wide range of applications due to their emulsifying, foaming, thickening or gelling properties. Knowledge of structure-dynamic-function relationships relating to their interactions in food systems is especially important as it often controls food texture, structure, processability and shelf life (Dickinson and Pawlowsky, 1998; Schmitt et al., 1998; Doublier et al., 2000; Weinbreck et al., 2004a; Mounsey et al., 2008; Liu et al., 2010a,b). Protein-polysaccharide interactions can also be tailored for the design of controlled delivery vehicles for carrying bioactive ingredients, or for developing coating and packaging materials (Liu et al., 2009). Depending on the nature of interactions and the biopolymers involved, formed electrostatic complexes (coacervates or precipitates) may have improved functionality than the biopolymers alone (Tolstoguzov, 1991; Schmitt et al., 1998).

Although the mechanism for complex coacervation has not been fully elucidated, the topic has been reviewed by Turgeon et al. (2007). Most studies have previously focused on complex

coacervation between animal-derived proteins, such as bovine serum albumin (Wang et al., 1996; Wen and Dubin, 1997), casein (Syrbe et al., 1998), whey proteins (Weinbreck et al., 2003a,b, 2004a,b) and β-lactoglobulin (Schmitt et al., 1999; Harnsilawat et al., 2006), and anionic polysaccharides. In contrast, mechanistic studies of coacervation involving plant proteins have been limited. Liu et al. (2009, 2010a,b) investigated the effect of pH, salt and biopolymer mixing ratio on complex formation involving pea protein-gum Arabic mixtures, and characterized both the nature of interactions and the functional attributes of formed complexes. Similar mechanistic studies were also performed for mixtures of canola protein-ι-carrageenan/alginate (Klassen et al., 2011), pea protein-alginate (Klemmer et al., 2012), pea protein-chitosan (Elmer et al., 2011), and pea globulin-gum Arabic (Ducel et al., 2004; Chourpa et al., 2006).

The present research investigates the effect of solvent (pH and salt) and biopolymer characteristics (polysaccharide-type, total biopolymer concentration and biopolymer mixing ratio) on mechanisms governing complex coacervation involving canola protein isolates (both rich in cruciferin and napin) and anionic polysaccharides (gum Arabic, carrageenan, pectin and/or alginate). Knowledge of these mechanisms could lead to the development of 'formulated protein-polysaccharide ingredients' with unique functionality.

3.2 Coacervation

In very dilute biopolymer mixtures, proteins and polysaccharides remain co-soluble (Fig. 3.1) with limited interactions within the aqueous solution (Weinbreck et al., 2003a; Ye, 2008). However, as the total biopolymer concentration is raised either segregative- or associative- type phase separation (Fig. 3.1) may occur depending on the solvent conditions (i.e., temperature, pH and salts), biopolymer characteristics (i.e., polysaccharide-type, reactive site, molecular weight, linear charged density and conformation), biopolymer concentration and mixing ratio, and physical processing (i.e., pressure, degree and time of shear) (Tolstoguzov, 2003; Gharsallaoui et al., 2010; Liu et al., 2009, 2010a). Segregative phase separation occurs when the two biopolymers are thermodynamically incompatible, typically driven by electrostatic repulsive forces between proteins and polysaccharides of similar net charges. Separation leads to both a protein-rich and polysaccharide-rich phase (Doublier et al., 2000; Weinbreck et al., 2003a,b; Liu et al., 2009, 2010a). In contrast, associative phase separation (also known as complex coacervation) occurs when the biopolymers carry opposite net charges and experience electrostatic attractive forces

(Bungenberg and Kruyt, 1929). This charge interaction leads to separation into a biopolymer-rich (proteins + polysaccharides) and a solvent-rich phase, and typically occurs over a narrow pH range between the pKa of the reactive site on the polysaccharide backbone and the isoelectric point (pI) of the protein (Doublier et al., 2000; Weinbreck et al., 2003a,b; Liu et al., 2009, 2010a). The formed 'electrostatic complexes' can either be present as a coacervate or a precipitate depending on the level of electrostatic attraction.

In either case, structure formation tends to follow a similar nucleation growth-type kinetic mechanism involving two main pH-dependent structure-forming events (Girard et al., 2004; Liu et al., 2009). During an acid titration involving a mixture of proteins and an anionic polysaccharide, structure formation is typically accessed by changes to turbidity (de Kruif and Tuinier, 2001; Turgeon et al., 2003; Weinbreck et al., 2003a; Liu et al., 2009) or scattering intensity (Semenova, 1996; Girard et al., 2004; Harnsilawat et al., 2006). The first experimentally detected rise in turbidity signifies the onset of structure formation in the form of soluble complexes, occurring at a pH denoted as pH_c (Fig. 3.2). As the pH is lowered further, macroscopic phase separation occurs as evident by a large rise in turbidity and a transition from a clear to cloudy solution (Weinbreck et al., 2003a; Liu et al., 2009). The onset of this rise is denoted as $pH_{\phi 1}$ (Fig. 3.2) and corresponds to the formation of insoluble complexes. *The terms 'soluble' and 'insoluble' are terms used in the coacervation literature to describe the various stages of growth and do not relate to 'solubility-like' functional testing.* As the pH is lowered further, the mixture reaches its electrical equivalent point and a maximum in turbidity or scattering intensity occurs. At this pH (denoted as pH_{opt}) (Fig. 3.2), electrostatic complexes become neutral and yield the greatest concentration of formed structures (Weinbreck et al., 2003a; Liu et al., 2009). At lower pH, the polysaccharide becomes protonated and previously formed structures begin to dissociate until reaching $pH_{\phi 2}$ (Fig. 3.2), where complete dissolution of complexes occurs (Weinbreck et al., 2003a; Liu et al., 2009).

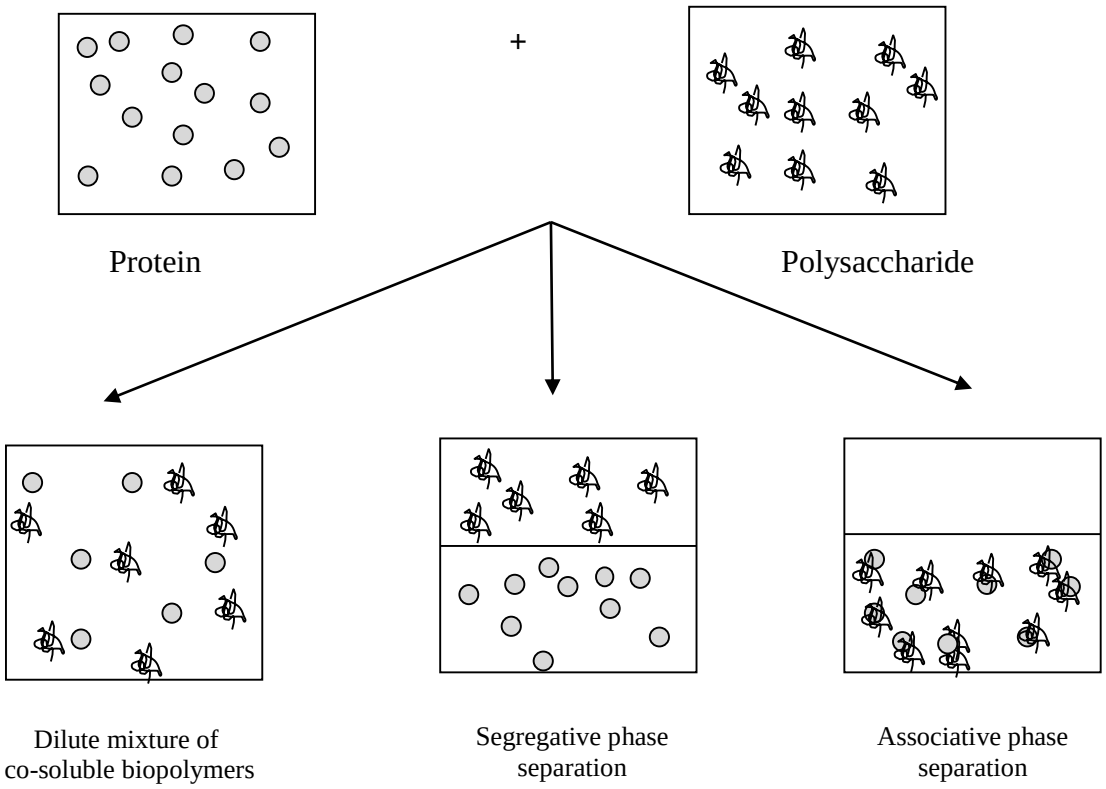

Figure 3.1 A schematic outlining segregative and associative phase behavior in admixtures of protein-polysaccharide systems (adapted from de Kruif and Tuinier, 2001).

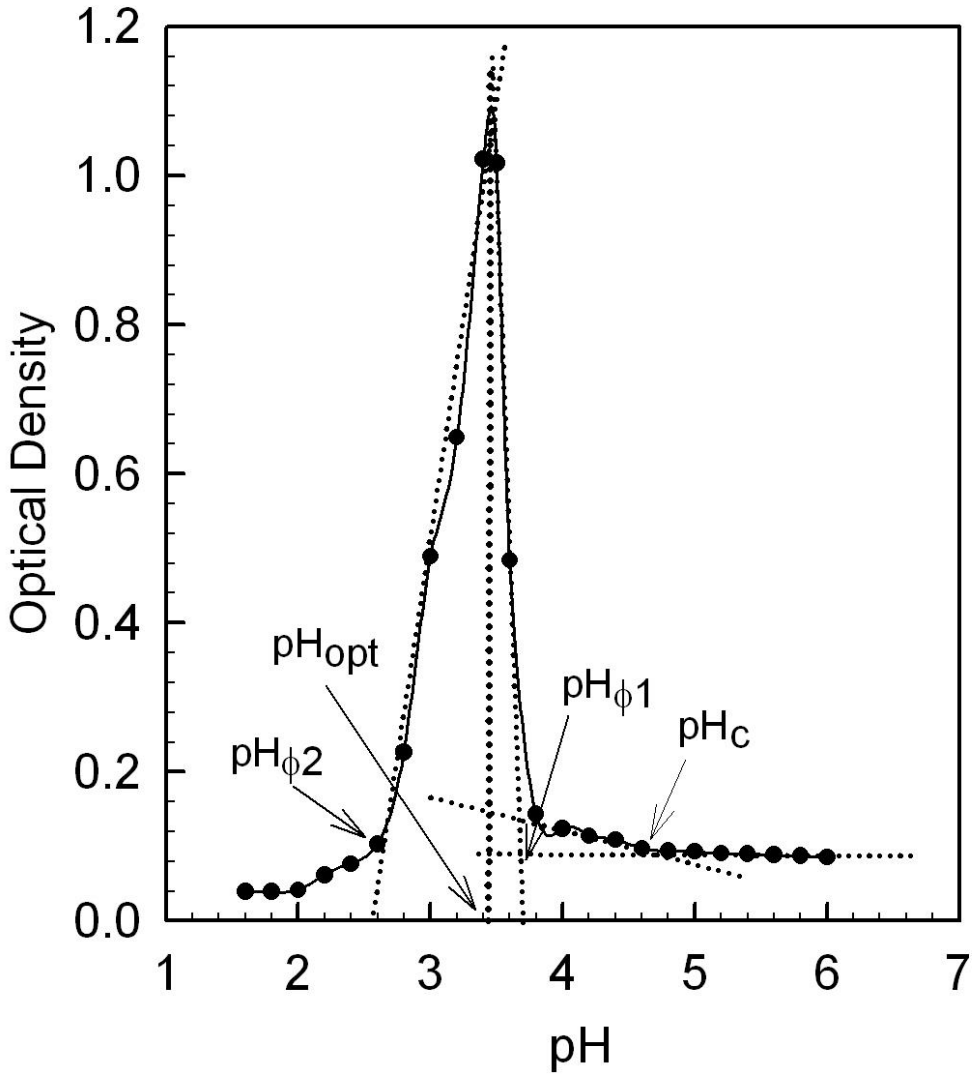

Figure 3.2 Schematic diagram showing how critical transition pHs (pH_c, $pH_{\phi 1}$, pH_{opt} and $pH_{\phi 2}$) are determined from a turbidity curve (Liu et al., 2009)

The coacervate structure is reversible, entraps a sufficient amount of solvent to remain suspended, and typically occurs within mixtures of proteins and weakly charged polysaccharides (i.e., those having a relative low linear charge density or weakly charge reactive group, such as the carboxyl sites found on gum Arabic and guar gum) (de Kruif et al., 2004). A stable coacervate structure is formed as entropies associated with biopolymer flexibility and solvent mixing become reduced, which offsets the enthalpic contribution associated with the release of water and

counterions during complex formation (Schmitt et al., 1999; Singh et al., 2007; Ye, 2008). In contrast, the precipitate structure tends to be only partially reversible and falls out of solution quickly. Biopolymers within the precipitate are more compact and entrap a lesser amount of solvent than the coacervate structure (Boral and Bohidar, 2010). In general, precipitation occurs within mixtures of proteins and strongly charged polysaccharides (i.e., those having a relatively high linear charge density of highly charge reactive group, such as carrageenan (sulfate group), chitosan (amine group) or exocellular polysaccharide B40 (phosphate group)) (Schmitt et al., 1998; Weinbreck et al., 2003b; de Kruif et al., 2004). Although complex coacervation is primarily driven by electrostatic attractive forces, the role of secondary forces, such as hydrophobic interactions and hydrogen bonding is less understood (Bungenberg and Kruyt, 1929; Schmitt et al., 1998; Doublier et al., 2000; Kaibara et al., 2000; de Vries et al., 2003; Weinbreck et al., 2003b; Wang et al., 2007; Liu et at., 2010a). Liu et al. (2010a) studied the nature of interactions within a mixture of pea protein isolate and gum Arabic an found that coacervation was governed primarily by electrostatic forces, with secondary stabilization by hydrogen bonding. The authors found that hydrophobic interactions played a role in stabilizing the protein-protein aggregates bound to the gum Arabic molecule, and reported that they were not involved in initial complex formation. However, in systems involving uncharged protein-polysaccharide mixtures, hydrophobic interactions have been reported to be the dominant driver for complex formation (Jönsson et al., 2003).

3.3 Factors affecting complex coacervation

Because complex coacervation involving proteins and charged polysaccharides is widely considered to be driven by electrostatic attractive forces, factors such as solvent pH, the presence of salts, biopolymer mixing ratio and polysaccharide-type are key to better understanding structure formation (Weinbreck et al., 2004a,b; Sanchez et al., 2006; Wang et al., 2007). The effect of each of these factors is briefly described below.

3.3.1 Effect of pH

Solvent pH is critical for altering the charge density on the protein's surface, which is required to trigger complexation with a charged polysaccharide (Schmitt et al., 1998; Jönsson et al., 2003; Weinbreck et al., 2004a,b; de Kruif et al., 2004). At pH>pI conditions, the protein

assumes a net negative charge, whereas at pH<pI a positive net charged is introduced. Complex coacervation typically occurs within a narrow pH range between the pKa of reactive groups along the polysaccharide backbone and the pI of the protein (Weinbreck et al., 2003b). As previously mentioned, as pH is lowered to pH<pI the protein assumes a positive net charge leading to the formation of an initial soluble complex at pH_c, by interacting with the negatively charged polysaccharide. In systems involving highly charged polysaccharides, such as carrageenan, pH_c can occur at pH>pI where both biopolymers carry a similar net positive charge (Weinbreck et al., 2003a, 2004a; Liu et al., 2009). Typically this phenomenon is thought to be associated with the interaction between the highly charged polysaccharide with positively charged patches of amino acids on the protein's surface (Weinbreck et al., 2003a, 2004a; Liu et al., 2009). As the pH is lowered during the acid titration, structure growth leads to the formation of insoluble complexes at $pH_{\phi 1}$, and then reaches pH conditions where charges along the protein and polysaccharide's surface are equivalent (pH_{opt}). At lower pH conditions, the reactive sites along the polysaccharide backbone become protonated leading to a weakening of the attractive forces between biopolymers until reaching $pH_{\phi 2}$ where dissolution of complexes occurs (Schmitt et al., 1998; Jönsson et al., 2003; de Kruif et al., 2004; Weinbreck et al., 2004a,b).

3.3.2 Effect of ionic strength

The presence of cations and anions has a dramatic effect on complex formation and their role is concentration dependent. As examples, in whey protein isolate-gum Arabic mixtures, NaCl levels >50 mM acted to suppress coacervation due to screening of the electric double layer on both the protein and the polysaccharide by bound and unbound ions (Weinbreck et al., 2003a). Liu et al. (2009) reported that critical pHs associated with complexation within pea protein isolate-gum Arabic mixtures were difficult to assess at levels >7.5 mM NaCl due to the increased prevalence of pea protein aggregates in the system. When investigating the nature of interactions involved with complexation of the same system, the authors found that complexation to be completely suppressed at 100 mM NaCl levels (Liu et al., 2010a). A number of research groups have reported similar findings, where the complexation of β-lactoglobulin-(high and low methoxy) pectin (Girard et al., 2002), canola protein isolate-(ι-carrageenan/alginate) (Klassen et al., 2011) and whey protein isolate-exocellular polysaccharide EPS B40 (Weinbreck et al., 2003a) mixtures were suppressed at 110, 100 and 75 mM NaCl respectively.

In contrast, in the presence of low salt concentration, complexation may be enhanced. As examples, Weinbreck et al. (2003a) reported that complexation within whey protein isolate-gum Arabic mixtures were improved at NaCl levels <50 mM. Under these ionic conditions, biopolymer-ion interactions may lead to slight conformational changes to the protein structure to expose or partially expose reactive sites and improve biopolymer flexibility within solution (Weinbreck et al., 2003a, Ducel et al., 2004). Low levels of NaCl may also play a role in enhancing protein solubility, which in turn will lead to greater interactions with polysaccharides in solution. The influence of NaCl addition has been well studied in literature for mixtures of pea protein isolate-gum Arabic (Liu et al., 2009, 2010a), β-lactoglobulin-pectin (Girard et al., 2004) and whey protein isolate-gum Arabic (Weinbreck et al., 2003a). Weinbreck et al. (2004a) reported for a whey protein isolate-carrageenan mixture that in the presence of NaCl, $pH_{\phi 1}$ is shifted to higher pH as NaCl levels increased up to 45 mM. At levels of 1.0 M NaCl, complexation of the same system was suppressed, with the higher amount of NaCl needed to suppress complexation attributed to the greater strength of the sulphated carrageenan versus the weaker carboxylated polysaccharides. The influence of others salts on complexation is less understood and studied. Weinbreck et al. (2004a) studied the effect of $CaCl_2$ addition on complex formation ($pH_{\phi 1}$) involving whey protein isolate and λ-type carrageenan mixtures. The authors reported a pH shift associated with complex formation to higher pH (8.00), which the authors attributed to calcium bridging.

3.3.3 Effect of biopolymer mixing ratio and total biopolymer concentration

Biopolymer mixing ratio also has a significant effect on complex formation, as it influences the level of available sites for electrostatic attraction between the two biopolymers. In general, the formation of soluble complexes is considered to be unaffected by mixing ratio, where it is thought that complexation involves the interaction between a single polysaccharide chain with a few protein molecule (Weinbreck et al., 2003a). However, this hypothesis was primarily shaped from studies involving 'aggregate-free' whey protein-polysaccharide mixtures (Weinbreck et al., 2003a,b, 2004a,b). In contrast, Klassen et al. (2011) and Liu et al. (2009, 2010a,b) reported for canola protein isolate (ι-carrageenan/alginate) and pea protein isolate-gum Arabic mixtures, respectively, that pH_c was dependent on the mixing ratio. The authors proposed that the mixing ratio dependence arose because the proteins were strongly aggregated, and initial complexes formed between small protein-protein aggregates with a single polysaccharide chain. The

biopolymer mixing ratio dependence reflects the progressive growth of protein–protein aggregates with increasing biopolymer concentration until a critical size is reached, after which a steady state occurs. Similar biopolymer mixing ratio dependence for pH_c was reported by Singh et al. (2007) involving mixtures of agar with type-A and type-B gelatin. In contrast, it is generally accepted that there is a mixing ratio dependence associated with the formation of insoluble complexes, where $pH_{\phi 1}$ increases with mixing ratio up to a critical value before reaching a steady state. This trend is believed to be attributed to a greater amount of protein molecules available per polysaccharide chain for binding (Weinbreck et al., 2003a,b, 2004a,b; Liu et al., 2009; Klassen et al., 2011). As an example, Weinbreck et al. (2003b) reported a shift in $pH_{\phi 1}$ to higher pH values as mixing ratios increased from 1:1 to 9:1 in whey protein isolate–exocellular polysaccharide B40 mixtures, above which charges along the protein's surface became saturated. A similar trend was reported for whey protein-carrageenan and pea protein isolate-gum Arabic mixtures where protein saturation occurred at mixing ratios of 30:1 and 4:1, respectively (Weinbreck et al., 2004a; Liu et al., 2009).

Typically, coacervation studies are prepared under very dilute biopolymer conditions (0.05-0.1%, w/w), since above a critical total concentration, coacervation of biopolymer is suppressed and interactions are more difficult to access via scattering techniques (e.g., turbidity). Suppression at higher total biopolymer concentrations arise due to competition for available solvent molecules between the two biopolymers, and an increased release of counterions into solution which screen reactive sites along the biopolymer's electric double layer (Weinbreck et al., 2003a; Ye, 2008; Liu et al., 2009). Liu et al. (2010b) studied the effect of pH on the functional attributes of pea protein isolate-gum Arabic complexes at high total biopolymer concentrations (5% w/w) and found that biopolymer complexation was still occurring.

3.3.4 Effect of polysaccharide-type

de Kruif et al. (2004) classified polysaccharides used in coacervation studies as being either weakly or strongly charged. Polysaccharides that have a relatively low charge density and weak reactive site are considered weakly charged and typically lead to the formation of coacervate-type structures. These polysaccharides include: gum Arabic, pectin, guar gum, carboxyl methyl cellulose and xanthan gum. In contrast, strongly charged polysaccharides have a high linear charge density and/or a highly charged reactive site (e.g., sulfate, amine or phosphate group). These polysaccharides could include: carrageenan, chitosan alginate, gellan gum, and exocellular

polysaccharide B40. Dickenson (1998) and Doublier et al. (2000) reported that $-OSO_3^-$ groups had greater attraction to $-N^+R_3$ groups on the protein's surface than $-COO^-$ groups. Depending on the polysaccharide-type, the reactive groups can differ resulting in differences in chain flexibility (or conformational entropy). Polysaccharides can also be linear in nature or branched; potentially affecting interactions with proteins due to steric hindrance. As previously mentioned, complex formation involving proteins and weakly charged polysaccharides typically occurs at pH<pI conditions, however in the presence of highly charged polysaccharides complexation can be initiated at pH>pI due to interactions with positively charged patches on the protein's surface.

3.3.5 Effect of molecular weight

The coacervation process has been predicted to be influenced by the molecular weight of the biopolymers within the mixed system where an increase in biopolymer molecular weight leads to an increase in the degree of coacervation (Overbeek and Voorn, 1957). Studies on the coacervation of soy globulin and dextran using light scattering have shown that the level of coacervation increased with increasing molecular weight of the dextran molecules (Semenova, 1996). The increased volume occupied by larger biopolymers is presumed to enable greater access to reactive sites for other macromolecules to react with during the coacervation process (Semenova, 1996; Schmitt et al., 1998). However, this trend is not always followed. Shieh and Glatz (1994) studied the complexation between lysozyme and polyacrylic acid (PAA) at different molecular weights ranging in size from 5 kDa to 4,000 kDa to find molecular weight played only a minor role in complex formation.

3.3.6 Effect of processing conditions

Complex formation and stability have been shown to be influenced by processing conditions, such as temperature, shearing and pressure (Schmitt et al., 1998). These processing conditions can influence the formation and/or stability of coacervates by partial or complete denaturation of proteins and hence influence their conformation by exposing buried hydrophobic groups which will favour non-polar interactions. High or low temperatures also break or favour hydrogen bonding (Schmitt et al., 1998). These processing conditions may induce protein-protein aggregation, effectively increasing the molecular weight of the interacting species. Post-harvest

processing of plant materials prior to protein extraction could also impact behavior and hence complexation.

3.3.7 Role of protein aggregation

Protein-protein aggregation influences complexation during an acid titration by: i) limiting the available reactive sites on the protein's surface for complex formation, ii) forming larger aggregates for interactions with polysaccharides and, iii) altering the biopolymer mixing ratio required to reach neutrality and maximum yield (Schmitt et al., 2000, 2001; Sanchez and Renard, 2002). Protein-protein aggregates have been reported to play a stabilizing role in β-lactoglobulin-acacia gum (Schmitt et al., 2000, 2001; Sanchez and Renard, 2002), pea protein isolate-gum Arabic systems (Liu et al., 2009, 2010a) due to protein aggregates size distribution and stabilizing hydrophobic interactions within the aggregated structure relative to aggregate-free systems; whey protein isolate-GA (Weinbreck et al., 2003a). Approximately 60-70% of the acacia gum has been reported to react to form aggregates and precipitates in a β-lactoglobulin-acacia gum system (Schmitt et al., 2001). In contrast, aggregate-free solutions formed complexes via electrostatic attraction only where polysaccharide chains interacted with only a few protein molecules to form complexes (Weinbreck et al., 2003a). Protein-polysaccharide ingredients that stay stable without the need for chemical crosslinkers could be formulated if the role that protein aggregates play in the stabilization of coacervates is better understood.

3.4 Functionality

Admixtures of protein and polysaccharides under conditions favoring associative phase separation affect the solubility profiles of proteins differently depending on the biopolymer-biopolymer and biopolymer-solvent characteristics. Solubility is highly dependent on the overall surface charge of the formed complexes, which relates to the level of surface hydrophobicity, biopolymer ratio and solvent conditions (Schmitt et al., 1998). In general, highly charged polysaccharides, low levels of surface hydrophobicity or biopolymer mixtures far from their electrical equivalence ratios, can exert an overall net negative charge on the formed complexes to improve its solubility relative to protein alone (especially at its pI) (Schmitt et al., 1998). However, depending on the biopolymers involved and complexation conditions, deviations from this behavior can occur. Ortiz et al. (2004) studied solubility profiles for soy protein isolate-

carrageenan complexes to find that as the polysaccharide level increased, the range of the pH from which minimum solubility occurred broadened towards the more acidic pHs.

The addition of polysaccharides to protein-stabilized oil-in-water emulsions leads to either stabilization or destabilization mechanisms depending on the nature of the biopolymers, solvent conditions and degree of complexation with the protein absorbed to the interface. In the case of absorbing polysaccharides, a destabilization phenomenon called 'bridging flocculation' may occur if at low biopolymer concentration (Jourdain et al., 2008). In this instance, there are insufficient polysaccharides present to span the entire oil droplet's surface, favoring instead to complex (or link) to proteins on more than one oil droplet (Dickinson, 1998). In contrast, at higher concentrations of absorbing polysaccharides, 'steric stabilization' is favored as multiple polysaccharides complex to, and saturate the protein-stabilized interface (Dickinson, 1998; Dickinson & Pawlowsky, 1998). The protective polysaccharide outer layer functions to improve the viscoelastic properties of the interfacial film; alters the surface charge on the dispersed droplets; and creates steric hindrance inhibiting the coalescence of neighboring droplets. Vikelouda & Kiosseoglou (2004) reported improved emulsion stability due to steric repulsive forces between droplets for a carboxylmethylcellulose-potato protein isolate stabilized interface. As polysaccharide levels increase, emulsion stability can further be enhanced through the formation of a 'network-like' structure within the continuous phase (Papalamprou et al., 2005). Jourdain et al. (2008) investigated the steps behind emulsion preparation involving a complexing system of sodium caseinate and dextran sulfate. Emulsions prepared using pre-formed complexes were more stable than those formed via a layer-by-layer assembly (or bilayer) whereby polysaccharides are triggered to absorb to an already formed protein-stabilized interface. The difference in observed stabilities were most probably related to the biopolymer film structure at the interface. In either case, stability was enhanced in the presence of the dextran sulfate.

The foam forming properties of proteins relate to their ability to diffuse to the air-water interface, adsorb to the interface, and re-align or undergo conformational changes at the interface to lower surface tension (Ganzevles et al., 2006; Martinez et al., 2007). In general, globular proteins act as good foam stabilizers but weak foam forming agents. As in emulsions, partial unraveling of the protein structure to expose hydrophobic moieties promotes greater interactions to the air-water interface. The addition of polysaccharides and subsequent formation of complexes contributes to foam stability through enhanced absorption at the interface and the formation of a

viscoelastic film between neighboring air bubbles (Marki & Doxastakis, 2007). The degree of stabilization by formed complexes is highly dependent on the characteristics of the biopolymer interactions (and solvent conditions) present. Polysaccharides themselves also contribute to foam stabilization, typically through increases to the bulk phase viscosity (Schmitt et al., 1998; Martinez et al., 2007; Dickinson, 2003), which result in higher cohesive forces among biopolymers (Marki & Doxastakis, 2007). The foaming properties of biopolymer admixtures has been previously studied for soy protein with hydroxylpropylmethylcellulose, λ-carrageenan and locust bean gum (Martinez et al., 2007), common bean protein isolates with xanthan gum, locust bean gum and gum Arabic (Marki & Doxastakis, 2007), and β-lactoglobulin with pectin (Ganzevles et al., 2006). Mechanisms for foam destabilization include coalescence, Ostwald ripening and drainage of the bulk phase (Marki & Doxastakis, 2007).

-Chapter 4-

Function attributes of commercial protein isolate ingredients

4.1 ABSTRACT

The functional properties of selected commercial protein isolate ingredients derived from pea, soy, wheat, egg and milk (whey) were investigated at pH 7.0, along with a laboratory prepared canola protein isolate, rich in cruciferin proteins for comparative purposes. Specifically, the solubility, foaming and emulsifying properties and, water hydration and oil holding capacities were assessed.

4.2 INTRODUCTION

Protein ingredients represent a multi-billion dollar industry, presently dominated by animal proteins, such as gelatin, ovalbumin, casein and whey. In 2011, the US protein ingredient market for food is estimated to be worth ~2.84 billion, with $1.17 (avg. annual growth rate, AAGR 6.4%) and ~1.67 (AAGR 1.7%) billion coming from plant and animal sources, respectively. The global protein market is expected to hit $24.5 billion by 2015. With increased concerns over the safety of animal-derived products, rising costs of dairy-based ingredients; growing dietary preferences and consumer demand for healthier foods; market trends are shifting towards lower cost and abundant plant-based alternatives. Plant proteins derived from agricultural crops have the potential to fill these market gaps, providing competition to soy products already in the market place. Plant proteins also have a significant price advantage over animal-based ingredients; for instance, casein is sold for ~$4.90 (USD) a pound, compared to soy or other plant proteins, which range between $0.42 to $2.08 (USD) per pound. Despite experiencing greater market growth than animal-derived protein ingredients, the wide spread use of plant proteins in the food and biomaterial sectors is hindered by their reduced solubility and functionality relative to animal-based products, and in the case of soy, its beany flavour, allergencity and tendency to cause flatulence.

Development of innovative knowledge and technology relating to proteins derived from agricultural crops will help support the movement of these products into existing markets (e.g., as food/biomaterial ingredients) and open up new market niches (e.g., functional foods and feed/pet food additives) for agricultural-based processors and producers. This strategy should lead to higher economic returns to producers through increased market demand for their crops/varieties and improved price stability.

The functionality of protein ingredients refers to any property other than their nutritional composition that influences their utilization. With the exception of solubility, many of the

common functionality tests to describe protein performance are not standardized by any professional body (e.g., American Oil Chemists Society). And as such, values found in literature are difficult to compare from one group to the next due to slight differences in methodologies and protein preparation. As part of this research, a standard set of 'in-house' methods of analysis were developed in order to evaluate differences among the commercial isolates, but also for (Chapters 5-8). This manual is included in Appendix A of this report, and has served as a guide for industrial training purposes by our group (e.g., to POS BioSciences Corp; Alliance Grain Traders; Sk. Food and Development Centre, etc.). Furthermore, a marketing study relating to food protein ingredients and the potential of canola protein products was also evaluated, and can be found in Appendix B of this report.

4.2.1 Protein structure and surface chemistry

Proteins are comprised of four structural levels: linear *primary* sequences comprised of long chains of amino acids containing varying side groups, which undergoes folding into *secondary* structures such as alpha-helices, beta-sheets, beta-turns and random coils. These undergo additional folding with other secondary structures to form subunits or its *tertiary* conformation. Finally, a protein's *quaternary* conformation is comprised of associated tertiary subunits. Depending on the nature of the amino acids (i.e., polar, non-polar, neutral, acidic, basic and aromatic) and the folded conformation, proteins can display different surface chemistries such as charge and hydrophobicity. The former fosters greater associations between the protein and water (or buffers) (protein- solvent interactions) enhancing their ability to remain in solution, migrate to an oil (or gas)-water interface in emulsions or foams, and abide water. In contrast, increased levels of hydrophobicity promote a greater amount of "protein-protein" interactions (or aggregation) and foster greater associations with non-polar mediums, such as air in the case of foams, and oil droplets in the case of emulsions. Depending on environmental (e.g., pH, temperature, and presence of salts) and processing conditions (e.g., time/temperature and shear), protein conformation and surface chemistry can be altered to an extent that could have a negative, neutral or positive impact on functionality. In most instances, proteins used by the food industry undergo some level of denaturation from their native state. Often a small amount is useful to induce partial unraveling of the protein structure to exposure reactive hydrophobic amino acids to the surface.

4.2.2 Protein functionality

a) Solubility

Protein solubility is often a perquisite to many other functional attributes; enabling them to be used as emulsifiers, foaming agents, gelling agents or thickeners in a wide range of applications. The solubility of a protein is related to its structure (charge and hydrophobicity, isoelectric point), along with solution pH, temperature and salts (type and concentration). At the protein's isoelectric point (pI), the structure has no net surface charge typically resulting in minimal solubility since neighboring proteins will have a tendency to aggregate into larger structures and sediment. In contrast, at solution pH away from its pI the protein will display either a positive (pH<pI) or negative (pH>pI) net surface charge and have maximum solubility. The presence of a surface charge acts to repel neighboring proteins away from each other to keep them in solution. The effect of salt on protein solubility is dependent on both the type and concentration present; leading to either a salting in or out effect. In general, mono- and divalent ions such as sodium, potassium, magnesium and calcium act to screen charges on the protein's surface to facilitate aggregation and loss of protein solubility. Temperature can also have both a positive and negative influence on solubility. At temperatures below the protein's denaturation temperature solubility is typically enhanced with increasing temperature. However, once the protein reaches its denaturation temperature its conformation begins to unravel and expose buried hydrophobic amino acids. As a result, neighboring proteins begin to aggregate and facilitate loss of solubility.

b) Emulsions

Emulsions are defined as mixtures of two (or more) immiscible liquids with one liquid being dispersed in a continuous phase of the other. Emulsions require some sort of energy input (e.g., high speed mixing or homogenization) to form, followed by a means to induce stability over time. Emulsions are widely found in food products, ranging from water-in-oil (W/O) emulsions, such as margarines and butter, or oil-in-water (O/W) emulsion, such as milk and salad dressings. Due to the immiscibility of oil and water, emulsions are inherently unstable and over time move to separate into two distinct phases. Depending on the system, instability in an O/W emulsion could take the form of: (1) *creaming*, where oil droplets float to the surface individually due to density differences between the two phases; (2) *flocculation*, where oil droplets reversibly aggregate into larger flocs (i.e., oil droplets remain separate entities within the larger cluster)

before floating to the surface; and (3) *coalescence*, where individual oil droplets irreversibly merge into larger droplets before floating to the surface. Proteins act to stabilize emulsions by coating the surface of individual oil droplets to prevent coalescence or flocculation; ensuring good dispersion of the oil droplets within the water continuous phase.

The effectiveness of proteins as emulsifiers stems from both their surface chemistry and conformation; both of which influences their ability to align at the oil-water interface. Within the protein coating, hydrophilic amino acids tend to align more towards the water phase, whereas hydrophobic amino acids orient towards the oil phase. Proteins that are more unraveled (e.g., casein) tend to integrate better at the interface versus more globular-type proteins (e.g., soy) which require greater time to align at the interface but form a thicker more stable film. Depending on the emulsion pH and the protein-type, oil droplets can repel one another at pH<pI or pH>pI to maintain good dispersibility within the water phase. At pHs close to the pI, oil droplets take on more of a neutral net charge and tend to aggregate leading to emulsion instability. Furthermore, depending on the distribution of hydrophilic and hydrophobic amino acids on the protein, integration and alignment at the oil-water interface may lead to sections of the protein extending out into solution. This effect creates steric forces which physically excludes neighboring droplets from coming together. Emulsion stability is also highly dependent on the shear rate and duration in which the emulsion is prepared. A greater amount of homogenization leads to the production of smaller droplets with improved emulsion stability.

c) Foams

Similar to emulsions, foams are mixtures of two immiscible phases with gases and water representing the dispersed and continuous phases, respectively. Protein-based foams are used in the food industry in meringues, mousses, beer and in whipped desserts. Similar to emulsions, foams form after an energy input (i.e., whipping, sparging, pouring) as proteins: migrate to the gas-water interface, re-orient to position hydrophobic amino acids towards the gas phase and hydrophilic amino acids towards the water phase, and then form a stiff gel-like film surrounding the gas bubbles that resists against rupturing. This film also connects with adjacent proteins to create a cage-like network with entrapped gas to constitute the foam structure. Foam formation is related to properties of the protein such as surface hydrophobicity, conformation/flexibility, size and level of denaturation. Foam stability is typically best at a pH near the pI of the protein, where

repulsive electrostatic forces are minimum. More viscous protein solutions tend to produce more stable foams, as liquid drainage from the protein cage-like network is reduced. A thicker protein solution in-between the gas bubbles also reduces Oswald Ripening (i.e., diffusion of gas from smaller gas bubbles to larger ones).

d) Water and oil holding

Water and fat holding properties of proteins are important for maintaining product quality and acceptability to consumers. They contribute to textural attributes, mouthfeel, and restrict expelled water on products (e.g., meats). The attraction of water to proteins or within a protein matrix can be considered in two parts: 1) bound water, which is no longer available for further reactions; and 2) trapped or retained water, which is free to participate in reactions and be expelled from the protein matrix or product if pressed. Proteins that are more highly charged tend to hold more water through electrostatic attractive forces, hydrogen bonding, and thus are related to protein composition (amino acid content and distribution), solution pH, salts and temperature. The pore structure of the protein network or food product is also important, as it influences the amount of protein-water interactions occurring as trapped water is pressed out. In contrast, oil holding properties of proteins or a protein matrix is related to protein composition (hydrophobic amino acid content and distribution); pore structure of the protein network or food product; and oil type and droplet size/distribution throughout the food.

4.3 MATERIALS AND METHODS

Materials

Commercial whey protein isolate (Davisco Foods International, Inc., Le Sueure, MN, USA, BiPRO JE Lot # 061-7-440), egg protein isolate (Ballas Egg Products Corp., Zanesville, OH, USA, Dried Egg Whites Type H-40), wheat protein isolate (ADM Milling, Keokuk, IA, USA, Pro Lite 100 Lot # 026706), soy protein isolate (Cargill Health & Food Technologies, Wayzata, MN, USA, Prolisse Lot # 020806PM-01), and pea protein isolate (Nutri-Pea Limited, Portage le Prairie, MB, Propulse), were kindly donated for this project. Canola seed (SP Desirable *Brassica napus*, Lot #: 168-8-129810) was kindly donated by Viterra (Saskatoon, SK). All chemicals used in this study were reagent grade, and purchased from Sigma-Aldrich Canada Ltd. (Oakville, ON). Protein determination of the commercial isolate products was performed by micro-Kjeldahl analysis (%N

x 6.25 –egg, wheat, soy and pea; %N 6.38-whey) (Appendix A). Protein levels were found to be 78.01%, 80.60%, 82.46%, 79.90% and 80.02% for the protein isolates from egg, whey, wheat, soy and pea, respectively.

Preparation of a canola protein isolate

Canola seeds (stored at 4^{o}C in a sealed container prior to use) were initially screened based on size using first a #8 (2.63 mm) Tyler mesh filter (Tyler, Mentor, OH, USA) and then a #12 (1.70 mm) filter. The screened seed was frozen at -40^{o}C overnight, and then were cracked using a stone mill (Morehouse-Cowles stone mill, Chino, CA, USA). The seed coat and cotyledons were then separated using an air classifier (Agriculex Inc., Guelph, ON, Canada). The cotyledons oil was removed up to ~13% mechanically using a continuous screw expeller (Komet, Type CA59 C; IBG Monforts Oekotec GmbH & Co., Mönchengladbach, Germany), which was operated at a speed of 59 rpm using a 3.50 mm choke. The residual oil in the meal was removed by hexane extraction (x3) at a 1:3 meal to hexane ratio for 8 h. The meal was then air-dried for an additional 8 h to allow for residual hexane to evaporate. CPI was prepared from defatted canola meal according to the method described by Folawiyo and Apenten (1996) and Klassen et al. (2011). In brief, 100 g defatted canola meal was dissolved in 1000 g 0.05 M Tris-HCl buffer containing 0.1M NaCl (pH = 7.0) at room temperature (21-23^{o}C) for 2 h under constant mechanical stirring at 500 rpm (IKAMAG RET-G, Janke & Kunkel GMBH & Co. KG, IKA-Labortechnik, Germany). The solution was then centrifuged (Sorvall RC Plus Superspeed Centrifuge, Thermo Fisher Scientific, Asheville NC, USA) at 3000 × *g* for 1 h to collect the supernatant. This was then filtered using # 1 Whatman filter paper (Whatman International Ltd., Maidstone, England), dialyzed (Spectro/Por tubing, 6-8 kDa cut off, Spectrum Medical Industries, Inc, USA) at 4 ^{o}C for 72 h with frequent changes of Milli-Q water (Millipore Corporation, MA, USA) to remove the salt, and then freeze-dried (Labconco Corporation, Kansas City, Missouri 64132) at temperature difference of 35 ^{o}C for 24 h to yield the CPI powder for later use. The crude protein composition of CPI powder was determined using the Association of Official Analytical Chemists Method 920.87 (AOAC, 2003). The CPI produced was found to be comprised of 90.45% protein (%N x 6.25).

Functionality testing of commercial food proteins and a non-commercial canola protein isolate

The functional properties of commercial protein isolates from egg, whey, wheat, soy and pea, and the non-commercial CPI were assessed using protocols outlined in Appendix A '*Protein Functionality Testing Manual*'. The Industry Manual gives a step-by-step guide to individual testing procedures, and includes: protein solubility, emulsification capacity, emulsification stability (by creaming), emulsifying stability and activity indices, water hydration capacity, oil holding capacity, and foaming stability and capacity. All tests were carried out at pH 7.0 with the exception of solubility, which was reported at pH 6.0 (Note: solubility was also measured at pHs 2.0, 4.0, 8.0 and 10.0 – reported in Appendix A for commercial proteins). All tests were also performed a 1% (w/w) protein concentration, with the exception of tests for emulsifying stability and activity indices which were carried out at a 0.25% (w/w) protein concentration. For all tests, concentrations used were corrected for protein content. All experiments were tested in triplet.

4.4 RESULTS AND DISCUSSION

Protein solubility

Protein solubility is often a perquisite to many other functional attributes; enabling them to be used as emulsifiers, foaming agents, gelling agents or thickeners in a wide range of applications. Solubility (at pH 6) for CPI was found to be comparable to that of animal-derived proteins from whey and eggs (>97%), and significantly higher than those from other plant sources, such as soy (~15%), pea (~5%) and wheat (<1%) (Table 4.1). The solubility of a protein relates to its structure (charge and hydrophobicity, isoelectric point), along with solution pH, temperature and salts (type and concentration). At the protein's isoelectric point (pI), the structure has no net surface charge typically resulting in minimal solubility since neighboring proteins will have a tendency to aggregate into larger structures and sediment. In contrast, at solution pH away from its pI the protein will display either a positive (pH<pI) or negative (pH>pI) net surface charge and have maximum solubility. The presence of a surface charge acts to repel neighboring proteins away from each other to keep them in solution.

Table 4.1. Functional properties of commercial protein isolates from various sources and a non-commercial (*) canola protein isolate prepared using a pH-salt extraction protocol. All functional tests were measured at pH 7.0, with the exception of solubility which was measured at pH 6.0, and at a 1% (w/w) protein concentration, with the exception of ESI and EAI tests which were done at a 0.25% (w/w) protein concentration. Data represent the mean ± one standard deviation (n=3).

Functional property	**Egg**	**Whey**	**Wheat**	**Soy**	**Pea**	**Canola***
Sol (%) (pH 6)	98.90 ± 0.90	97.00 ± 0.91	0.70 ± 0.00	14.93 ± 0.79	5.02 ± 0.10	97.22 ± 0.49
EC (g/g)	197.92 ± 7.22	210.42 ± 14.43	106.25 ± 0.00	172.92 ± 7.22	177.08 ± 7.22	202.08 ± 7.22
ES (%)	94.67 ± 2.31	100.00 ± 0.00	24.67 ± 3.06	100.00 ± 0.00	80.67 ± 3.06	75.33 ± 1.15
ESI (min)	11.59 ± 0.42	11.28 ± 0.18	11.77 ± 0.30	10.72 ± 0.02	23.87 ± 4.46	11.68 ± 0.19
EAI (m^2/g)	18.81 ± 0.32	31.47 ± 0.95	4.53 ± 0.15	19.77 ± 0.37	1.49 ± 0.25	17.57 ± 0.15
WHC (g/g)	CD[1]	CD[1]	NM[2]	12.39 ± 0.32	3.09 ± 0.11	0.39 ± 0.11
OHC (g/g)	1.96 ± 0.01	1.39 ± 0.07	2.84 ± 0.01	1.85 ± 0.13	0.96 ± 0.02	1.63 ± 0.06
FC (%)	115.56 ± 16.78	276.67 ± 5.77	182.22 ± 10.18	171.11 ± 16.78	81.11 ± 17.11	257.78 ± 3.85
FS (%)	72.71 ± 5.29	75.53 ± 2.55	49.20 ± 8.45	67.69 ± 2.96	27.15 ± 7.40	71.97 ± 2.08

Abbreviations: Protein content (PC), solubility (Sol), emulsification capacity (EC), emulsification stability (ES), emulsifying activity index (EAI), emulsifying stability index (ESI), water hydration capacity (WHC), oil holding capacity (OHC), foam capacity (FC) and foam stability (FS).

[1]CD = Completely dissolved.

[2]NM = Not measurable, remained suspended in water as particulates (not dissolved).

Emulsifying properties

Emulsions are defined as mixtures of two (or more) immiscible liquids with one liquid being dispersed in a continuous phase of the other. Emulsions require some sort of energy input (e.g., high speed mixing or homogenization) to form, followed by a means to induce stability over time. Due to the immiscibility of oil and water, emulsions are inherently unstable and over time move to separate into two distinct phases. Proteins act to stabilize emulsions by coating the surface of individual oil droplets to prevent coalescence or flocculation; ensuring good dispersion of the oil droplets within the water continuous phase. CPI was found to have similar emulsion capacities (*i.e., the amount of oil that can be emulsified by a protein relative to the total weight of emulsion, after which the emulsion undergoes an inversion from an oil-in-water emulsion to a water-in-oil emulsion*) as whey and egg proteins (~203 g/g); which were slightly higher than that of soy and pea proteins (~175 g/g), and substantially higher than that of wheat (~106 g/g) (Table 4.1). Despite CPI's ability to form an emulsion, its stability was reduced (~75%) relative to that of egg, whey and soy (~98%) as measured by creaming; and was more comparable to that of pea (~81%). Emulsions prepared using wheat proteins were highly unstable (~25%), most likely caused by pour alignment at the oil-water interface, which stemmed form its poor solubility in water/buffer (Table 4.1). Emulsion stability as measured by creaming, refers to the ability of the protein-stabilized emulsion to resist creaming. As an emulsion becomes unstable, oil droplets come together and migrate upwards to form a cream layer at the top of the emulsion. A protein's emulsifying activity index refers to the ability of a protein to form of an emulsion with the index providing an estimate of the interfacial area stabilized per unit weight of protein – based on a highly dilute emulsion test. Activity indices were found to be greatest for whey proteins (~31.5 m^2/g) most likely due to their high solubility, affinity for the oil-water interface and small structure. Egg, soy and CPI proteins had relatively similar indices (~18.7 m^2/g), suggesting that the interfacial area stabilized by each protein was the same. Wheat and pea proteins showed poor interfacial stabilization, giving indices less than 5 m^2/g (Table 4.1). In contrast, the emulsion stability index provides an estimate to the stability of that same dilute emulsion over a defined time period. Indices for the dilute emulsions appeared similar for proteins from wheat, egg, whey, soy and canola (~11.4 min) (Table 4.1). In contrast, the stability index was quite high for pea (~23.9 min), however the emulsion generated was very low (Table 4.1).

Water hydration and oil holding properties

Water hydration capacities (*i.e., the amount of water that can be absorbed by one gram of protein)* of CPI was found to be very low (0.39 g/g) due its high solubility at pH 7 (Table 4.1). The water hydration test relates to the amount of water absorbed to insoluble protein in solution; where water may be bound or trapped within the protein matrix. Water hydration capacities could also not be detected for whey or egg proteins, since the proteins, like CPI, almost completely dissolved. Soy in contrast, had poor solubility (<20%) at pH 7, and was able to absorb a significant amount of water, having a capacity value of ~12 g/g. In contrast, pea protein (also having poor solubility) showed significantly lower amounts of absorbed water (~3 g/g) (Table 4.1). Differences in the protein's effectiveness to absorb water relate back to the protein's structure. In general, proteins with higher amounts of hydrophilic groups near the surface abide more water. Testing was unsuccessful for the wheat protein isolate, where proteins formed particulate structures that remained suspended but not dissolved. In terms of the protein's oil holding capacities (*i.e., the amount of oil that can be absorbed by one gram of protein*), wheat proteins were able to retain the largest amount of oil (~2.8 g/g), followed by egg and soy (~1.9 g/g), CPI (~1.6 g/g) and whey (~1.4 g/g) and then pea (~1.0) (Table 4.1). In general, proteins with higher amounts of exposed hydrophobic sites on the surface tend to absorb a greater amount of oil per gram protein.

Foaming properties

Foams are mixtures of two immiscible phases with gases and water representing the dispersed and continuous phases, respectively. Similar to emulsions, foams form after an energy input (i.e., whipping, sparging, pouring) as proteins: migrate to the gas-water interface, re-orient to position hydrophobic amino acids towards the gas phase and hydrophilic amino acids towards the water phase, and then form a stiff gel-like film surrounding the gas bubbles that resists against rupturing. This film also connects with adjacent proteins to create a cage-like network with entrapped gas to constitute the foam structure. Foaming capacity *(i.e., the ability for a protein at a given concentration to generate a foam)* of CPI (~258%) was found to be similar to that of proteins from whey (~277%). In contrast, reduced foam volume was found in the following descending order: wheat > soy and > egg ≈ pea (Table 4.1). In contrast, foam stability *(i.e., ability of that protein to maintain its foam volume over a defined period of time*) for CPI was also reasonably good (~72%) and comparable to that of egg, whey and soy (~72%) (Table 4.1). Stability

of the foams produced by wheat and pea proteins was significantly reduced relative to the others (Table 4.1). Foam formation is related to properties of the protein such as surface hydrophobicity, conformation/flexibility, size and level of denaturation. Foam stability is typically best at a pH near the pI of the protein, where repulsive electrostatic forces are minimum. More viscous protein solutions tend to produce more stable foams, as liquid drainage from the protein cage-like network is reduced. A thicker protein solution in-between the gas bubbles also reduces Oswald Ripening (i.e., diffusion of gas from smaller gas bubbles to larger ones).

-Chapter 5-

Formation and functional attributes of canola protein isolate - gum Arabic electrostatic complexes[1]

Andrea K. Stone, Anzhelika Teymurova and Michael T. Nickerson

Department of Food and Bioproduct Sciences, University of Saskatchewan
51 Campus Drive, Saskatoon, SK, Canada, S7N 5A8

[1]Food Biophysics, 9, 203-212 (2014)

5.1 ABSTRACT

The formation of electrostatic complexes within mixtures of canola protein isolates (CPI) and gum Arabic (GA) was investigated by turbidity during an acid pH titration (7.00-1.50) as a function of mixing ratio (1:1 to 8:1 CPI: GA), and the resulting functional properties (e.g., flow behavior, solubility, foaming and emulsification) of formed complexes were studied. Complexation typically follows two pH-dependent structure forming events associated with the formation of soluble (pH_c) and insoluble complexes ($pH_{\phi 1}$). Both pH_c and $pH_{\phi 1}$, was found to shift to higher pHs with increasing mixing ratio until reaching a plateau at a 4:1 CPI-GA ratio. Maximum coacervation occurred at pH 4.20 at a ratio of 2:1 CPI-GA, prior to complete dissolution at pH 2.20. The coacervate phase was pseudoplastic in nature, with some evidence of elastic-like behavior associated with a weakly interconnected network or entangled polymer solution. Solubility of CPI and CPI-GA was found to be pH-dependent with minimum solubility occurring at pH 4.00 and 3.00, respectively. Foaming and emulsifying properties of CPI-GA remained unaffected relative to CPI alone, except foaming capacity which was reduced for the mixed system.

5.2 INTRODUCTION

Protein-polysaccharide interactions play an important role in controlling food quality and texture (Tolstoguzov, 2003), as well as in the formation of edible packaging (Murillo-Martínez et al., 2011) and controlled delivery carriers for pharmaceutical and functional food purposes (McClements, 2006). Depending on the solvent and biopolymer conditions, protein-polysaccharide interactions may lead to either segregative or associative phase separation. The former arises when biopolymers carry a similar net charge and repel one another into both a protein-rich and polysaccharide-rich phase (Turgeon et al., 2003). In the case of the latter, biopolymers carrying opposing net charges experience electrostatic attraction, leading to separation into both a biopolymer-rich and a solvent-rich phase (de Kruif et al., 2004; Schmitt and Turgeon, 2011). Associative phase separation typically involves two pH-dependent structure forming events during an acid pH titration associated with first the formation of soluble complexes (denoted at pH_c). At pH_c, a small inflection within a pH-turbidity profile is evident as the first experimentally detectable protein-polysaccharide interaction arises (Kizilay et al., 2011). Typically this occurs at or near the protein's isoelectric point (pI); below which the protein assumes a net positive charge and starts to interact with anionic polysaccharides. As pH decreases, soluble

complexes continually grow in size and number until a point where macroscopic phase separation and the formation of insoluble complexes (occurring at $pH_{\phi 1}$) occurs (Li et al., 1994; de Kruif et al., 2004). At $pH_{\phi 1}$, solutions transition from transparent to cloudy and large increases in turbidity occurs up to a maximum (denoted at pH_{opt}) where the biopolymer mixture reaches an electrical equivalence point (Li et al., 1994; de Kruif et al., 2004). Beyond which, turbidity declines as complexes break up as reactive groups along the polysaccharide backbone begin to become protonated. Complete dissolution of complexes occurs at $pH_{\phi 2}$ near the pKa of the reactive site of the polysaccharide (Li et al., 1994; de Kruif et al., 2004).

Associative phase separation within plant protein-polysaccharide mixtures has been relatively limited (Ducel et al., 2004; Chourpa et al., 2006; Dong et al., 2013) compared to those involving milk proteins (Weinbreck et al., 2004; Ye et al., 2006; Wang et al., 2007). Previous research from our group has focused on interactions involving pea protein isolates with both weakly charged (e.g., gum Arabic (Liu et al., 2009; Liu et al., 2010a; Liu et al., 2010b)) and strongly charged (e.g., alginate (Klemmer et al., 2012) and chitosan (Elmer et al., 2011)) polysaccharides. In all cases (Liu et al., 2009; Liu et al., 2010a; Liu et al., 2010b; Elmer et al., 2011; Klemmer et al., 2012), initial interactions were thought to be between small protein-protein aggregates, driven by electrostatic attraction with secondary stabilization by hydrogen bonding. Hydrophobic interactions were thought to play a role in the stabilization of the complex structure, especially under acidic pHs (<3.50) rather than with its formation (Liu et al., 2010a). However, interactions with the gum Arabic polysaccharides and pea proteins led to the formation of a coacervate structure, whereas interactions with the more highly charged polysaccharides with pea proteins led to precipitate formation soon after $pH_{\phi 1}$. Work involving canola protein isolate and highly charged polysaccharides (e.g., alginate and ι-carrageenan) also suggested a similar mechanism of formation as with pea (Klassen et al., 2011).

The functionality of protein-polysaccharide complexes vary considerably within the literature, depending on the biopolymer, solvent and processing conditions used during testing. For instance, solubility is highly dependent upon the overall surface characteristics (charge and hydrophobicity) of the formed complex. In some instances, formed complexes may be electrically neutral, whereas in the other cases the presence of a strongly charged polysaccharide may result in a charged complex in solution regardless of the pH. Liu et al. (2010b) studied the solubility of pea protein isolate and gum Arabic mixtures to find the pH-solubility minimum to shift relative to

the pea protein alone to more acidic pHs. Similar findings were reported by Ortiz et al. (Ortiz et al., 2004) studying soy protein isolate-carrageenan complexes. The presence of polysaccharides at protein-stabilized oil-in-water (i.e., emulsion) or air-water (i.e., foam) interface can also have a positive or negative impact on functionality depending on the nature of the biopolymer, solvent and processing conditions. For instance, the addition of polysaccharides to the outside of an oil droplet may lead to steric stabilization or exert a charge into solution leading to repulsive stabilizing forces (Liu et al., 2010b). However, bridging flocculation may also occur, if the polysaccharide electrostatically interacts with multiple oil droplets leading to emulsion instability. In foams, the addition of polysaccharides may lead to enhance absorption at the interface of complexes; help strengthen the viscoelastic film surrounding the gas bubbles; and increase the viscosity of the continuous phase (Liu et al., 2010b).

The focus of the present study is to better understand canola protein - gum Arabic interactions during complex formation, and the rheological and functional behavior of the formed canola protein – gum Arabic complexes. Greater understanding of plant-derived proteins, their performance and association with other food ingredients is important as the food industry moves to find alternatives to animal-derived proteins based on dietary restrictions, food/ingredient preferences and perceived fears by consumers (e.g., Bovine spongiform encephalopathy).

Canola is primarily grown for its high healthy oil content, used mainly in cooking and biofuel applications. In order for the industry to become more sustainable, greater value is being sought for its underutilized protein- and fibre-rich meal which is currently being sold as low cost animal feed supplement. Canola proteins are increasingly being explored for their commercial potential as a new food ingredient because of their well-balanced amino acid profile and functional attributes. However, since these proteins are primarily extracted from defatted canola meal, their quality may be negatively impacted by the oil processing conditions. It is hypothesized that by inducing electrostatic interactions between the canola proteins and anionic polysaccharides, such as gum Arabic would alter the surface chemistry to give new and hopefully improved functionality over the protein alone. Canola protein isolates (CPI) are dominated by two main storage proteins: 12 S (S, Svedberg unit) cruciferin and 2 S napin. Cruciferin is a hexameric glycosylated (~12.9 % saccharides) protein with a molecular weight of ~300 kDa with six subunits comprised of α- (30 kDa) and β- (20 kDa) chains linked together by a total of 12 intramolecular disulfide bonds (Lampart-Szczapa et al., 2001). In contrast, napin (2S) is a water-soluble albumin (12-14 kDa),

containing two polypeptide chains of 4.5 kDa and 10 kDa held together by disulfide bonds (Bérot et al., 2005). In contrast, gum Arabic (GA) is an anionic arabinogalactan polysaccharide-protein complex comprised of three fractions. The major faction (~89 % of the total; ~250 kDa) consists of a β-(1→3) galactopyranose (galactan) polysaccharide backbone that is highly branched with β-(1→6) galactopyranose residues terminating in arabinose and glucuronic acid and/or 4-O-methyl glucuronic acid units (Dror et al., 2006). The second fraction (~10% of the total) is comprised of a covalently linked arabino glatactan-protein complex, whereas the remaining fraction (~1% of the total) is a glycoprotein. Gum Arabic has been widely used in coacervation studies due to its overall low linear charge density, allowing it to complex with highly charged proteins (Liu et al., 2009; Liu et al., 2010a; Liu et al., 2010b). If both the protein and polysaccharide is highly charged, then precipitation typically ensues due to the degree of electrostatic interactions occurring. In the present study, electrostatic interactions will be discussed in terms of the negatively charged glucuronic acid residues of the side changes of the major galactan polysaccharide fraction (i.e., pH > 1.89 (Liu et al., 2009)) with the positively charged canola proteins, when the pH of the solvent is below the isoelectric point (i.e., pH < 5.78 (Stone et al., 2013)).

5.3 MATERIALS AND METHODS

Materials

Canola seed (SP Desirable *Brassica napus*, Lot #: 168-8-129810) and GA (Gum Arabic FT Pre-Hydrated, Lot #: 11229, 2007) were kindly donated by Viterra (Saskatoon, SK, Canada) and TIC Gums (Belcamp, MD, USA), respectively. All chemicals used in this study were reagent grade, and purchased from Sigma-Aldrich Canada Ltd. (Oakville, ON, Canada).

Preparation of canola protein isolates

Canola protein isolates were prepared as described by Klassen et al. (2011). In brief, defatted canola meal was prepared by pressing the seeds with a continuous screw expeller (Komet Type CA59 C, IBG Monforts Oekotec GmbH & Co., Monchengladbach, Germany), followed by hexane extraction at a 1:1 meal: hexane ratio for 16 h. The meal was then air-dried for 8 h, followed by a second hexane extraction. Proteins from the defatted meal were extracted using a Tris-HCl buffer (pH 7.0) with 0.1 M NaCl at a ratio of 10 mL buffer/g meal for 2 h under constant mechanical stirring at room temperature (~21-22°C). The dispersion was then centrifuged

(Beckman J2-HC, Beckman Coulter Canada Inc., Mississauga, ON, Canada) at 18,600 x g for 1 h at 4 °C, and supernatant was recovered. A second centrifuge step for 30 min was used to further clarify the supernatant of insoluble residues, followed by dialysis (Spectro/Por® tubing, 6-8 kDa cut off, Spectrum Medical Industries, Inc, USA) at 4 °C for 48 h with frequent changes of the with Milli-Q^{TM} water (Millipore Corporation, MA, USA) to remove the salt content. Precipitated salt soluble proteins were recovered by centrifugation at 18,600 x *g* for 2 h at 4 °C (Folawiyo and Apenten, 1996), and then subsequently freeze dried (Labconco Corp., Kansas City, MO, USA) to yield a protein isolate powder.

Proximate analysis

Chemical analyses on the CPI and GA materials were performed according to the Association of Official Analytical Chemists (AOAC, 2003) Methods 925.10, 923.03, 920.87 and 920.85 for moisture, ash, crude protein and lipid (% wet weight basis), respectively. Carbohydrate content was determined based on percent differential from 100 %. Composition of CPI was found to consist of 94.95 % protein (N x 5.70), 0.70 % moisture, 0.32 % lipid, 2.32 % ash and 1.71 % carbohydrate, whereas the commercial GA powder was comprised of 0.86 % protein (% N x 6.25), 9.56 % moisture, 0.11 % lipid, 5.19 % ash and 84.28 % carbohydrate. CPI and GA concentrations used in this study reflect the protein and carbohydrate content, respectively, rather than powder weight.

pH-turbidimetric assessments

Changes in turbidity during a pH acid titration were investigated for mixtures of CPI and GA as a function of pH (1.50-7.00) and biopolymer mixing ratio (0.5:1 – 8:1 CPI: GA) at a total biopolymer concentration of 0.1 % (w/w), in order to identify critical pH values associated with complex formation according to Klassen et al. (2011). Individual CPI and GA solutions were also measured under the same conditions, each at a 0.1 % (w/w) concentration. Biopolymer solutions were prepared by dissolving the respective amount of each powder within Milli-Q (Millipore Milli-Q^{TM}) water at pre-selected mixing ratios. Solution pH was then adjusted to pH 8.00 using 1M NaOH and continuously stirred for 2 h (500 rpm) at room temperature (21-23 °C). Readings of optical density were measured as a function of pH (7.00–1.50) using a Genesys 10 UV/Vis spectrophotometer (Thermo Scientific, Waltham, MA, USA) at 600 nm in plastic cuvettes (1 cm

path length). Critical pH values were determined graphically as the intersection point of two curve tangents (Weinbreck et al., 2003; Liu et al., 2009). All measurements were performed in triplicate.

Surface charge

The ζ-potential of 0.05% (w/w) NPI solutions as a function of pH and NaCl concentration was determined by measuring the electrophoretic mobility (U_E) using a Zetasizer Nano-ZS90 (Malvern Instruments, Westborough, MA, USA). Zeta potential (units: mV) was calculated using U_E by applying Henry's equation:

$$U_E = \frac{2\varepsilon \times \zeta \times f\,(k\alpha)}{3\eta} \qquad \text{(eq. 5.1)}$$

where, ε is the permittivity (units: F (Farad)/m), $f(\kappa\alpha)$ is a function related to the ratio of particle radius (α; units: nm) and the Debye length (κ; units: nm^{-1}), and η is the dispersion viscosity (units: mPa·s). The Smoluchowski approximation $f(\kappa\alpha)$ was set as 1.5. All measurements are reported as the mean ± one standard deviation (n = 3).

Rheological measurements

Rheological measurements were performed on the coacervate phase after centrifugation for a 2:1 CPI: GA mixing ratio and at 2.00 % (w/w) total biopolymer concentration under pH conditions where they are interacting (pH 4.20). All measurements were performed using a AR-G2 rheometer (TA Instruments, New Castle, USA) with a cone-and-plate geometry (diameter 40 mm, cone angle 2°). Biopolymer solutions were prepared by dispersing powders of each biopolymer in Milli-Q water (Millipore Milli-Q™), adjusted to pH 8.00 and constantly stirred for 2 h (500 rpm) at room temperature. The mixed solution was adjusted to pH 4.2 and re-adjusted if needed within 15 min. Adjusted solutions to pH 4.20 were transferred into 50 mL centrifuge tube and gently centrifuged at 1,050 x *g* (VWR clinical centrifuge 200, VWR International, Mississauga, Canada). The supernatant was discarded and the pellet was used for rheological measurements. For comparative purposes the measurements were performed for 2.00 % (w/w) CPI-GA biopolymer solutions prepared by dissolving the biopolymer powders in Milli-Q water and adjusting to pH 7 (non-interacting conditions). Samples were loaded onto the rheometer at room temperature (21-23 °C) and allowed to equilibrate for 10 min. Measurements were performed in rotational (steady-shear) and small-deformation oscillatory modes. Steady shear viscosity readings were performed as a function of shear rate (0.1-100 s^{-1}) and were fitted using the Power

law model (Nickerson and Paulson, 2004) in the range of 1-10 s^{-1} (representing the linear portion of the curve) shear rate using eq. 5.2,

$$\eta = m \times \dot{\gamma}^{n-1} \quad \text{(eq. 5.2)}$$

where η is the apparent viscosity (Pa·s), m is the consistency coefficient ($Pa \cdot s^n$), $\dot{\gamma}$ is shear rate m (s^{-1}) and n is the flow behavior index (dimensionless). The flow behavior index (n) and consistency coefficient (m) were calculated using Microsoft Office Excel 2007 (Microsoft Corporation, Redmond, WA, USA). The dynamic storage (G′, Pa) and loss (G″, Pa) moduli, and complex viscosity (η^*) were measured only for the coacervate phase (pH 4.20) as a function of angular frequency (0.1-100 Hz) and at a constant strain of 2 % within the linear viscoelastic region. The complex viscosity is defined as the frequency-dependent viscosity as a function of a oscillating shear stress, and is equivalent to the difference between the dynamic viscosity and the out-of-phase viscosity. All viscoelastic parameters were determined using the TA Instrument Software. All the measurements were performed in triplicate.

Functional properties

Solubility. Percent solubility was determined for 1.00 % (w/w) CPI and CPI-GA (2:1 ratio; 0.66% w/w CPI: 0.34% w/w GA) solutions as a function of pH (2.00-8.00). CPI alone and CPI-GA solutions were dissolved by stirring (500 rpm) for 2 h at a room temperature (21-23 °C) then centrifuged at 4,180 x *g* for 10 min (VWR clinical centrifuge 200, VWR International, Mississauga, ON, Canada). Protein content was determined in the supernatant by means of micro-Kjeldahl method (N x 5.70). Percent protein solubility was determined by dividing the water-soluble protein content by the total protein content (x 100 %). All measurements were performed in triplicate.

Foam capacity and stability. Foam capacity and stability were tested for 1.00 % (w/w) CPI alone and CPI-GA (at mixing ratio 2:1; 0.66% w/w CPI: 0.34% w/w GA) solutions at pH 4.20 using a modified method Liu et al. (2010b). Foams were generated from 15 mL (V_{li}, initial volume of biopolymer solution used to make the foam) of biopolymer solution using an Omni Macro Homogenizer (Omni International, Inc., Marietta, GA, USA) at 8,000 rpm for 5 min then transferred into a 100 mL graduated cylinder (inner diameter = 26 mm; height = 25 mm; as measured by a digital caliper). The percentage foam capacity and stability values were calculated using eq. 5.3 and 5.4, respectively, where V_{f0} is the foam volume generated initially after

homogenization and V_{f30} is the foam volume remaining after 30 min. Foam stability was measured after an arbitrary time of 30 min. All measurements were performed in triplicate.

$$\%Foam\ Capacity = \frac{V_{f0}}{V_{li}} \times 100\% \quad \text{(eq. 5.3)}$$

$$\%Foam\ Stability = \frac{V_{f30}}{V_{f0}} \times 100\% \quad \text{(eq. 5.4)}$$

Emulsion capacity. In brief, a series of emulsions with different amounts of oil was prepared from a 1.00 % (w/w) CPI solution or CPI: GA mixture (2:1 mixing ratio; 0.66% w/w CPI: 0.34% w/w GA) at pH 4.20, and canola oil. Aliquots of each solution (2.0 g) were mixed with canola oil (3-4 g) in 50 mL centrifuge tubes followed by homogenization using an Omni Macro Homogenizer (Omni International, Inc., Marietta, GA, USA) equipped with a 20 mm diameter saw tooth generating probe, at 8,000 rpm for 5 min. Immediately after homogenization the conductivity of each emulsion was measured. As an emulsion inverts from an oil-in-water to water-in-oil emulsion (inversion point) a significant drop in conductivity will be observed. Percent emulsion capacity was reported as the average weight (g) of canola oil per gram of protein before and after the inversion point.

Emulsion stability. In brief, oil-in-water (50/50) emulsions were prepared from a 1.00 % (w/w) CPI solution or CPI: GA mixture (2:1 mixing ratio; 0.66% w/w CPI: 0.34% w/w GA) at pH 4.20, with canola oil. Aliquots of each solution (4.0 mL) were mixed with canola oil (4.0 mL) in 50 mL centrifuge tubes followed by homogenization using an Omni Macro Homogenizer (Omni International, Inc., Marietta, GA, USA) equipped with a 20 mm diameter saw tooth generating probe, at 8,000 rpm for 5 min. Immediately after homogenization emulsions were transferred into individual 10 mL graduated cylinders (inner diameter 10.80 mm; height 100.24 mm) and left for separation for 30 min. Percent emulsion stability was determined using eq. 5.5,

$$\%Emulsion\ Stability = \frac{V_B - V_A}{V_B} \times 100\% \quad \text{(eq. 5.5)}$$

were V_B and V_A are the volume of the aqueous (or serum) layer before emulsification (4.0 mL) and after 30 min of drainage, respectively. All measurements were performed in triplicate.

Statistics

A paired Student's T-test was used to test statistical differences in critical pHs and max OD data for CPI-GA solutions, and for foaming and emulsifying properties between CPI, GA and CPI-GA solutions. Statistical analyses were performed using Microsoft Excel 2010 (Microsoft Corporation, Redmond, WA, USA).

5.4 RESULTS AND DISCUSSION

Effect of pH and biopolymer mixing ratio

Optical density (OD) as a function of pH during an acid titration was investigated for individual CPI and GA solutions (0.1% w/w), along with a 1:1 CPI: GA mixture (total of 0.1% w/w) (Figure 5.1A). In the case of CPI alone, OD followed a bell shaped profile occurring between pHs of 6.60 and 4.00, with the maximum OD (0.950) occurring at pH 5.40. The rise in OD as the pH was lowered is thought to be associated with CPI-CPI aggregation corresponding to pHs where charge repulsion between proteins is reduced. This maximum OD value corresponds to the pI of an individual CPI solution as shown in the ζ-potential data as a function of pH where net surface charge equals 0 mV at a pH of 5.45 (Figure 5.2). In contrast, GA displayed no optical activity (not shown). Net neutrality for the gum Arabic solution was found to occur at pH 1.73 corresponding to the protonation of the carboxyl group on the polysaccharide backbone (Figure 5.2). In the mixed system, the addition of GA to CPI resulted in a shift in the turbidity profile to lower pHs (Figure 5.1A). The formation of soluble (pH_c) and insoluble ($pH_{\phi 1}$) electrostatic complexes occurred at pH 4.13 ± 0.07 and 3.82 ± 0.01, respectively. Maximum OD (0.760) occurred at pH_{opt} 3.57 ± 0.01, with complete dissolution of electrostatic complexes occurring at $pH_{\phi 2}$ (2.14 ± 0.07) (Figure 5.1A).The shift in the turbidity profile to lower pHs, and reduction in the OD maximum relative to CPI alone are thought to reflect electrostatic repulsive forces between GA chains that inhibit CPI-CPI-aggregation. A shift in net neutrality (0 mV) was also evident in the ζ-potential data for the mixed 1:1 CPI-GA system occurring at pH 3.73, which also was near the pH_{opt} value representing maximum CPI-GA interactions (Figure 5.2).

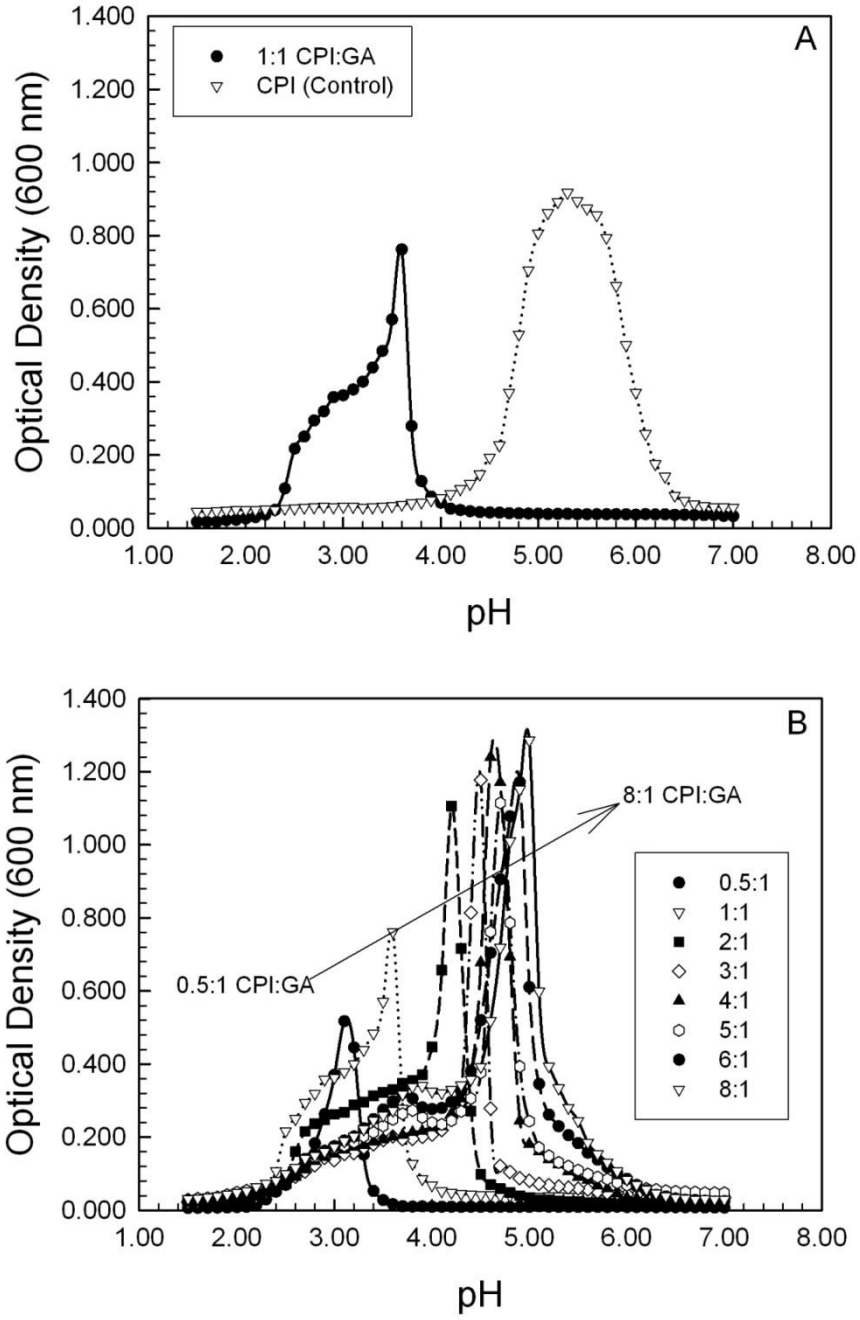

Figure 5.1 Mean turbidity curves for a 1:1 canola protein isolate (CPI) – gum Arabic (GA) mixture and an individual CPI solution at a total biopolymer concentration of 0.1% (w/w), as a function of pH (A); and CPI-GA mixtures as a function of mixing ratio (B). Data represent the mean ± one standard deviation (n = 3).

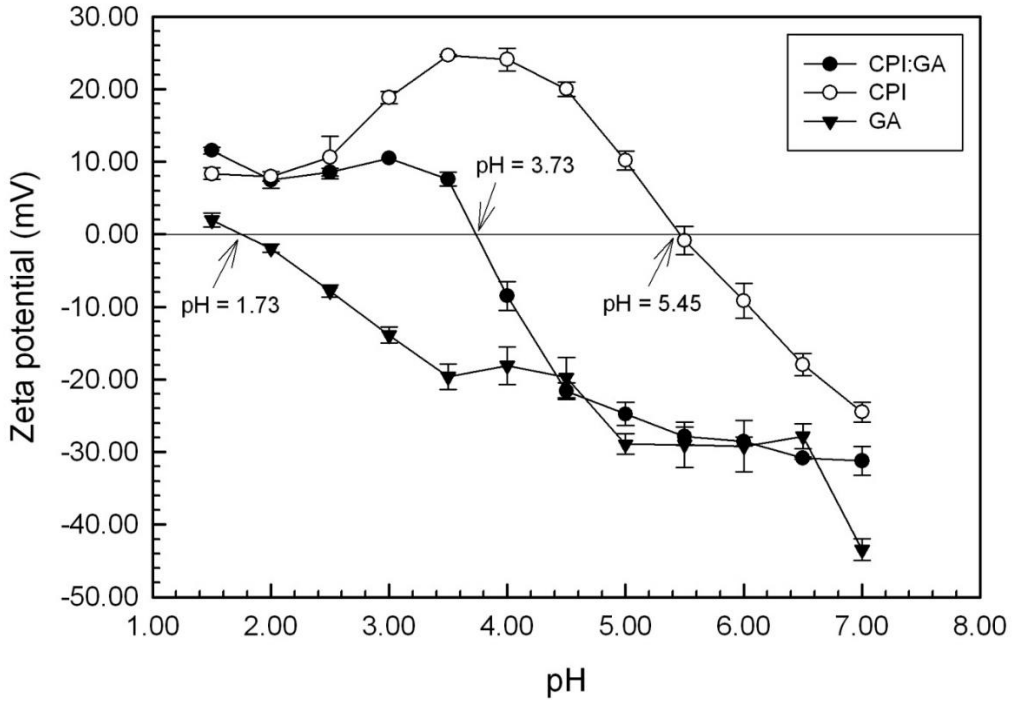

Figure 5.2 Zeta potential values (mV) as a function of pH for individual canola protein isolate (CPI) and gum Arabic (GA) solutions, and a 1:1 CPI-GA mixture at a total biopolymer concentration of 0.1% (w/w). Data represent the mean ± one standard deviation (n = 3).

Furthermore, unlike the individual CPI profile, the mixed system's turbidity profile is skewed towards acidic pHs due to the presence of stronger Coulombic forces. It was hypothesized that GA interacts with small CPI-CPI aggregates already formed to form the coacervate structure due to the overlapping turbidity curves (Figure 5.1A). Particle size measurements were not made within this study, since aggregates were too large for dynamic light scattering, and too poor of scatters for conventional static light scattering. The presence of aggregates stabilized by hydrophobic interactions are thought to play a key role in inhibiting the dissolution of electrostatic complexes at acidic pHs (~>2.50). However, once the carboxyl site along the GA backbone is protonated, complete dissolution of the coacervate structure occurs as the electrostatic attractive forces with the CPI is lost, as evident by the lack of OD at pH< 2.14 ($pH_{\phi 2}$) (Figure 5.1A). A similar phenomenon was evident in other plant protein-polysaccharide mixtures such as: lentil protein isolate - gum Arabic (Aryee and Nickerson, 2012) and partially purified pea proteins

(legumin and vicilin) – gum Arabic (Klassen et al., 2011). In contrast, for systems in which aggregates were filtered prior to coacervation, such as in whey protein – carrageenan (Weinbreck et al., 2004) and whey protein – gum Arabic admixtures (Weinbreck et al., 2003), no such skewed profile occurred. Liu et al. (2010a) investigated this phenomenon further by studying the effect of temperature on turbidimetric behavior within mixtures of pea protein isolate and GA and the associated structures by confocal scanning laser microscopy. As temperatures were elevated from room temperature (23 °C) to 60 °C, the OD between pH_{opt} and $pH_{\phi 2}$ increased along with the size of the electrostatic complexes formed. The rise in OD and size is associated with an increased amount of hydrophobic interactions occurring within and between CPI aggregates; leading to enhanced stability.

The effect of increasing the biopolymer mixing ratio from 0.5:1 to 8:1 CPI: GA resulted in a shift towards higher pHs as the number of GA chains became reduced at higher mixing ratios (Figure 5.1B). As a result, inhibition of CPI-CPI aggregation also subsequently became reduced as evident by a rise in OD. A phase diagram of critical pHs indicated pH_c, $pH_{\phi 1}$ and pH_{opt} all increased with increasing mixing ratio between 1:1 to ~4:1 CPI: GA, afterwards a plateau is reached between 4:1 and 8:1 CPI: GA (Figure 5.2A). The mixing ratio-dependence of pH_c (formation of soluble complexes) suggests that initial GA interaction is occurring with mostly small CPI-CPI aggregates rather than individual CPI molecules. Some works in the literature have filtered protein aggregates prior to complexation studies to find a ratio independence of pH_c, as was the case for whey protein-polysaccharide (Weinbreck et al., 2004) and beta-lactoglobulin-pectin mixtures (Wang et al., 2007) where the polysaccharide chains were though to interact with individual protein molecules. Mixing ratio dependence of $pH_{\phi 1}$ (formation of insoluble complexes) and pH_{opt} (pH corresponding to maximum interactions and electrostatic complexes formed) is hypothesized to be associated with growing CPI-CPI aggregates as mixing ratio increases, until the aggregates reach a critical size. Interactions after this with GA result in the plateau observed in the state diagram. In contrast, $pH_{\phi 2}$ remained constant as a function of mixing ratio. Maximum OD corresponding to pH_{opt} as a function of mixing ratio was found to increase from 1:1 CPI: GA mixing ratio to 2:1, before reaching a plateau between 2:1 and 8:1 CPI: GA (Figure 5.3B); suggesting at the 2:1 CPI: GA mixing ratio maximum interactions and coacervation is occurring. Based on Figure 5.3B, rheology and functional properties were assessed only at the 2:1 CPI: GA ratio.

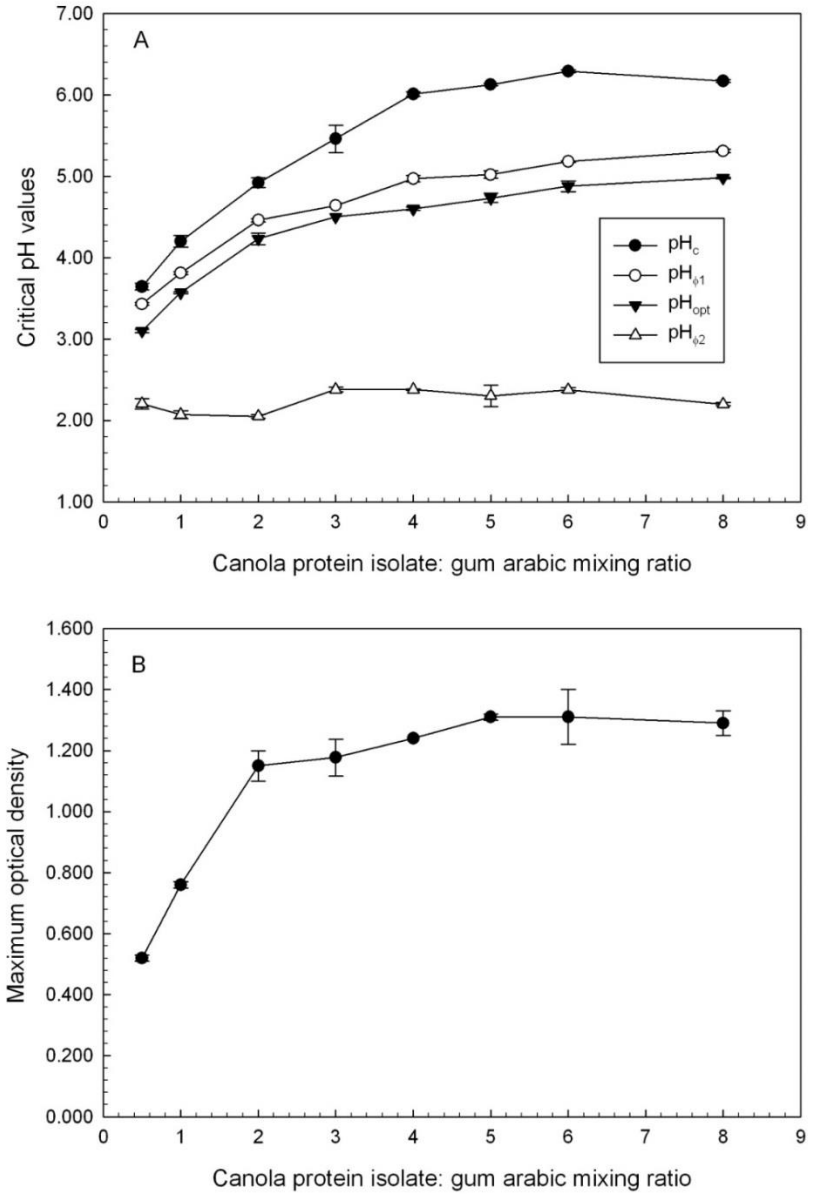

Figure 5.3 Critical pHs (pH_c, $pH_{\phi 1}$, pH_{opt} $pH_{\phi 2}$) (A) and maximum optical density (B) of canola protein isolate (CPI) – gum Arabic (GA) mixtures as a function of biopolymer mixing ratio at a total biopolymer concentation of 0.1% (w/w). Data represent the mean ± one standard deviation (n = 3).

Rheological behavior

The flow behavior of mixtures of CPI-GA under interacting (pH 4.20) and non-interacting (pH 7.00) conditions was measured as a function of shear rates (Figure 5.4). In both cases, pseudoplastic behavior was observed as is expected for a biopolymer solution. The apparent viscosity at pH 7.00 was found to decrease from ~0.05 to 0.00 Pa·s as shear rates increased from 1 to 100 s^{-1}, having a flow behavior index and consistency coefficient of 0.57 and 33.77 $Pa \cdot s^n$, respectively (R^2 = 0.999) (Figure 5.4A). In contrast, under interacting conditions the coacervate phase was substantially higher, also having its apparent viscosity decrease from ~4534.67 to 19.69 Pa·s over the same shear rate range, having a flow behavior index and consistency coefficient of 0.28 and 676.08 $Pa \cdot s^n$, respectively (R^2= 0.944) (Figure 5.4B). The higher viscosity of the coacervate phase (at pH 4.20) is hypothesized to be induced by electrostatic attractive interactions between CPI and GA chains, and as a result the formation of a loosely packed coacervate structure (with entrapped solvent). Upon reversing the shear rate (100-0.1 s^{-1}) no hysteresis effects were observed under non-interacting conditions (at pH 7.00) with the exception of shear rates <1 s^{-1}. Hysteresis found at these low shear rates may be the result of loss of sensitivity of the rheometer. In contrast, hysteresis was evident between upwards and downwards flow curves under interacting conditions (at pH 4.20) over the entire shear rate range, except at rates >80 s^{-1} indicating that it was behaving as a thixotropic material (Figure 5.4B). Hysteresis found for the coacervate phase was thought to be associated with shear rate induced disruption of the coacervate structure, which then reforms once shearing rates decline overtime. de Kruif and co-workers (2004) reported shear-thinning phenomenon for a whey protein isolate (WPI)-GA coacervate phase under interacting (pH 4.0) and non-interacting (pH 7.0) conditions, respectively. Higher viscosity and greater shear thinning was evident for the coacervate phase relative to conditions where the WPI and GA were non-interacting, which the authors attributed to stronger electrostatic interactions occurring in the coacervate phase, similar to the present study.

The viscoelastic storage and loss moduli were also measured as a function of frequency under interacting conditions only (pH 4.20) (Figure 5.5). Oscillatory shear was not reported for solutions at pH 7.00 due to lack of instrument sensitivity to any structures present (data not shown). Data from pH 4.20 suggests some frequency dependence of the storage and loss moduli, and G′ was greater than G″ indicating the formation of elastic-like properties, possibly the result of a weakly interconnected coupled network. The complex viscosity was also decreased with

frequency, showing evidence of shear-thinning and weak gel properties within the coacervate phase. Similar phenomenon was observed within coacervate phases of bovine serum albumin-pectin (Ru et al., 2012), β-lactoglobulin-pectin (Wang et al., 2007), WPI-chitosan (Bastos et al., 2010) and fish gelatin-laponite (Karimi et al., 2013) mixtures.

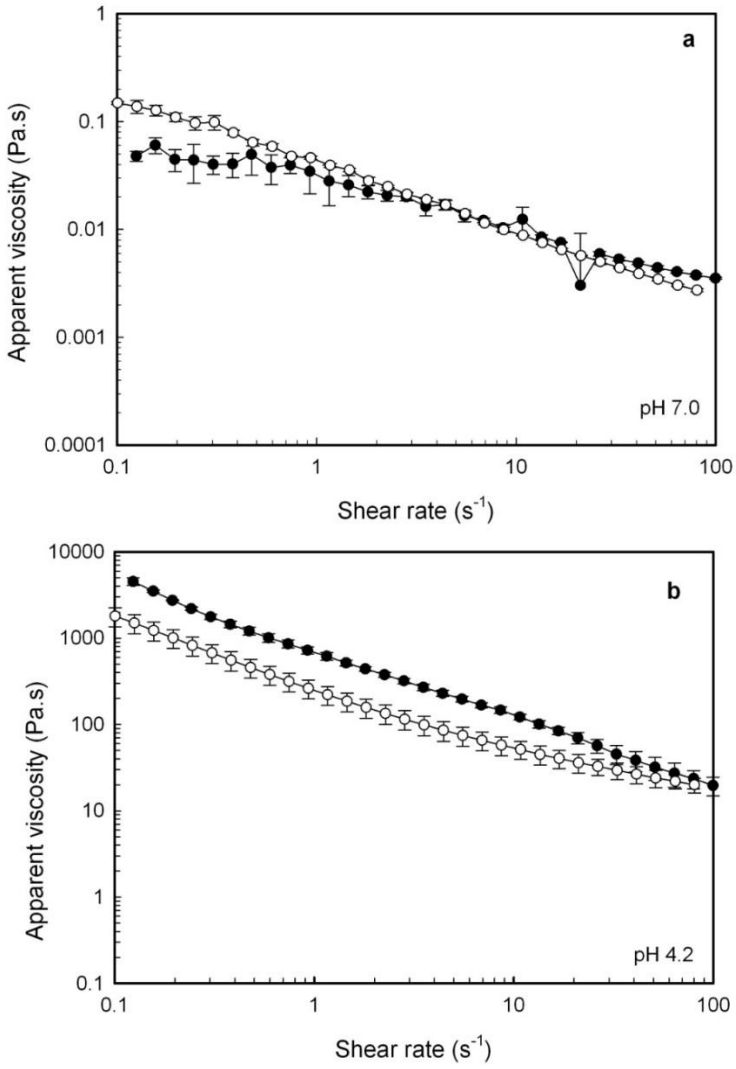

Figure 5.4 Flow curves for a canola protein isolate (CPI) – gum Arabic (GA) mixture at pH 7.00 (non-interacting conditions) (A) and at pH 4.20 (interacting conditions) (B) as a function of shear rate during an upwards (solids) and downwards (open) sweep. The total biopolymer concentration was 2.0% (w/w). Data represent the mean ± one standard deviation (n = 3).

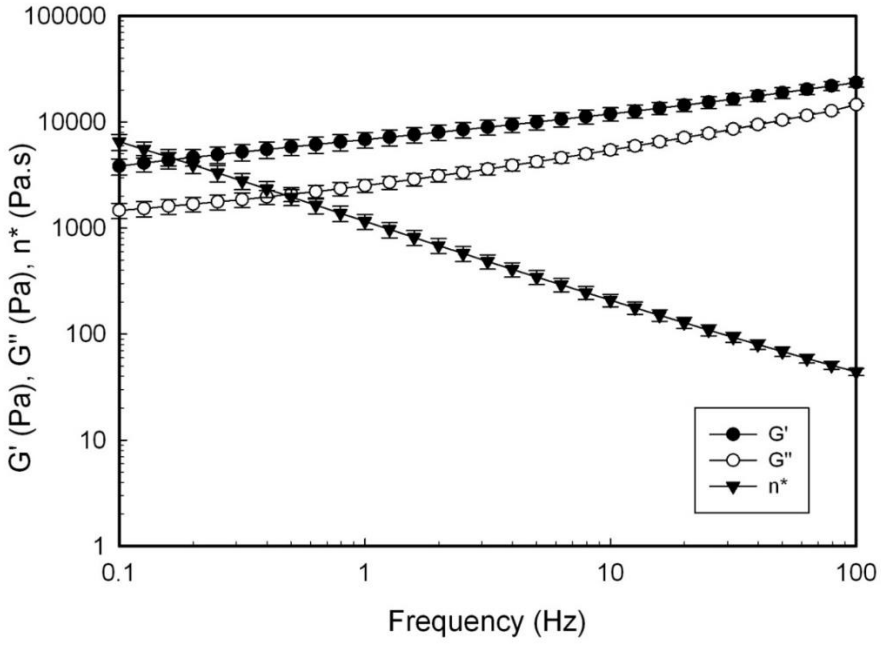

Figure 5.5 Dynamic storage (G′) and loss (G″) moduli, and complex viscosity (η^*) for a canola protein isolate (CPI) – gum Arabic (GA) solution (interacting conditions, pH 4.20, coacervate phase only) as a function of frequency. The total biopolymer concentation was 2.0% (w/w). Data represent the mean ± one standard deviation (n = 3).

Functional properties

Solubility of CPI-GA mixtures and individual CPI solutions was investigated as a function of pH (Figure 5.6). In the range of pH 5.00 to 8.00, solubility of CPI alone was found to be quite high (~85-95%), whereas at pH 4.00 solubility sharply decreased to ~55% which was hypothesized to be due to the presence of protein-protein aggregates (Figure 5.6). Further acidification (pH < 4.00) was presumed to lead to a disruption of these aggregates and a rise in the solubility curve to 90%. Similarly to CPI alone, solubility of CPI-GA mixture remained high (90%) within pHs 5.00-8.00 (non-interacting pHs), yet the minimum of the U-shaped solubility profile shifted from pH 4.00 to pH 3.00, and had reduced solubility at the minimum relative to the CPI alone (Figure 5.6). At pH <3.00 solubility of the CPI-GA mixture sharply increased to ~90% (non-interacting conditions, pH<$pH_{\phi 2}$, Figure 5.1B). Liu et al. (2010b) and Ortiz et al. (2004) reported a broadening of the typical U-shaped solubility curve towards acidic pHs in mixed systems of soy protein

isolate-carrageenan and pea protein isolate-gum Arabic. In most instances, complexation leads to a decrease in protein solubility as was the case for whey proteins-carboxymethocellulose (Hansen et al., 1971), potato protein isolate-carboxymethocellulose (Vikelouda and Kiosseoglou et al., 2004) and canola protein isolate – carrageenan (Stone et al., 2013). In the case of the latter, differences in complex solubility was observed depending on the carrageenan-type (i.e., κ, ι and λ) present associated with different levels of biopolymer interactions. The linear charge density on the carrageenan is influenced by the number of charged groups present (i.e., κ, ι and λ-types have 1, 2 and 3 sulphate groups per disaccharide unit), as well as their conformation (i.e., κ and ι form double helices, whereas λ remains as a random coil), and therefore impacts how strongly it bonds to the canola proteins. The more strongly bound complexes (canola protein-λ-carrageenan) led to greater precipitation and solubility loss (Stone et al., 2013). However, cases have been reported where enhanced solubility occurred, such as for soy protein – xanthan gum (Xie and Hettiarachchy, 1997) indicating that is highly system dependent.

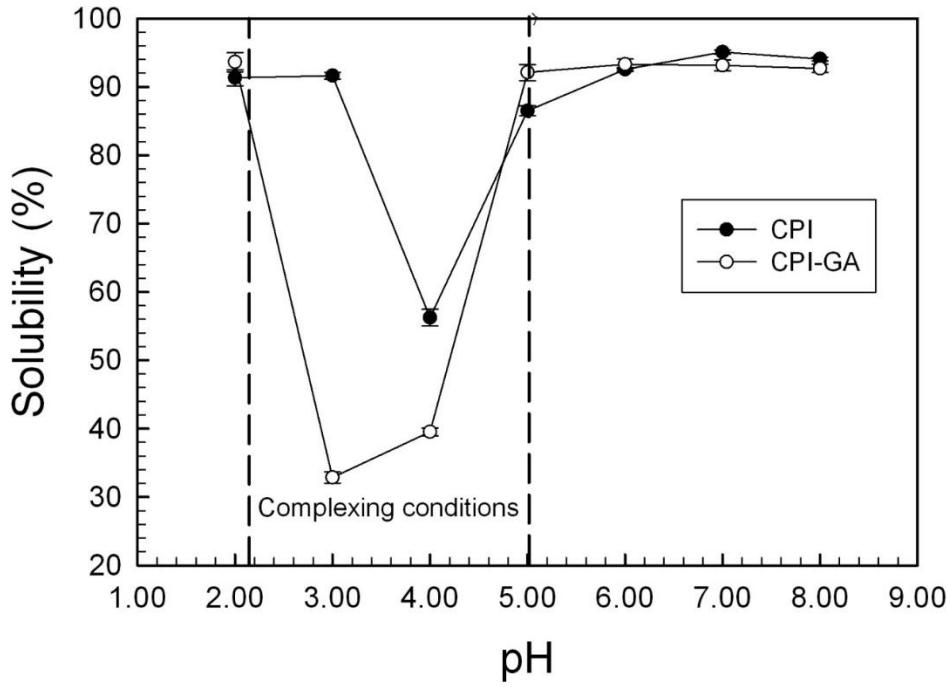

Figure 5.6 Solubility pH-profile for individual canola protein isolate (CPI) solutions, and a 1:1 CPI-gum Arabic mixture. The total biopolymer concentration was 1.0% (w/w). Data represent the mean ± one standard deviation (n = 3).

During foam and emulsion formation, proteins or protein-polysaccharide complexes migrate to the interface, re-orient so that the hydrophobic groups are positioned towards the non-polar phase and the hydrophilic groups are positioned towards the polar phase, and then precipitate to form a viscoelastic film surrounding a gas bubble or oil droplet. Foam capacity reflects the amount of foam per amount of protein (or complex) that can be generated upon homogenization, whereas foam stability relates to the degree of foam breakdown over an arbitrarily defined time. In the current study, the presence of GA led to a decrease in foam capacity from ~160 to ~115% relative to CPI alone ($p<0.01$), yet had no significant impact on foam stability which remained constant at ~80%. In the case of GA alone, no foaming occurred under the concentrations used in this study (Table 5.1). The loss in foaming capacity may be the result of reduced solubility at pH 4.20 in the mixed system (~40%) compared to CPI alone (~55%). Furthermore, the presence of GA may interfere with CPI ability to integrate fully into the interface, partially inhibiting its formation capacity. Stone et al. (2013) also reported a decline in foam capacity for CPI with carrageenan polysaccharides (κ-, ι-, and λ-type), without a change in foam stability. Foam stability remained unchanged in the present study, most likely because of the electrostatic CPI-GA complexes remain within the continuous phase raising its viscosity. Ganzevles et al. (2006) proposed various mechanisms relating to protein-polysaccharide interactions at the interface, to include: a) the absorption of free protein only to the air-water interface; b) competitive or mixed absorption between proteins and protein-polysaccharide complexes, caused by differences in diffusion rates from the bulk to the interface; and c) partial dissociation of bound proteins within the complexes, allowing the disassociated proteins to adsorb to the interface. In the present study, the reduced foam formation is the result of competitive absorption of free proteins and protein-polysaccharide complexes. However, as complexes interact with the interface, they might then partial dissociate and release proteins. The foams in the mixed system would then be stabilized by both free and released proteins, to give the same stability as that of CPI alone. Others such as Makri and Doxatakis (2007) and Liu et al. (2010b) reported an increase in foam stability in mixed systems of bean protein isolates and gums from Arabica, locust bean and xanthan, and that of pea protein isolate – gum Arabic under complexing conditions, respectively. The authors attributed the rise in stability to increased bulk phase viscosity and in the creation of weak gel that inhibited coalescence.

Table 5.1 Foaming and emulsifying properties of CPI, GA and CPI-GA solutions at pH 4.20. Data represent the mean ± one standard deviation (n = 3). Signifcant differences within each test are denoted by different superscripts ($p<0.05$).

Material	FC (%)	FS (%)	ES (%)	EC (%)
CPI-GA	115.56 ± 7.70^{a}	83.04 ± 3.22^{a}	75.33 ± 1.15^{a}	61.58 ± 1.05^{a}
CPI	161.11 ± 1.92^{b}	79.99 ± 1.42^{a}	76.00 ± 0.00^{a}	63.34 ± 0.95^{a}
GA	NF	NF	22.00 ± 2.00^{b}	-

Note: Canola protein isolates (CPI); gum Arabic (GA); foaming stability (FS) and capacity (FC); emulsion stability (ES) and capacity (EC); no foam (NF); not measured (-).

The emulsifying properties of a protein and/or protein-polysaccharide complex depends how strongly they adsorb the oil-water interface and resist creaming. Emulsion stability refers to the ability of an emulsion to resist gravitational phase separation through first droplet coalescence followed by creaming. In contrast, emulsification capacity refers to the amount of oil (g) of defined amount of protein (g) can support within an oil-water emulsion prior to undergoing phase inversion into a water-oil emulsion. In the present study both emulsion stability and capacity were found to be similar with the addition of GA to the CPI, and the CPI alone system, being constant at 76 and 62%, respectively ($p>0.05$) (Table 5.1). In the case of GA alone, low emulsifying properties (emulsion stability ~ 22%) were revealed under the conditions examined (Table 5.1). Stone et al. (2013) reported that the emulsion capacity and stability values for canola protein-carrageenan complexes were reduced and enhanced, respectively depending on the type of carrageenan present. And Furthermore, Liu et al. (2010b) reported that for pea protein-gum Arabic mixtures improved emulsion stability values at pH conditions were complexation is occurring. The authors suggested the rise in stability may be due to electrostatic repulsion, steric stabilization and a thicker viscoelastic film surrounding the droplets. Li et al. (2012) reported for bovine serum albumin-pectin mixtures both enhanced and reduced emulsion stability depending on the pH and level of biopolymer interactions. Under conditions, where biopolymers were non-interacting, emulsion stability values remained similar between the complexes and the proteins due to a depletion flocculation process. In the present study, it suggests that the oil-water interface is being stabilized by either free proteins within the mixed system, or released proteins after partial dissociation of

the complex structure near the oil-water interface. If the complex was truly adsorbed to the oil-water interface we would likely observe an increase in the emulsion stability due to aforementioned reasons described by Liu et al. (2010b), or would see a decrease of bridging flocculation.

5.5 SUMMARY

The complex coacervation between CPI and GA was strongly affected by biopolymer mixing ratio and pH highlighting the importance of electrostatic interactions, most likely between small CPI-CPI aggregates and GA chains. Maximum CPI-GA interactions were found to occur at a mixing ratio of 2:1 and at a pH of 4.20. Flow behavior of the coacervate phase indicated pseudoplastic flow and elastic-like properties indicative of a weakly interconnected electrostatic network. Complexation also reduced the solubility of CPI in the presence of GA and shifted the minimum from pH 4.00 to 3.00. Complexation also showed a negative effect on foaming capacity, whereas foam stability, and emulsion capacity and stability were similar to CPI alone at pH 4.20. For food applications, mixing CPI and GA under interacting conditions would have the greatest impact on products where thickening, pouring and suspension attributes were needed (e.g., salad dressings, sauces).

-Chapter 6-

Formation and functionality of soluble and insoluble electrostatic complexes within mixtures of canola protein isolate and (κ-, ι- and λ-type) carrageenan[2]

Andrea K. Stone, Lamlam Cheung, Chang Chang and Michael T. Nickerson

Department of Food and Bioproduct Sciences, University of Saskatchewan,
51 Campus Drive, Saskatoon SK, Canada S7N 5A8

[2]Food Research International, 54, 195-202 (2013)

6.1 ABSTRACT

The formation of electrostatic complexes between a canola protein isolate (CPI) and (κ-, ι-, and λ-type) carrageenan (CG) was investigated as a function of pH (1.50-7.50) and biopolymer weight mixing ratio (1:1 – 75:1, CPI-CG) by turbidimetric measurements during an acid titration. The addition of CG to CPI suppressed CPI-CPI aggregation. Critical pHs designating structure forming events (pH_c, $pH_{\phi 1}$ – soluble and insoluble complexes, respectively) shifted to more acidic pHs as the mixing ratio increased then plateaued at the 15-20:1 ratio. The functional properties (solubility, foaming capacity/stability, emulsion capacity, emulsion stability) of the complexes (20:1, CPI-CG) at pH_c (6.75) and $pH_{\phi 1}$ (5.00), were compared to CPI alone. At both pHs, solubility, foaming capacity and emulsion capacity of CPI was reduced upon complexation with CG. Emulsion stability of the complexes was high at ~87-96% depending on pH and CG type. Differences in functionality based on CG type was related to the structure and charge of the CG molecules. The pH of net neutrality was reduced from pH 5.78 for CPI alone to pH 5.35 for CPI-κ-CG and pH 4.95 for both CPI-κ- and ι-CG.

6.2 INTRODUCTION

Protein and polysaccharides are widely used by the food industry for their functionality and ability to control food structure (Tolstoguzov, 2002; Ye, 2008; Schmitt and Turgeon, 2011). Their interactions can also be carefully tailored for protein separation/purification purposes (Xu et al., 2011) or in the design of biopolymer adhesives, edible films (Schmitt et al., 1998) and controlled delivery applications (Schmitt and Turgeon, 2011). A better understanding of biopolymer interactions and factors/conditions leading to their phase behaviour could increase their usefulness for tailoring food structure or in the development of more high value applications (e.g., capsules, films, etc.).

Mixtures of proteins and polysaccharides generally exhibit either segregative or associative phase behaviour due to the electrostatic forces arising between the two (Schmitt et al., 1998; Tolstoguzov, 2002; Ye, 2008). Segregative phase behaviour is the result of electrostatic repulsive forces between similarly charged biopolymers, leading to separation into both a protein-rich and polysaccharide-rich phase (Tolstoguzov, 1991; Schmitt et al., 1998; Boral and Bohidar, 2010; Schmitt and Turgeon, 2011). In contrast, associative phase behaviour (also known as complex coacervation) occurs with biopolymers of opposing net charges through primarily electrostatic

attractive forces, with secondary stabilization by hydrogen bonding (Liu et al., 2010a). Complex coacervation leads to both a biopolymer-rich and solvent rich phase (Tolstoguzov, 1991; Schmitt et al., 1998; Boral and Bohidar, 2010; Schmitt and Turgeon, 2011). The biopolymer-rich phase consists of soluble and insoluble complexes that re-orient into either a coacervate or precipitate-type morphology depending on the strength of the polyelectrolytes present. Coacervates are comprised of complexed biopolymers, typically involving a strong (e.g., protein) and weakly (e.g., gum Arabic) charged polyelectrolyte, which entrap small amounts of solvent to remain quite mobile (Klassen et al., 2011). In contrast, complexes that precipitate typically involve mixtures with both strongly charged proteins and polysaccharides, such as carrageenan, alginate, chitosan and pectin, andv tend to form over a much narrower pH range before precipitating out of solution. Complexation in either case is driven by a loss in entropy associated with conformational freedom and solvent mixing, which offsets the enthalpic contribution from the release of counterions and water (Liu et al., 2009; Boral and Bohidar, 2010).

Due to the electrostatic nature of complexation, biopolymer interactions are strongly influenced by solvent properties, such as pH, temperature and ionic strength; biopolymer characteristics, such as molecular weight, charge density, distribution/type of reactive sites, conformation, and hydration; and mixing conditions, such as biopolymer mixing ratio and level and duration of shear processing (Semenova et al., 1991; Schmitt et al., 1998; Ye, 2008). Typically, researchers study associative phase behaviour during a turbidimetric pH-titration, in which multiple pH-induced structure forming events can be observed. For instance, in mixtures of proteins and an anionic polysaccharide at solvent pH higher than the protein's isoelectric point (pI), the system is co-soluble (under dilute biopolymer conditions). However, as pH is lowered below the pI, the protein takes on a positive net charge and begins to experience electrostatic attraction with the negatively charged polysaccharide. Initial interactions, first experimentally detected by an inflection point in the turbidity-pH profile signify the formation of soluble complexes (denoted by the critical pH, pH_c). As the solution is acidified further, a dramatic rise in turbidity occurs corresponding to macroscopic phase separation and the formation of insoluble complexes (denoted by the critical pH, $pH_{\phi 1}$) (Xia and Dubin, 1994; Weinbreck et al., 2004; Liu et al., 2009). Complexation becomes greatest once biopolymers reach an electrical equivalence point to become electrically neutral (denoted by maximum turbidity vs. pH at pH_{opt}) (Liu et al., 2009). Complex formation then becomes weaker at $pH<pH_{opt}$ until complete dissolution occurs

(denoted by the critical pH, $pH_{\phi 2}$), where the reactive sites on the polysaccharide become protonated. If complexation leads to precipitate formation, only pH_c and $pH_{\phi 1}$ may be determined, and structures begin to follow out of solution near pH_{opt} creating scattering in the O.D. vs. pH data at lower pHs. In some cases involving two highly charged biopolymers, initial interactions can occur at pH>pI where they have similar net charges thought to be due to surface patch binding or interactions between negatively charged polysaccharides and positively charged patches on the protein's surface (Gupta et al., 2007; Boral and Bohidar, 2010).

CPI is typically extracted from canola meal, which is a protein-rich (≤ 50%, dry basis) by-product of canola oil extraction that is most commonly used for animal feed (Uruakpa and Arntfield, 2005; Wu and Muir, 2008; Aider and Barbana, 2011). However because of canola protein's well balanced amino acid profile and functionality, it is increasingly being investigated for its potential as a new food ingredient (Aider and Barbana, 2011). Canola proteins consist of two major storage proteins, cruciferin and napin. Cruciferin, is a 12 S hexameric globulin protein (~300 kDa) containing 6 subunits (~50 kDa), with each comprising of two polypeptide chains (α-chain, 30 kDa; β-chain 20 kDa) joined by a disulphide bond (Lampart-Szczapa, 2001; Aider and Barbana, 2011). In contrast, napin is a 2 S albumin with a low molecular weight (12-14.5 kDa) and two polypeptide chains (4.5 and 10 kDa) linked primarily by disulphide bonds (Monsalve and Rodriguez, 1990; Berot et al., 2005).

Carrageenan is an anionic linear sulfated polysaccharide derived from red algae (*Rhodophyceae*) and is commonly used in the food industry for gelling and thickening applications (Clark and Ross-Murphy, 1987). Structurally it is comprised of partially sulphated repeating (1-3) linked β-D-galactose and (1-4) linked 3,6-anhydro-α-D-galactose residues (Clark and Ross-Murphy, 1987). The three main classes of CG, κ-, ι-, and λ-type, are based on the number of sulphate groups (1, 2 and 3, respectively) per repeat unit. Kappa and ι-CG exist as random coils at sufficiently high temperatures and undergo a disordered-ordered transition when the temperature is reduced resulting in a double helical structure (Morris et al., 1980). Side-by-side aggregation of the helices, and subsequent gelation, occurs in the presence of gel-promoting salts (Morris et al., 1980). Kappa- and ι-CG are known to have different salt sensitivities in respect to gelation, κ-CG is K^+ sensitive with an intramolecular bridge forming between K^+ and the sulphate group of D-galactose and the K^+ and the anhydro-O-3,6 ring of the second D-galactose unit, through an ionic bond and electrostatic association, respectively (te Nijenhuis, 1997). Calcium promotes gelation

more than other cations in ι-CG. This specificity involves intramolecular bridging between the two sulphate groups of the same repeat unit through ionic forces with Ca^{2+} and intermolecular bridging between sulphate groups of different residues through ionic and electrostatic forces with Ca^{2+} (te Nijenhuis, 1997). It was believed that λ-CG does not have gelation abilities but forms only viscous solutions due to its high linear charge density and lack of an ordered conformation (te Nijenhuis, 1997; Weinbreck et al., 2004; Piculell, 2006).

Complexation studies involving plant proteins and polysaccharides are limited compared to those systems involving animal-derived proteins in the literature. In addition, although there are a few studies relating the functionality of mixed complexed biopolymer systems (Gu et al., 2005; Liu et al., 2010b; Schmidt et al., 2010; Stone and Nickerson, 2012), very few studies compare both soluble and insoluble complex functionality. Klassen et al. (2011) investigated complex formation involving CPI with alginate and ι-CG under various pH and mixing ratio conditions, and also studied the impact of complexation on protein solubility as a function of pH. In both mixtures, complexation leads to the formation of precipitate-type structures, with only the CPI-alginate mixture experiencing improved solubility near CPI's pI. The present study focuses on understanding the effects of pH and biopolymer mixing conditions on the formation of soluble and insoluble electrostatic complexes involving a canola protein isolate and (κ-, ι-, and λ-type) carrageenan (CG); as well as the resulting functional attributes of the formed complexes relative to CPI alone.

6.3 MATERIALS AND METHODS

Materials

Canola seeds (SP Desirable *Brassica napus*, Lot#: 168-8-129810) were kindly provided by Viterra (Saskatoon, SK, Canada), whereas κ-, ι - and λ-type CG were purchased from Sigma-Aldrich Canada Ltd. (Oakville, ON, Canada). Canola protein isolate was prepared according to the defatting protocol and salt extraction method of Folawiyo and Apenten (1996) as previously described (Klassen et al., 2011). Chemical analyses of the materials found CPI to be comprised of 95% protein (N x 5.70), 0.70 % moisture, 0.32 % lipid, 2.32 % ash and 1.71 % carbohydrate as determined by Association of Official Analytical Chemists (AOAC, 2003) methods; 925.10 (moisture), 923.03 (ash), 920.87 (crude protein), and 920.85 (lipid). Carbohydrate content was determined on the basis of present differential from 100%. In the case of CG, the κ-type was

comprised of 66.50% carbohydrate, 10.65% moisture and 22.86% ash (including: 2.4% Ca^{2+}, 0.16% Mg^{2+}, 5.4% K^{+} and 0.49% Na^{+}); ι-type was comprised of 64.40% carbohydrate, 10.82% moisture and 24.97% ash (including: 3.4% Ca^{2+}, 0.18% Mg^{2+}, 3.2% K^{+} and 1.2% Na^{+}); and the λ-type comprised of 63.79% carbohydrate, 12.26% moisture and 23.95% ash (including: 3.0% Ca^{2+}, 0.83% Mg^{2+}, 2.4% K^{+} and 1.3% Na^{+}). In all cases, protein and lipid contents was considered to be negligible. All chemicals used in this study were of reagent grade and purchased from Sigma-Aldrich (Oakville, ON, Canada).

Turbidimetric pH-acid titrations

Critical pH values (pH_c and $pH_{\phi 1}$) associated with the formation of soluble and insoluble complexes within CPI-CG mixtures was investigated by turbidimetric pH acid titrations as a function of pH (7.50-1.50) and biopolymer mixing ratio (1:1-35:1; CPI:CG) at a constant biopolymer concentration of 0.05% (w/w). CPI and CG solutions were prepared by dissolving each powder in Milli-Q water at pre-determined mixing ratios and stirring for 2 h at room temperature (~21-23ºC) before adjusting solutions to pH 8.00 using 0.5 M NaOH. Solutions were then allowed to stir overnight at 4°C to help facilitate solubility. Optical density measurements were made at room temperature over a pH range (7.50 to 1.50) using a UV/Vis spectrophotometer (Thermo Scientific, Waltham, MA) at 600 nm using plastic cuvettes (1 cm path length). The pH of the solutions was lowered by drop wise addition of HCl using a gradient of HCl concentrations (0.05 M > pH 6.00; 0.1 M > pH 3.50; 0.5 M > pH 3.00; 1 M > pH 2.50 and 2 M > pH 1.50) to reduce dilution effects associated with the titration (i.e., < 3 mL of HCl was added to 100 g of solution upon completion of the titration). Turbidity measurements were made on individual CPI and CG solutions (0.05% w/w) as controls. Critical pH values associated with structure forming events were determined graphically on individual turbidity curves as described by Weinbreck et al. (2003) and Liu et al. (2009). All measurements were made in triplicate.

Electrophoretic mobility

Electrophoretic mobility (U_E) (i.e., velocity of a particle within an electric field) for individual and mixed CPI-CG (20:1 CPI-CG mixing ratio) solutions (0.05% w/w - total biopolymer concentration) was measured as a function of pH (7.00-2.00) using a Zetasizer Nano-ZS90 (Malvern Instruments, Westborough, MA). Samples were prepared and acidified as

previously described in Section 2.2. Measurements were made every one pH increment and were performed in duplicate. Electrophoretic mobility was used to calculate the zeta potential (estimate of surface charge on biopolymer, ζ) using the Henry equation:

$$U_E = \frac{2\varepsilon \times \zeta \times f(\kappa\alpha)}{3\eta} \qquad \text{(eq. 6.1)}$$

where η is the dispersion viscosity, ε is the permittivity, and *f*(κα) is a function related to the ratio of particle radius (α) and the Debye length (κ). Using the Smoluchowski approximation *f*(κα) equalled 1.5.

Functional properties of electrostatic complexes

Functional properties of CPI-CG mixtures (20:1 CPI-CG mixing ratio) were determined at a 1% (w/w) total biopolymer concentration at pHs 6.75 and 5.00 corresponding to where soluble and insoluble complexes exist, respectively (described in section 6.4-Results and Discussion and Figure 6.3). Individual CPI solutions were also tested at corresponding pHs and concentrations as the mixed systems. Unless otherwise stated, samples were prepared in a similar manner as described previously. All measurements were performed in triplicate.

Protein solubility

The solubility of CPI-(κ-, ι- and λ-type)-CG complexes and individual CPI solutions were determined by a modified method of Morr et al. (1985) at pH 6.75 and 5.00. CPI and CG powders were dissolved in 0.1 N NaCl. Solutions were allowed to stir (500 rpm) for 1 h at the desired pH to facilitate the formation of complexes, then centrifuged (Sorvall® SS-1 Superspeed Angle Centrifuge, DJB Labcare Ltd., England) at 1,000 x *g* for 10 min at room temperature. Protein content of the supernatant was determined by micro-Kjeldahl (%N x 5.7) analysis. Percent protein solubility was determined by dividing the protein content of the supernatant by the total sample protein content.

Foaming capacity and stability

Foaming capacity (FC) and stability (FS) were determined according to modified methods of Liu et al. (2010b). In a 400 mL beaker (inner diameter = 69 mm; height = 127 mm; as measured by a digital caliper) 15 mL (V_{li}, initial volume of liquid used to make foam) of biopolymer solution

at the required pH was foamed at 8,000 rpm using an Omni Macro homogenizer (Omni International Inc., Marietta, GA) equipped with a 20 mm diameter saw tooth generating probe (positioned slightly below the air-water interface) for 5 min. Immediately following homogenization, the foam was transferred to a 100 mL graduated cylinder (inner diameter = 26 mm; height = 25 cm). Foam capacity and FS were determined using eqs. 5.2 and 5.3, respectively, where V_{fi} is the volume of foam immediately after homogenization and V_{ft} is the volume of foam remaining after time. Foaming stability was determined after 30 min.

$$\%FC = \frac{V_{fi}}{V_{li}} x\, 100\% \qquad \text{(eq. 6.2)}$$

$$\%FS = \frac{V_{ft}}{V_{fi}}\, x\, 100\% \qquad \text{(eq. 6.3)}$$

Emulsion stability

Emulsion stability (ES) was determined for 50/50 (5 mL canola oil/ 5 mL biopolymer solution (V_B)) oil-in-water emulsion (Stone and Nickerson, 2012). Emulsions were prepared in 50 mL screw capped plastic centrifuge tubes and were homogenized for 5 min at 8000 rpm with the Omni Macro homogenizer equipped with a saw tooth generating probe, positioned at the oil-water interface. Emulsions were then transferred to 10 mL graduated cylinder (inner diameter = 10.80 mm; height = 100.24 mm; as measured by a digital caliper) and allowed to separate for 30 min. Emulsion stability was determined using eq. 4 where V_A is the volume of the aqueous layer after 30 min of drainage.

$$\%ES = \frac{V_B - V_A}{V_B}\, x\ 100\% \qquad \text{(eq. 6.4)}$$

Emulsion capacity

Two grams of biopolymer solution along with canola oil (3-5 g) were added to 50 mL centrifuge tubes to obtain a series of emulsions with varying amounts of oil. Immediately after homogenization of each emulsion (5 min, 8,000 rpm, Omni Macro Homogenizer equipped with a saw tooth generating probe), conductivity was measured using an Orion 3-star conductivity meter with a 4-electrode conductivity cell (Thermo Scientific, Waltham, MA, USA). Emulsion capacity

(EC) was determined at the inversion point when an oil-in-water emulsion changed to a water-in-oil emulsion as indicated by a large drop in emulsion conductivity. Emulsion capacity was expressed as g oil emulsified per g protein as the average oil amount before and after the inversion.

Statistics

A one-way analysis of variance (ANOVA) with a Scheffe post-hoc test was used to measure statistical differences within state diagrams for each critical pH value as a function of biopolymer mixing ratio and to measure statistical differences within soluble complexes and insoluble complexes functionality. All statistical analyses were performed using Systat software (SPSS Inc., Ver. 10, 2000, Chicago, IL).

6.4 RESULTS AND DISCUSSION

Effect of pH and mixing ratio on the formation of electrostatic complexes

Optical density (OD) for individual solutions of canola protein isolate (Figure 6.1) and (κ-, ι- and λ-type) CG (not shown) was investigated during a pH acid titration between pH 7.00 and 1.50. The turbidity profile for CPI followed a bell-shaped profile with a rapid rise in OD initiating at pH 7.00, until reaching a maximum (near OD 0.970) at pH 5.60, and then declining in magnitude to pH 3.50 below which minimal OD was observed (Figure 6.1). Klassen et al. (2011) found a similar bell shaped profile for salt extracted CPI. The rise in OD is thought to be associated with CPI-CPI aggregation which is strongest near the protein's pI where electrostatic charge repulsion is reduced significantly between neighbouring molecules. As the OD of the CPI solution increases it is thought that the size and number of CPI-CPI aggregates are increasing. No OD was observed for the carrageenan materials over the pH range 7.00 – 1.50 (data not shown).

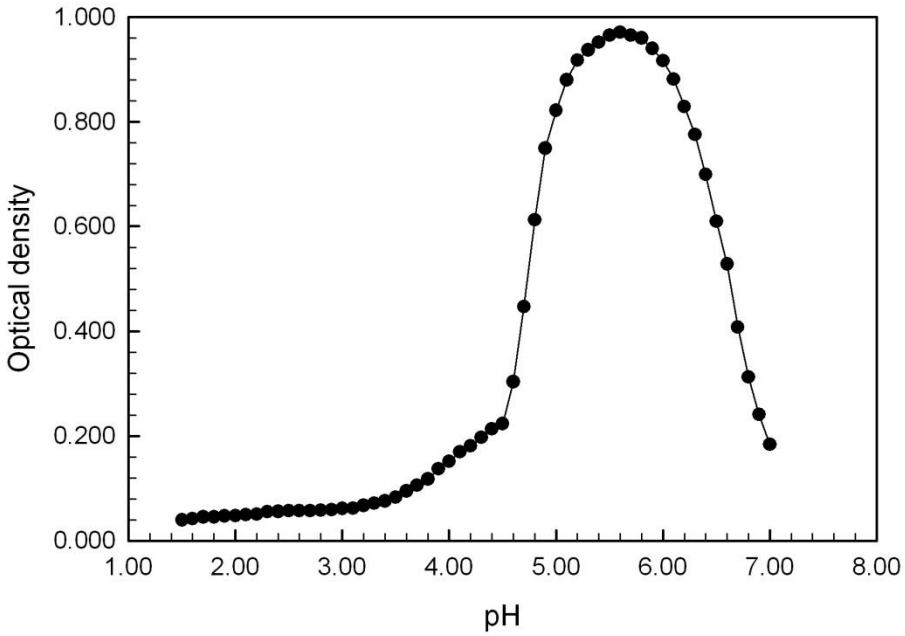

Figure 6.1 Mean turbidity curve for an individual homogenous CPI solution as a function of pH (n = 3).

In the mixed CPI-CG system the addition of CG (regardless of CG-type) resulted in significant suppression of CPI-CPI aggregation relative to the individual CPI system as seen by substantially reduced OD in the mixed systems and a shift in initial OD rise during the acid titration towards more acidic pHs (Figure 6.2). Both of these trends were less pronounced as the concentration of CG was decreased, i.e. as mixing ratio increased. For the 1:1 CPI-(κ-, ι- and λ-type) CG system, OD data as a function of pH was relatively flat, with maximum OD occurring at < 0.150 indicating very little CPI-CPI aggregation was occurring (Figure 6.2). Suppression of CPI-CPI aggregation was thought to be associated with the presence of strong electrostatic forces arising from sulphate groups along the CG backbone of free molecules in solution.

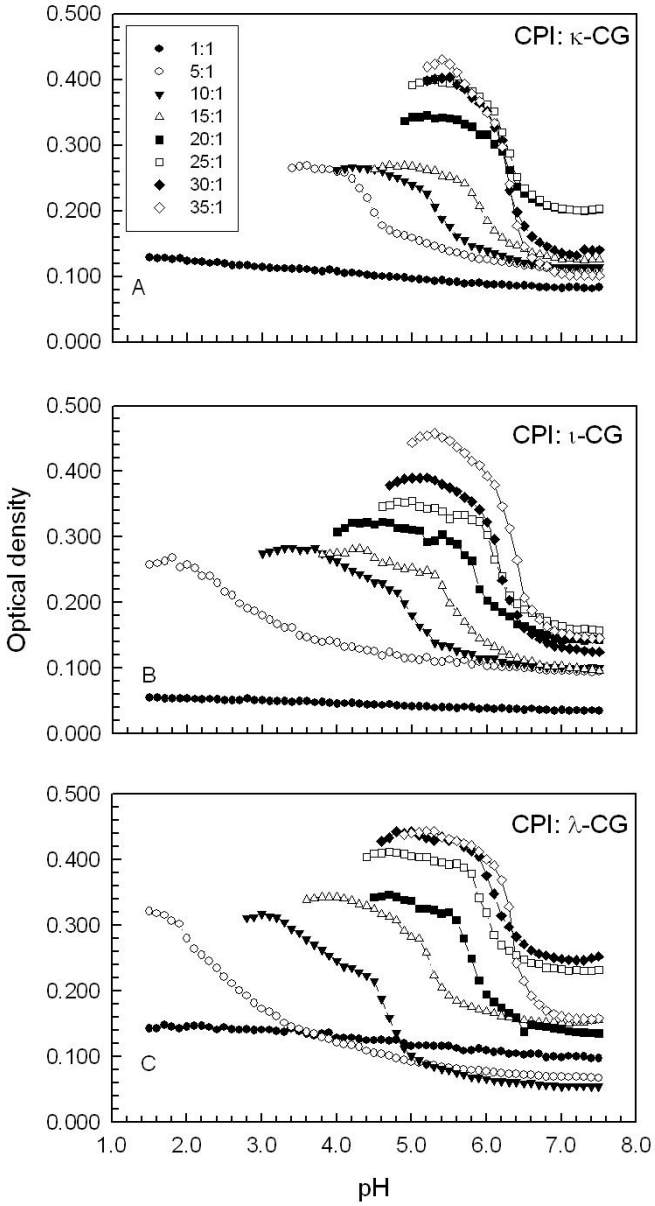

Figure 6.2 Mean turbidity curves for CPI-κ-GG (A), CPI-ι-CG (B), and CPI-λ-CG (C) mixtures as a function of pH and biopolymer mixing ratios (n = 3).

At higher mixing ratios, critical pH's associated with the formation of soluble and insoluble complexes were found to occur at pHs all above the pI of CPI, where both biopolymers carried a net negative charge (Figures 6.2 and 6.3). In all cases, complex formation led to the formation of precipitate-type structures, which began to fall out of solution soon after the maximum OD was

reached (Note; data corresponding to pHs where precipitation occurred was removed from Figure 6.2). In contrast to a coacervate morphology, precipitates are more compact, entrap less solvent and tend to be irreversible. This initial electrostatic attraction (denoted by pH_c) between the two biopolymers at pH > pI is presumed to be associated with the interaction of CG molecules with positively charged patches distributed on the protein's surface (Dickinson, 1998; de Vries et al., 2003; Weinbreck et al., 2004). This has previously been reported in several systems including whey protein isolate (WPI)-CG (Weinbreck et al., 2004; Stone and Nickerson, 2011) and, CPI-alginate and CPI-ι-CG (Klassen et al., 2011).

For all mixed systems (with the exception of the 1:1 mixing ratio), pH_c and $pH_{\phi 1}$ shifted to higher pHs as the mixing ratio increased (i.e., less CG is present at higher ratios), until nearing a plateau at a 20:1 CPI-CG ratio, with the exception of pH_c for κ-CG which plateaued at the 15:1 ratio (Figure 6.3). The mixing ratio dependence suggests the presence of CPI-CPI aggregates participating with complex formation, where it was hypothesized that aggregates increased in size as the mixing ratio increased up to a critical point (corresponding to the plateau region of the curve). Similar findings were reported for mixtures of pea protein isolate -gum Arabic (Liu et al., 2009), pea protein-alginate (Klemmer et al., 2012), gelatin-agar (Singh et al., 2007) and CPI-alginate/ι-CG (Klassen et al., 2011). Weinbreck et al. (2004) and Girard et al. (2004) investigated complexation within WPI-CG and β-lactoglobulin-pectin mixtures, respectively, using protein solutions where aggregates were pre-filtered prior to complexation. Both authors reported the absence of mixing ratio dependence of pH_c, where they hypothesized that complexation involved individual proteins and polysaccharide molecules. In the case of $pH_{\phi 1}$, mixing ratio dependence was observed for both systems thought to be attributed to an increase in the number of proteins interacting with the same number of polysaccharide chains.

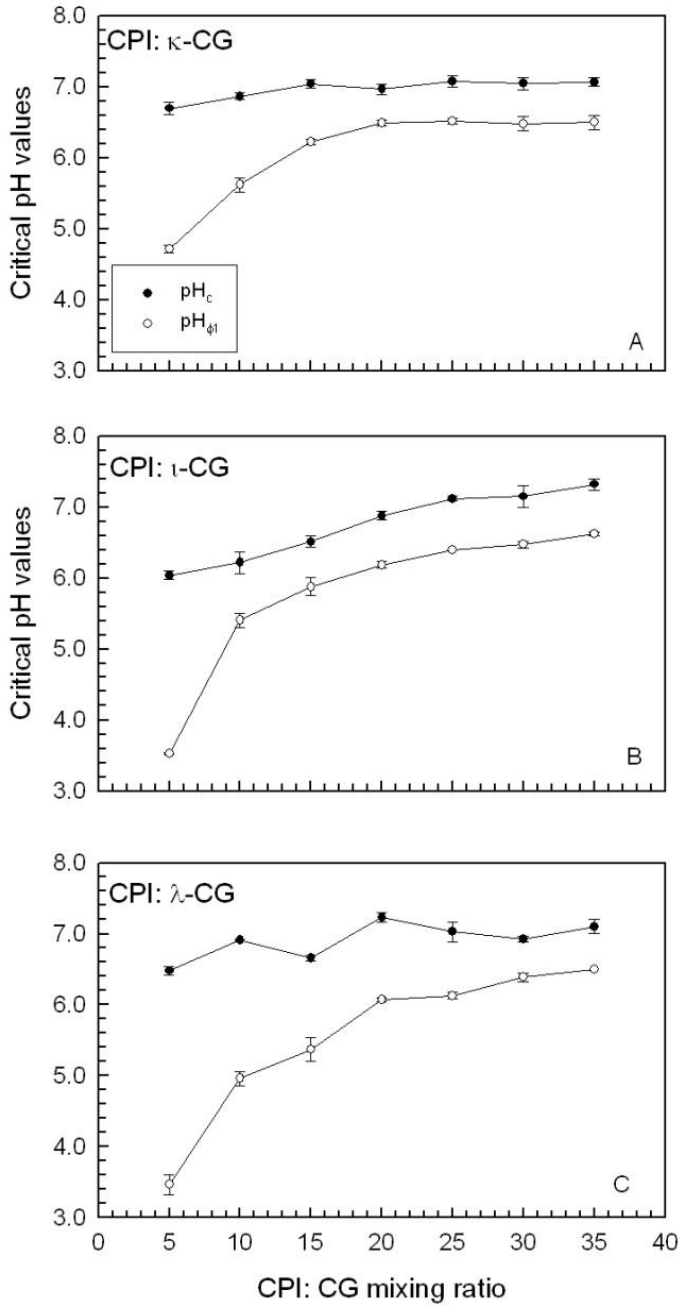

Figure 6.3 Critical pH values associated with the formation of soluble (pH_c) and insoluble ($pH_{\phi 1}$) complexes within admixtures of CPI-κ-GG (A), CPI-ι-CG (B), and CPI-λ-CG (C) mixtures as a function of biopolymer mixing ratios. Data represent the mean ± one standard deviation.

At the 20:1 CPI-CG mixing ratio, the size of complexes was presumed to be similar involving κ- and λ-type CG as the maximum OD was similar (OD ~0.350), whereas the maximum OD reading involving the ι-type CG was lower (~0.326) (Figure 6.2). Differences in the maximum OD readings as a function of CG-type are presumed to be associated structure of the various CG molecules in solution, and how this then impacts the formation of complexes. For instance, the number of sulphate groups available for complexation with CPI increases from 1, 2 and 3 per disaccharide repeat unit for κ-, ι- and λ-type CG, respectively; and the ordered conformation of CG differs at room temperature where both κ- and ι-types form double helical structures whereas λ-type remains in a random coil. CG conformation will impact chain flexibility and the amount of exposed reactive sites available for complexation with CPI. Stone and Nickerson (2011) reported that within WPI-(κ-, ι- and λ-type) CG mixtures, the ι-type had the greatest effect on inhibiting complex formation, where maximum complexation was found to occur at a 20:1 WPI-CG mixing ratio versus a 12:1 ratio for the κ- and λ-CG types. The authors hypothesized that although λ-CG has a greater number of sulfate groups per repeat unit than ι-type, its ability to inhibit CPI-CPI aggregation was less since λ-CG remained in a random coil conformation (rather than double helical structure), and as such, may not have all sulfate groups available for binding with the protein. Gu et al. (2005) concluded that magnitude of electrostatic interactions between the three CG types and β-lactoglobulin was influenced not just by the relative charge density of the CGs but also by the CG conformation.

Electrophoretic mobility was measured for 20:1 CPI-CG mixtures and individual solutions of CPI and CG as a function of pH (7.00 – 1.50) (Figure 6.4). The individual CPI solution indicated its pI value to be at a pH of 5.78 (Figure 6.4), corresponding closely to where the CPI turbidity curve peaked (pH 5.60) (Figure 6.1). In contrast, individual CG molecules, regardless of their type remained highly negatively charged (~-40 to -80 mV) over the entire pH range (Figure 6.4). The pI for CPI in the present study was lower than typically reported in the literature for cruciferin (pI 7.2) and napin (pI ~11.0), which are usually determined based on their amino acid composition. In the present study, pI is determined based on the electrophoretic mobility of the protein in solution. CPI constitutes a mixture of proteins, in which are most likely experiencing some level of aggregation in which exposes some, and buries other amino acids from the surface to influence mobility. Where mobility ceases, CPI displays no net charge (zeta potential = 0 mV). In the mixed systems, the presence of CG shifted the pH of net neutrality to

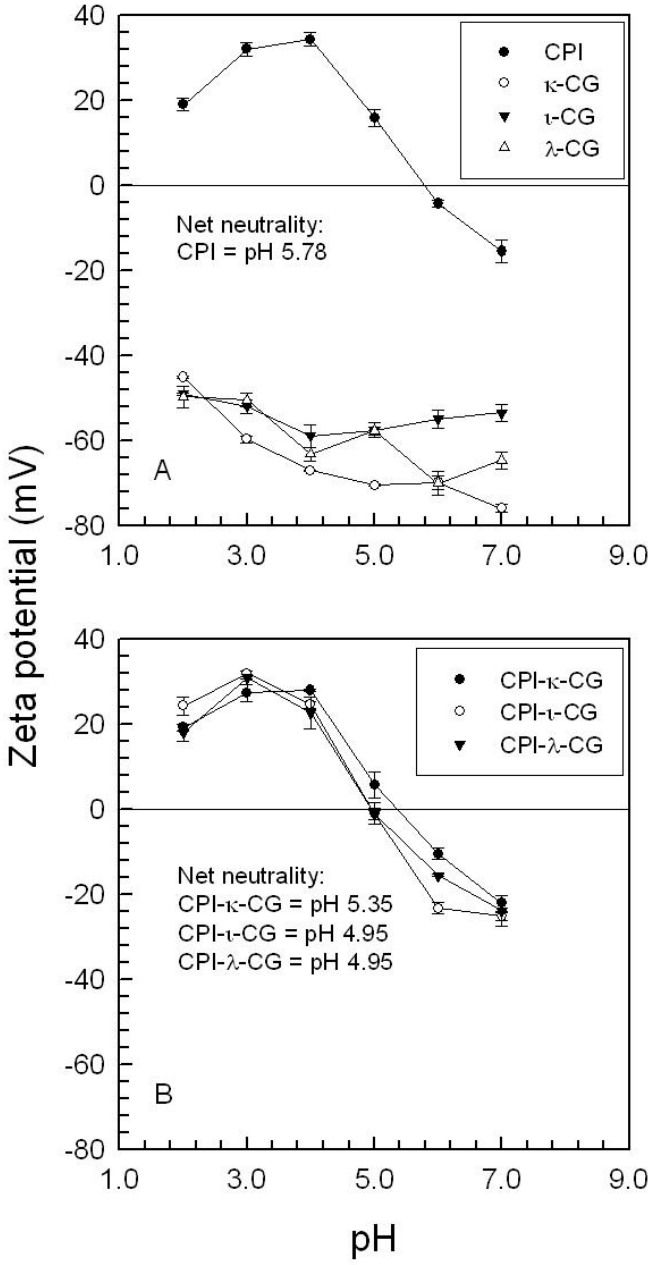

Figure 6.4 Surface charge (zeta potential, mV) of homogenous (CPI and κ-, ι- and λ-type CG) (A) and mixed (CPI- (κ-, ι- and λ-type) CG, 20:1 ratio) (B) biopolymer solutions (20:1 mixing ratio) as a function of pH. Data represent the mean ± one standard deviation.

more acidic pHs relative to the individual CPI system due to the complexation of CG molecules to the CPI-CPI aggregates surface. Mixtures of both CPI-ι- and λ-CG shifted net neutrality to occur a pH 4.95, whereas in the case of CPI-κ-CG, net neutrality shifted to only pH 5.35. A similar trend was found WPI-CG complexes with WPI-κ-CG having a higher pH of net neutrality compared to WPI mixed with ι- or λ-CG. Klassen et al. (2011) reported CPI-ι-CG complexes having net neutrality at pH 4.55 which was consistent with our findings.

Functional properties of soluble and insoluble CPI-CG complexes vs. CPI alone

a) Solubility

The functional properties of CPI and CPI-CG mixtures were investigated at pH 6.75 and 5.00 corresponding to pH conditions where soluble and insoluble complexes, respectively, were present in solution (Table 6.1). 'Insoluble complexes' refers to terminology associated with the protein-polysaccharide complex occurring and not its functional properties; solubility of said complexes refers to how much of the complex can remain suspended in solution. At pH 6.75, solubility for individual CPI solutions (~96.5%) was significantly higher than for the mixed CPI-CG systems as soluble complexes ($p<0.001$) (Table 6.1). CPI-κ-CG complexes showed greater solubility (~84.3%) than the other CG-types (ι-, λ-) ($p<0.01$), which were similar in magnitude (~68.3% CPI-ι-CG; ~61.9% CPI-λ-CG; $p>0.05$). As pH was lowered to 5.0, individual CPI solutions showed slightly reduced solubility (~90.6%) relative to that at higher pH, and to that of the mixed systems ($p<0.001$) (Table 6.1). However, the solubility of insoluble complexes was reduced further, as strong electrostatic attraction between biopolymers resulted in precipitated structures. All three mixtures were found to be statistically different ($p<0.001$), where CPI-ι-CG showed the greatest solubility (~61.9%), followed by κ-CG (~47.5%) and then λ-CG (~25.9%) (Table 6.1). The greater solubility of CPI-ι-CG over the other two CG types may be due to less interactions occurring between CPI and ι-CG, and therefore less precipitation out of solution, as evident by the CPI-ι-CG turbidity curve having a lower magnitude than the CPI-κ- or λ-CG curves (Figure 6.2). Differences in order (based on solubility) within the mixed system as soluble and insoluble complexes is proposed to reflect difference is biopolymer mobility within the complexes during the process of forming the precipitate-type structures. Having reduced solubility at higher pH's within mixed systems is advantageous for protein separation applications. Klassen et al. (2011) and Liu et al. (2010b) reported decreases in solubility at pH

Table 6.1 Functional attributes of canola protein isolate (CPI)- (κ-, ι- and λ-type) carrageenan (CG) mixtures under biopolymer (20:1 CPI-CG mixing ratio) and pH conditions where soluble and insoluble complexes exist. Data represent the mean ± one standard deviation (n=3).

	Solubility (%)	**Foaming Capacity (%)**	**Foaming Stability (%)**	**Emulsion Stability (%)**	**Emulsion Capacity (g/g)**
Soluble complexes (pH 6.75)					
CPI-κ-CG	84.27 ± 2.37	144.44 ± 10.18	69.95 ± 3.42	91.67 ± 5.13	194.69 ± 7.58
CPI-ι-CG	68.35 ± 2.29	120.00 ± 5.77	70.87 ± 0.98	96.00 ± 2.00	190.31 ± 0.00
CPI-λ-CG	61.90 ± 5.74	111.11 ± 3.85	64.40 ± 4.88	87.33 ± 3.06	164.06 ± 0.00
CPI (control)	96.50 ± 0.44	271.11 ± 10.18	74.20 ± 0.70	86.00 ± 2.00	225.31 ± 7.58
Insoluble complexes (pH 5.00)					
CPI-κ-CG	47.46 ± 1.19	97.78 ± 3.85	81.75 ± 4.32	96.00 ± 0.00	181.56 ± 15.16
CPI-ι-CG	61.89 ± 0.54	71.11 ± 3.85	77.88 ± 6.82	94.67 ± 2.31	190.31 ± 13.13
CPI-λ-CG	25.94 ± 2.48	73.33 ± 6.67	86.72 ± 7.21	96.00 ± 0.00	190.31 ± 13.13
CPI (control)	90.62 ± 0.50	211.11 ± 10.18	73.76 ± 2.56	92.00 ± 0.00	247.19 ± 7.58

where insoluble complexes were formed in CPI-ι-CG and pea protein isolate-gum Arabic, respectively. Protein-polysaccharide complexes can also increase the solubility of the protein, particularly near its pI, as the polysaccharide acts to inhibit protein-protein aggregation (Ye, 2008). An increase in solubility at acidic pH (pH 4) has been found for soy protein isolate-chitosan complexes (Yuan et al., 2013). Burova et al. (2007) reported the addition of ι- and κ-CG increased the solubility of β-casein in the range of pH 3-5 where β-casein precipitates when alone in solution. The increase in solubility was more pronounced for κ-CG over ι-CG.

b) Foaming

Foam capacity reflects the amount of foam per amount of protein that can be generated upon application of mechanical shear. FC was found to decrease significantly at pH 6.75 for the mixed CPI-CG systems relative to individual CPI solutions (~271%) ($p<0.001$). CPI-κ-CG soluble complexes (~144%) were found to be significantly higher than the other two types ($p<0.001$), which were similar (~115%) ($p>0.05$). As pH was lowered to 5.00, FC for individual CPI solutions was reduced (~211%) relative to that at higher pH (~271%), and for all mixed systems as well ($p<0.001$) (Table 6.1). FC of insoluble complexes followed a similar trend as the soluble complexes, where CPI-κ-CG showed the higher FC (~98%) than the other two types ($p<0.001$), whereas FC for CPI-ι-CG (~71%) and CPI-λ-CG (~73%) types were similar ($p>0.05$) (Table 6.1). Reduced FC for the latter two types (CPI-ι-CG and CPI-λ-CG) relative to CPI-κ-CG complexes, between individual and mixed systems and between soluble and insoluble complexes is proposed to be associated with reduced solubility of the electrostatic complexes within the continuous phase. In order for FC to be high, biopolymer must migrate to the air-water interface and unfold to expose hydrophobic groups towards the gaseous phase and hydrophilic groups to the aqueous phase to form a viscoelastic film around the air bubble. Electrostatic complexation is expected to influence both diffusion of proteins to that interface and re-alignment once there.

Foam stability relates to the degree of foam breakdown over a defined time period. At pH 6.75, FS was found to be relatively similar for the individual and all soluble CPI-CG complexes after 30 min, ranging between ~64 and 74% ($p>0.05$; Table 6.1). However, as pH was reduced to 5.00, CPI-CG insoluble complexes showed slightly improved FS over the soluble complexes, whereas individual CPI solutions remained relatively unchanged. No statistical differences were apparent among the various CPI-CG insoluble complexes ($p>0.05$) (Table 6.1). The slightly

improved FC for the insoluble complexes is thought to be associated with increased continuous phase viscosity associated with precipitated complexes that remain within the interstitial phases of the form. Schmidt et al. (2010) reported that the addition of pectin to napin solutions led to improved FS relative to napin alone, where the authors thought improved FS was associated to both unbound and bound proteins within the continuous phase that acted to delay liquid drainage from the foam structure. Miquelim et al. (2010) investigated FS of egg-albumin-κ-CG complexes relative to the albumin alone. The authors concluded the addition of κ-CG improved the FS by decreasing the surface tension to less than that of albumin alone, for pH's below the pI of albumin. Liu et al. (2010a) found percent foam expansion to be similar for pea protein isolate alone and when complexed with gum Arabic regardless of pH. However the authors reported pea protein isolate FS to increase greatly with gum Arabic under pH conditions where complexation was occurring. This was hypothesized to be due to increased surface hydrophobicity of the pea protein isolate-gum Arabic complex over pea alone, leading to better adsorption and integration at the air-water interface and increased strength of the viscoelastic film due to the electrostatic interactions of the pea protein isolate-gum Arabic complexes.

c) Emulsification

The emulsification properties of soluble and insoluble complexes were evaluated in terms of their emulsion capacity (EC) and stability (ES) – by creaming. During emulsion formation, proteins and protein-polysaccharide complexes migrate to the oil-water interface, and then re-align to form a viscoelastic film around an oil droplet with hydrophobic residues oriented towards the oil phase and hydrophilic residues towards the aqueous phase (Walstra and van Vliet, 2008). Stability can be enhanced with increased electrostatic repulsion, steric hindrance between neighbouring droplets and increased continuous phase viscosity (Walstra and van Vliet, 2008). Emulsion capacity refers to the amount of oil (g) a certain amount of protein (g) can support within an oil-in-water emulsion prior to inverting into a water-in-oil emulsion (Crenwelge et al., 1974). At pH 6.75, CPI-CG soluble complexes showed reduced EC over the CPI control ($p<0.001$) with CPI-κ- and ι-CG mixtures having greater EC than CPI- λ-CG ($p<0.001$) (Table 6.1). In contrast, EC for all mixed systems was similar (~190 g/g) ($p>0.05$) in their insoluble complex state (pH 5.00), however the EC for CPI alone was significantly higher (~247 g/g) ($p<0.01$). Emulsion stability relates the ability of an oil-in-water emulsion to resist gravitational phase separation as a

consequence of droplet coalescence and creaming (McClements, 2007). Overall at pH 6.75, the ES for individual CPI and soluble CPI-CG complexes (regardless of type) were similar in magnitude ($p>0.05$; Table 6.1). In contrast for ES data at pH 5.00, insoluble CPI-κ-CG and CPI-λ-CG complexes were found to be similar in magnitude (~96%, $p>0.05$), but higher than that of CPI alone (~92%) ($p<0.05$). Insoluble CPI-ι-CG complexes gave similar ES to that of CPI alone ($p>0.05$). In the present study, surface charge of both individual CPI and mixed systems at pH 5.00 and 6.75 were relatively low (i.e., ~±20 mV) (Figure 6.4), therefore its contribution to ES stability was quite low. At pH 5.00, solubility of the insoluble CPI-κ-CG and CPI-λ-CG complexes were lower compared to the individual CPI and CPI-ι-CG complexes, and as such most likely lead to slightly increased continuous phase viscosities resulting in the higher observed emulsion stability data.

Gu et al. (2005) reported that under conditions where weak complexes were formed between β-lactoglobulin and CG the order of creaming stabilities was κ-CG > ι -CG > λ-CG. In a β-lactoglobulin-CG system at pH where strong electrostatic interactions were occurring no differences were found for creaming stabilities between the three CG types below a critical CG concentration (Gu et al., 2005). Uruakpa and Arntfield (2005) found that adding κ-CG to CPI, at pH where the biopolymers were oppositely charged, increased the emulsion stability of CPI. Stone and Nickerson (2012) reported that an increase in WPI emulsion stability when complexed with CG may be due to charge repulsion between droplets, viscoeleastic film formation with protein-polysaccharide complexes saturating the oil-water interface and steric stabilization caused by the CG chains. Li et al. (2012) reported that bovine serum albumin (BSA)-sugar beet pectin either increased or decreased emulsion stability depending on the level of interactions occurring between the protein and polysaccharide. At increased pHs where little to no complexation was taking place no increase in emulsion stability was found due to depletion flocculation and competitive adsorption. Under conditions where soluble BSA-pectin complexes were formed an increase in emulsion stability was found which the authors attributed to the thick protein-polysaccharide layer at the interface causing strong steric stabilisation of the droplets. And finally insoluble BSA-pectin complexes led to extremely unstable emulsions due to bridging flocculation.

6.5 SUMMARY

The formation of soluble and insoluble complexes was investigated in CPI-(κ-, ι- and λ-type) CG mixtures as a function of pH and biopolymer mixing ratio. Complexes formed at pHs > pI and critical pHs plateaued at a 15:1-20:1 CPI-CG mixing ratio. CPI-CPI aggregates were thought to be formed based on the pH dependence of pH_c. Complex formation between CPI and (κ-, ι- and λ-type) CG was found to have a significant negative effect on solubility, foaming capacity, and emulsion capacity at pHs where soluble (pH 6.75) and insoluble (pH 5.00) complexes exist, whereas the foaming stability and emulsion stability properties of CPI were similar or increased with the addition of CG at these pHs. Increases in foam and emulsion stability are mostly likely associated with increase in the continuous phase viscosities. Within the mixed systems CPI-κ-CG had the greatest FC at pHs where soluble and insoluble complexes exist and CPI-λ-CG had significantly less EC and solubility than the other CG types at pH corresponding to the presence of soluble complexes. Overall, complexation-induced changes to protein solubility offered the most dramatic results of all the functionality tests measured, with possible applications in protein (or other charged particles) separation techniques where precipitation is desired.

-Chapter 7-

Formation and functionality of canola protein isolate with both high- and low-methoxyl pectin under associative conditions[3]

Stone, Andrea K., Teymurova, Anzhelika, Chang, Chang, Cheung, Lamlam, and Nickerson, Michael T.

Department of Food and Bioproduct Sciences, University of Saskatchewan
51 Campus Drive, Saskatoon, SK, Canada, S7N 5A8

[3]Submitted to Food Science and Biotechnology (August 2014)

7.1 ABSTRACT

Electrostatic interactions within mixtures of a canola protein isolate (CPI) and both low- (LMP) and high-methoxy (HMP) pectins were studied by measurements of turbidity (pH 8.0-1.5) as a function of mixing ratio (1:1 to 30:1; CPI-pectin) and electrophoretic mobility (pH 7.0 -1.5). The rheological (flow behavior) and functional (solubility, foaming and emulsifying properties) attributes of the formed CPI-pectin complexes were also studied. Increasing biopolymer mixing ratios shifted both the formation of soluble and insoluble complexes to higher pHs until plateauing ~10:1. Maximum coacervation for CPI-HMP and CPI-LMP occurred at the 10:1 biopolymer mixing ratio at pH 5.30 and 4.83 whereas pHs of net neutrality occurred at ~4.50 and 4.27, respectively. Complex formation did not affect the functional attributes of CPI, except for a slight increase in solubility for CPI-HMP and a large reduction in foaming capacity for CPI-LMP, however it did increase solution viscosity substantially.

7.2 INTRODUCTION

Interactions between proteins and polysaccharides within foods play an integral role in terms of maintaining product quality (Tolstoguzov, 1991). A greater understanding of these interactions, and the factors affecting them could lead to greater ingredient tailoring for a wide range of food applications. Depending on the pH of the system, these macromolecules may experience electrostatic attraction whereby the anionic polysaccharides associate with positively charged proteins (pH < pI, pI – isoelectric point); or electrostatic repulsion between negatively charged proteins and polysaccharides at pHs > pI (Schmitt et al., 1998). The former condition leads to associative phase separation in which a solvent-rich and biopolymer (protein + polysaccharide)-rich phase develops; whereas the latter is referred to as segregated phase separation where a polysaccharide-rich and protein-rich phase forms (Schmitt et al., 1998; de Kruif et al., 2004). Typically this process is investigated using light scattering, turbidity or by titration within biopolymer mixtures as solvent pH is lowered. Structure forming events are typically associated with the formation of soluble complexes, as evident by a slight reflection in the scattering intensity over the baseline during acidification (relating to the first experimental detectable indication of biopolymer interactions) (denoted as pH_c); and by the formation of insoluble complexes as evident by large changes in scattering intensity upon acidification (denoted as $pH_{\phi 1}$) (Li et al., 1994; de Kruif et al., 2004; Liu et al., 2009). Biopolymer interactions are considered optimal at the pH

corresponding to maximum scattering intensity (pH_{opt}) where the two biopolymers are reaching an electrical equivalence point (or electrical equivalence pH) (Schmitt et al., 1998). At $pH<pH_{opt}$, formed complexes begin to break down as the pKa on the reactive sits along the polysaccharide backbone start to progressively become protonated (Li et al., 1994; de Kruif et al., 2004).

Most coacervation studies have focused on understanding the process from a mechanistic stand point (Weinbreck et al., 2004; Bohidar et al., 2005; Lizarraga et al., 2006; Wang et al., 2007; Ru et al., 2012), rather than the functionality of the resulting complexes where they can be tailored depending on the solvent (temperature, pH, salts) and biopolymer characteristics (mixing ratio, concentration, biopolymer type) used.

High protein solubility is an important attribute for many food applications, coacervation with a polysaccharide can improve protein solubility especially near a proteins pI (Ye, 2008). The effects of coacervation on protein solubility have been investigated for soy protein- chitosan complexes as a function of mixing ratio and temperature (121°C, 15 min) (Yuan et al., 2013); soy protein- κ-carrageenan (CG) mixtures as a function of pH and mixing ratio (Ortiz et al., 2004); and faba bean legumin- chitosan complexes as a function of pH (Plashchina et al., 2001). Protein-polysaccharide complexes can also form at water-air/oil interfaces to produce and stabilize emulsions and foams. Emulsifying properties have been investigated for canola protein-κ-CG under varied pH, and protein, polysaccharide, salt concentration and denaturant type (Uruakpa et al., 2005); legumin and pectin under complexing and non-complexing conditions (Tolstoguzov, 1991); bovine serum albumin and sugar beet pectin at various pHs and mixing ratios (Li et al., 2012); β-lactoglobulin-κ-, ι-, λ-CG complexes as a function of pH (Gu et al., 2005); and denatured soluble soy whey proteins with soluble soybean polysaccharides as a function of mixing ratio and pH (Ray and Rousseau, 2013). The stability of foams has been investigated in egg albumin- k-CG, xanthan gum and guar gum as a function of pH (Miquelim et al., 2010); and napin protein-pectin complexes as a function of ionic strength, protein concentration and pectin charge density (Schmidt et al., 2010). Emulsion formation and stability through complex coacervation technology is also useful for the encapsulation of flavor compounds and essential oils (Xiao et al., 2014).

Canola contains two major storage protein fractions: cruciferin (12S globulin) and napin (2S albumin). Cruciferin, with a molecular weight ~300 kDa, consists of α- and β-chains linked by disulfide bonds (Lampart-Szczapa, 2001). Napin (~20% of total protein content) consists of two polypeptide α-chains (4.5 kDa and 10 kDa) connected by disulfide bonds (Berot et al., 2005).

Canola protein is considered to be an emerging protein to the food industry, receiving GRAS status in North America with research efforts expanding as the canola industry searches to add value to the protein-rich underutilized meal, left over after oil processing. In contrast, pectin is an anionic heteropolysaccharide comprised of primarily α-(1→4) D-galacturonic acid residues (Voragen et al., 1995). The behavior of pectin in food applications may vary depending on the ratio of esterified to non-esterified galacturonic acid. Typically, pectins are classified in two types depending of the degree of methyl-esterification (DM) of galacturonic acid carboxyl groups: low-methoxyl pectin (LMP) with DM<50% and high-methoxyl pectin (HMP) with DM>50%.

The overall goal of this research is to investigate the effect of pH and mixing ratio on complex formation between CPI and both HMP and LMP, and to explore the functional attributes of these formed complexes. Findings could lead to the development of mixed biopolymer ingredients with unique properties over the materials alone.

7.3 MATERIALS AND METHODS

Materials

Canola seed (SP Desirable *Brassica napus*, Lot #: 168-8-129810) was kindly supplied by Viterra (Saskatoon, SK, Canada). Low-methoxyl (LMP) (≥ 6.7% esterified) and high-methoxyl (HMP) (≥ 85.0% esterified) pectins were obtained from Sigma-Aldrich Canada Ltd. (Oakville, ON, Canada). All other chemicals used in this study were of reagent grade, and purchased from Sigma-Aldrich Canada Ltd. (Oakville, ON, Canada). Canola protein isolates were prepared as described by Klassen et al. (2011). In brief, defatted canola meal was prepared by pressing the seeds with a continuous screw expeller (Komet Type CA59 C, IBG Monforts Oekotec GmbH & Co., Monchegladbach, Germany), followed by hexane extraction at a 1:1 meal: hexane ratio for 16 h. The meal was then air-dried for 8 h, followed by a second hexane extraction. Proteins from the defatted meal were extracted using a Tris-HCl buffer (pH 7.0) with 0.1 M NaCl at a ratio of 10 mL buffer/g meal for 2 h under constant mechanical stirring at room temperature (~21-22°C). The dispersion was then centrifuged (Beckman J2-HC, Beckman Coulter Canada Inc., Mississauga, ON, Canada) at 18,600 x g for 1 h at 4°C, and the supernatant was recovered. A second centrifuge step for 30 min was used to further clarify the supernatant of insoluble residues, followed by dialysis (Spectro/Por® tubing, 6-8 kDa cut off, Spectrum Laboratories, Inc., Rancho Dominguez, CA, USA) at 4°C for 48 h with frequent changes of Milli-Q water (Millipore Corporation,

Billerica, MA, USA) to remove the salt content. Precipitated salt soluble proteins were recovered by centrifugation at 18,600 x g for 2 h at 4°C (Folawiyo and Apenten, 1996), and then subsequently freeze dried using a Labconco FreeZone 6 freeze drier (Labconco Corp., Kansas City, MO, USA) to yield a protein isolate powder. Chemical analyses on the CPI, LMP, HMP materials were performed according to the Association of Official Analytical Chemists (AOAC, 2003) Methods 925.10, 923.03, 920.87 and 920.85 for moisture, ash, crude protein and lipid (%wet weight basis), respectively. Carbohydrate content was determined based on percent differential from 100%. CPI consisted of 94.95% protein (wet basis) (%N x 5.70), 0.70% moisture, 0.32% lipid, 2.32% ash and 1.71% carbohydrate, whereas the commercial HMP and LMP powders were comprised of 89.08% and 86.16% carbohydrate, respectively. CPI, HMP, LMP concentrations used in this study reflect the protein and carbohydrate content, respectively, rather than powder weight.

pH-turbidimetric titrations

Changes in turbidity during a pH acid titration were investigated for mixtures of CPI with HMP and LMP as a function of pH (1.50-8.00) and biopolymer mixing ratio (1:1 –30:1 CPI: HMP or LMP) at a total biopolymer concentration of 0.05% (w/w), in order to identify critical pH values associated with complex formation according to Klassen et al. (2011). Individual CPI, HMP and LMP solutions were also measured under the same conditions, each at a 0.5% (w/w) concentration. Biopolymer solutions were prepared by dissolving the respective amount of each powder within Milli-Q water at pre-selected mixing ratios. Solution pH was then adjusted to pH 8.00 using 1 M NaOH and solutions were allowed to stir overnight (~16 h) at 4°C. Readings of absorbance (or optical density) were measured as a function of pH (8.00–1.50) at room temperature (~21-23°C) using a Genesys 10 UV/Vis spectrophotometer (Thermo Scientific, Waltham, MA, USA) at 600 nm in plastic cuvettes (1 cm path length). Critical pH values were determined graphically as the intersection point of two curve tangents as previously described by Weinbreck et al. (2003) and Liu et al. (2009). All measurements were performed in triplicate.

Electrophoretic mobility

Electrophoretic mobility (*U*) for individual CPI and mixed CPI-HMP, CPI-LMP biopolymer solutions were investigated as a function of pH (7.0-1.5) using a Zetasizer Nano-ZS90 instrument (Malvern Instruments, Westborough, MA, USA). Hydrochloric acid (0.05 M and 1 M)

was used to lower the pH in 1.0 unit increments. Samples were prepared as previously described. Electrophoretic mobility was related to the zeta potential using the Henry equation (eq. 7.11):

$$U = \frac{2\varepsilon \times \zeta \times f(\kappa\alpha)}{3\eta} \quad \text{(eq. 7.1)}$$

where η is the dispersion viscosity, ε is the permittivity, and f($\kappa\alpha$) is a function related to the ratio of particle radius (α) and the Debye length (κ). Using the Smoluchowski approximation, f($\kappa\alpha$) equaled 1.5. All measurements were made in triplicate.

Rheological properties

Rheological measurements were performed on the lower phase of CPI-HMP and CPI-LMP solutions prepared at a 2.00% (w/w) total biopolymer concentration and 10:1 mixing ratio using an AR-G2 rheometer (TA Instruments, New Castle, DE, USA) and cone-and-plate geometry (Diameter 40 mm; Cone angle 2°). Biopolymer solutions were prepared by dispersing powders of each biopolymer in Milli-Q water, adjusting to pH 8.0 and then stirring for 2 h (500 rpm) at room temperature. Mixed solutions were then adjusted to pH 5.3 and 4.8 (pH of maximum CPI-pectin interactions as determined by turbidity measurements) for CPI-HMP and CPI-LMP respectively, and re-adjusted if needed within 15 min. pH adjusted solutions were transferred to 50 mL centrifuge tubes and gently centrifuged at 1,050 x *g* (VWR clinical centrifuge 200, VWR International, Mississauga, ON, Canada). The supernatant (upper phase) was discarded and the pellet (lower phase) was used for rheological measurements. For comparative purposes the same measurements were performed for 2.00% (w/w) CPI-HMP and CPI-LMP biopolymer solutions at pH 7.0 (non-interacting conditions). Steady shear viscosity was measured as a function of shear rate (0.1-100 s^{-1}) at room temperature and fitted to the Power law model in the range of 1-10 s^{-1} shear rate using eq. 7.2,

$$\eta = m \times \dot{\gamma}^{n-1} \quad \text{(eq. 7.2)}$$

where η is the apparent viscosity (Pa s), m is the consistency coefficient (Pa s^n), $\dot{\gamma}$ is the shear rate (s^{-1}) and n is the flow behavior index (dimensionless). All the measurements were performed four times.

Functional properties

All functionality tests (solubility, foaming capacity/stability, emulsion capacity and emulsion stability) were performed on 1.00 % (w/w) CPI-HMP and CPI-LMP solutions at a 10:1 mixing ratio at pH 5.3 and 4.8, respectively, corresponding to mixing ratio and pH of maximum coacervation (determined by turbidity measurements; Figs. 7.1,2) where insoluble CPI-pectin complexes exist. For comparative purposes functionality tests were performed on CPI alone at the corresponding pHs and concentrations as in the mixed systems.

Solubility

Percent solubility was determined for 1.00% (w/w) CPI-HMP and CPI-LMP solutions at a 10:1 mixing ratio using a modified method of Morr et al. (1985) and compared to CPI alone. CPI, CPI-HMP and CPI-LMP solutions were dissolved in 0.1 N NaCl and stirred (500 rpm) for 1 h at a room temperature (21-22°C) then centrifuged at 4,180 x g for 10 min (21-22°C) (VWR clinical centrifuge 200, VWR International, Mississauga, ON, Canada). Protein content was determined in the supernatant by means of micro-Kjeldahl (%N x 5.7). Percent protein solubility was estimated by dividing the water-soluble protein content by the total protein content (100%). All measurements were performed in triplicate.

Foam capacity and stability

Foam capacity (*FC*) and foam stability (*FS*) were determined by a modified method Liu et al. (2010). Foams were generated from 15 mL (V_{li}, initial volume of biopolymer solution used to make the foam) of CPI or CPI-pectin solutions using an Omni Macro Homogenizer (Omni International, Inc., Marietta, GA, USA) with a 20 mm saw tooth generating probe at 8,000 rpm for 5 min then transferred into a 100 mL graduated cylinder (inner diameter = 26 mm; height = 25 mm; as measured by a digital caliper). The *%FC* and *%FS* values were calculated using Eq. (7.3) and (7.4), respectively, where V_{fo} is the foam volume generated initially after homogenization (time = 0) and V_{f30} is the foam volume remaining after 30 min. Foam stability was measured after an arbitrary time of 30 min. All measurements were performed in triplicate.

$$\%FC = \frac{V_{fo}}{V_{li}} \times 100\% \qquad \text{(eq. 7.3)}$$

$$\%FS = \frac{V_{f30}}{V_{f0}} \times 100\% \quad \text{(eq. 7.4)}$$

Emulsion capacity (EC)

In brief, series of emulsions were prepared from 1.00 % (w/w) biopolymer solutions (CPI, CPI-pectin) with differing amounts of canola oil (2.5-5.5 g). Aliquots (2 g) of each solution were added to canola oil in 50 mL centrifuge tubes followed by homogenization using an Omni Macro Homogenizer (Omni International, Inc., Marietta, GA, USA) equipped with a 20 mm diameter saw tooth generating probe, at 8,000 rpm for 5 min. Immediately after homogenization the conductivity of the emulsion was measured. Percent emulsion capacity (*EC*) was estimated by the average weight of canola oil per gram of protein before and after the emulsion conversion (from oil-in water to water-in-oil) which is observed by a significant drop in conductivity.

Emulsion stability (ES)

In brief, oil-in-water (50/50) emulsions were prepared from 1.00% (w/w) biopolymer solutions (CPI, CPI-pectin) with canola oil. Aliquots (5 mL) of each solution were added with canola oil (5 mL) to 50 mL centrifuge tubes followed by homogenization using an Omni Macro Homogenizer (Omni International, Inc., Marietta, GA, USA) equipped with a 20 mm diameter saw tooth generating probe, at 8,000 rpm for 5 min. Emulsions were transferred into individual 10 mL graduated cylinders (inner diameter 10.80 mm; height 100.24 mm) and left for separation for 30 min. Percent emulsion stability (*ES*) was determined using eq. 7.5,

$$\%ES = \frac{V_B - V_A}{V_B} \times 100\% \quad \text{(eq. 7.5)}$$

were V_B and V_A are the volume of the aqueous (or serum) layer before emulsification (5.0 mL) and after 30 min of drainage, respectively. All measurements were performed in triplicate.

Statistics

A paired Student's T-test was used to test statistical differences in critical pHs and max OD data for CPI-HMP and CPI-LMP solutions, and for the functional properties between CPI and CPI-pectin solutions. Statistical analyses were performed using Microsoft Excel 2010 (Microsoft Corporation, Redmond, WA, USA).

7.4 RESULTS AND DISCUSSION

Effect of pH and biopolymer mixing ratio

Turbidity measurements were performed for individual CPI, HMP and LMP solutions as well as for CPI-HMP and CPI-LMP mixed solutions (Fig. 7.1). In the case of CPI alone a bell-shaped turbidity curve was observed with a decrease in pH from 7.00 and 3.00, with maximum absorbance (0.777) reached at pH 5.70 which is likely due to CPI-CPI aggregation. In contrast, both HMP and LMP did not show any optical density (OD) readings along the entire pH range (data not shown). Optical density was plotted as function of biopolymer ratio (1:1 to 30:1; CPI-pectin) during an acid titration for CPI-HMP and CPI-LMP mixed solutions. At the 1:1 ratio the CPI-HMP profile was shifted towards lower pHs and significantly decreased OD (0.245), as compared to CPI alone, which is thought to be associated with predominantly electrostatic repulsion between HMP chains and CPI which hinders CPI-CPI aggregation. Upon increasing the biopolymer ratio from 1:1 up to 10:1 for CPI-HMP, turbidity profiles shifted towards higher pHs with progressively increased absorbance magnitude which reached the CPI alone maximum (0.797) (Fig. 7.1A). At higher ratios from 15:1 to 30:1 there were no significant changes in turbidity profiles (Fig. 7.1B).

In the case of the CPI-LMP mixture the shift towards lower pHs and reduced OD was also observed at the 1:1 mixing ratio, whereas at higher ratios, 5:1 and 10:1, CPI-LMP OD maximum was increased to 0.892 and 1.039, respectively (Fig. 7.1C). Similar to CPI-HMP, further increase in CPI-LMP mixing ratios from 15:1 to 30:1 did not cause any shifts from the10:1 ratio profile (Fig. 7.1D). At higher biopolymer mixing ratios CPI-CPI aggregation in CPI-HMP and CPI-LMP mixtures was not hindered because the number CPI molecules exceeded the number of pectin chains. Unlike the CPI alone profile, CPI-LMP profiles at all mixing ratios (except 1:1) were slightly skewed towards acidic pHs. It is hypothesized that in these conditions CPI-CPI small aggregates were formed and further complexed with LMP chains. In contrast, CPI-HMP profiles

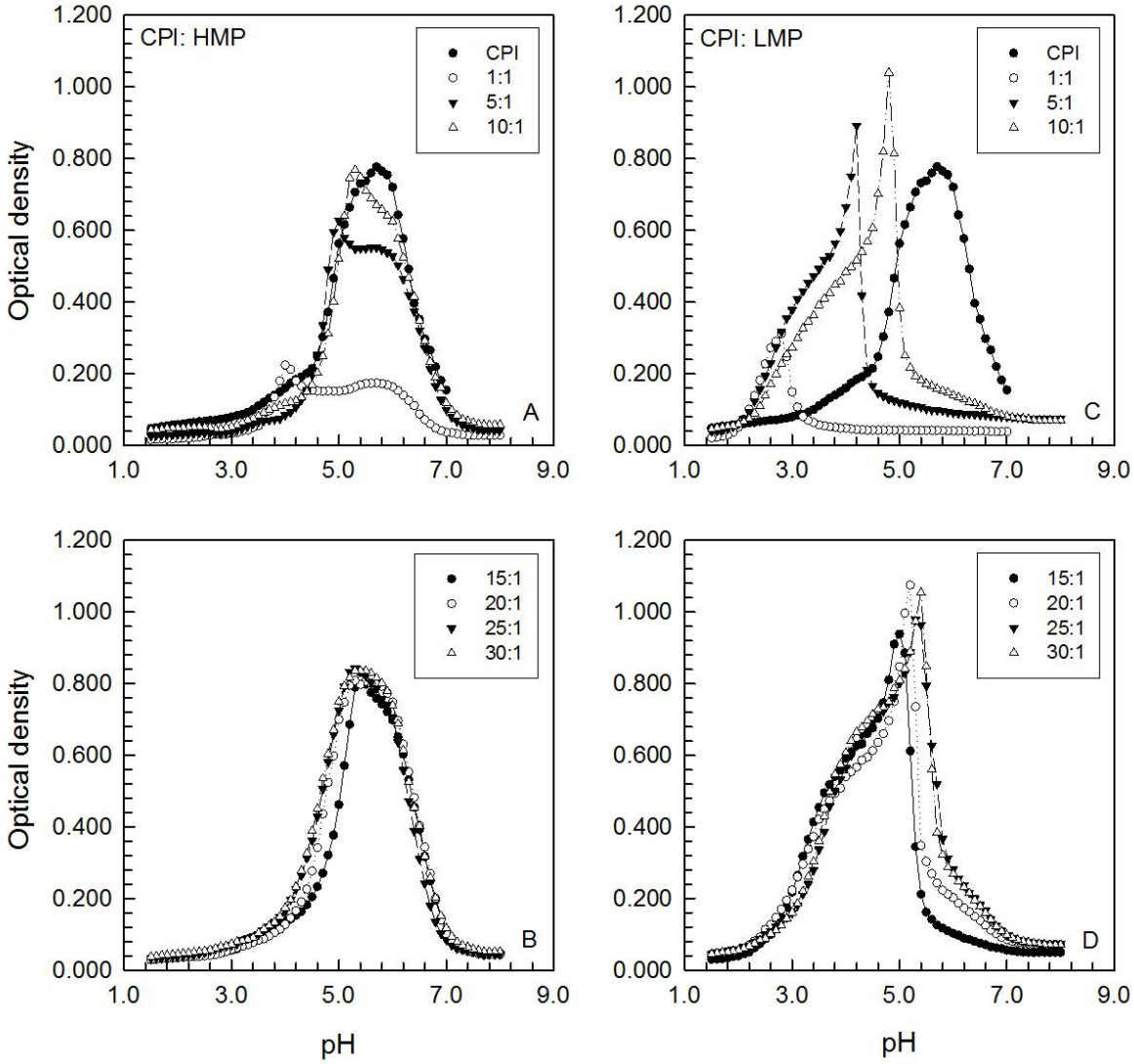

Figure 7.1 Mean turbidity curves for and an individual CPI solution, CPI-HMP (A,B) and CPI-LMP (C,D) as a function of pH and biopolymer mixing ratio (1:1 to 10:1, A,C; 15:1 to 30:1, B,D) (n = 3).

were skewed towards higher pHs in the range of lower mixing ratios (1:1 to 10:1) which is thought to be due to initial formation of small CPI-CPI aggregates at pHs around the CPI alone maximum OD reading and then their disruption followed by complex formation. For example, at the 10:1 mixing ratio the formation of soluble (pH_c) complexes for CPI-HMP and CPI-LMP mixtures was found to occur at pHs 7.57 ± 0.13 and 7.42 ± 0.14 ($p>0.01$) with the transition to insoluble complexes at pHs 6.96 ± 0.21 and 5.02 ± 0.02 ($p>0.01$), respectively. Maximum OD occurred at pH_{opt} 5.30 ± 0.1 and 4.83 ± 0.06 with further dissolution and complete disruption of complexes at pHs 3.05 ± 0.08 and 2.00 ± 0.06 for 10:1 CPI-HMP and CPI-LMP mixtures, respectively, which shows that small CPI-CPI aggregates play an important role in stabilization of the CPI-LMP coacervate structure in acidic pH conditions (pHs<3.00) (Fig. 7.1C).

A similar phenomenon was observed in our previous work on plant protein-anionic polysaccharide mixed systems, namely in partially purified pea proteins (legumin and vicilin) – gum Arabic (Klassen and Nickerson, 2012) and lentil protein isolate - gum Arabic (Aryee and Nickerson, 2012). Critical pHs (pH_c, $pH_{\phi 1}$, pH_{opt} and $pH_{\phi 2}$) for CPI-HMP and CPI-LMP mixtures were plotted versus biopolymer mixing ratio (Fig. 7.2 A,C). For the CPI-HMP mixture pH_c and $pH_{\phi 1}$ were found to be independent of mixing ratio, whereas pH_{opt} and $pH_{\phi 2}$ slightly increased in the 1:1 to 10:1 range then plateaued between 10:1 and 30:1 (Fig. 7.2A). In contrast, for the CPI-LMP mixture pH_c, $pH_{\phi 1}$ and pH_{opt} increased between 1:1 to ~15:1 then plateaued between the 15:1 and 30:1 ratios which is thought be associated with small CPI-CPI aggregates involved in complex formation and growth of the intermolecular complexes until maximum size is reached (~15:1 ratio) (Fig. 7.2C). In contrast $pH_{\phi 2}$ remained unchanged for the entire range of mixing ratios. Greater interactions between CPI and LMP versus HMP are hypothesized to be due to the lower DM in LMP and consequently more carboxylic groups available for binding with CPI. Girard et al. (2002) and Sperber et al. (2009) investigated complex formation of β-lactoglobulin with LMP and HMP using potentiometric titrations and suggested that in case of LMP more ionic groups were involved in electrostatic complexation with β-lactoglobulin than with HMP. Both the CPI-HMP and CPI-LMP mixtures' maximum OD was increased upon raising the mixing ratio from 1:1 to 10:1 and remained unchanged between 10:1 and 30:1 in which the maximum of intermolecular interactions between biopolymers had been reached (Fig. 7.2B,D). Further experiments on rheological and functional properties were performed at the 10:1 ratio ~pH_{opt} (HMP pH 5.3; LMP pH 4.8) for both mixtures.

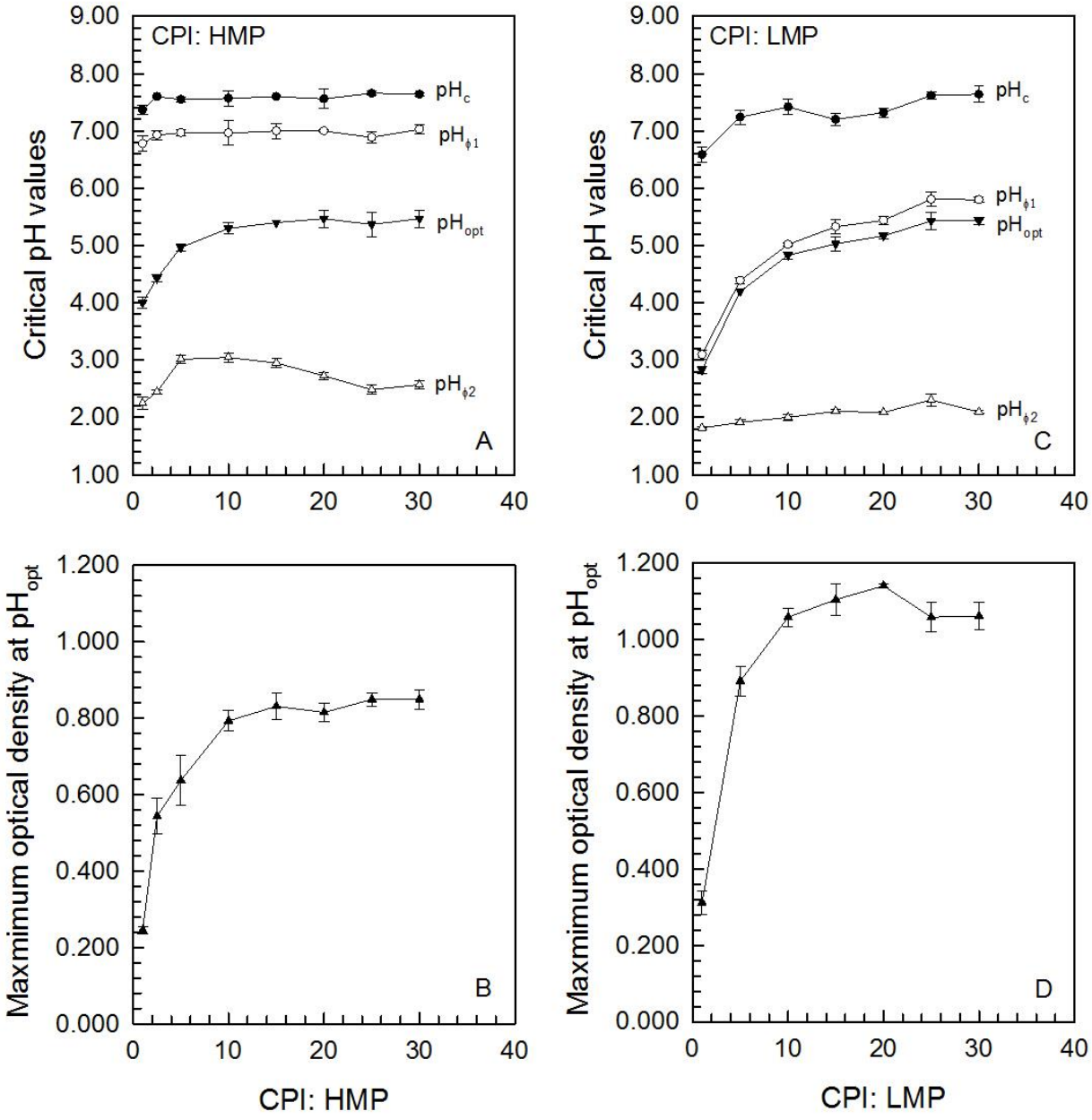

Figure 7.2 Critical pHs (pH_c, $pH_{\phi1}$, pH_{opt}, $pH_{\phi2}$) and maximum optical density of CPI-HMP (A,B) and CPI-LMP (C,D) mixtures as a function of biopolymer mixing ratio. Data represent the mean ± one standard deviation (n = 3).

Figure 7.3A and B display electrophoretic mobility measured as a function of pH (7.00-2.00) for individual CPI, HMP, LMP solutions and mixed CPI-HMP, CPI-LMP solutions, respectively. For CPI alone net neutrality (zeta potential = 0 mV) occurred at pH 5.78 corresponding to CPI pI, whereas at pH< pI and pH> pI the CPI is net positively and negatively charged, respectively. In contrast, HMP remained negatively charged along most of pH range (7.00-2.00) until reaching net neutrality at pH 2.3 corresponding to protonation of carboxylated reactive sites (pKa $–COO^-$ ~1.88) (Liu et al., 2009), whereas LMP became less negatively charged with decreasing pH but did not reach net neutrality and was much more negatively charged than HMP especially between ~pH 7-4. In the mixed solutions net neutrality was reached at pHs 4.50 and 4.27 for CPI-HMP and CPI-LMP, respectively, suggesting that favorable conditions of complex formation occur when two biopolymers are oppositely charged.

Rheological behavior of CPI-pectin complexes

Flow curves for CPI-HMP and CPI-LMP mixtures under non-interacting (pH 7.00) and interacting (pHs 5.3 and 4.8 for CPI-HMP and CPI-LMP, respectively) conditions were plotted as a function of shear rates (Fig. 7.4). Both mixtures under non-interacting conditions exhibited slightly non-Newtonian fluid behavior with flow behavior indices of 0.75 and 0.82 for CPI-HMP and CPI-LMP mixtures, respectively, and the consistency coefficient being 0.01 $Pa{\cdot}s^n$ for both mixtures (R^2 = 0.959) (Fig. 7.4A,C). No time dependence was observed. In contrast, the flow behavior of coacervate phases for both mixtures displayed strong shear thinning behavior. The apparent viscosity of the CPI-HMP coacervate phase at pH 5.30 decreased from ~35.50 to 2.10 Pa·s between 1 and 100 s^{-1} with a flow behavior index and consistency coefficient of 0.19 and 34.00 $Pa{\cdot}s^n$, respectively (R^2 = 0.999) (Fig. 7.4B), whereas for the CPI-LMP coacervate phase at pH 4.8 viscosity was reduced from ~402.17 to 1.89 Pa·s having a flow behavior and consistency coefficient of 0.06 and 432.71 $Pa{\cdot}s^n$, respectively (R^2 = 0.979) (Fig. 7.4D). Pseudoplastic flow behavior and higher viscosity have previously been reported for coacervate phases and are thought to be associated with strong electrostatic attractive interactions between CPI and pectin chains. The greater number of reactive sites in LMP due to lower DM makes it more attractive for complexation with CPI and results in the formation of a more dense and compact coacervate structure versus CPI-HMP. These results are in agreement with our turbidity

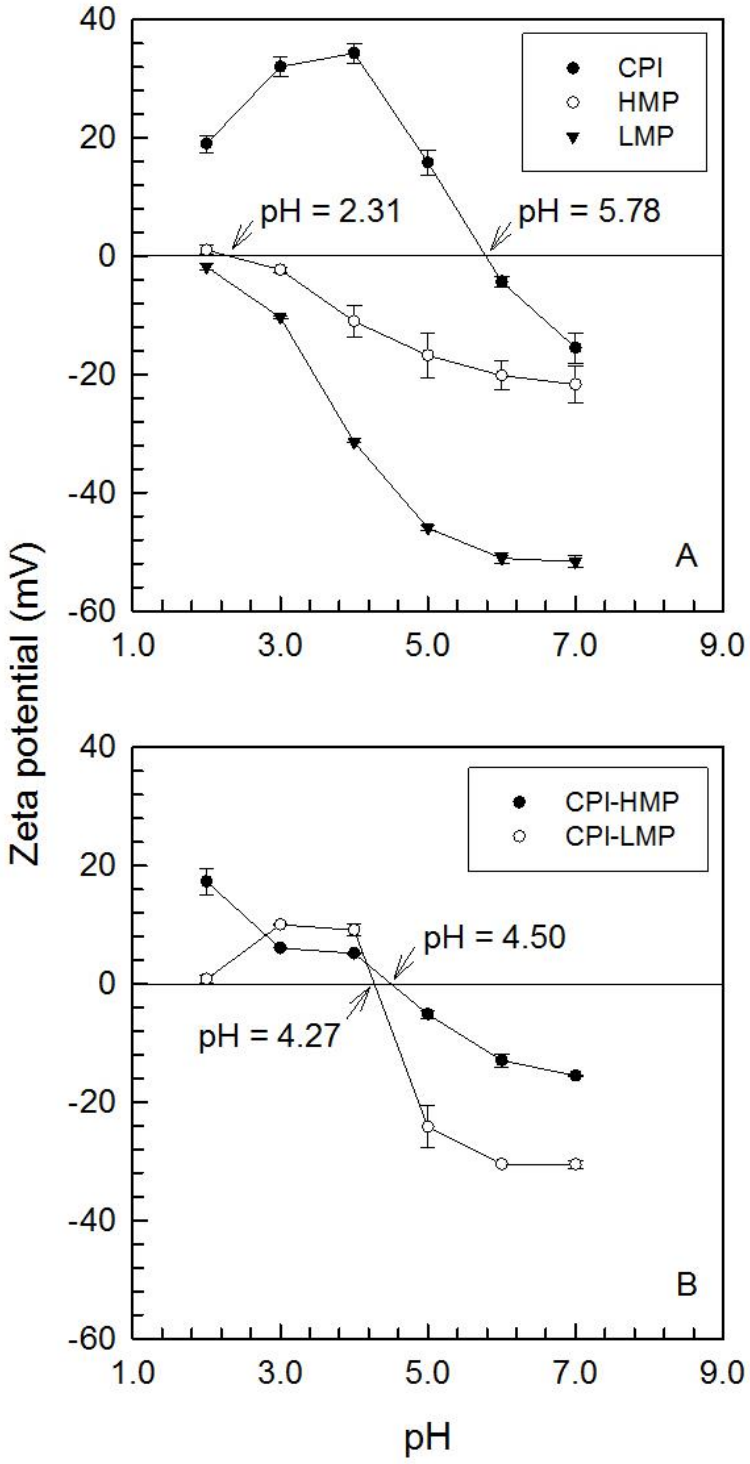

Figure 7.3 Surface charge (zeta potential, mV) for individual (CPI, HMP, LMP) (A) and mixed (CPI– HMP and LMP) (B) biopolymer (10:1 mixing ratio) solutions as a function of pH. Data represent the mean ± one standard deviation (n = 3).

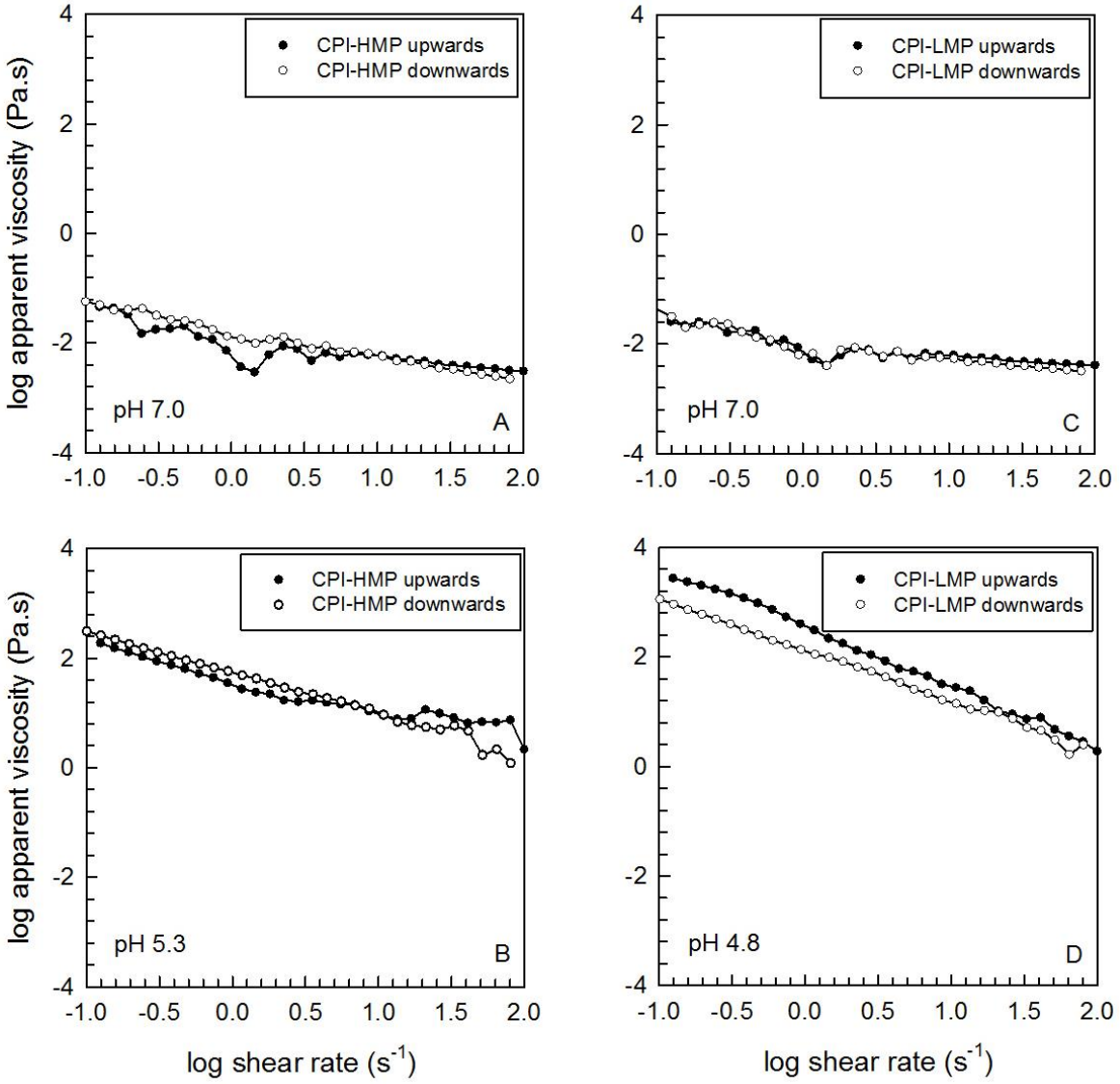

Figure 7.4 Flow curves for CPI-HMP (A) and CPI-LMP mixtures (C) under non-interacting (pH 7.0) and interacting conditions (pH 5.3 CPI-HMP (B); pH 4.8 CPI-LMP (D)) as a function of shear rate (n = 3).

data. Shear thinning phenomenon and compact weak gel structure was also observed within other protein-pectin mixtures (Wang et al., 2007; Lutz et al., 2009; Ru et al., 2012). Hysteresis was observed only in the CPI-LMP mixture which was hypothesized to be due to shear-rate induced break down of the coacervates (Fig. 7.4D).

Functional attributes of CPI-pectin complexes

Functional properties of CPI-HMP and CPI-LMP complexes were obtained under conditions of maximum coacervation (10:1 biopolymer mixing ratio; pHs 5.3 (CPI-HMP) and 4.8 (CPI-LMP)) and compared to CPI alone at the respective pHs (Table 7.1). Solubility of the CPI-HMP mixture was slightly increased (96%) compared to CPI alone (93%) ($p<0.05$), whereas there was not a significant difference between CPI-LMP (~95%) and CPI alone (~93%) ($p>0.05$). The slight increase in solubility of CPI with the addition of HMP, at pH (5.30) near the protein's pI (~5.7), may be due to decreased protein aggregation induced by electrostatic interactions with HMP. Increased solubility in coacervate mixtures near the protein's pI has been previously reported by Yuan et al. (2013) (soy protein and chitosan) Burova et al. (2007) (whey protein and ι-, κ-carrageenan) and Plashchina et al. (2001) (faba bean legumin and chitosan). The ability of a protein to form and stabilize emulsions and foams is an important functional property of the protein and depends on its structure, hydrophilic and hydrophobic residues, conformational stability and interactions/realignment at the oil-water/ air water interface and the experimental conditions being used (Tolstoguzov, 1991). The addition of LMP to CPI greatly decreased the foaming capacity (FC) of CPI from ~200% to ~64% ($p<0.01$), however the foaming stability (FS) of CPI was not affected ($p>0.05$). For the CPI-HMP mixture FC (~190%) and FS (~68%) were not significantly different ($p>0.05$) from the CPI control. Schmidt et al. (2010) reported that the addition of pectin (DM 43% and DM 74%) did not change the FC of napin but did increase napin's FS through delayed liquid drainage from the foam caused by the presence of napin-pectin complexes. The emulsion properties of a protein can be improved by the addition of a complexing polysaccharide by increasing the viscosity of the continuous phase, steric hindrance between neighboring oil droplets by polysaccharide tails and a stronger electrostatic viscoelastic layer at the interface induced by protein polysaccharide electrostatic interactions. Neither pectin type affected the emulsion stability (ES) of CPI which was relatively high at both pHs tested (pH 5.30, ES ~86%; pH 4.80, ES ~90%). Similar to ES the emulsion capacity (EC) of CPI remained unchanged

($p>0.05$) with the addition of HMP or LMP which at the corresponding pHs had EC of ~250-273 g/g and ~177-202 g/g, respectively. The lack of increased CPI ES or EC under coacervation conditions with pectin may be due to the low concentration of both protein and polysaccharide used or the already high emulsifying properties that CPI possesses. In contrast to the present findings Uruakpa et al. (2005) found the addition of an anionic polysaccharide (κ-carrageenan) to CPI under complexing conditions increased the emulsifying properties (emulsifying activity index and emulsion stability) of CPI, however the concentration of both protein (10-20%) and polysaccharide (1-3%) used was much higher than in the present study. Tolstoguzov (1991) attributed an increase in stability from 67% for legumin alone to 96% for pectin-legumin stabilized emulsions under acidic complexing conditions to be due to an increased charge density of the protein-polysaccharide layer adsorbed at the interface and an increase in hydrophobic residues exposed to the interface due to the change in conformational arrangement of legumin induced by the addition of pectin.

7.5 SUMMARY

In conclusion, complex formation between CPI and both HMP and LMP was mainly governed by pH and biopolymer mixing ratio and driven by electrostatic interactions occurring between small CPI-CPI aggregates and pectin chains. At lower biopolymer mixing ratios (<10:1) repulsion between pectin chains slightly inhibited complex formation with CPI. Maximum CPI-HMP and CPI-LMP interactions were found to occur at pHs 5.30 and 4.80, respectively, and at the 10:1 biopolymer mixing ratio. Higher mixing ratios (>10:1) did not further enhance complex formation. The coacervate phase exhibited pseudoplastic flow behavior. Complex coacervation slightly increased the solubility of CPI in the presence HMP, yet had no effect in the presence of LMP. Except for decreased foaming capacity of the CPI-LMP complexed mixture, the foaming stability, emulsion capacity and emulsion stability of CPI remained unchanged regardless of both HMP and LMP addition. Complexed CPI-pectin may be applicable as a thickening agent, as well as for enhancing pouring and suspension properties of food products.

Table 7.1 Functional attributes of CPI-pectin (10:1 mixing ratio) electrostatic complexes at a pH corresponding to conditions where maximal biopolymer interactions occurs. Data represent the mean ± one standard deviation (n=3). Abbreviations: Canola protein isolate (CPI); high methoxy pectin (HMP); low methoxy pectin (LMP).

Biopolymers	pH	Solubility (%)	Foaming Capacity (%)	Foaming Stability (%)	Emulsion Stability (%)	Emulsion Capacity (g/g)
CPI-HMP	5.30	96.14 ± 1.19	195.56 ± 13.88	69.68 ± 2.73	87.33 ± 3.06	251.25 ± 8.66
CPI	5.30	93.53 ± 1.13	186.67 ± 6.67	66.64 ± 2.34	85.33 ± 4.16	272.92 ± 7.22
CPI-LMP	4.80	95.05 ± 1.43	64.44 ± 3.85	72.59 ± 4.49	93.33 ± 1.15	177.08 ± 7.22
CPI	4.80	93.20 ± 0.68	200.00 ± 13.33	79.94 ± 1.34	88.67 ± 4.16	202.08 ± 7.22

-Chapter 8-

Formation and functional attributes of electrostatic complexes involving napin protein isolate and anionic polysaccharides[4]

Andrea K. Stone, Anzhelika Teymurova, Qian Dang, Sujeema Abeysekara, Anna Karalash and Michael T. Nickerson

[+]Department of Food and Bioproduct Sciences, University of Saskatchewan, 51 Campus Drive, Saskatoon SK, Canada, S7N 5A8

[4]European Food Research and Technology, 238, 773-780 (2014)

8.1 ABSTRACT

The formation of napin protein isolates (NPI) and carboxylated (alginate) (AL) and sulphated (κ-, ι-, λ-type carrageenan) (CG) polysaccharide complexes were investigated at a biopolymer mixing ratio of 10:1 (NPI: polysaccharide) as a function of pH (4.0-12.0) using turbidity and electrophoretic mobility. The functionality of the ensuing complexes was tested on the basis of their solubility, emulsion stability, and foaming capacity and stability relative to NPI alone. Complexation follows two pH-dependent structure forming events associated with the formation of 'soluble' and 'insoluble' complexes. Soluble and insoluble complexes for NPI-AL, NPI-κ-CG, NPI-ι-CG and NPI-λ-CG mixtures occurred at pHs 7.1 and 6.2, 8.6 and 7.0, 9.5 and 9.3, and 9.0 and 8.7, respectively. Complexation resulted in a shift in net neutrality from 5.0 for NPI alone, to pH 4.2, 3.7, 3.2 and 2.3 in the presence of κ-CG, ι-CG, λ-CG and AL, respectively. Solubility and foaming capacity of NPI were reduced with the addition of polysaccharide. Foaming stability was similar for NPI-κ-CG and NPI-λ-CG mixtures relative to NPI, but increased and decreased for NPI-ι-CG and NPI-AL mixtures, respectively. Emulsion stability was found to be similar for all mixtures relative to NPI, except for the NPI-ι-CG mixture which had reduced emulsion stability.

8.2 INTRODUCTION

Canola (*Brassica napus L.*) is an economically important crop grown in Canada primarily for its oil content for use in cooking and biofuel applications (Wu and Muir, 2008). The remaining meal after oil extraction tends to be rich in protein (~50% on a dry basis) and fibre, and used in low value feed applications for improved animal health. Tremendous opportunity exists to further extract the valuable protein fraction from the meal for use in food and/or biomaterial applications. However, a greater understanding of the protein's functionality and interactions with other ingredients is needed prior to market integration.

Canola is comprised of two major storage proteins: cruciferin, a 12S hexameric globulin-type protein with a molecular mass of ~300 kDa and isoelectric point (pI) of 7.2; and napin, a 2S dimeric albumin-type protein with a molecular mass of 14-17 kDa and a varying pI point depending on the extraction method used and isoforms present. Cruciferin is comprised of two polypeptide chains (α-chain, 30 kDa; β-chain 20 kDa) joined by a disulphide bond (Lampart-Szczapa, 2001; Aider and Barbana, 2011), whereas napin is comprised of two smaller polypeptide

chains (4.5 and 10 kDa) also linked primarily by a disulphide bond (Monsalve and Rodriguez, 1990; Bérot et al., 2005). Cruciferin and napin account for ~60% and ~20% of the total protein content within the meal, respectively (Höglund et al., 1992). The functionality (e.g., emulsifying, foaming and gelling abilities, and solubility) of canola proteins have typically been tested using mixed isolates, with little or no fractionation (Aluko and McIntosh, 2005; Yoshie-Stark et al., 2006; Wu and Muir, 2008; Khattab and Arntfield, 2009; Guo et al., 2010), or using chemically modified proteins (e.g., acetylation and succinylation) (Gruener and Ismond, 1997). However, functional studies on canola proteins in the presence of polysaccharides has been limited and typically restricted to solutions of high concentrations (~20%) (Uruakpa and Arntfield, 2005a,b; Arntfield, 2006).

Depending on the solution pH and biopolymer characteristics, segregative or associative phase separation may occur within protein-polysaccharide mixtures. The former involves the electrostatic repulsion between two similarly charged biopolymers, whereas the latter involves the electrostatic attraction between two biopolymers of opposing net charges (de Kruif et al., 2004; Schmitt and Turgeon, 2011). Associative phase separation typically involves the attraction of a positively charged protein (pH<pI) with an anionic polysaccharide. However, in the presence of highly charged polyelectrolytes (e.g., carrageenan and alginate) initial intermolecular interactions may occur at pH>pI where biopolymers are of similar net charges, due to polysaccharide interactions with positive patches on the protein's surface (de Kruif et al., 2004; Weinbreck et al., 2004; Fang et al., 2006; Stone and Nickerson, 2012). In either case, initial interactions lead to two pH-dependent structure forming events associated with the formation of soluble (denoted at pH_c) and insoluble (denoted at $pH_{\phi 1}$) complexes and are evident by a minor and major increases in turbidity, respectively, as a function of pH (Li et al., 1994; Weinbreck et al., 2004; Liu et al., 2009). It is noteworthy to mention the 'soluble' and 'insoluble' terms are used to describe the state of phase separation, rather than relate to a specific functionality measurement. The formation of electrostatic complexes can then lead to either liquid-solid phase separation into a solvent-rich or precipitate phase, or liquid-liquid phase separation into a solvent-rich and coacervate phase (de Kruif et al., 2004; Stone and Nickerson, 2012). Biopolymers within the coacervate phase tend to be more mobile, less compact and have a greater amount of entrapped solvent, than biopolymers within a precipitate (de Kruif et al., 2004).

The overall goal of the present study is to investigate the effect of pH and polysaccharide-type on the formation of electrostatic complexes involving a mixture of NPI with (κ-, ι- and λ-type) carrageenan (CG) and alginate (AL) polysaccharides. And then study the functionality of the mixed complexes versus NPI alone to better characterize negative, neutral or positive effects on protein functionality. Carrageenan is an anionic linear sulfated polysaccharide derived from red algae (*Rhodophyceae*), comprised of partially sulphated repeating, (1- 3) linked β-D-galactose and (1-4) linked 3,6-anhydro-α-D-galactose, disaccharide units (Clark and Ross-Murphy, 1987). The three main classes of CG, κ-, ι-, and λ-type, are based on the number of sulphate groups (1, 2 and 3, respectively) per repeat unit. In contrast, alginate is a linear polyuronic polysaccharide extracted from brown seaweed (*Phaeophyceae*), and consists of (1→4)-linked blocks of poly-β-D-mannuronic acid (M), poly-α-L-guluronic acid (G) and mixed MG blocks (Harnsilawat et al., 2006).

8.3 MATERIALS AND METHODS

Materials

Canola seed *(B. napus* /variety VI-500) was obtained from Viterra Inc. (Saskatoon, SK, Canada), whereas all polysaccharide-types (AL, κ-CG, ι-CG and λ-CG) were purchased from Sigma Aldrich Canada Ltd. (Oakville, ON, Canada). Chemical analyses for all materials were performed according to the Association of Official Analytical Chemists Methods 925.10, 923.03, 920.87 and 920.85 for moisture, ash, crude protein (N% x 6.25) and lipid (% wet basis (wb)), respectively. Carbohydrate content was determined based on percent differential from 100%. In the case of all polysaccharides, protein and lipid contents were assumed to be negligible. Proximate composition for all biopolymers is given in Table 8.1. Biopolymer concentrations used in this study reflect the protein (napin) or carbohydrate (AL, κ-, ι-, λ-CGs) content rather than powder weight. Canola oil was purchased from Loblaws Inc. (Toronto, ON, Canada). All chemicals used in this study were reagent grade, and purchased from Sigma Aldrich Canada Ltd. (Oakville, ON, Canada).

Table 8.1 Chemical composition of NPI and anionic polysaccharides (%, wet basis (w.b). Data represent the mean ± one standard deviation (n = 3)

Biopolymer	Protein (%, wb)	Moisture (%)	Ash (%, wb)	Lipid (%, wb)	Carbohydrate[a] (%, wb)
Napin	93.58 ± 0.65	3.01 ± 0.27	0.75 ± 0.09	0.51 ± 0.27	2.15
Alginate	-	12.34 ± 0.06	23.46 ± 0.15	-	64.20
κ-Carrageenan	-	7.51 ± 0.78	21.45 ± 0.10	-	71.04
ι-Carrageenan	-	10.82 ± 0.28	24.97 ± 0.46	-	64.40
λ-Carrageenan	-	12.26 ± 0.47	23.95 ± 0.34	-	63.79

[a]Carbohydrate levels were determined as the percent difference from 100% after protein, moisture, ash and lipid were determined. Mean values were used in this calculation

Preparation of the NPI

Prior to use, canola seeds were stored in containers at 4°C. At room temperature (21-23°C), small seeds were first removed using a #12 (1.7 mm mesh size) Tyler mesh filter (Tyler, Mentor, OH, USA) in order to maximize the cracking efficiency of the screened seeds. The latter was then placed in a -40°C freezer overnight to aid in the dehulling processes. Frozen seeds were then cracked using a stone mill (Morehouse-Cowles stone mill, Chino, CA, USA), followed by separation of the seed coat and cotyledons using an air blower (Agriculex Inc., Guelph, ON, Canada) which separates based on density differences between the two. The dehulled seeds were then pressed using a continuous screw expeller (Kornet, Type CA59 C; IBG Monforts Oekotec GmbH & Co., Mönchengladbach, Germany) to remove the majority of the oil. The screw expeller was operated at speed 6.5 using a 3.5 mm choke, resulting in a meal temperature of ~75°C. The meal was ground into a powder and residual oil was reduced using hexane (1:3 meal: hexane ratio) at room temperature for 16 h, twice. The defatted meal was left in a fume hood overnight to allow residual hexane to evaporate.

NPI was prepared based on methods of Wanasundara and McIntosh (2008). In brief, 100 g of defatted ground meal was dispersed in 1 L of Milli-Q™ water containing 0.75% NaCl, adjusted to pH 3.0 using 1.0 M HCl, and then allowed to stir continuously (500 rpm) for 90 min at room temperature (21-23°C). The dispersion was centrifuged at 17,700 × *g* for 20 min at 4°C using a Sorvall RC-6 Plus centrifuge (Thermo Scientific, Asheville, NC). The supernatant was collected

through vacuum filtration using Whatman No. 1 filter paper (Whatman International Ltd., Maidstone, UK). Afterwards, the filtered supernatant was adjusted to neutral pH (6.8-7.0) using 1.0 M NaOH, followed by centrifugation at 17,700 × *g* for 20 min at 4°C using the same centrifuge to separate the precipitant. The supernatant was then diafiltrated with Pellicon-2 Tangential flow membrane filtration system through a 5 kDa regenerated cellulose membrane (using 3 membranes with area size 0.1 m^2 each) (Millipore Corporation, Milford, MA) to remove salt and larger molecular weight substances from the liquid (Wanasundara and McIntosh, 2008). The concentrated supernatant was stored at -30°C until freeze-drying took place to yield a free flowing powder.

Sodium dodecyl sulfate polyacrylamide gel electrophoresis (SDS-PAGE) under reducing conditions

Sodium dodecyl sulphate-polyacrylamide gel electrophoresis (SDS-PAGE) was performed on NPI using a Protean III mini system (Bio-Rad Laboratories, Inc., Hercules, CA, USA). In brief, samples were prepared by dissolving 2 mg of NPI in 1 mL of 0.1 M Tris-HCl buffer (containing 5% SDS (w/v) and 2% β-Mercaptoethanol, pH 8.00), followed by heating at 95°C (Incu Block model 285, Denville Scientific Inc., South Plainfield, NJ, USA) for 10 min to unravel and disassociate the protein. Solutions were then cooled to room temperature (21-23°C) before centrifuging with a microcentrifuge (Hetovac VR-1, Heto Lab Equipment, Denmark) at 12,000 x *g* for 10 min to remove any insoluble material. A 1 µL volume of the NPI samples and a set of molecular mass standards (Bio-Rad Broad Range Marker, 7,100–209,000 MW, Bio-Rad Laboratories, Inc., Hercules, CA, USA) were added to wells on a 15% Tris-HCl precast polyacrylamide gel (Bio-Rad Laboratories, Inc., Hercules, CA, USA) at 100-110 V for ~1.5 h. Protein bands were stained by using a Coomassie blue R-250 solution for 45 min, and then de-stained with a 10% acetic: 20% methanol solution.

Turbidimetric acid-pH titrations

Optical density (O.D.) was investigated as a function of pH (12.0-4.0) during an acid titration for both individual and mixed biopolymer solutions at a total biopolymer concentration of 0.1% (w/w) at room temperature (21-23°C). A 10:1 NPI: polysaccharide ratio was used for all mixed systems. Biopolymer solutions were prepared by dispersing their respective powders in 50

mL of Milli-Q water (Millipore Milli-Q^{TM}), followed by a pH adjustment to 12.0 with 1 M NaOH, and then allowed to stir (500 rpm) for 1 h at room temperature. Solution pH was re-adjusted periodically during stirring. Optical density was then followed at 600 nm using an ultraviolet visible spectrophotometer (Genesys 10-S, Thermo Scientific, Asheville, NC, USA) and plastic cuvettes (1 cm path length) during an pH-acid titration using HCl to lower the pH. Critical pH values (pH_c and $pH_{\phi 1}$) were determined graphically on individual turbidity curves by the intersection point of two curve tangents as described by Liu et al. (2009) and Weinbreck et al. (2003). All measurements were made in triplicate.

$$\%FC = \frac{V_{fo}}{V_{li}} \times 100\% \qquad \text{(eq. 8.2)}$$

$$\%FS = \frac{(V_{fo})}{(V_{f30})} \times 100\% \qquad \text{(eq. 8.3)}$$

Emulsion stability (ES): ES was measured using a modified method of Liu et al. (2010). In brief a 50/50 oil-in-water emulsion was prepared by transferring 5 mL of the aqueous biopolymer solution and 5 mL of canola oil into a 50 mL centrifuge tube. An emulsion was formed by homogenization using an Omni Macro Homogenizer equipped with a 20 mm diameter saw tooth generating probe, at 8,000 rpm for 5 min. After homogenization, emulsions were transferred into individual 10 mL graduated cylinders (inner diameter 10.80 mm; height 100.24 mm) and left for separation over 30 min. The *%ES* was determined using eq. 8.4,

$$\%ES = \frac{V_B - V_A}{V_B} \times 100\% \qquad \text{(eq. 8.4)}$$

where V_B and V_A are the volume of the aqueous (or serum) layer before emulsification (5.0 mL) and after 30 min of drainage, respectively.

Statistical analysis

A paired Student's T-test was used to test for statistical differences in functional properties between the mixed system and NPI. Statistical analyses were performed using Microsoft Excel 2010 (Microsoft Corporation, Redmond, WA).

10.4 Protein-stabilized emulsions

The stability of protein-stabilized emulsions is dependent upon the protein (e.g., globular vs. fibrous, conformational flexibility, molecular weight) and surface (e.g., hydrophobic and hydrophilic residues) characteristics, processing conditions (e.g., shear and heat) and solvent properties (e.g., temperature, pH and salts). During emulsion formation, soluble proteins diffuse towards the interface, then re-arrange and re-organize at the interface to orient hydrophobic amino groups towards the non-polar oil phase and the hydrophilic amino groups towards the aqueous phase forming a viscoelastic film (Dalgleish, 1997) (Figure 10.2a). This process is highly depended on the molecular flexibility and packing of the protein (Freer et al., 2004). Film strength is then enhanced via protein-protein interactions, hydrogen bonding and electrostatic interactions and van der Waals attractive forces. Moreover, the addition of macromolecules such as protein would increase the overall viscosity of the medium and restrict random movements of the oil droplets. In some studies cross-linking agents (e.g., transglutaminase) is added to improve stability (Fñrgemand et al., 1998; Dickinson et al., 1999) of O/W emulsions.

Although the majority of the hydrophobic groups are buried within the interior of the 3-dimensional structure, some remain on the surface amongst the hydrophilic residues as hydrophobic patches. As such, a prerequisite to achieving good emulsion stabilization is partial or complete denaturation or unraveling of the protein to expose reactive non-polar sites (Damodaran, 2005). Depending on the primary structure, and the spatial arrangement of the protein at the interface, tails or loops comprised of protein chains may extend into the aqueous solution leading to steric forces or interactions. In contrast, low molecular weight surfactants tend to form micelles in the aqueous phase, and diffuse towards the interface at a much faster rate (Figure 10.2b). Alignment at the interface tends to result in complete coverage rather than having irregular intermittent breaks in the viscoelastic films due to the presence of loops or tails, or from incomplete absorption to the oil-water interface.

Protein absorbed to the interface often forms a thin film around the dispersed droplet. The viscoelastic film typically provides an electric charge to the droplet, which depending on the pH, may lead to attraction or repulsion between neighboring droplets (Friberg et al., 2004). The concentration of protein absorbed at the interface could also affect the film formation, and could have detrimental effects on emulsion stability. For instance, insufficient protein at the interface could lead to a thinner film, which is more susceptible to film rupture or incomplete coating of the

droplet (Tcholakova et al., 2002; McClements, 2004). In turn, this could increase the chance of coalescence when droplets are of close proximity. When there is sufficient protein absorbed at

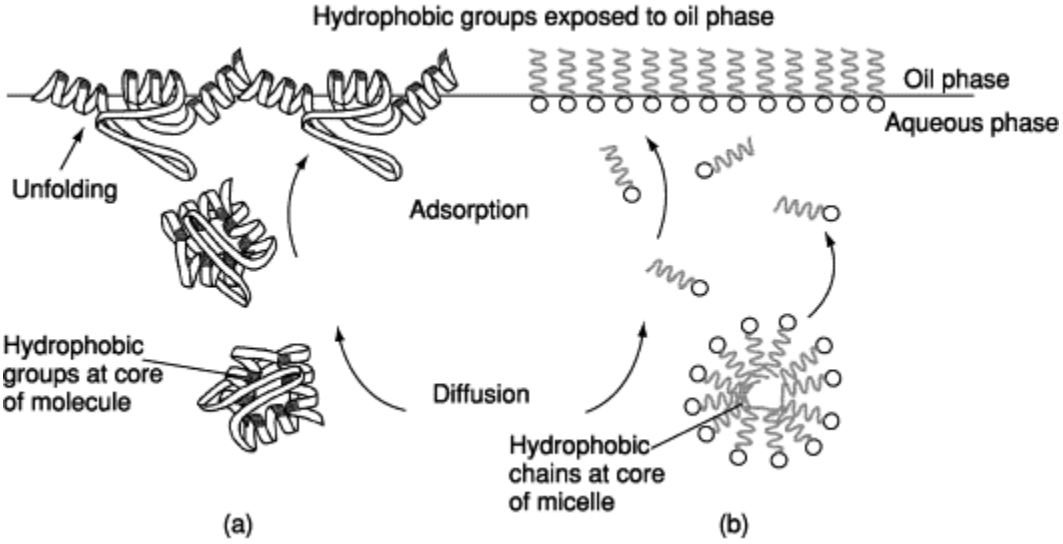

Figure 10.2 Schematic diagram of protein (a) and low molecular weight surfactant (b) absorption to an oil-water interface (reproduced with permission from Robins and Wilde, 2003).

the interface, the stability of emulsion is mainly affected by the mechanical force input to form smaller droplets which could reduce the density differences of the dispersed phase and the continuous phase and delay gravitational separation (McClements, 2004). The relationship of mean droplet size and protein as emulsifier concentration can be illustrated mathematically (eq. 10.2).

$$r_{\min} = \frac{a\Gamma_{sat}\phi}{cs} = \frac{a\Gamma_{sat}\phi}{cs'(1-\phi)} \qquad \text{(eq. 10.2)}$$

Where, Γ_{sat} is the excess surface concentration of the emulsifier at saturation (in kg m^{-2}), ϕ is the disperse phase volume fraction, *CS* is the concentration of emulsifier in the emulsion (in kg m^{-3}) and *CS'* is the concentration of emulsifier in the continuous phase (in kg m^{-3}) (McClements, 2004). Excess protein or protein that cannot be absorbed at the interface could cause depletion flocculation due to competition of solvent around and between the droplets similar with the "salting out"

phenomenon (McClements, 2000). A critical flocculation concentration (CFC) has to be reached before depletion flocculation occurs and CFC value reduces as droplet size increases and protein volume fraction increases (McClements, 2000). Proteins rich in sulfur containing amino acids such as rapeseed proteins, could form disulfide bonds with other protein molecules as the protein unravel at the interface (Wu et al., 2011). Disulfide bonds formed between proteins at the same interface could enhance emulsion stability (Tcholakova et al., 2002). However, disulfide bonds formed between two different interfaces might lead to flocculation and followed by coalescence and it is also known as bridging flocculation (Joshi et al., 2012; Wang et al., 2012). Joshi et al. (2012) also suggested reducing inter and intra disulfide bonding all together could improve overall emulsion stability in a lentil protein stabilized emulsion.

Protein stabilized emulsions are most stable at pHs away from its pI value because of the presence of an electric charge on the oil droplet's surface which acts to repel neighboring droplets. In contrast, when solution pH is close to the pI of the protein, electrostatic repulsive forces are minimal between droplets enabling them to flocculate or undergo partial or complete coalescence (Xu et al., 2005; Foegeding and Davis, 2011). Larger droplets are than more prone to gravitational separation. Furthermore, protein solubility tends to be reduced near the pI of the protein, also leading to flocculation and/or partial or complete coalescence and subsequent reduced absorption to the oil-water interface (Kinsella, 1979). Often low protein solubility is associated with poor emulsifying properties (Dickinson, 2003; Can Karaca et al., 2011).

Protein stabilized emulsion are also very sensitive to ionic strength, which when levels exceed certain concentration, emulsion stability can be reduced (McClements, 2004). Multivalent ions such as Ca^{2+}, Mg^{2+},Fe^{2+} or Fe^{3+} are more prone to cause emulsion instability than monovalent ions such as Na^{+}, Cl^{-} or K^{+} because they are more effective at screening electrostatic repulsive forces between surfaces to reduce the zeta potential (ζ), which is a measure of the protein's surface charge (Keowmaneechai and McClements, 2002). Demetriades and co-workers (1997) found that an oil-in-water emulsion stabilized by 2% whey protein was unstable when pH was close to pI of whey protein (pH 4.6). The authors also reported the addition of NaCl up to 100 mM resulted in large droplet sizes, and high levels of flocculation and creaming. Kulmyrzaev et al. (2000) found emulsions prepared with diluted whey protein isolate (0.5% w/w) showed that the addition of only 20 mM of $CaCl_2$ resulted in 3 times reduction in the zeta potential around the droplets both below and above the isoelectric point of whey protein. The authors also found emulsion stability was

relatively insensitive to $CaCl_2$ (<20 mM) when pH was below the pI of whey protein, however creaming occurred at pH above the pI of whey protein at levels > 5 mM and above $CaCl_2$ (Kulmyrzaev et al., 2000). Solubility and zeta potential of canola protein isolate was also found lowest near the isoelectric point (pH 4-5) and reduced substantially with the addition of 350 and 700 mM NaCl by Paulson and Tung (1987).

According to the Stokes' Law (eq. 10.1), creaming rate has a reciprocal relationship with bulk phase viscosity. Increasing bulk phase viscosity could reduce the chances of droplet-droplet collision which might induce coalescence (McClements, 2004). Previous studies have shown the addition of sucrose was able to improve the thermal stability of milk protein stabilized emulsions (Kim et al., 2003). The authors also found the addition of sucrose before thermal treatments prevented extensive droplet aggregation, however if the sucrose was added after thermal treatment, it promoted droplet aggregation. The author speculated that sucrose affects emulsion stability mainly by stabilizing the conformation of the adsorbed protein rather than changing the properties of the bulk phase condition since the results showed dependency on the order of addition of sucrose before or after thermal treatment (Kim et al., 2003).

The other important aspect to the emulsifying properties of plant protein is the extraction methods because it can impact the purity, quantity and the conformational structure of the protein extracted (Aider and Barbana, 2011; Can Karaca et al., 2011). For oilseed proteins, the defatting process used to create an oil free meal involves the use of both heat and chemicals, and often leads to partial or complete denaturation of the protein (Khattab and Arntfield, 2009). Table 10.1 provides some brief methodology for extracting proteins from various oilseeds found in literature, along with their emulsifying properties, using emulsifying activity index (EAI) and emulsion stability (ES) as indicators. EAI indicates the area of interface covered per one gram of protein, whereas ES is the measure of creaming after a standard period of time to quantify the ability of the protein film to stabilize the emulsion to delay droplet aggregation.

Many plant protein materials contain undesirable compounds which will affect the organoleptic and/or functional properties of the protein. For instance, oilseed proteins often contain phenolic compounds and phytates that make them undesirable as a human food ingredient because of the inferior organoleptic properties or poor functional properties (Schwenke, 1994; Krause et al., 2002; Wanasundara, 2011). Fortunately, with proper extraction, these undesirable compounds

Table 10.1 Summary of various extraction processes for oilseed protein isolates, and their emulsifying properties reported in literature (modified from Moure et al., 2006).

Protein in oilseeds	**Extraction Solvent/pH/time(h)/temperature ºC**	**Purification**	**EAI (m^2/g)**	**ES (%)**	**Reference**
Almond	20 mM Tris-HCl/8.1/1/25	Dissolve defatted meal. Filter through glass wool, followed by centrifugation. Supernatant is then filtered to remove debris, and dialyzed against 5 L of distilled deionized water. Supernatant is then freeze-dried.	51.77	-	Sze-Tao and Sathe, 2000
Canola	0.1 M NaOH/–/0.33/23	Dissolve defatted meal. Filter with filter paper, adjust to pH 4.0, centrifuge, wash to remove salt, and then centrifuge again to recover the pellet.	28.27	71.0	Aluko and McIntosh , 2001
Canola	0.1 M NaOH/–/0.33/23	Dissolve defatted meal. Filter with filter paper, adjust to pH 6.0, add $CaCl_2$ up to 1 M, and centrifuge. The supernatant is diluted in 200 volume of water to remove salt, and then recover protein after centrifugation.	32.34	26.9	Aluko and McIntosh, 2001
Canola	0.3 M NaCl/-/4/23	Dissolve defatted meal. Centrifuge, filter the supernatant, further concentrate the supernatant by ultrafiltration, and then dilute the supernatant with 6x volume of water, and recover protein micelle by centrifugation.	39.80	68.0	Gruener and Ismond, 1997a,b

Table 10.1 Summary of various extraction processes for oilseed protein isolates, and their emulsifying properties reported in literature (modified from Moure et al., 2006) (Continued).

Flaxseed	0.5 M NaCl/5.5-6.5/1/25	Dissolve defatted meal and collect clear supernatant. Concentrated supernatant by ultrafiltration, dilute with 5x volume of cold water, and then centrifuge to recover the protein micelle.	2550	80.0	Krause et al., 2002
Flaxseed	Water/8.5/–/25	Dissolve defatted meal. Adjust pH to 4.5 to precipitate the protein, and then centrifuge to obtain protein material.	2100	81.5	Krause et al., 2002
Sesame	1 M NaOH/9.5/1/50	Dissolve defatted meal. Sample is centrifuged, the supernatant liquid is adjusted to pH 4.9, and then stirred for 1 h at 50−55 °C and again centrifuged, the solid residue is collected and dried.	114.33	35.5	Bandyopadhyay and Ghosh, 2002
Soybean	20 mM Tris-HCl/8.1/1/25	Dissolve defatted meal. Filter through glass wool, and then centrifuge. The supernatant is adjusted to pH 4.5 and centrifuged to precipitate the proteins. Proteins were dialyzed against distilled deionized water.	11.61	–	Sze-Tao and Sathe, 2000
Soybean	Acetic acid-acetate buffer/4.5/–/25	Dissolve defatted meal. Protein is fractionated by ultrafiltration with 10, 30 and 50 kDa cut off (centrifugation prior to ultrafiltration is optional) and concentrated using a 5 kDa membrane.	106.7	27.6	Moure et al., 2005

could be reduced to safe levels suitable for human consumption (Ismond and Welsh, 1992). Krause and co-workers (2002) extracted flaxseed protein isolate with conventional isoelectric precipitation (IP) and protein micellar mass (PMM) methods and found although 11S globulin was the main fraction in both isolates, the isolate produced by IP had lower solubility and EAI compared with the isolate produced by the PMM method. In the same study, isolates produced by the PMM method also achieved much lower phenolic and phytic acid levels. The authors stated that PMM method preserved the protein's native form with minimal amount of undesirable compounds, whereas IP produced isolate might have undergone partial denaturation and irreversible protein aggregation (Krause et al., 2002).

8.4 RESULTS AND DISCUSSION

Characterization of the biopolymer materials

The NPI was found it to be comprised of ~93.6% (w.b.), ~3.0% moisture, ~0.8% (w.b.) ash, ~0.5% (w.b.) lipid and ~2.1% (w.b.) carbohydrate (Table 8.1). An SDS-PAGE (under reducing conditions) gel of the NPI found only the presence of two bands of low molecular mass at ~5 and 7 kDa (Figure 8.1). Based on the molecular mass profile, it was hypothesized that disulfide bonds linking the polypeptides together within napin were broken, leading to the respective bands. However further protein sequencing would be required for positive confirmation of the napin molecule. Wanasundara et al. (2012) found under similar extraction and electrophoresis conditions the presence of two bands with molecular masses of 7.2–7.6 and 4.6–4.8 kDa. Extraction under acidic conditions (pH 3.0) is thought to pre-select for basic isomers from the napin proteins. The carbohydrate, ash, and moisture content for the polysaccharides studied (AL, κ-CG, ι-CG, λ-CG) ranged between ~63.8% to ~71.0%, ~21.4% to ~25.0%, and ~7.5% to ~12.3%, respectively (Table 8.1). The high ash content reflects the counter and co-ions used to neutralize the polysaccharides in the commercial extraction process.

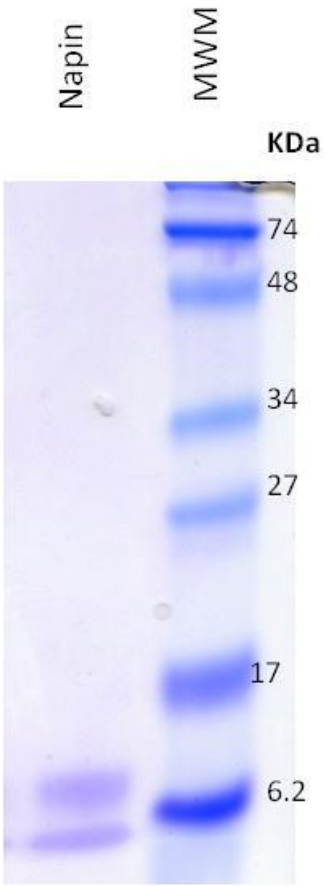

Figure 8.1 SDS-PAGE gel under reducing conditions for a napin protein isolate (NPI) and a molecular weight maker (MWM) solution.

Formation of electrostatic complexes

The formation of electrostatic complexes involving admixtures of NPI and anionic polysaccharides were investigated as a function of pH and polysaccharide-type. Specifically, similarities and differences in complex formation with NPI and a carboxylated polysaccharide (e.g., AL) and a family of sulfated polysaccharides with differing charge densities (e.g., κ-, ι-, λ-type CG) were investigated. Individual NPI and all polysaccharide solutions were found to have no O.D. at the 0.1% (w/w) concentration during an acid titration over the pH range (12.0-4.0) (results not shown). However, significant changes in O.D. were observed in the mixed systems as a function of pH (Figure 8.2). In the case of NPI-AL, the formation of soluble and insoluble complexes was found to occur at pH 7.12 ± 0.08 and 6.21 ± 0.09, followed by a rapid rise to a peak at pH 6.0 and an O.D. maximum of ~1.360, followed by precipitation (Figure 8.2). Optical

density data was removed from the turbidity curves in Figure 8.2, once precipitation led to irreproducible O.D. readings.

Based on electrophoretic mobility studies as a function of pH, NPI was found to have an isoelectric point (pI) at pH 5.0, where at pH>pI and <pI the protein molecule assumes a net negative and positive charge, respectively (Figure 8.3). Figure 8.3A and 8.3B shows the zeta potential as a function of pH for individual and mixed systems, respectively. NPI alone shows only a very weakly charged molecule, ranging from <+5 mV at pH 2.0 to < -30 mV at pH 10.0. In contrast, AL chains remain very negatively charged, ~-80 mV for the majority of the pH range (4.0-10.0), then increased significantly to ~-8 mV at pH 2.0, as carboxylate sites become protonated (pK_a $–COO^-$ ~1.88) (Liu et al., 2009). Findings from this study indicate that NPI-AL complexation initially occurring at pHs where the two biopolymers carry a similar net negative charge. However, it is believed that this initial complexation is occurring between AL chains and positively charged patches of the NPI's surface. A similar phenomenon has been reported in other mixed systems involving a protein and a highly charged polyelectrolyte, as was the case for gelatin-κ-CG (Antonov and Goncalves, 1999), ovalbumin-CG (Galazka et al., 1999) and whey protein-CG (Weinbreck et al., 2004). The mixed complex resulted in a steady rise in zeta potential from pH 10.0 to 2.0, in which net neutrality (0 mV) was reached at pH 2.1. Electrostatic interactions between NPI and AL also led to an increase in negative charge on the NPI molecule (Figure 8.3).

In contrast to AL, mixtures involving CG resulted in a much greater shift towards higher pHs where initial complexation was believed to be associated with a more electronegative sulfate group on the CG backbone which can interact more strongly to positive patches on the NPI's surface. For instance, the formation of soluble and insoluble complexes were found to occur at pH 8.25 ± 0.10 and 7.02 ± 0.08, respectively for NPI-κ-CG mixtures, and at pH 9.53 ± 0.12 and 9.27 ± 012, respectively for NPI-ι-CG mixtures. Maximum O.D. occurred at ~pH 5.0 (O.D. ~0.500) and ~pH 8.0 (O.D. ~0.800) for the NPI-κ-CG and NPI-ι-CG mixtures, respectively (Figure 8.2), followed by precipitation. Complexation of NPI was greater with ι-CG than κ-CG which was hypothesized to be due to the higher linear charge density (2 sulfate groups vs. 1 sulfate group per disaccharide repeating unit) of ι-CG. Unbound (free) sulfate groups in the NPI-κ-CG mixture may have suppressed NPI-NPI-aggregation and, therefore, led to the reduced magnitude of O.D. For both CG types, a double helix model is the most widely accepted secondary structure in solution (Rees et al., 1969, Nilsson and Piculell, 1991). The higher O.D. maximum values in the NPI-AL

mixture relative to the NPI-CG mixtures (excluding λ-CG) may be explained by the presence of CG sulphated groups which would provide charge repulsion to suppress structure formation.

In the case of λ-CG, the formation of soluble and insoluble complexes occurred at pHs 8.97 ± 0.03 and 8.61 ± 0.05, respectively, which was in-between the pH shift for NPI-κ-CG and NPI-ι-CG mixtures. Maximum O.D. for the NPI-λ-CG mixture occurred near pH 7.0 with a value of ~1.440 (Figure 8.2). Differences between the NPI-λ-CG and mixtures with other CG-types may be the result of the polysaccharide conformation rather than its charge density. Although λ-CG has a higher linear charge density than the other types (3 sulfate groups per disaccharide repeat unit), its secondary structure is more flexible remaining as a random coil in solution rather than a double helical structure (Rees et al., 1969). Stone and Nickerson (2012) also reported significantly different turbidity spectrums within whey protein isolate-CG mixtures among the different CG-types. In the present study, electrophoretic mobility as a function of pH indicated net neutrality to occur at pH 4.2, 3.7 and 3.1 for NPI and κ-CG, ι-CG and λ-CG mixtures, respectively, a shift from pH 5.0 for NPI alone (Figure 8.3B).

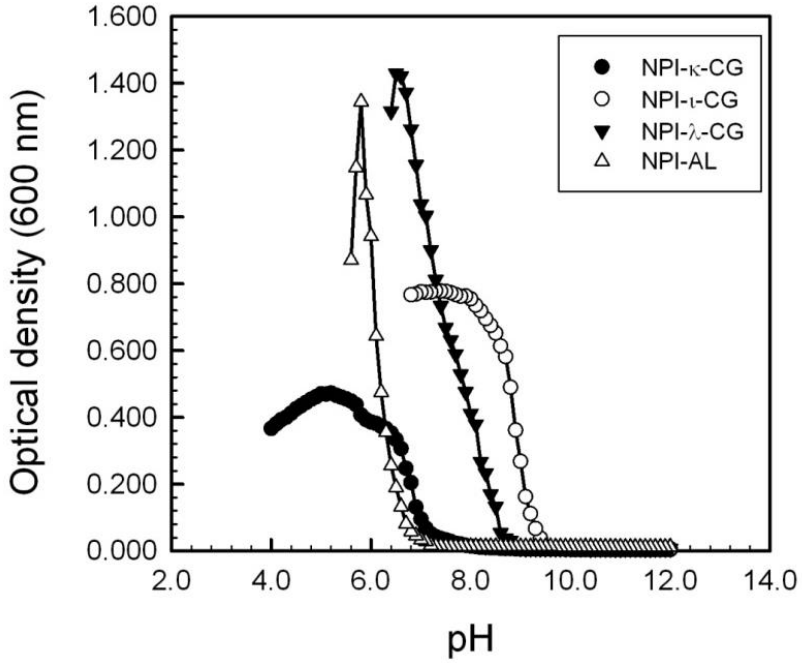

Figure 8.2 Mean turbidity curves of NPI-AL, NPI-(κ-, ι-, λ -)-CG mixtures as a function of pH (n = 3).

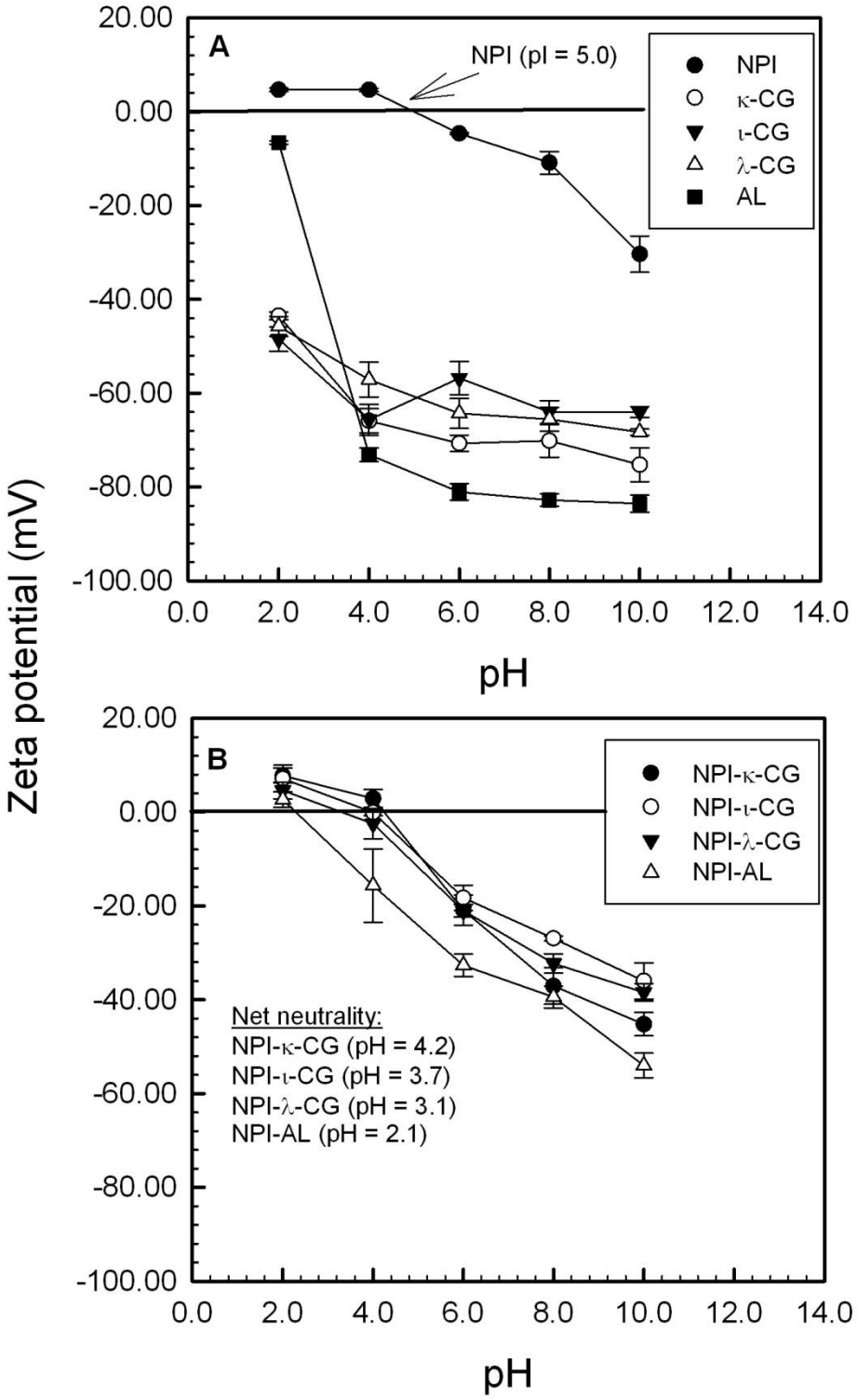

Figure 8.3 Mean zeta-potential (mV) for (a) individual (NPI, AL, κ-, ι-, λ-type CG) and (b) mixed (NPI-AL, NPI-(κ-, ι-, λ-type) CG) solutions. Data represent the mean ± one standard deviation (n = 3).

Functional properties of NPI and NPI-polysaccharide complexes

The functional attributes of NPI and NPI-polysaccharide complexes were compared at pHs corresponding to where the maximum O.D. occurred for each mixture (Figure 8.2). For instance NPI was compared with NPI-κ-CG, NPI-ι-CG, NPI-λ-CG and NPI-AL mixtures at pH 5.0, 8.0, 6.5 and 6.0, respectively (Table 8.2). In the case of solubility, individual NPI solutions were found to be completely soluble regardless of the pH (5.0-8.0). However, the addition of polysaccharides in all cases reduced the solubility of the NPI significantly ($p<0.001$) (Table 8.2). For instance, protein solubility declined in the following order: NPI-κ-CG (~61.7%), NPI-ι-CG (~43.0%) and NPI-λ-CG (~30.4%) as it related to CG-type, and to ~43.4% for NPI-AL mixtures (Table 8.2). Findings were in agreement to turbidity studies where electrostatic interactions were thought to lead to the formation of precipitates, and are in agreement with the interactions between a protein and a strong polyelectrolyte (de Kruif et al., 2004).

In the case of foam capacity, the addition of all polysaccharides led to a decline in FC relative to NPI alone. However, the magnitude of reduction was mixture specific. For instance, the addition of κ-CG to NPI caused only a small reduction in FC from ~231% to ~188% ($p<0.01$), similarly the addition of ι-CG to NPI resulted in a comparable reduction from ~233% to ~189% ($p<0.01$) (Table 8.2). In contrast, the addition of λ-CG to NPI resulted in a much more significant reduction in foam forming abilities, where FC was reduced from ~215% to ~127% ($p<0.001$) (Table 8.2). A similar effect was also found with the addition of AL, where FC was reduced from ~~198% to ~85% ($p<0.001$) (Table 8.2). The decrease in FC of the NPI-polysaccharide complexes relative to NPI alone is hypothesized to be due to the lower solubility of the complexes as compared to the highly soluble NPI. In order to generate a good foam, complexes need to be soluble in order to migrate to the air-water interface and entrap air through the formation of a viscoelastic film.

Foam stability remained unchanged between NPI and NPI-κ-CG at ~76%, and NPI and NPI-λ-CG at ~56% ($p>0.05$) (Table 8.2). In the case of NPI and NPI-ι-CG, FS was improved from ~65% to ~77% ($p<0.01$), whereas FS for the NPI and NPI-AL comparison was reduced from ~73% to ~61% ($p<0.01$) (Table 8.2). The NPI-AL mixture is very highly charged at pH 6.0 as compared to the NPI alone and this may have resulted in electrostatic charge repulsion between the NPI-AL complexes forming the viscoelastic film at the air water interface leading to the decreased FC relative to NPI alone.

Table 8.2 Functional properties of NPI and NPI-polysaccharide complexes. Data represent the mean ± one standard deviation (n = 3).

Material	pH	Sol (%)	FS (%)	FC (%)	ES (%)
NPI	5.0	100.41 ± 1.75	75.99 ± 0.85	231.11 ± 7.70	34.00 ± 3.46
NPI-κ-CG	5.0	61.75 ± 2.28	76.79 ± 1.79	186.67 ± 0.00	40.00 ± 2.00
Statistics		$p<0.001$	NS	$p<0.01$	NS
NPI	8.0	101.75 ± 2.26	65.26 ± 1.21	233.33 ± 6.67	65.33 ± 2.31
NPI-ι-CG	8.0	43.01 ± 1.38	77.07 ± 1.38	188.89 ± 3.85	45.33 ± 2.31
Statistics		$p<0.001$	$p<0.01$	$p<0.01$	$p<0.05$
NPI	6.5	100.76 ± 0.97	56.71 ± 2.41	215.55 ± 3.85	38.67 ± 2.31
NPI-λ-CG	6.5	30.44 ± 3.15	56.15 ± 1.53	126.67 ± 6.67	37.33 ± 2.31
Statistics		$p<0.001$	NS	$p<0.001$	NS
NPI	6.0	98.54 ± 0.76	73.54 ± 4.68	197.78 ± 3.85	42.00 ± 2.00
NPI-AL	6.0	43.43 ± 3.59	61.01 ± 2.85	85.33 ± 6.81	39.33 ± 3.06
Statistics		$p<0.001$	$p<0.01$	$p<0.001$	NS

Abbreviations: Napin protein isolates (NPI); carrageenan (CG); solubility (Sol); foaming stability (FS) and capacity (FC); and emulsion stability (ES).

In the case of emulsion stability, no differences were found between NPI and NPI-polysaccharide mixtures ($p>0.05$), with the exception of NPI and NPI-ι-CG in which ES was found to decline with the addition of the polysaccharide from ~65% to ~45% ($p<0.05$) (Table 8.2). However, this decline was only minor.

8.5 SUMMARY

The formation of NPI-polysaccharide electrostatic complexes within admixtures of NPI and anionic polysaccharides (AL and (κ-, ι-, λ-type) CG) was found to be highly dependent upon polysaccharide-type and pH. All mixtures began interacting at pHs>pI where biopolymers carried

a similar net negative charge. The complexation of polysaccharides to NPI led to significant reductions in solubility and foaming capacity, whereas little to no changes were evident between complexes and NPI for foam and emulsion stabilities. Findings from this study indicated that complexation had largely a negative effect on NPI solubility, however interactions with polysaccharides could be used in the development of protein separation technologies after further exploration.

-Chapter 9-

Summary

In part II of this report, the formation of soluble and insoluble complexes were investigated involving a canola protein isolate (rich in cruciferin) or a napin protein isolate with a variety of polysaccharides as a function of pH and biopolymer mixing ratio. In all cases, protein–polysaccharide interactions followed a typical complex coacervation process in which interactions typically occur via electrostatic attraction leading to the formation of a '*supra-macromolecular*' complex. The functionality of these complexes were also assessed in mixtures of canola/napin protein-polysaccharide mixtures at pH and biopolymer mixing conditions corresponding to the presence of soluble and insoluble conditions. Specifically, protein solubility, foaming capacity and stability, and emulsion capacity and stability were tested. Tables 9.1 and 9.2 summarizes the functional attributes of the soluble and insoluble complexes for the cruciferin-rich protein isolate mixed with polysaccharides, respectively, relative to a CPI control (done at corresponding pH and concentrations used, as in the mixed system); Table 9.3 summaries the functionality of only insoluble complexes of the napin protein isolate and polysaccharides; and Table 9.4 summarizes the functionality of the commercial protein isolates as a reference point.

Functionality of CPI-polysaccharide <u>soluble</u> complexes

The addition of carrageenan to CPI resulted in a loss in total protein solubility of ~14%, ~41% and ~57% for the κ-, ι- and λ-types, respectively (Table 9.1). The loss in solubility corresponded to reduced ability to migrate to the oil-water (emulsions) or air-water (foam) interfaces leading to reduced emulsion and foaming capacities. As complexes begin to form, polysaccharides act to neutralize charges on the protein's surface leading to reduced electrostatic repulsion within solution. As such, complexes tend to aggregate and are more likely to fall out of solution. In contrast the addition of polysaccharides once at the oil/air-water interface did not seem to influence the stability of the emulsions or foams relative to CPI alone (Table 9.1). The addition of high methoxy pectin or gum Arabic to CPI resulted in similar functionality, with the exception of emulsion stability in which the pectin chain lead to only a slight improvement (Table 9.1). Improved emulsion stability is believed to be enhanced by slightly improved viscosity of the continuous phase. The addition of low methoxy pectin to CPI was did not impact CPI solubility,

however the CPI- low methoxy pectin had reduced foaming capacity and stability, and emulsion capacity. Emulsion stability however was slightly improved (Table 9.1).

Functionality of CPI-polysaccharide <u>insoluble</u> complexes

Complexation of carrageenan to CPI resulted in a loss in protein solubility, which in turn had a negative effect on both foam and emulsion formation. Lambda-type carrageenan showed the greatest loss in solubility (~26% total solubility) relative to CPI alone (~91% total solubility), followed by κ-type (~47% total solubility) and ι-type (~62% total solubility) (Table 9.2). Loss in protein solubility was thought to influence the CPI's ability to migrate to the air-water or oil-water interface in order for it to form either a foam or an emulsion, respectively. In the present study, both foam and emulsion capacities were reduced in CPI-carrageenan (all types) systems relative to CPI alone, however stabilities for both slightly improved (Table 9.2). Foam and emulsion stabilities may be enhanced due to the slight increase in viscosity versus the control as the result of a slightly higher total biopolymer concentration. In the case of CPI-pectin (high methoxy) slightly improved solubility, foam capacity/stability and emulsion stability was observed relative to CPI alone, whereas emulsion capacity declined slightly. In contrast, CPI-pectin (low methoxy) had similar solubility and emulsion stability to CPI alone, but lower foam capacity/stability and emulsion capacity values (Table 9.2). 'High versus low methoxy' refers to the amount of esterified galacturonic acid residues with methanol, with the latter being more reactive, especially towards calcium salts. The higher foaming/emulsifying properties of high methoxy pectin-CPI mixtures than with low methoxy may be a consequence of increased hydrophobicity associated with the methanol group. For CPI-gum Arabic mixtures, only foam capacity was reduced relative to CPI alone, with foam stability, emulsion capacity and emulsion stability remaining similar. Solubility of the mixed CPI-gum Arabic system was significantly improved however over CPI alone, increasing from ~39.5% to 56.2% at pH 4.2 (Table 9.2).

Table 9.1. Functional attributes of canola protein isolate (CPI) (Cruciferin-rich)-polysaccharide mixtures under biopolymer and pH conditions where soluble complexes exist. Data represent the mean ± one standard deviation (n=3).

Biopolymer mixtures	Mixing ratio	pH	Solubility (%)	Foaming Capacity (%)	Foaming Stability (%)	Emulsion Stability (%)	Emulsion Capacity (g/g)
CPI (control)	20:1	6.75	96.50 ± 0.44	271.11 ± 10.18	74.20 ± 0.70	86.00 ± 2.00	225.31 ± 7.58
CPI-κ-carrageenan	20:1	6.75	84.27 ± 2.37	144.44 ± 10.18	69.95 ± 3.42	91.67 ± 5.13	194.69 ± 7.58
CPI-ι-carrageenan	20:1	6.75	68.35 ± 2.29	120.00 ± 5.77	70.87 ± 0.98	96.00 ± 2.00	190.31 ± 0.00
CPI-λ-carrageenan	20:1	6.75	61.90 ± 5.74	111.11 ± 3.85	64.40 ± 4.88	87.33 ± 3.06	164.06 ± 0.00
CPI (control)	10:1	7.25	97.80 ± 0.47	280.00 ± 8.82	72.79 ± 1.46	77.50 ± 1.32	194.80 ± 7.94
CPI-pectin (high methoxy)	10:1	7.25	97.29 ± 0.78	282.22 ± 6.94	73.43 ± 0.41	88.00 ± 2.00	203.96 ± 7.94
CPI (control)	10:1	6.00	96.36 ± 1.04	227.78 ± 6.94	72.92 ± 1.29	81.33 ± 2.31	249.80 ± 7.94
CPI-pectin (low methoxy)	10:1	6.00	95.39 ± 1.27	191.11 ± 3.85	56.98 ± 1.73	100.00 ± 0.00	213.13 ± 0.00
CPI (control)	2:1	4.75	91.22 ± 0.66	164.45 ± 3.85	75.35 ± 2.09	76.00 ± 2.00	296.88 ± 10.83
CPI-gum Arabic	2:1	4.75	90.87 ± 0.88	104.45 ± 3.85	74.44 ± 0.96	94.33 ± 0.58	278.13 ± 10.82

Table 9.2. Functional attributes of canola protein isolate (CPI) (Cruciferin-rich) -polysaccharide mixtures under biopolymer and pH conditions where insoluble complexes exist. Data represent the mean ± one standard deviation (n=3).

Biopolymer mixtures	Mixing ratio	pH	Solubility (%)	Foaming Capacity (%)	Foaming Stability (%)	Emulsion Stability (%)	Emulsion Capacity (g/g)
CPI (control)	20:1	5.00	90.62 ± 0.50	211.11 ± 10.18	73.76 ± 2.56	92.00 ± 0.00	247.19 ± 7.58
CPI-κ-carrageenan	20:1	5.00	47.46 ± 1.19	97.78 ± 3.85	81.75 ± 4.32	96.00 ± 0.00	181.56 ± 15.16
CPI-ι-carrageenan	20:1	5.00	61.89 ± 0.54	71.11 ± 3.85	77.88 ± 6.82	94.67 ± 2.31	190.31 ± 13.13
CPI-λ- carrageenan	20:1	5.00	25.94 ± 2.48	73.33 ± 6.67	86.72 ± 7.21	96.00 ± 0.00	190.31 ± 13.13
CPI (control)	10:1	5.30	93.53 ± 1.13	186.67 ± 6.67	66.64 ± 2.34	85.33 ± 4.16	300.21 ± 7.94
CPI-pectin (high methoxy)	10:1	5.30	96.14 ± 1.19	195.56 ± 13.88	69.68 ± 2.73	87.33 ± 3.06	277.29 ± 7.94
CPI (control)	10:1	4.80	93.20 ± 0.68	200.00 ± 13.33	79.94 ± 1.34	88.67 ± 4.16	220.30 ± 7.94
CPI-pectin (low methoxy)	10:1	4.80	95.05 ± 1.43	64.44 ± 3.85	72.59 ± 4.49	93.33 ± 1.15	194.79 ± 7.94
CPI (control)	2:1	4.2	39.52 ± 0.56	161.11 ± 1.92	79.99 ± 1.42	76.00 ± 0.00	259.38 ± 10.83
CPI-gum Arabic	2:1	4.2	56.26 ± 1.24	115.56 ± 7.70	83.04 ± 3.22	75.33 ± 1.15	240.63 ± 10.83

Functionality of NPI-polysaccharide insoluble complexes

The functional properties of complexes formed involving a napin-rich protein isolate and a variety of polysaccharides was also explored under conditions favoring only insoluble complexes, and then compared with NPI alone at corresponding pH and biopolymer conditions. The solubility of each NPI-polysaccharide mixture was much lower than the NPI alone which was almost completely soluble (98-100%) at each pH tested. Kappa-carrageenan reduced NPI solubility by ~38%, however the reduced solubility did not influence either foaming or emulsion stability but did result in a reduction in foaming capacity from ~230% to ~187%. NPI solubility was also reduced further with the addition of ι-CG, CG-λ and AL by ~57%, ~70% and ~55% respectively (Table 9.3). The addition of ι-CG to NPI lead to an increase in the foaming stability by ~10% but decreased both foam capacity and emulsion stability from ~233 to ~189%, and ~65% to ~45%, respectively (Table 9.3). The low solubility of the NPI-λ-CG mixture did not impact the foaming or emulsion stability of NPI, but again reduced foaming capacity significantly from ~215% to ~126%. Napin protein isolate-alginate mixtures followed a similar trend, where foaming capacity was reduced from ~187% to 85%, with no changes in emulsion or foaming stability (Table 9.3).

9.4 Summary

Overall, the functionality of both soluble and insoluble complexes involving either protein had a neutral or negative effect on protein functionality. Solubility and foaming capacity were the greatest properties negatively affected in all cases. This trend was found for most systems with the exception of CPI and gum Arabic at pH 4.2 (near its isoelectric point), where a rise in solubility from ~39% to ~56% was observed with the addition of the polysaccharide. Despite rejecting our null hypothesis that the addition of the polysaccharide would improve protein functionality, findings arising from this work will aid the food industry in understanding complex ingredient interactions occurring in food and during product development. The ability to reduce solubility so drastically could have implications in the development of new separation procedures for protein isolation from canola meal or in clarification applications. Furthermore the protein produced (CPI and NPI) performed much better than expected as a control material, and had very comparable functionality relative to commercial protein ingredients derived from egg and milk which was highlighted in depth in Chapter 4 of this report (leaving little room for improvement). Possibly a

more degraded denatured protein extracted after harsher oil processing conditions might respond differently to this caoacervation approach for industial non-food appliations. Although it was difficult to directly compare the functional properties of CPI and NPI due differences in pHs used, the CPI generally performed better near pH 7 (pH 6.75, Table 9.1) than NPI (pH 6.5, Table 9.3). Solubility of both proteins were similar (96-100%), however CPI had higher foaming capacity (271% vs. 215%), foaming stability (74% vs. 56%) and emulsion stability (86% vs. 38%) than NPI (Tables 9.1 and 9.3).

Since the addition of polysaccharides showed only neutral or negative benefits to CPI and NPI functionality, only the proteins alone (CPI and NPI) were investigated more in-depth in terms of emulsification (Part III). Furthermore, due to the low recovery of NPI during Part II and III of this project, sufficient quantities of NPI could not be generated for the gelation studies (Part IV). Consequently, only the CPI (cruciferin-rich) material was used and compared to that of commercial soy protein isolate ingredient.

Table 9.3. Functional attributes of napin protein isolate (NPI)-polysaccharide mixtures under biopolymer (10:1 mixing ratio) and pH conditions where insoluble complexes exist. Data represent the mean ± one standard deviation (n=3). Note: Emulsion capacity was not tested (as in Table 9.1 and 9.2) due to limited sample availability.

Biopolymer mixtures	pH	Solubility (%)	Foaming Stability (%)	Foaming Capacity (%)	Emulsion Stability (%)
NPI (control)	5.00	100.41 ± 1.75	75.99 ± 0.85	231.11 ± 7.70	34.00 ± 3.46
NPI-κ-carrageenan	5.00	61.75 ± 2.28	76.79 ± 1.79	186.67 ± 0.00	40.00 ± 2.00
NPI (control)	8.00	101.75 ± 2.26	65.26 ± 1.21	233.33 ± 6.67	65.33 ± 2.31
NPI-ι-carrageenan)	8.00	43.01 ± 1.38	77.07 ± 1.38	188.89 ± 3.85	45.33 ± 2.31
NPI (control)	6.50	100.76 ± 0.97	56.71 ± 2.41	215.55 ± 3.85	38.67 ± 2.31
NPI-λ-carrageenan)	6.50	30.44 ± 3.15	56.15 ± 1.53	126.67 ± 6.67	37.33 ± 2.31
NPI (control)	6.00	98.54 ± 0.76	73.54 ± 4.68	197.78 ± 3.85	42.00 ± 2.00
NPI-alginate	6.00	43.43 ± 3.59	61.01 ± 2.85	85.33 ± 6.81	39.33 ± 3.06

Part III: Emulsifying properties of canola proteins

-Chapter 10-

Literature review

10.1 Food emulsions

Emulsions consist of a mixture of two (or more) immiscible liquids formed after an input of mechanical energy (e.g. homogenization) where one liquid becomes dispersed as small droplets within a continuous phase of the other (Hill, 1996; Schultz et al., 2004; McClements, 2005). Depending on the ingredient formulation and processing conditions, various structures, flavor release and textural attributes can be achieved in foods by forming emulsions, leading to improved organoleptic quality for consumers. Physicochemical and sensory attributes of the emulsion product are controlled by tailoring characteristics of the dispersed droplets, such as concentration, size distribution, surface charge and level of interactions (e.g., flocculation, aggregation, and coalescence) (McClements, 2007). In food emulsions, droplet sizes typically range between 0.1 to 100 μm in diameter, and are classified either as water-in-oil (W/O) (e.g., margarine and butter) and oil-in-water (O/W) (e.g., salad dressings, ice cream, milk, soups, dips/sauces and beverages) emulsions based on their continuous phase. Emulsion-based technology is also important in terms of drug or bioactive molecule delivery where multiple emulsions (e.g., O/W/O or W/O/W) or nanoemulsions are used for carrying, protecting and releasing sensitive bioactive ingredients (Garti and Bisperink, 1998; Cho and Park, 2003).

Emulsions are typically formed under high shear conditions using homogenizers, high pressure valve homogenizers, microfluidizers or high shear mixers (McClements, 2005, 2007). However, they are inherently unstable and tend to separate over time due to various mechanisms of instability. The rate of which depends on many factors, including droplet characteristics (size distribution, surface charge and level of interactions), continuous phase viscosity, the presence of emulsifiers and solvent conditions (e.g., presence of salts, temperature and pH) (Dickinson and Stainsby, 1988; Wu and Muir, 2008; Can Karaca et al., 2011). The Stoke's law has commonly been used to describe the rate of gravitational separation of dispersed droplets within the continuous phase. Stoke's law is as follows (eq. 10.1),

$$U = -2gr^2\Delta\rho / 9\eta \qquad \text{(eq. 10.1)}$$

where, U is separation rate (mm/day), r is the radius of droplet, $\Delta\rho$ is the difference density of the two phases and η is the viscosity of the continuous phase.

Emulsifiers are surface active molecules or macromolecules that absorb to the surface of the dispersed droplets forming a viscoelastic film or coating that prevent aggregation (Dalgleish, 1997; McClements, 2007). Examples of emulsifiers include low molecular weight surfactants (e.g., Tween, Span), phospholipids (e.g., lecithin), and biopolymers (e.g., polysaccharides and proteins) (Friberg et al., 2004). Emulsifiers act to reduce interfacial tension between the oil and water phases by positioning their hydrophobic amino acid group within the oil phase and hydrophilic amino acid groups within the polar phase. Emulsifiers act by reducing the energy needed to form an emulsion, and then delay the likelihood of phase separating into two immiscible phases. Macromolecules such as polysaccharides and proteins can act to raise the continuous phase viscosity or form a gel network, significantly inhibiting Brownian motion and emulsion droplet interactions (McClements, 2007). Proteins, are either filamentous (e.g., casein and gelatin) or globular in nature, and comprise of both hydrophobic and hydrophilic amino acid residues at their surface making it capable of interacting with both the aqueous and lipid phases. Protein at the interface sometimes form "loops" and "tails" that can also provide steric hindrance which physically prevent the emulsion droplets come into close proximity of each other depending on the conformation, protein molecular size and amino residues of the protein. (Damodaran, 2005).

10.2 Mechanisms of emulsion instability

As previously discussed, emulsions are inherently unstable comprised of two (or more) thermodynamically incompatible phases, which overtime moves towards a more energetically favorable state that minimizes Gibb's free energy within the system (Gupta and Muralidhara, 2001; Tolstoguzov, 2003). In this state, oil and water phases are completely separated into distinct layers to give the least amount of contact surface area, rather than having one dispersed within the other. Thermodynamic equilibrium in emulsions is maintained with the addition of emulsifiers, which act to minimize the driving energy to phase separation (i.e., reduces interfacial tension between the two phases) (Damodaran, 2005).

Food emulsions become unstable due to various interconnected processes including gravitational separation (i.e., creaming/sedimentation), flocculation, coalescence (or partial

coalescence), Oswald ripening (also called disproportion) and phase inversion (McClements, 2007). These mechanisms are each summarized in Figure 10.1. In brief, gravitational separation refers to either an upward migration of droplets to the surface to form a cream layer, in the case of creaming, or the downward migration of droplets to form sediment, in the case of sedimentation. Migration rate and separation depends on density differences between the two phases, and the level of droplet aggregation, whereby larger droplets either cream or sediment at much faster rates than smaller droplets (McClements, 2007). Aggregation of droplets may be reversible in the case of flocculation, where adjacent droplets stick together but remain distinct as their viscoelastic membranes which encase the droplets. In the case of coalescence or partial coalescence, membranes surrounding adjacent droplets become ruptured leading to complete or partial exchange of dispersed materials and the formation of one larger irregular sized droplet (McClements, 2007). Oswald ripening (more common in foams) occurs based on the diffusion of the dispersed phase from a small droplet through the continuous phase to merge into larger droplets. The process is also known as disproportion. In the case of phase inversion, an oil-in-water emulsion will invert into a water-in-oil emulsion or vice versa (McClements, 2007).

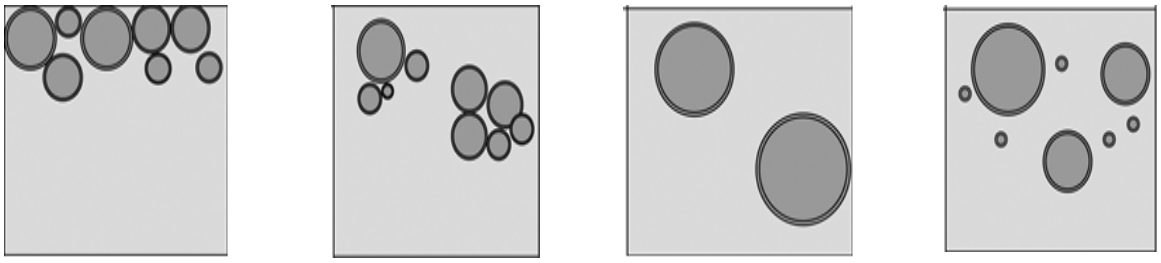

Figure 10.1 Schematic diagram describing mechanism for emulsion instabilities (modified from Robins and Wilde, 2003).

10.4 Protein-stabilized emulsions

The stability of protein-stabilized emulsions is dependent upon the protein (e.g., globular vs. fibrous, conformational flexibility, molecular weight) and surface (e.g., hydrophobic and hydrophilic residues) characteristics, processing conditions (e.g., shear and heat) and solvent properties (e.g., temperature, pH and salts). During emulsion formation, soluble proteins diffuse

towards the interface, then re-arrange and re-organize at the interface to orient hydrophobic amino groups towards the non-polar oil phase and the hydrophilic amino groups towards the aqueous phase forming a viscoelastic film (Dalgleish, 1997) (Figure 10.2a). This process is highly depended on the molecular flexibility and packing of the protein (Freer et al., 2004). Film strength is then enhanced via protein-protein interactions, hydrogen bonding and electrostatic interactions and van der Waals attractive forces. Moreover, the addition of macromolecules such as protein would increase the overall viscosity of the medium and restrict random movements of the oil droplets. In some studies cross-linking agents (e.g., transglutaminase) is added to improve stability (Fñrgemand et al., 1998; Dickinson et al., 1999) of O/W emulsions.

Although the majority of the hydrophobic groups are buried within the interior of the 3-dimensional structure, some remain on the surface amongst the hydrophilic residues as hydrophobic patches. As such, a prerequisite to achieving good emulsion stabilization is partial or complete denaturation or unraveling of the protein to expose reactive non-polar sites (Damodaran, 2005). Depending on the primary structure, and the spatial arrangement of the protein at the interface, tails or loops comprised of protein chains may extend into the aqueous solution leading to steric forces or interactions. In contrast, low molecular weight surfactants tend to form micelles in the aqueous phase, and diffuse towards the interface at a much faster rate (Figure 10.2b). Alignment at the interface tends to result in complete coverage rather than having irregular intermittent breaks in the viscoelastic films due to the presence of loops or tails, or from incomplete absorption to the oil-water interface.

Protein absorbed to the interface often forms a thin film around the dispersed droplet. The viscoelastic film typically provides an electric charge to the droplet, which depending on the pH, may lead to attraction or repulsion between neighboring droplets (Friberg et al., 2004). The concentration of protein absorbed at the interface could also affect the film formation, and could have detrimental effects on emulsion stability. For instance, insufficient protein at the interface could lead to a thinner film, which is more susceptible to film rupture or incomplete coating of the droplet (Tcholakova et al., 2002; McClements, 2004). In turn, this could increase the chance of coalescence when droplets are of close proximity. When there is sufficient protein absorbed at

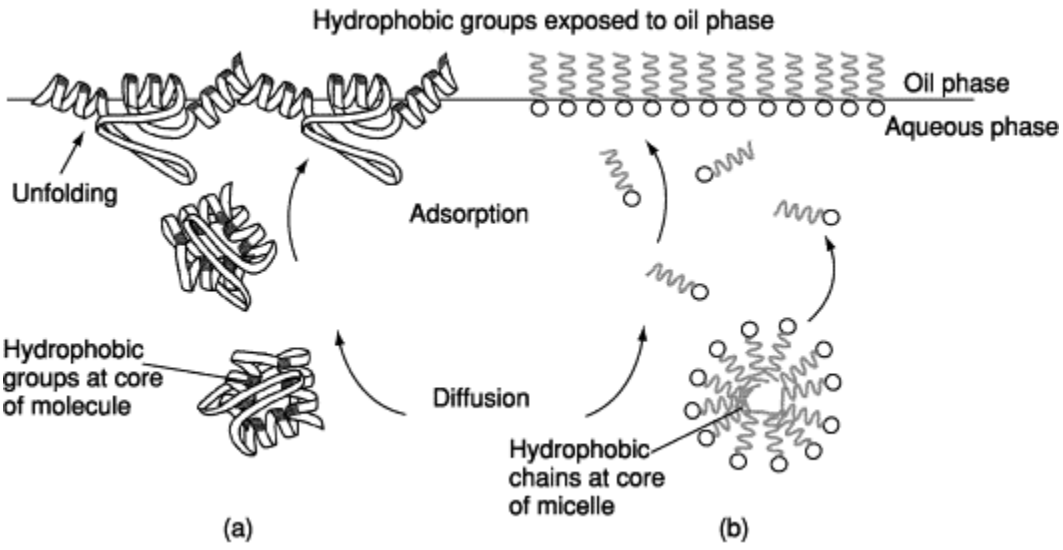

Figure 10.2 Schematic diagram of protein (a) and low molecular weight surfactant (b) absorption to an oil-water interface (reproduced with permission from Robins and Wilde, 2003).

the interface, the stability of emulsion is mainly affected by the mechanical force input to form smaller droplets which could reduce the density differences of the dispersed phase and the continuous phase and delay gravitational separation (McClements, 2004). The relationship of mean droplet size and protein as emulsifier concentration can be illustrated mathematically (eq. 10.2).

$$r_{\min} = \frac{a\Gamma_{sat}\phi}{cs} = \frac{a\Gamma_{sat}\phi}{cs'(1-\phi)} \qquad \text{(eq. 10.2)}$$

Where, Γ_{sat} is the excess surface concentration of the emulsifier at saturation (in kg m^{-2}), ϕ is the disperse phase volume fraction, *CS* is the concentration of emulsifier in the emulsion (in kg m^{-3}) and *CS'*is the concentration of emulsifier in the continuous phase (in kg m^{-3}) (McClements, 2004). Excess protein or protein that cannot be absorbed at the interface could cause depletion flocculation due to competition of solvent around and between the droplets similar with the "salting out" phenomenon (McClements, 2000). A critical flocculation concentration (CFC) has to be reached before depletion flocculation occurs and CFC value reduces as droplet size increases and protein volume fraction increases (McClements, 2000). Proteins rich in sulfur containing amino acids such

as rapeseed proteins, could form disulfide bonds with other protein molecules as the protein unravel at the interface (Wu et al., 2011). Disulfide bonds formed between proteins at the same interface could enhance emulsion stability (Tcholakova et al., 2002). However, disulfide bonds formed between two different interfaces might lead to flocculation and followed by coalescence and it is also known as bridging flocculation (Joshi et al., 2012; Wang et al., 2012). Joshi et al. (2012) also suggested reducing inter and intra disulfide bonding all together could improve overall emulsion stability in a lentil protein stabilized emulsion.

Protein stabilized emulsions are most stable at pHs away from its pI value because of the presence of an electric charge on the oil droplet's surface which acts to repel neighboring droplets. In contrast, when solution pH is close to the pI of the protein, electrostatic repulsive forces are minimal between droplets enabling them to flocculate or undergo partial or complete coalescence (Xu et al., 2005; Foegeding and Davis, 2011). Larger droplets are than more prone to gravitational separation. Furthermore, protein solubility tends to be reduced near the pI of the protein, also leading to flocculation and/or partial or complete coalescence and subsequent reduced absorption to the oil-water interface (Kinsella, 1979). Often low protein solubility is associated with poor emulsifying properties (Dickinson, 2003; Can Karaca et al., 2011).

Protein stabilized emulsion are also very sensitive to ionic strength, which when levels exceed certain concentration, emulsion stability can be reduced (McClements, 2004). Multivalent ions such as Ca^{2+}, Mg^{2+},Fe^{2+} or Fe^{3+} are more prone to cause emulsion instability than monovalent ions such as Na^{+}, Cl^{-} or K^{+} because they are more effective at screening electrostatic repulsive forces between surfaces to reduce the zeta potential (ζ), which is a measure of the protein's surface charge (Keowmaneechai and McClements, 2002). Demetriades and co-workers (1997) found that an oil-in-water emulsion stabilized by 2% whey protein was unstable when pH was close to pI of whey protein (pH 4.6). The authors also reported the addition of NaCl up to 100 mM resulted in large droplet sizes, and high levels of flocculation and creaming. Kulmyrzaev et al. (2000) found emulsions prepared with diluted whey protein isolate (0.5% w/w) showed that the addition of only 20 mM of $CaCl_2$ resulted in 3 times reduction in the zeta potential around the droplets both below and above the isoelectric point of whey protein. The authors also found emulsion stability was relatively insensitive to $CaCl_2$ (<20 mM) when pH was below the pI of whey protein, however creaming occurred at pH above the pI of whey protein at levels > 5 mM and above $CaCl_2$ (Kulmyrzaev et al., 2000). Solubility and zeta potential of canola protein isolate was also found

lowest near the isoelectric point (pH 4-5) and reduced substantially with the addition of 350 and 700 mM NaCl by Paulson and Tung (1987).

According to the Stokes' Law (eq. 10.1), creaming rate has a reciprocal relationship with bulk phase viscosity. Increasing bulk phase viscosity could reduce the chances of droplet-droplet collision which might induce coalescence (McClements, 2004). Previous studies have shown the addition of sucrose was able to improve the thermal stability of milk protein stabilized emulsions (Kim et al., 2003). The authors also found the addition of sucrose before thermal treatments prevented extensive droplet aggregation, however if the sucrose was added after thermal treatment, it promoted droplet aggregation. The author speculated that sucrose affects emulsion stability mainly by stabilizing the conformation of the adsorbed protein rather than changing the properties of the bulk phase condition since the results showed dependency on the order of addition of sucrose before or after thermal treatment (Kim et al., 2003).

The other important aspect to the emulsifying properties of plant protein is the extraction methods because it can impact the purity, quantity and the conformational structure of the protein extracted (Aider and Barbana, 2011; Can Karaca et al., 2011). For oilseed proteins, the defatting process used to create an oil free meal involves the use of both heat and chemicals, and often leads to partial or complete denaturation of the protein (Khattab and Arntfield, 2009). Table 10.1 provides some brief methodology for extracting proteins from various oilseeds found in literature, along with their emulsifying properties, using emulsifying activity index (EAI) and emulsion stability (ES) as indicators. EAI indicates the area of interface covered per one gram of protein, whereas ES is the measure of creaming after a standard period of time to quantify the ability of the protein film to stabilize the emulsion to delay droplet aggregation.

Many plant protein materials contain undesirable compounds which will affect the organoleptic and/or functional properties of the protein. For instance, oilseed proteins often contain phenolic compounds and phytates that make them undesirable as a human food ingredient because of the inferior organoleptic properties or poor functional properties (Schwenke, 1994; Krause et al., 2002; Wanasundara, 2011). Fortunately, with proper extraction, these undesirable compounds could be reduced to safe levels suitable for human consumption (Ismond and Welsh, 1992). Krause and co-workers (2002) extracted flaxseed protein isolate with

Table 10.1 Summary of various extraction processes for oilseed protein isolates, and their emulsifying properties reported in literature (modified from Moure et al., 2006).

Protein in oilseeds	**Extraction Solvent/pH/time(h)/temperature ºC**	**Purification**	**EAI (m^2/g)**	**ES (%)**	**Reference**
Almond	20 mM Tris-HCl/8.1/1/25	Dissolve defatted meal. Filter through glass wool, followed by centrifugation. Supernatant is then filtered to remove debris, and dialyzed against 5 L of distilled deionized water. Supernatant is then freeze-dried.	51.77	-	Sze-Tao and Sathe, 2000
Canola	0.1 M NaOH/–/0.33/23	Dissolve defatted meal. Filter with filter paper, adjust to pH 4.0, centrifuge, wash to remove salt, and then centrifuge again to recover the pellet.	28.27	71.0	Aluko and McIntosh , 2001
Canola	0.1 M NaOH/–/0.33/23	Dissolve defatted meal. Filter with filter paper, adjust to pH 6.0, add $CaCl_2$ up to 1 M, and centrifuge. The supernatant is diluted in 200 volume of water to remove salt, and then recover protein after centrifugation.	32.34	26.9	Aluko and McIntosh, 2001
Canola	0.3 M NaCl/-/4/23	Dissolve defatted meal. Centrifuge, filter the supernatant, further concentrate the supernatant by ultrafiltration, and then dilute the supernatant with 6x volume of water, and recover protein micelle by centrifugation.	39.80	68.0	Gruener and Ismond, 1997a,b

Table 10.1 Summary of various extraction processes for oilseed protein isolates, and their emulsifying properties reported in literature (modified from Moure et al., 2006) (Continued).

Flaxseed	0.5 M NaCl/5.5-6.5/1/25	Dissolve defatted meal and collect clear supernatant. Concentrated supernatant by ultrafiltration, dilute with 5x volume of cold water, and then centrifuge to recover the protein micelle.	2550	80.0	Krause et al., 2002
Flaxseed	Water/8.5/–/25	Dissolve defatted meal. Adjust pH to 4.5 to precipitate the protein, and then centrifuge to obtain protein material.	2100	81.5	Krause et al., 2002
Sesame	1 M NaOH/9.5/1/50	Dissolve defatted meal. Sample is centrifuged, the supernatant liquid is adjusted to pH 4.9, and then stirred for 1 h at 50−55 °C and again centrifuged, the solid residue is collected and dried.	114.33	35.5	Bandyopadhyay and Ghosh, 2002
Soybean	20 mM Tris-HCl/8.1/1/25	Dissolve defatted meal. Filter through glass wool, and then centrifuge. The supernatant is adjusted to pH 4.5 and centrifuged to precipitate the proteins. Proteins were dialyzed against distilled deionized water.	11.61	–	Sze-Tao and Sathe, 2000
Soybean	Acetic acid-acetate buffer/4.5/–/25	Dissolve defatted meal. Protein is fractionated by ultrafiltration with 10, 30 and 50 kDa cut off (centrifugation prior to ultrafiltration is optional) and concentrated using a 5 kDa membrane.	106.7	27.6	Moure et al., 2005

conventional isoelectric precipitation (IP) and protein micellar mass (PMM) methods and found although 11S globulin was the main fraction in both isolates, the isolate produced by IP had lower solubility and EAI compared with the isolate produced by the PMM method. In the same study, isolates produced by the PMM method also achieved much lower phenolic and phytic acid levels. The authors stated that PMM method preserved the protein's native form with minimal amount of undesirable compounds, whereas IP produced isolate might have undergone partial denaturation and irreversible protein aggregation (Krause et al., 2002).

10.5 Protein extraction methods

Canola oil production ranks second only to soy bean among the oilseed crops (Table 10.2) (Food and Agriculture Organization of UN, 2012). Canola represents a significant economic value to Canada, especially Saskatchewan, which is the major canola growing province along with Alberta. Canola meal, the co-product of oil processing is rich in protein (36- 39%) and crude fibre (~12%), which to date is commonly used in low cost livestock feed for its nutritional value (Khattab and Arntfield, 2009; Newkirk, 2009). The meal contains high levels of phenolic compounds and phytic acid which can lead to poor protein functionality depending on the extraction method used due to the interaction between the protein and phenolic compounds and phytic acid (Wu and Muir, 2008; Aider and Barbana, 2011). Depending on the canola variety used, processing practices and methods of extraction, protein functionality can vary considerably (Aluko and McIntosh, 2001; Khattab and Arntfield, 2009; Can Karaca et al., 2011). Successful processing innovations and product characterization could lead to the development of a new plant sourced protein food ingredient.

Table 10.2 World production of major oilseeds (million tonnes).

Oilseed	2010/11	2011/12 (estimate)	2012/13 (forecast)
Soybean	265.2	239.8	268.6
Canola/Rapeseed	60.8	61.5	60.1
Cottonseed	43.7	46.5	43.3
Groundnut	36.9	36.6	37.0
Sunflower	33.1	38.8	35.2
Palm kernel	12.6	12.8	13.5
Copra	4.9	5.3	5.4
Total	457.2	441.4	463.3

Source: FAO, 2012

As mentioned previously, extraction and purification methods can cause great variations in the physicochemical and functional properties of the protein isolates. In general, canola protein extraction found in literature could be generalized to be either, alkali extracted followed by acid precipitation (Mieth et al., 1983; Aluko and McIntosh, 2001; Can Karaca et al., 2011) or using the PMM method developed by Murray et al. (1980). In the case of the former, NaOH is often used to bring the solvent pH to strongly basic conditions (pH 11-12) in order to have high protein recovery rate (Tan et al., 2011). Sodium hexametaphosphate (SHMP) at pH 7.0 is another alkaline medium used to extract canola proteins followed by acid precipitation (Thompson et al., 1976). Tzeng et al. (1988) found that a canola protein isolate produced by SHMP had better color and taste, but lower protein recovery than if extracted using NaOH. Once the proteins are dissolved, solutions are acidified to bring the pH closer to the isoelectric point to allow the protein to precipitate with HCl or CH_3COOH in the presence or absence of NaCl (Klockeman et al., 1997; Aluko and McIntosh, 2001). Ghodsavali et al. (2005) reported that a range of pHs between 4.5 and 5.5 was the optimum precipitation pH for canola proteins.

In the case of the PMM approach, defatted meal is often stirred with NaCl to achieve an ionic strength at least 0.2 M and then diluted with 6-10 parts of cold water to reduce ionic strength to 0.06-0.1 M in order to precipitate the salt soluble proteins in the form of protein micelles (Murray et al., 1980). The PMM approach first provide conditions to solubilize protein with elevated ionic strength (salting-in), and then reduce the ionic strength to promote hydrophobic

interactions between protein molecules by diluting the solution with cold water to form protein micelle. PMM method tends to be less harsh on the native protein than other extraction means, possibly leading to the production of a higher quality (i.e., non-denatured) protein. However, the PMM method was found to have relatively lower protein yield (~71.3%- 78.5%) in comparison to alkali extraction methods (Ismond and Welsh, 1992). Some extraction methods found in literature using the alkali extraction/acid precipitation and PMM methods are summarized in Table 10.3.

10.6 Canola proteins

Canola protein is dominated by a salt soluble 12S globulin, cruciferin, representing up to 60% of the total protein. The remaining composition consists of water soluble albumin (Napin, 2S) and alcohol soluble prolamins (Hoglund et al., 1992). The exact ratio of these two proteins varies among cultivar and extraction processes used. A significant variation of globulin: napin ratios have been reported, ranging from 0.7 to 2.0 (Raab et al., 1992; Aider and Barbana, 2011).

10.6.1 Cruciferin proteins

Cruciferin is a hexamer (molecular mass of ~300 kDa) with each monomer comprised of two polypeptides; an α- chain (~30 kDa) and a β- chain (~20 kDa) stabilized by a disulfide bridge (Schwenke et al., 1983). The reversible dissociation of 12S subunits into 7S trimmers has been reported depending on the ionic strength (<0.5) (Schwenke and Linow, 1982). It was also found that 12S cruciferin can further dissociate into 2-3S components irreversibly after dialyzing the protein solution against 6 M urea (Bhatty et al., 1968). Similarly, the 12S cruciferin can dissociate into a 7S trimer at low pH (<3.6). Cruciferin has a neutral pI (~pH 7.2), and its secondary structures are composed of high levels of β-sheets (~50%) and low levels of α-helices (~10%) (Zirwer et al., 1985).

The emulsifying properties of 12S *Brassicaceae* protein were investigated (Krause and Schwenke, 2001; Wu and Muir, 2008). Krause and Schwenke (2001) found higher concentrations of cruciferin was needed to form a stabilized viscoelastic film around an oil droplet as compared to napin, indicating the need for high packing density of the protein at the interface. Cruciferin was also able to have more intermolecular interactions at the interface due to its lower surface charge compared with napin molecules. In the same study, cruciferin was found to have a much lower emulsifying activity index (168 m^2/g) compared with napin (418 m^2/g) (Krause and Schwenke,

Table 10.3 Summary of alkali extraction/acid precipitation and PMM methods for rapeseed protein found in literature.

(a) Alkaline extraction (followed by acid precipitation)	
Aluko and McIntosh, 2001	Defatted meal is dissolved in 10 volumes of solution of 0.1 M NaOH, stirred at room temperature for 20 min. Acid adjustment to pH 4.0 by 0.1 M HCl.
Pedroche et al., 2004	Defatted meal is dissolved in 10 volumes of 0.2% NaOH, stirred at room temperature for 1 h twice. Acid adjustment to pH 2.5- 6.0 in 0.5 increments by 0.5 N HCl.
Klockeman et al., 1997	Defatted meal is dissolved in 0.4% NaOH, stirred at room temperature for 1 h. Acid adjustment to pH 3.5 by acetic acid.
Tzeng et al., 1988	Defatted meal is dissolved in 1.0% aqueous SHMP at room temperature for 30 min. Acid adjustment to pH 3.5 by 6 N HCl.
(b) PMM method extraction	
Gruener and Ismond, 1997a,b	Defatted meal is stirred in 0.3 M NaCl (1:10 meal: solvent) for 4 h at room temperature. Supernatant is ultrafiltrated and concentrated through 10 kDa molecular weight cut off spiral ultrafiltration, pressure maintained at 20 psi, the volume of the supernatant is reduced 8 times and then diluted with 6 times volume of cold water.
Ismond and Welsh, 1992	Defatted meal is stirred in buffer (NaH_2PO_4) at room temperature with either 0.01 or 0.1 M NaCl ranging from pH 5.5-6.5. Supernatant is concentrated through ultrafiltration with 100 kDa molecular weight cut off, pressure maintained at 60-70 psi, the volume reduced 4 times, and then diluted with 15 times volume of cold water.
Ser et al., 2008	Defatted meal is stirred in buffer (NaH_2PO_4) with 0.5 M NaCl at pH 5.5-6.5. Supernatant is concentrated through ultrafiltration with 10 kDa molecular weight cut off, pressure maintained at 60-70 psi and then diluted with 15 times volume of cold water.

2001). Wu and Muir (2008) found cruciferin prepared emulsions resulted in smaller droplet sizes (<1μm) compared with napin prepared emulsions (>10 μm) as well as higher emulsion stability (97.74% compared with 77.41% for napin). Schwenke (1994) reported unmodified cruciferin is more surface active than napin, this could be due to the higher hydrophobicity of cruciferin. Surface hydrophobicity was found to be positively correlated with emulsifying properties in soy protein, sunflower protein and rapeseed protein (Nakai et al., 1980; Townsend and Nakai, 1983).

10.6.2 Napin proteins

Napin in *Brassicaceae* seed possess a homologous structure with a group of closely related low molecular weight 2S albumin proteins in many plants such as Brazil nuts, mustard, sunflower seeds, etc. (Lönnerdal and Janson, 1972). Napin is a basic protein with a calculated pI > 10 and molecular weight 12-14 kDa (Bhatty et al., 1968; Schwenke et al., 1988). Napin is comprised of one small (~4.5 kDa) and one large subunit (~10 kDa) stabilized by two disulfide bonds (Schwenke, 1990; Gehrig et al., 1998). It was reported that chemical modification such as acetylation and succinylation would not change the secondary or tertiary structure of napin unless the disulfide bonds are broken such as under S-S bond reduction conditions, indicating napin is a highly stabilized structure (Schwenke et al., 1988; Schwenke, 1994). Structural stabilization of napin by disulfide bonds would reduce the molecular flexibility of napin and could become a disadvantage for napin during the formation of emulsions when the molecules need to rearrange and realign at the interface (Schwenke, 1994). The secondary structure of napin is characterized by a high content of α- helix (40-46%) and low content of β- sheet (12%) at pH range from 3-12 (Schmidt et al., 2004). Positively charged amino acids on the surface of napin also tend to be highly reactive towards chemical modification, however, this could be a disadvantageous because it is easy to form insoluble complexes with phytic acid and/ or phenolic compounds through electrostatic attractive forces (Schwenke, 1990).

Crucifer 2S napin is considered the main allergen in mustard seed and was identified as structurally homologous with 2S albumin in many mono- and di-cotyledonous plants such as cotton seeds, Brazil nuts, sunflower seeds and castor bean, etc. (Monsalve, 1991; Moreno and Clemente, 2008). So far four proteins of *Brassicaceae* 2S fraction have been identified as mustard seed allergens: Sin a 1 from *Sinapis alba*, Bra j 1 from *Brassica juncea*, Bra n 1 from *Brassica*

napus and Bra r 1 from *Brassica rapa*. (Wanasundara, 2011). Because of the highly stabilized molecular structure of 2S albumin, it was found that 2S protein is able to cross the gut mucosal barrier to sensitize the mucosal immune system to trigger an allergic response (Monreno and Clemente, 2008). There were attempts of transferring 2S albumin coding gene from Brazil nut, which is homologous with napin, into soybean (Nordlee et al., 1996). It was found that the transgenic soybean retained the 2S albumin allergenicity and triggered allergic reactions on skin-prick tests.

Functionality of native and modified napin has been investigated (Schwenke, 1990; Krause and Schwenke, 2001; Wu and Muir, 2008). Krause and Schwenke (2001) reported that napin has a higher diffusion rate and is highly surface active with higher emulsifying activity index (EAI) than its globulin counterpart. The authors also found that a smaller concentration of napin was needed to form a saturated protein film on droplets; however the film was not as protein packed compared with cruciferin which could be due the electrostatic repulsive force between napin molecules that prevent close stacking on the film (Krause and Schwenke, 2001). On the contrary, Wu and Muir (2008) reported a napin prepared emulsion had lower stability (77.41%) compared with cruciferin (97.74%) and a canola protein isolate (89.95%), and concluded napin content in canola protein is a major factor contributing to the inferior functionality of canola protein. Wu and Muir (2008) suspected high level of basic amino acid residues on napin might favor electrostatic interaction which might be responsible for the inferior emulsifying properties of canola protein. Protein solubility of *Brassicaceae* meals was investigated by Wanasundara and others (2012) and showed that napin has high solubility across pH 2.0 to 10.0 in many of the crucifer oilseeds, this could explain the findings of Krause and Schwenke (2001), where napin has higher diffusion rate compared with cruciferin due to its high protein solubility at neutral pH. Jyothi et al. (2007) found napin has low binding constant to extrinsic fluorescence probes which indicated napin molecule may have lesser number of hydrophobic sites on the surface. Nitecka et al. (1986) found that upon succinylation and acetylation, surface hydrophobicity of napin increased linearly with the level of reactions and the modified napin showed aggregation at pH below its pI value. The authors also found acetylation reduced the emulsifying activity of napin simply due to the linear increase of surface hydrophobicity. Schwenke (1994) stated that based on the studies done on native and modified canola main storage protein, napin showed excellent foaming ability comparable with egg white, however, napin has poorer emulsifying properties than cruciferin. Chemical

modification of napin such as succinylation and acetylation resulted in poor foaming and emulsifying properties due to reduced solubility and higher surface hydrophobicity (Nitecka et al., 1986; Schwenke, 1990).

10.7 Anti-nutritional properties

107.1 Phytates

Phytic acid (PA) is found as salt of calcium, magnesium and potassium in crystal form inside the storage protein bodies of *Brassicaceae* seed (Yiu et al., 1983). Phytic acid content was reported to be 2.0-4.0% in whole seed and the level of phytic acid increases to 5.0-7.5% in protein concentrate to 1.0-9.8% in protein isolates depending on the protein extraction methods (Ismond and Welsh, 1992). Phytic acid has six phosphate groups and 12 protons that are dissociable in pH range from 1.92 to 9.53 (Schwenke, 1994). As a result, PA could undergo attractive electrostatic reaction with the storage proteins at pHs below their isoelectric point (Wanasundara, 2011). Phytic acid-protein complexes are often insoluble during solvent extraction of protein; therefore the presence of PA could reduce the overall protein yield if the extraction pH is under the isoelectric point of the protein. Fortunately, the addition of salt such as NaCl is able to reduce the level of PA effectively during extraction (Ismond and Welsh, 1992). Ismond and Welsh (1992) found the addition of 0.01 M and 0.1M NaCl reduced total PA level in the protein isolate to 0.96% and 0.49% respectively, by limiting the electrostatic attraction between the PA and protein. Phytic acid could potentially cause changes in the physicochemical and functional properties of the canola protein. Krause and Schwenke (2001) reported the protein isolate had slightly different interfacial behavior which the authors speculated might be due to complex formation of protein with PA. Phytic acid is also known as one of the antinutritional compounds present in rapeseed due to its ability to reduce the bioavailability of essential dietary minerals (Wanasundara, 2011).

10.7.2 Phenolic compounds

Phenolic compounds in *Brassicaceae* are considered to be the major contributor of the poor organoleptic properties of rapeseed flour or protein products (Schwenke, 1994; Aider and Barbana, 2011). Level of phenolic compounds in rapeseed meal were found to be 5 times higher than soybean meal and thus has become one of the limiting factors to utilize rapeseed meals and rapeseed protein concentrate or isolate in the food or feed industry (Ismond and Welsh, 1992;

Aider and Barbana, 2011). Phenolic compounds exist in many forms in rapeseed meal, the predominant type of phenolic compound in rapeseed meal and its derivative products is sinapic acid, which could constitute 70-85% of total phenolic compounds present in rapeseed meal (Naczk et al., 1998). Similar to phytic acid, phenolic compounds are also capable of altering the physicochemical and functional properties of rapeseed proteins (Schwenke, 1994). Spencer and others (1988) suggested that phenolic compounds might be binding protein through hydrophobic interaction with aromatic groups or hydrocarbon side chain, and then the binding is reinforced by hydrogen bonds between phenolic residues and polar groups of the protein. The binding of free sinapic acid is high when pH is lower than 7.0 without NaCl, however, Ismond and Welsh (1992) found the addition of 0.1M NaCl to NaH_2PO_4 buffer at pH 5.5 reduced total phenolic compounds in the protein isolate by 85.3%.

10.7.3 Glucosinolates

Glucosinolates are a group of compounds commonly but not exclusively found in the plants of the family *Cruciferae* which includes many economically valuable crops such as the *Brassicaceae* genus, used for edible oil and animal feeds from meal (McDanell et al., 1988). All glucosinolates have a fundamental backbone comprised of a β-D-thioglucose group, a sulphonated oxime moiety and a variable side-chain derived from methionine, tryptophan or phenylalanine (Mithen et al., 2000). Glucosinolates undergo enzymatic hydrolysis to produce a variety of breakdown products that are catalyzed by the indigenous enzyme myrosinase which co-exists with glucosinolates in the seeds but in separate compartments (Fahey et al., 2001). Upon the crushing of the seeds and/or other physical injuries occurring to the seeds, myrosinase can be released and initiate the hydrolysis process of glucosinolates. Some of the major glucosinolate breakdown products such as isothiocyanates, are responsible for the pungent aroma and hot/ bitterness of mustard seeds and mustard products (McDanell et al., 1988). Another major glucosinolate degradation product, thiocyanate ion, is considered goitrogenic and reduces the bioavailability of iodine causing goiter in extreme cases (Fenwick and Heaney, 1983). The level of total glucosinolates in *Brassicaceae* seeds are dependant upon the species of the plants and agronomic factors Often researchers are also interested in the level of specific types of glucosinolates because of the distinct physical, chemical and physiological properties of their break- down compounds

(McDanell et al., 1988; Fahey et al., 2001). Problems associated with glucosinolates in canola meal were limited due to the low total glucosinolate level in the seeds.

-Chapter 11-

Effect of pH and NaCl on the physicochemical and emulsifying properties of a cruciferin-rich protein isolate[5]

Lamlam Cheung[+], Janitha Wanasundara[++], and Nickerson, Michael T.[+]

[+]Department of Food and Bioproduct Sciences, University of Saskatchewan,
51 Campus Drive, Saskatoon SK, Canada, S7N 5A8

[++]Saskatoon Research Centre, Agriculture and Agri Food Canada,
107 Science Place, Saskatoon, SK, Canada, S7N 0X2

[5] Food Biophysics, 9, 105-113 (2014)

11.1 ABSTRACT

The influence of pH (3.0, 5.0, and 7.0) and ionic strength (0, 50, 100 mM NaCl) on the physicochemical and emulsifying properties of a cruciferin-rich protein isolate (CPI) was investigated. Surface charge on the CPI was found to substantially reduced in the presence of NaCl. Surface hydrophobicity was found to be the lowest for CPI at pH 7.0 with 100 mM NaCl, and highest at pH 3.0 without NaCl. Solubility was found to be lowest at pH 5.0 and 7.0 without NaCl (<20%), however greatly improved for all other pH and NaCl conditions (>80%). Interfacial tension was found to be lowest at 10-11 mN/m for pH 5.0 – 0 mM NaCl and pH 7.0 – 50/100 mM NaCl, whereas under all other conditions interfacial tension was higher (15+ mN/m). Overall, NaCl has no effect on EAI at pH 3.0 where it ranged between 18.8 and 19.4 m^2/g. At pH 5.0, EAI decreased from 21.1 to 12.8 m^2/g as NaCl levels increased from 0 to 100 mM. At pH 7.0, EAI values were found to decrease from 14.9 to 5.2 m^2/g as NaCl levels were raised from 0 to 100 mM. Overall, ESI was reduced with the addition of NaCl from ~15.7 min at 0 mM NaCl to ~11.6 min and ~12.0 min for the 50 and 100 mM NaCl levels, respectively.

11.2 INTRODUCTION

Canola is primarily grown in Canada is for its oil content, used for cooking and biofuel purposes. The remaining meal after oil extraction is considered rich in protein (up to 50 % dry basis) and fibre, and currently used as a low cost animal feed for nutritional purposes (Mieth et al., 1983; Aider and Barbana, 2011). Despite its well-balanced amino acid profile, canola protein remains still underutilized for human consumption because of its inferior functional and organoleptic properties, and presence of antinutritional factors such as phytic acid and phenolic compounds (Schwenke, 1994; Nesi et al., 2008; Tan et al., 2011). Over the past few decades, research has focused on trying to understand structure-function relationships involving canola proteins, and ways to improve them through enzymatic or chemical means (Gruener and Ismond, 1997; Pinterits and Arntfield, 2008; Klassen et al., 2011). Unfortunately, the physicochemical and functional properties of canola proteins can vary depending on the degree of processing of the meal and the protein extraction process used (Can Karaca et al., 2011a; Tan et al., 2011; Wanasundara et al., 2012). Other studies have focused on significantly lowering the antinutritional factors to improve the digestibility and functionality of the protein product (Ismond and Welsh, 1992; Ser et al., 2008). Successful innovation and optimization of processing parameters could

yield canola proteins with superior functionality that could compete on the vegetable ingredient market as an alternative to soy.

Canola storage protein is dominated by the salt soluble globulin 12S cruciferin, up to 60% of total protein, the rest being composed of water soluble albumin (napin) and alcohol soluble prolamin proteins (Hoglund et al., 1992). The exact ratio of which, however varies among the cultivar and extraction processes used (Raab et al., 1992; Aider and Barbana, 2011). Cruciferin is a hexamer (~300 kDa) with six monomers, where each monomer contains one α- chain polypeptide (~30 kDa) and one β- chain polypeptide (~20 kDa) stabilized with a disulfide bridge (Simard et al., 1979; Schweke et al., 1983). The reversible dissociation of 12S cruciferin to 7S trimers dependS on the ionic strength (<0.5) has been observed (Schwenke and Linow, 1982). It was also found that 12S cruciferin can further dissociate into a 2-3S component irreversibly after dialyzing the protein solution against 6 M urea (Bhatty et al., 1968). The same authors also reported the 12S cruciferin would dissociate into the 7S trimer at pH <3.6. Cruciferin has a neutral pI (~pH 7.2), and has secondary structures composed of high level of β-sheets (~50%) and low level of α-helices (~10%) (Zirwer et al., 1985).

The functional properties of 12S rapeseed protein were investigated such as foaming properties (Nitecka et al., 1986; Gruener and Ismond, 1997) and emulsifying properties (Krause and Schwenke, 2001; Wu and Muir, 2008). Great variations of data regarding the emulsifying properties of 12S cruciferin has been found in literature possibly due to different extraction methods and experimental conditions used. For instance, Krause and Schwenke (2001) found cruciferin had poor emulsifying properties due to its lack of structural flexibility at the oil/ water interface. However, Wu and Muir (2008) found cruciferin has better emulsifying properties than the water soluble napin protein. Schwenke (1994) reported unmodified cruciferin to also be more surface active than napin. The overall goal of this study was to investigate underlying structure-function mechanisms associated with the emulsifying properties of a cruciferin-rich protein isolate in response to changes in pH and NaCl content.

11.3 MATERIAL AND METHODS

Materials

Canola seeds (*B. napus*/ variety VI- 500) were kindly donated by Viterra (Saskatoon, SK, Canada) for this research. All chemicals used in this study were of reagent grade and purchased from Sigma- Aldrich Canada Ltd. (Oakville, ON, Canada). Water used in this research was double deionized water produced from a Millipore Milli-Q^{TM} water purification system (Millipore Corporation, Milford, MA).

Preparation and characterization of a cruciferin-rich protein isolate

Prior to use, canola seeds were stored in containers at 4^{o}C. At room temperature (21-23^{o}C), small seeds were first removed using a #12 (1.7 mm mesh size) Tyler mesh filter (Tyler, Mentor, OH) in order to maximize the cracking efficiency of the screened seeds. The latter was then placed in a -40^{o}C freezer overnight to aid in the dehulling processes. Frozen seeds were then cracked using a stone mill (Morehouse-Cowles stone mill, Chino, CA), followed by separation of the seed coat and cotyledons using an air blower (Agriculex Inc., Guelph, ON, Canada) which separates based on density differences between the two. The dehulled seeds were then pressed using a continuous screw expeller (Kornet, Type CA59 C; IBG Monforts Oekotec GmbH & Co., Mönchengladbach, Germany) to remove the majority of the oil. The screw expeller was operated at speed 6.5 using a 3.5 mm choke and resulting in a meal temperature of ~75^{o}C. The meal was then ground into a powder. Residual oil was then reduced using hexane (1:3 meal: hexane ratio) at room temperature for 16 h, twice. The meal was then left in fume hood overnight to allow residual hexane to evaporate.

A cruciferin-rich protein isolate (CPI) was prepared based on methods of Murray et al. (1980) with slight modifications. In brief, 20 g of defatted ground meal was dispersed in 200 mL of Milli-Q^{TM} water containing 0.2 M NaCl, and then maintained at pH (5.8- 6.3) with continuous stirring (500 rpm) for 90 min at room temperature (21-23^{o}C). The dispersion was then centrifuged at 17,700 × *g* for 20 min at 4^{o}C using Sorvall RC-6 Plus centrifuge (Thermo Scientific, Asheville, NC). The supernatant was then collected through vacuum filtration using Whatman No. 1 filter paper (Whatman International Ltd., Maidstone, UK). Afterwards, the filtered supernatant was diluted with prepared cold Milli-Q^{TM} water (<4^{o}C) up to 2000 mL and allowed to settle overnight. Protein micelles were collected by decanting the clear upper layer and pooling the protein micelles

in separatory funnels. The concentrated protein liquid was then dialyzed (Spectro/ Pro® tubing, 6-8 kDa cut off, Spectrum Medical Industries Inc., Rancho Dominguez, CA) at 4°C for 48 h against Milli-Q water with several changes of water until the conductivity reached ~2.0–2.5 mS/cm. Desalted protein micelles were then freeze dried to obtain a CPI powder. Protein content was determined according to the Association of Official Analytical Chemists (AOAC, 2003) method 920.87, using a micro-Kjeldhal digestion and distillation unit (Labconco Corp., Kansas City, MO) and a nitrogen conversion factor of 6.25.

The amino acid composition analysis was performed by POS (POS Bio- Science, Saskatoon). Amino acid profile of the NPI was determined using a pico-tag amino acid analysis system (Waters Corporation, Milford, MA, USA) and HPLC. In general, fifteen amino acid residues were quantified according to method developed by Bidlingmeyer et al. (1987) in which 15 mL of 6N HCl was added to the sample for hydrolysis prior to HPLC separation. The amount of sulfur- containing amino acid residues were determined according to AOAC official methods 985.28 (AOAC, 2003), in which 10 mL cold performic acid was added to oxidize cysteine and methionine before hydrolysis with 15 mL 6N HCl. Quantity of tryptophan was determined according to AOAC method 988.15 (AOAC, 2003) which 10 mL of 4.2M NaOH was added to samples to hydrolyze tryptophan before separation. Sample amino acid concentration was normalized for the isolate based on its crude protein content.

The CPI was also subjected to sodium dodecyl sulphate (SDS) polyacrylamide gel electrophoresis (PAGE) under reducing conditions to observe the molecular weight band profile, according to the Laemmli procedure (Laemmli, 1970) and using the PhastSystem equipped with separation and development capabilities (Amersham Pharmacia, Uppsasla, Sweden). In brief, samples were prepared by dissolving 2 mg of protein with 1 mL in a 0.1 M Tris-HCl buffer (containing 5% SDS (w/v) at pH 8.00) with addition of β-mercaptoethanol (5%, v/v), followed by heating at 99°C (Incu Block model 285, Denville Scientific Inc., South Plainfield, NJ) for 10 min to unravel and disassociate the protein, followed by cooling the solution to room temperature (21-23°C). Mixtures were then centrifuged at 16,873 x *g* for 10 min to remove any insoluble material (Marcone et al., 1998). A sample of 1 μg protein solution was applied into each well and standard proteins (Sigma wide range molecular weight markers) of 170, 130, 95, 72, 55, 43, 34, 26, 17 and 10 kDa were applied to a separate well. Gradient mini gels (resolving 8–25%T (T, denotes the total amount of acrylamide present) and 2%C (C, denotes the amount of cross-linker), stacking

zone 4.5%T and 3%C, 43 mm × 50 mm × 0.45 mm, polyacrylamide gels cast on GelBond® plastic backing, buffer 0.112 M acetate, 0.112 M Tris, pH 6.4) were used to separate proteins. Following separation, the proteins were fixed and stained using PhastGel blue R (Coomassie R-350) and developed to obtain suitable background colour. Molecular weights of each band and relative percentage were estimated using the ImageQuant® (Ver. 3.0; Amersham Pharmacia Biotech, Piscataway, NJ, USA) software based on the darkness intensity of each band (Marambe et al., 2013).

Sample preparation

Protein solutions (0.25%, w/w - unless otherwise stated) were prepared for all experiments by dispersing CPI powder (corrected for protein content) within Milli-Q water containing 0, 50 or 100 mM NaCl under continuous stirring (500 rpm) at room temperature (21-23ºC). Solution pH was then adjusted (pH 8.0- 8.5) using either 0.1 M HCl or 0.1 NaOH. CPI solutions were then allowed to stir overnight, prior to use (with the exception of solubility testing).

Surface charge

The zeta potential of 0.05% (w/w) CPI solutions as a function of pH and NaCl concentrations were determined by measuring the electrophoretic mobility (U_E) using a Zetasizer Nano-ZS90 (Malvern Instruments, Westborough, MA, USA). Zeta potential (ζ; units: mV) was calculated by the zetasizer with U_E by applying Henry's equation:

$$U_E = \frac{2\varepsilon \times \zeta \times f\,(k\alpha)}{3\eta} \qquad \text{(eq.11.1)}$$

where ε is the permittivity (units: F (Farad)/m), $f(\kappa\alpha)$ is a function related to the ratio of particle radius (α; units: nm) and the Debye length (κ; units: nm^{-1}), and η is the dispersion viscosity (units: mPa·s). The Smoluchowski approximation $f(\kappa\alpha)$ was set as 1.5. All measurements are reported as the mean ± one standard deviation (n = 3).

Average surface hydrophobicity using a fluorescent probe method

The average surface hydrophobicity of CPI as a function of pH and NaCl concentrations were estimated using a FluoroMax-4 spectrofluorometer (Horiba Jobin Yvon Inc., Edison, NJ) by

the ANS (8-anilino-1-naphthalenesulfonic acid) fluorescent probe method based on the original work of Kato and Nakai (1980) and later modified by Can Karaca et al. (2011a,b). In brief, CPI solutions were diluted into concentrations of 0.1%, 0.08%, 0.06%, 0.04% and 0.02%. (w/w) with Milli-Q water containing the desired NaCl level. For each diluted CPI concentration, two 15 mL test tubes containing 4 mL of CPI solution were prepared, with and without 20 µL of 8 mM ANS solution in Milli-Q water with salt level the same as the samples, and then vortex for 10s. All solutions were then stored in the dark for 15 min at room temperature (21-23^{o}C). Fluorescence intensity at 390 nm excitation and 470 nm emission wavelengths were measured for: (a) an ANS blank (containing only the ANS probe); (b) a CPI blank (containing only the CPI solution); and (c) the CPI solution containing the ANS probe. The net fluorescence intensity was obtained by subtracting the ANS (a) and CPI (b) blanks from the sample (c), at equivalent protein concentrations. The net fluorescence intensity was then plotted against protein concentration, where the slope (as determined by linear regression) of the initial rise was taken (arbitrarily divided by 10000) as an index of average protein surface hydrophobicity. All measurements are reported as the mean ± one standard deviation (n = 3).

Protein solubility

Protein solubility of CPI was investigated as a function of pH and NaCl content, according to Can Karaca et al. (2011a,b) with slight modifications. In brief, 20 mL of protein solutions were prepared as previously described (except stirring for 1 h at room temperature). For each solution, 12 mL was then transferred to a 15 mL centrifuge tube and centrifuged (VWR clinical centrifuge 200, VWR International, Mississauga, ON, Canada) at 4,180 × *g* for 10 min at room temperature (21-23^{o}C). Protein content was determined by measuring the total nitrogen levels in ~5 g of supernatant using a micro-Kjeldahl digestion and distillation unit (Labconco Corp., Kansas City, MO) and a 6.25 conversion factor. Protein solubility (%) was determined by dividing the total amount of protein within the supernatant by the original amount in the sample, multiplied by 100%. All measurements are reported as the mean ± one standard deviation (n = 3).

Interfacial tension

The interfacial tension between canola oil and each CPI solution (as a function of pH and NaCl) was measured using a semi-automatic tensiometer (Lauda TD2, GmbH & Co., Lauda-

KÖnigshofen, Germany) according to the Du Noüy ring method. Interfacial tension for a water (without CPI)-canola oil system served as a control. Interfacial tension was calculated from the maximum force *(F_{max}; units: milli-Newtons; instrument measures mg x gravity)* using the following equation:

$$\gamma = \frac{F_{\max}}{4\pi R\beta} \quad \text{(eq. 11.2)}$$

where, γ is the interfacial tension (mN/m), R is the radius of the ring (20 mm), β is a correction factor that depends on the dimensions of the ring and the density of the liquid involved (McClements, 2005). All measurements are reported as the mean ± one standard deviation (n = 3).

Emulsifying properties

Emulsification activity (EAI) and stability (ESI) indices were determined according to Pearce and Kinsella (1978). In brief, 5.0 g of the CPI solution (prepared as a function of pH and NaCl content) was homogenized with 5.0 g of canola oil using an Omni Macro Homogenizer (Omni International, Marietta, GA) with a 20 mm saw tooth generating probe at speed 4 (~7,200 rpm) for 5 min. Fifty microliters of the emulsion was immediately taken from the bottom of the tube and diluted in 7.5 mL of 0.1% sodium dodecyl sulphate (SDS), followed by vortexing for 10 s. A Genesys 10 UV-visible spectrophotometer (Thermo Scientific, Madison, WI) was used to determine the absorbance of the diluted emulsion samples at 500 nm using a plastic cuvette (1 cm path length). A second absorbance reading was taken from the dilution after 10 min. EAI and ESI were calculated by following equations.

$$EAI\ \left(\frac{m^2}{g}\right) = \frac{2\times 2.203\times A_0\times N}{c\times\varphi\times 10000} \quad \text{(eq. 11.3)}$$

$$ESI\ (\text{min}) = \frac{A_0}{\Delta A}\times t \quad \text{(eq. 11.4)}$$

where, A_0 is the absorbance of the diluted emulsion immediately after homogenization, N is the dilution factor, c is the weight of protein per volume (g/mL), φ is the oil volume fraction of the emulsion, and ΔA is the difference in absorbance between 0 and 10 min ($A_0 - A_{10}$) and t is the time interval (10 min). All measurements are reported as the mean ± one standard deviation (n = 3).

Statistical analyses

All statistics were performed using SPSS Ver. 20.0 software (SPSS Inc., 2012, Chicago, IL). A two-way analysis of variance (ANOVA) was used to test the significance of the main effects (pH and NaCl) and associated interaction on the physicochemical (surface hydrophobicity, solubility and interfacial tension) and emulsifying (EAI and ESI) properties. A simple Pearson correlation was also performed to describe the relationship between the emulsifying and physicochemical properties.

11.4 RESULTS AND DISCUSSION

Characterization of the CPI material

The protein content of CPI was determined to be 90.35% (w.b.). Ismond and Welsh (1992) obtained a 78.5% (w.b.) protein content using a similar extraction procedure. Figure 11.1 shows an SDS-PAGE profile of CPI under reducing conditions with bands occurring between ~17 and ~65 kDa accounting for 85.6% of the total bands as determined by densitometry (lane 1, CPI). The results are presumed to correspond to the molecular mass of the individual subunits of cruciferin (~50 kDa), along with their α- (~30 kDa) and β- (~20 kDa) chains (Dalgalarrondo et al., 1986), aligning with the results of Wu and Muir (2008). The amino acid composition of CPI was found to be high in glutamine (+ glutamic acid) (17.90%), along with asparagine (+ aspartic acid) (9.49%), leucine (7.21%) and arginine (6.97%) (Table 11.1). Chabanon and others (2007) and Schwenke (1990) reported cruciferin to be rich in glutamine (+ glutamic acid) and arginine, accounting for ~20 and 10% of the total amino acids, respectively. The most abundant amino acid group, glutamine has a pK_a of 4.1; leaving its reactive side group negatively charged at pHs > 4.1. In contrast, arginine has a very high pK_a at 12.5, and its reactive side group assumes a positive charge at pHs less than this pH.

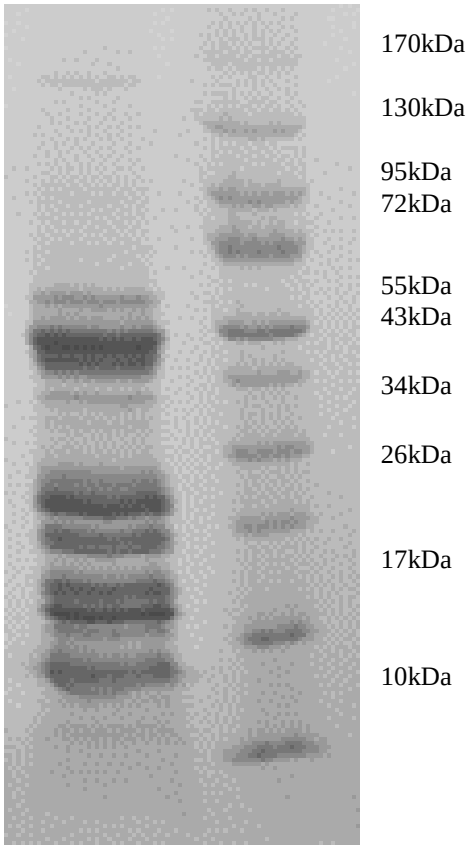

Figure 11.1 SDS-PAGE (reducing) (1 μL of 2 mg mL^{-1} CPI solution) applied to gradient 8-25% PhastGels. Lanes: (1) CPI and (2) standard.

Table 11.1 Amino acid profile for the cruciferin-rich protein isolate.

Amino acid	**Percent**
(Aspartic acid + Aspargine)	9.49
(Glutamic acid + Glutamine)	17.9
Alanine	3.76
Arginine	6.97
Cysteine	1.33
Glycine	5.18
Histidine	2.19
Isoleucine	4.06
Leucine	7.21
Lysine	3.37
Methionine	1.52
Phenylalanine	4.28
Proline	5.00
Serine	5.00
Threonine	4.07
Tryptophan	1.32
Tyrosine	2.89
Valine	4.65
Total:	**90.19**

Surface characteristics

Surface charge on the protein is highly dependent upon on the amino acid composition, protein conformation and solvent conditions (e.g., pH and salt content). Figure 11.2 shows the change in zeta potential (mV) for CPI solutions as a function of pH and salt concentration. For CPI in the absence of added NaCl, zeta potential rose from ~-33 mV at pH 8.0 relatively linearly to pH 4.8 (isoelectric point) where it became 0 mV, then increased further to +33 mV at pH 3.0, before declining slightly to ~+22 mV at pH 2.0. In contrast, the addition of both 50 and 100 mM NaCl

resulted in only a slight charge ranging between ~-10 mV at pH 8.0 and ~+10 mV at pH 2.0, the pI values (pH 4.6) remained relatively similar to the sample without added NaCl. The addition of NaCl acts to screen charged amino groups on the protein's surface, functioning to reduce the relative thickness of the electric double layer and the charge exerted out into solution (McClements, 2004). Paulson and Tung (1987) reported similar findings with the addition of 350 and 700 mM NaCl for unmodified CPI where the zeta potential was reduced from -18 mV to -5 mV at pH 5.0 and from -40 mV to -20 mV at pH 7.0. Schwenke (1990) and Mieth et al. (1983) both reported pI values of ~7.2 for cruciferin extracted from *B. napus*. However, cruciferin rich isolates has been recorded to have pIs ranging from pH 4-10 depending on the extraction method (Paulson and Tung, 1987; Can Karaca et al., 2011; Wanasundara et al, 2012).

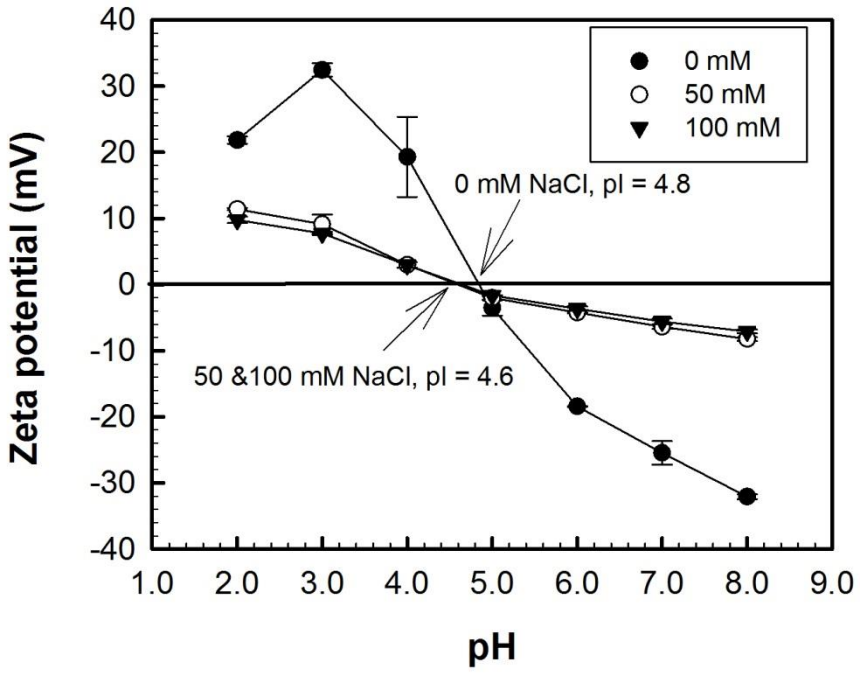

Figure 11.2 Zeta potential (mV) of CPI in the function of pH and NaCl (mM) content. Data represent the mean ± one standard deviation (n = 3).

Surface hydrophobicity plays an important role in driving protein-protein aggregation and the protein's interfacial activity (Dickinson, 2003). Higher amounts of protein-protein interactions may also have a negative impact on protein solubility in aqueous solutions and alignment at the interface if hydrophobic moieties become re-buried (Jung et al., 2005; Avramenko et al., 2013).

Gerbanowskia and co-workers (2003) also reported that hydrophobicity can impact the rate of interfacial tension reduction in terms of protein diffusion, adsorption, conformational change and molecular rearrangement at the interface. In the present study, the effects of pH and NaCl on surface hydrophobicity was shown to be significant ($p<0.001$). Overall, surface hydrophobicity was found to be at the highest level at low pH, however the effects of salt level were different at each pH (Figure 11.3). At pH 3.0, surface hydrophobicity was similar for solutions with 0 and 50 mM of added NaCl (100 and 98.4 arbitrary units, A.U.); however surface hydrophobicity was significantly reduced with the addition of 100 mM NaCl (68.8 A.U.). At pH 5.0, hydrophobicity was found to increase linearly with NaCl content from 45.3 A.U. at 0 mM NaCl to 74.0 A.U. at 100 mM NaCl. At pH 7.0, hydrophobicity was found to increase from 16.4 A.U. at 0 mM NaCl to 25.0 A.U. for 50 mM NaCl; and then declined to 5.04 A.U. as NaCl content increased to 100 mM. At pH 3.0, it was hypothesized that hydrophobicity was overall higher than the other pHs due to possibly dissociation of protein subunits which would expose hydrophobic moieties. At pH 5.0, the CPI carried a relatively neutral charge (~ 0 - -5 mV), where the addition of NaCl most likely resulted an increase in conformational entropy allowing for greater mobility of the proteins in solution. It was hypothesized that because of these conformational changes, a greater amount of aromatic groups became exposed and available for interaction with the ANS probe. In contrast, at pH 7.0 the rise and fall of hydrophobicity with increased NaCl content is thought to be due to conformational change of the cruciferin molecules which affect the binding efficiency of ANS probes. Paulson and Tung (1987) have also reported similar trends for canola salt soluble globulins where the effect of salt was opposite at pH < pI and pH> pI. Alizadeh-Pasdar and Li-Chan (2000) reported that hydrophobicity results obtained by ANS probes need to be treated with caution because the charges carried by the probes might affect the ability of the probe to bind to the protein surface especially at pHs above the pI value of the protein.

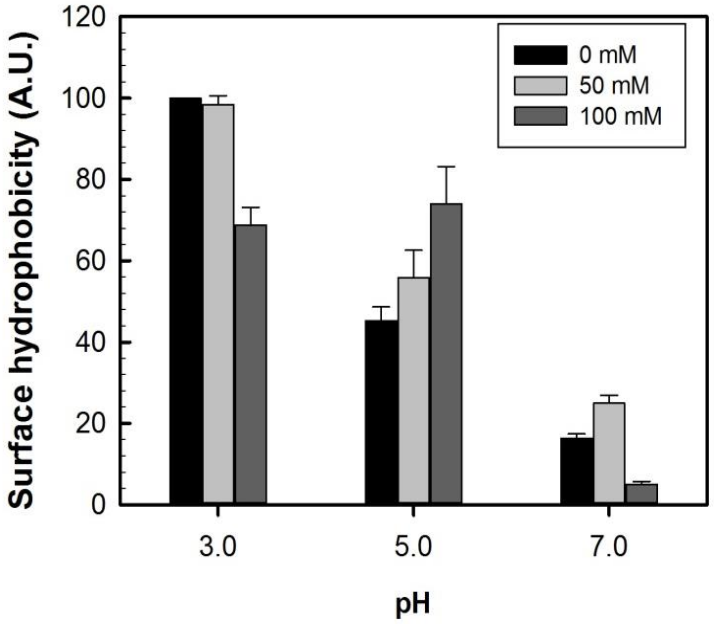

Figure 11.3 Surface hydrophobicity for CPI solutions as a function of pH and NaCl (mM) content. Data represent the mean ± one standard deviation (n = 3).

CPI solubility

The solubility of CPI as a function of pH and NaCl concentration is shown in Figure 11.4. A two-way analysis of variance found the main effects of pH ($p<0.001$) and NaCl concentration ($p<0.001$) along with their associated interaction ($p<0.001$) to be significant. Overall solubility was found to be highest at pH 3.0 regardless of the concentration of NaCl (~91%), whereas at pH 5.0, solubility increased from 10.7% at 0 mM NaCl to 77.4 % and 88.2% with the addition of 50 mM and 100 mM NaCl, respectively. A similar trend was reported for pH 7.0, where solubility increased from 15.7% at 0 mM NaCl to 86.6 % and 90.4% with the addition of 50 mM and 100 mM NaCl, respectively. Findings from the present study indicated that NaCl had a salting in effect on the CPI, in which Na^+ ions contributed to the ordering of the hydration layer to improve protein-water interactions; resulting in relatively high solubility (Dickinson, 2003). For CPI solutions in the absence of added NaCl, solubility was good at pH 3.0 due to a sufficient amount of electrostatic repulsive forces between proteins in solution to keep them dispersed. In contrast, at pH 5.0 (near the pI) and at pH 7.0, electrostatic repulsion was less leading to protein-protein interactions and aggregation.

Can Karaca et al. (2011) found a CPI solution at pH 7.0 showed very poor solubility at a ~5% level. Paulson and Tung (1987) reported poor solubility of cruciferin at pH 5.0 (~5%) in the absence of NaCl, which was increased to ~20% with the addition of 0.35 and 0.7 M NaCl. The authors also reported that solubility was improved at pH < pI with the addition of NaCl due to a salting-in process, however was adversely affected at pH > pI due to a salting-out process. Although this pH-salt dependence contradicts our findings, Paulson and Tung (1987) used much higher NaCl levels than in the present study. The overall lower solubility found by the authors versus the present study is also presumed to be attributed to the much higher protein concentration used (11.4% vs 0.25%).

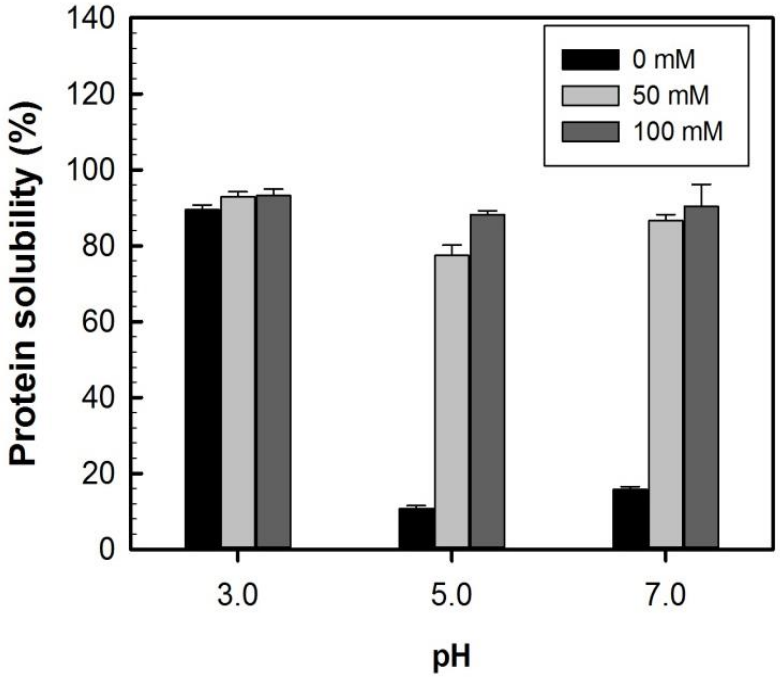

Figure 11.4 Percent protein solubility for CPI solutions as a function of pH and NaCl (mM) content. Data represent the mean ± one standard deviation (n = 3).

Interfacial tension

Interfacial tension is defined as the work required creating a unit area of interface at a constant temperature, pressure, and chemical potential (Drelich et al., 2002). The ability for CPI to reduce interfacial tension at an oil-water interface was investigated as a function of pH and salt content, and is given in Figure 11.5. A two-way analysis of variance found that the main effect of pH and (salt x pH) interaction term to be significant ($p<0.001$), whereas the effect of salt alone was not significant ($p>0.05$). The addition of CPI to the aqueous phase at all pHs and NaCl concentrations was found to reduce the interfacial tension at an oil-water interface from 22.5 mN/m (control, no protein) to 10-17 mN/m. Overall, interfacial tension declined from ~16.7 mN/m at pH 3.0, to 14.0 mN/m at pH 5.0, and then to 12.0 mN/m at pH 7.0, however the influence of salt was different at each pH. At pH 3.0, interfacial tension remained similar regardless of the salt content at 16.5-17.3 mN/m. At pH 5.0, the addition of salt had a negative effect on the ability of CPI to lower interfacial tension, where values were found to be 15.3 and 15.6 mN/m for solutions with 50 and 100 mM NaCl, respectively relative to that without NaCl at 11.1 mN/m. Furthermore, at pH 7.0 the addition of NaCl showed a positive effect on reducing interfacial tension by lowering values to 10.3 and 11.0 mN/m for the 50 and 100 mM NaCl levels, respectively relative to that solution without added NaCl (14.8 mN/m). A simple Pearson correlation shown that interfacial tension is positively correlated with surface hydrophobicity ($r= 0.765$, $p<0.01$) which indicated higher hydrophobicity might promote protein- protein interaction and have negative impacts on the CPI molecules ability to migrate and realign at the interface due to reduced structural flexibility. Krause and Schwenke (2001) found that although cruciferin had lower diffusion rate compared with napin, cruciferin achieved greatest decrease in interfacial tension. Previous study also found the surface hydrophobicity has significant effect to the interfacial tension where the sample with modified cruciferin through succinylation (at 66.0%) had the lowest interfacial tension (Gueguen et al., 1990).

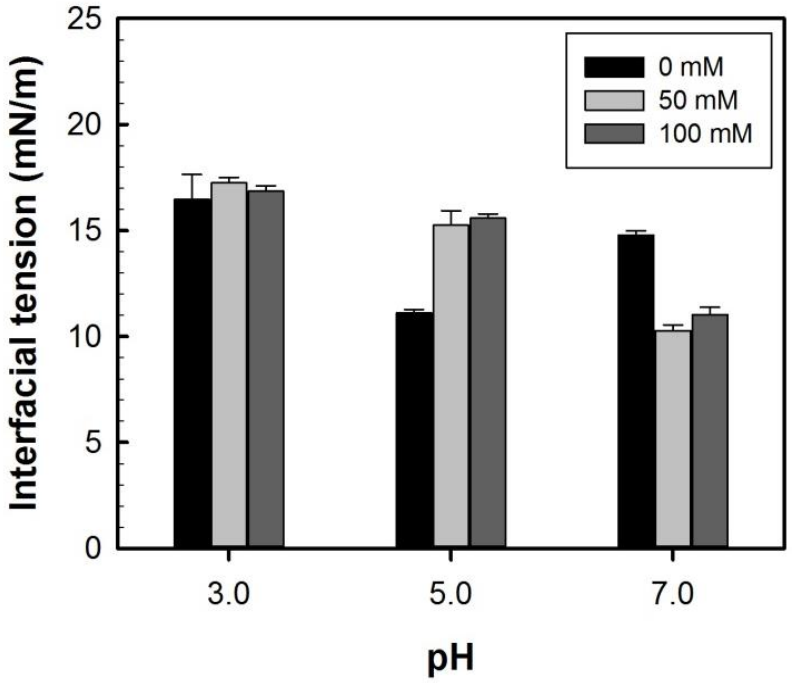

Figure 11.5 Interfacial tension (mN/m) for CPI solutions as a function of pH and NaCl (mM) content. Data represent the mean ± one standard deviation (n = 3).

Emulsifying properties

The emulsifying activity index (EAI) gives a measure of interfacial area coated by an emulsifier such as protein during the formation of an emulsion and is a good predictor for protein surface activity (Pearce and Kinsella, 1978). The EAI for CPI under the influence of pH and NaCl was investigated, and was found that the main effects of NaCl and pH were significant ($p<0.001$), along with their associated interaction ($p<0.01$). Overall, NaCl had no significant effect on EAI at pH 3.0 where EAI values ranged between 18.8 and 19.4 m^2/g. The effect of NaCl was more pronounced at pH 5.0 and pH 7.0 in which the addition of NaCl reduced the EAI values (Figure 11.6A). For instance, at pH 5.0, EAI values declined from 21.1 m^2/g to 18.8 m^2/g and then to 12.8 m^2/g as NaCl levels increased from 0 mM to 50 mM and then to 100 mM, respectively. A similar trend was observed at pH 7.0, where the addition of NaCl reduced EAI values from 14.9 m^2/g at 0 mM NaCl to 5.2 m^2/g at 100 mM NaCl. A simple Pearson correlation

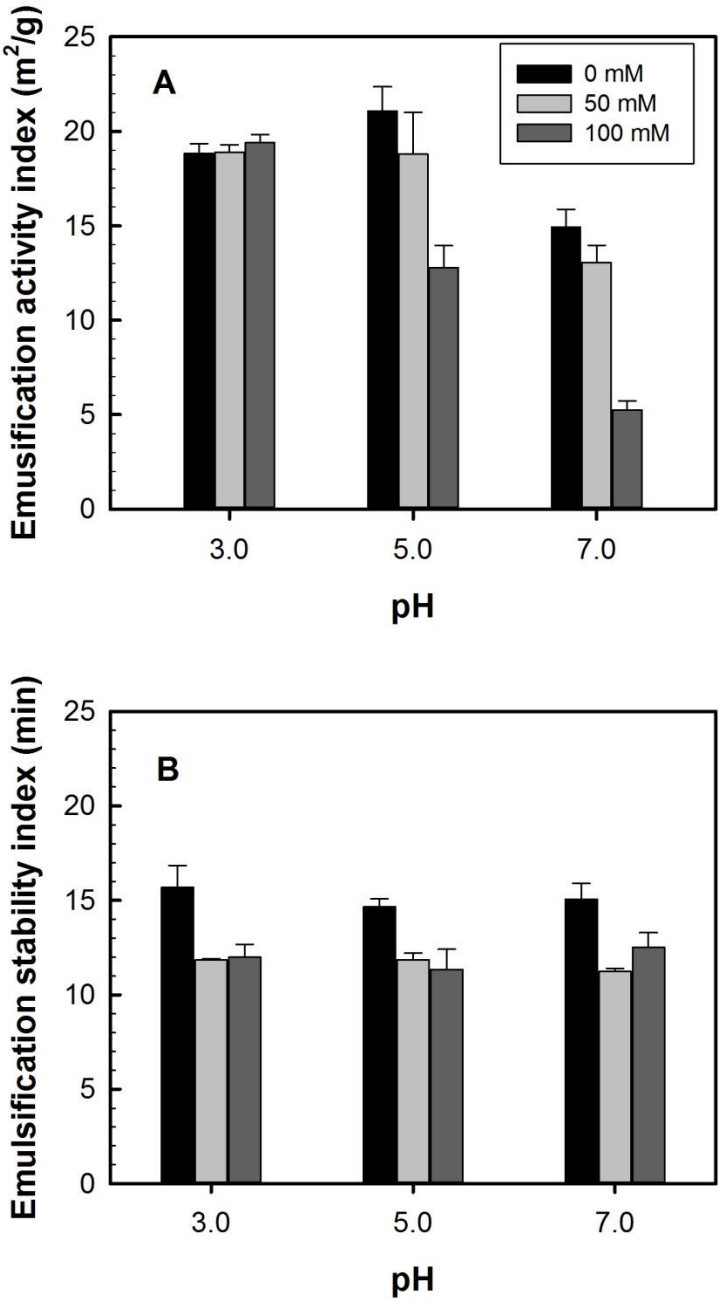

Figure 11.6 Emulsification activity (m^2/g) (A) and stability (min) (B) indices for CPI solutions as a function of pH and NaCl (mM) content. Data represent the mean ± one standard deviation (n = 3).

analysis found that EAI was positively correlated with surface hydrophobicity ($r = 0.642$; $p<0.01$). It is believed that having high hydrophobicity leads to greater alignment and integration of protein into the oil-water interface, allowing interfacial tension to be reduced and greater to occur (Kato and Nakai, 1980; Zayas, 1997). Paulson and Tung (1987) and, Wanasundara and Shahidi (1997) suggested that the ratio of hydrophobic to hydrophilic sites on the protein's surface impacts the ability for a viscoelastic film to form. Krause and Schwenke (2001) reported that under neutral conditions, EAI for rapeseed globulin was relatively lower than the albumin fraction, and that of a mixed rapeseed protein comprised of 30% albumin and 70% globulin. The larger molecular mass of proteins of CPI may have a negative effect during the formation of emulsion due to the lack of conformational changes at the interface in its globular undissociated state (Wanasundara, 2011).

The emulsifying stability index (ESI) provides a measure of the stability of the diluted emulsion over a fixed period of time (Can Karaca et al., 2011). ESI for CPI as a function of pH and salt content was investigated and is given in Figure 11.6B. An analysis of variance found that only the effect of salt was significant ($p<0.001$). Overall, ESI was reduced with the addition of NaCl from ~15.1 min at 0 mM NaCl to ~11.6 min and ~12.0 min for the 50 and 100 mM NaCl levels, respectively. In this study, the ESI results were corresponded with the surface charge where the addition of NaCl reduced overall surface charge which would lead to droplets flocculation and coalescence due to lack of electrostatic repulsion between droplets. ESI values were also found to be negatively correlated with solubility ($r = -0.582$, $p<0.01$), where it was thought that reduced solubility was important for additional proteins to precipitate and adhere to the viscoelastic film surrounding the droplets. Solubility was higher for CPI solutions with NaCl present than without added NaCl, possibly due to a salting-in effect which kept a greater amount of protein in solution, despite pHs near its pI value (5.0, 7.0). Zhang et al. (2009) reported the effect of NaCl on the emulsion stability of chickpea proteins by measuring changes in mean droplet size over time, to find greater instability with the addition of NaCl as a result of coalescing droplets. In the study of Can Karaca et al. (2011), there were no significant differences of ESI between CPI extracted by different methods which was believed to be dominated by globulin or globulin/albumin mixed fraction. The authors found ESI of canola protein isolates around 10.5-15.5 min at pH 7.0 which was similar to the ESI values in the present study.

11.5 SUMMARY

In general, the physicochemical properties of CPI varied with increasing ionic strength depending on the pH level. For instance, the addition of NaCl greatly improved solubility at pHs 5.0 and 7.0 but had no effect at pH 3.0. In contrast, surface hydrophobicity was found to decline with increasing ionic strength at pHs 3.0 and 5.0. Increasing ionic strength increased interfacial tension at pH 5.0 but had opposite effect at pH 7.0. Overall, the emulsifying properties of CPI were strongly influenced by the physicochemical properties of the protein, pH and NaCl content. For instance, EAI was positively correlated with the protein's surface hydrophobicity and ability to reduce interfacial tension, whereas ESI was negatively influenced by the solubility of the protein. EAI was reduced with the addition of NaCl at pH close to pI value and at pH 7.0. Emulsion stability was also reduced with the addition of NaCl at all tested pH levels.

-Chapter 12-

Effect of pH and NaCl on the emulsifying properties of a napin protein isolate[6]

Cheung, Lamlam[+], Wanasundara, Janitha P.D.[++], and Nickerson, Michael T.[+]

[+]Department of Food and Bioproduct Sciences, University of Saskatchewan,
51 Campus Drive, Saskatoon SK, Canada, S7N 5A8

[++]Agriculture and Agri-Food Canada, Saskatoon Research Centre,
107 Science Place, Saskatoon, SK, Canada, S7N 0X2

[6]Food Biophysics, Accepted June 2014, *In press*

12.1 ABSTRACT

The physicochemical and emulsifying properties of a napin protein isolate (NPI) were examined as a function of pH (3.0, 5.0 and 7.0) and NaCl content (0, 50 and 100 mM). Specifically, surface charge and hydrophobicity, interfacial tension (IT), solubility, and the emulsifying activity (EAI) and stability (ESI) indices were studied. Surface charge in the absence of NaCl ranged between ~ +10 mV to ~ -5 mV depending on the pH, becoming electrically neutral at pH 6.6. Overall, surface hydrophobicity decreased as the pH increased, whereas it increased as NaCl levels were raised. Solubility was high (~93-100%) regardless of the conditions. NPI's ability to reduce IT was enhanced at higher pHs, however the effect of NaCl was pH dependent with the addition of NaCl enhancing and decreasing NPI's ability to reduce IT at pH 3.0 and 7.0, respectively. Overall, EAI values were similar in magnitude at pH 3.0 and 5.0, and lower at pH 7.0. The effect of NaCl on EAI was similar at pH 3.0 and 7.0, where EAI at the 0 mM and 100 mM NaCl level were similar in magnitude, but increased significantly at the addition of 50 mM NaCl. However, the EAI values at pH 5.0 decreased as the level of NaCl increased. Overall, the stability of NPI-stabilized emulsions degraded rapidly and the addition of salt induced faster emulsion instability.

12.2 INTRODUCTION

Canola was originally bred from rapeseed varieties (e.g., *Brassica napus* L.*)* to have low levels of erucic acid (<2%) and glucosinolates (<30 µmol/g) for use as an edible healthy oil. (Canola Council of Canada, 2011). Canola meal, the co-product of oil processing is rich in protein (36- 39%) and fibre (~12%), which to date is commonly used in low cost livestock feed for its nutritional value (Khattab and Arntfield, 2009; Newkirk, 2009). The meal also contains high levels of phenolics compounds and phytic acid which can lead to poor protein functionality depending on the extraction method used (Wu and Muir, 2008; Aider and Barbana, 2011) Research surrounding adding value to the under-utilized and under-valued meal has intensified recently, particularly as it relates to the protein fraction. Despite its well-balanced amino acid profile (Ohlson and Anjou, 1979), the utilization of canola protein by the food industry has been limited due to its poorer functionality compared to animal-derived protein ingredients. Depending on the canola variety used, processing practices and methods of extraction, protein functionality can vary considerably (Aluko and McIntosh, 2001; Khattab and Arntfield, 2009; Can Karaca, Low and

Nickerson, 2011a,b). Successful processing innovations and product characterization could lead to the development of a new plant sourced protein food ingredient.

Canola proteins are dominated by two types of protein: cruciferin and napin. Cruciferin and napin constitute roughly 70% and 30% of the total protein, respectively (Krause and Schwenke, 2001; Dong et al., 2011; Tan et al., 2011). Cruciferin (12 S; molecular mass ~240-300 kDa) is a salt-soluble globulin with a isoelectric point (pI) of ~ 7.2 (Schwenke, 1994), and is comprised of high level of β-sheets (~50%) and low level of α-helices (~10%) (Zirwer et al., 1985). Napin (1.7-2.0 S; molecular mass ~12-14 kDa) is water soluble albumin and comprised of higher level of α-helices (~45%) than β-sheets (~12%) (Crouch et al., 1983; Schwenke, 1994). Napin proteins consist of a small (~ 4.5 kDa) and large (~ 10 kDa) subunits stabilized by two disulfide bonds (Schwenke, 1990; Gehrig et al., 1998). Structural stabilization of the napin protein by disulfide bond reduces the molecular flexibility of the protein, negatively impacting on the functional performance (Schwenke, 1994). The majority of studies in the literature have focused on evaluating the functionality of isolates produced with a mixture of proteins, or have the canola proteins modified chemically.

The overall goal of this present study is to evaluate only the emulsifying properties of the napin fraction. Emulsions consist a mixture of two (or more) immiscible liquids formed after an input of mechanical energy (e.g., homogenization), where one liquid becomes dispersed as small droplets within a continuous phase of the other (Hill, 1996; McClements, 2005). During emulsion formation, soluble proteins diffuse towards the interface, then re-arrange and re-organize at the interface to orient hydrophobic amino groups towards the non-polar oil phase and the hydrophilic amino groups toward the aqueous polar phase in order to reduce interfacial tension and forming a viscoelastic film (Dalgleish, 1997). The viscoelastic film typically induces an electric charge on the droplet, which depending on the pH may lead to attractive or repulsive forces between neighboring droplets. At solution pHs close to the pI of the protein, droplets would exert little to no repulsive charge leading to flocculation and/or aggregation due to hydrophobic interaction, followed by partial or complete coalescence (Xu et al., 2005). In contrast, at pHs away from the pI, proteins exert a repulsive force between neighboring droplets to keep the emulsions stable. The addition of NaCl or other salts can cause shielding of the repulsive charge on the droplets, inducing droplet flocculation even if the solution pH is away from the pI.

Napin was selected, despite concerns surrounding allergens (Aider and Barbana, 2011), because of its high solubility in aqueous solutions. Information relating to the emulsifying properties of napin is limited in literature, and somewhat variable. Krause and Schwenke (2001) reported that napin had a higher diffusion rate than cruciferin, leading to higher values of the emulsifying activity index (EAI) in dilute emulsion systems. In contrast, Wu and Muir (2008) reported napin to have lower EAI values, formed larger oil droplets and had lower stability than cruciferin, and was a major factor contributing to the inferior functionality of mixed canola protein isolates. And, Malabat et al. (2001) reported napin could only form an emulsion when chemically modified.

In the present study, the overall objective to better understand structure-function relationships driving the stability/instability of oil-in-water emulsions prepared using a napin protein isolate, as a function of pH and NaCl. Napin was selected, despite concerns surrounding allergens (Aider and Barbana, 2011), because of its high solubility in aqueous solutions.

12.3 MATERIAL AND METHODS

Materials

Canola seeds (*Brassica napus*/variety VI- 500) were kindly donated by Viterra (Saskatoon, SK, Canada) for this research. All chemicals used in this study were of reagent grade and purchased from Sigma-Aldrich Canada Ltd. (Oakville, ON, Canada). For all reagent preparation, water from a Millipore Milli-Q^{TM} water purification system (Millipore Corporation, Milford, MA, USA) was used.

Preparation and characterization of a napin-rich protein isolate

Prior to use, canola seeds were stored in containers at 4°C. Canola seeds were dehulled as described by Wanasundara and McIntosh (2008). First small seeds were screened using a #12 (1.7 mm mesh size) Tyler mesh filter (Tyler, Mentor, OH, USA) to maximize seed cracking efficiency. Screened seeds were frozen at -40°C overnight, cracked using a stone mill (Morehouse-Cowles stone mill, Chino, CA, USA), followed by separation of the seed coat and cotyledons using an air aspirator (Agriculex Inc., Guelph, ON, Canada) which separating based on density differences between the two. The dehulled seeds were then pressed using a continuous screw expeller (Komet, Type CA59 C; IBG Monforts Oekotec GmbH & Co., Mönchengladbach, Germany) to remove a

large fraction of oil. The screw expeller was operated at speed 6.5 using a 3.5 mm choke, resulting in a meal temperature of ~75°C. The meal was then ground into a powder. Residual oil was then extracted using hexane (1:3 w/v, meal: hexane) at room temperature for 16 h, twice with change of solvent after 16 h. The defatted meal was left in a fume hood overnight to allow residual hexane to evaporate.

A napin- rich protein isolate (NPI) was prepared based on methods of Wanasundara and Mcintosh (2008). Briefly, 100 g of defatted ground meal was dispersed in 1 L of water containing 0.75% (w/v) NaCl, adjusted to pH 3.0 using 1.0 M HCl, and then allowed to stir continuously (500 rpm) for 90 min at room temperature (21-23°C). The dispersion was centrifuged at 17,700 × *g* for 20 min at 4°C using a Sorvall RC-6 Plus centrifuge (Thermo Scientific, Asheville, NC). The supernatant was collected through vacuum filtration using Whatman No. 1 filter paper (Whatman International Ltd., Maidstone, UK). Afterwards, the filtered supernatant was adjusted to neutral pH (6.8-7.0) using 1.0 M NaOH, followed by centrifugation at 17,700 × *g* for 20 min at 4°C using the same centrifuge to separate any precipitate. The supernatant was then diafiltered with Pellicon-2 Tangential flow membrane filtration system through a 5 kDa regenerated cellulose membrane (using 3 membranes with area size 0.1 m^2 each) (Millipore Corporation, Milford, MA) to remove salt and small molecular weight substances in the protein extract (Wanasundara and McIntosh, 2008). The concentrated supernatant was stored in -30°C and freeze-dried to yield a free flowing powder. The protein content of the resulting powder was determined according to the Association of Official Analytical Chemists (AOAC, 2003) method 920.87, using a micro-Kjeldahl digestion-distillation unit (Labconco Corp., Kansas City, MO, USA) and a nitrogen conversion factor of 6.25.

The amino acid composition of the NPI was determined using a pico-tag amino acid analysis system (Waters Corporation, Milford, MA, USA) and HPLC. In brief, three sets of 20 mg NPI were prepared for pre-separation hydrolysis according methods developed by Bidlingmeyer et al. (1987), AOAC official methods 985.28 for sulfur containing amino acid residues, and 988.15 for tryptophan (AOAC, 2003). To one set of NPI sample, 10 mL cold performic acid was added to oxidize cysteine and methionine then followed by hydrolysis with 15 mL 6N HCL. To second set of NPI sample, 10 mL of 4.2M NaOH was added to hydrolyze tryptophan before separation. To the third set of NPI sample, 15 mL of 6N HCl was added to hydrolyze the other amino acids

residues. Sample amino acid concentration was normalized for the isolate based on its crude protein content.

SDS-PAGE was performed on NPI according to Laemmli (1970) procedure as described by Marambe et al. (2008) using the PhastSystem equipped with separation and development capabilities (Amersham Pharmacia, Uppsasla, Sweden). β-Mercaptoethanol (2%) was added in the samples where reducing conditions were needed. Samples were prepared by dissolving 2 mg of protein in 1 mL of 0.1 M Tris-HCl buffer (containing 5% SDS (w/v), pH 8.00), followed by heating at 99°C (Incu Block model 285, Denville Scientific Inc., South Plainfield, NJ, USA) for 10 min. Solutions were then cooled to room temperature (21-23°C) before centrifuging with Labnet Spectrafuge 16M microcentrifuge (Mandel Scientific, NJ) at 16,873 × *g* for 10 min to remove any insoluble material. A 1 μg sample was applied to each well and standard proteins (Sigma-Aldrich – Wide range molecular weight markers) of 170, 130, 95, 72, 55, 43, 34, 26, 17 and 10 kDa were applied to a separate well. Gradient mini gels (resolving 8–25%T and 2%C, stacking zone 4.5%T and 3%C, 43 mm × 50 mm × 0.45 mm, polyacrylamide gels cast on GelBond® plastic backing, buffer 0.112 M acetate, 0.112 M Tris, pH 6.4) were used to separate proteins. Following separation, the proteins were fixed and stained using PhastGel blue R (Coomassie R-350) and developed to obtain suitable background colour. Molecular weights of bands and quantity present on the SDS-PAGE gel were estimated as described by Marambe et al. (2013) using the ImageQuant® (version 3.0; Amersham Pharmacia Biotech, Piscataway, NJ, USA) software based on the darkness intensity of each band.

Sample preparation

Protein solutions (0.25%, w/w, unless otherwise stated) were prepared for all experiments by dispersing NPI powder (corrected for protein content) within Milli-Q water containing 0, 50 or 100 mM NaCl under continuous stirring (500 rpm) at room temperature (21-23°C). Solution pH was then adjusted to desired values (3.0, 5.0 and 7.0) using either 0.1 M HCl or 0.1 M NaOH. NPI solutions were then stirred overnight at 4^{o}C prior to use (with the exception of solubility testing).

Surface charge (or zeta potential)

The zeta potential of 0.05% (w/w) NPI solutions as a function of pH and NaCl concentration was determined by measuring the electrophoretic mobility (U_E) using a Zetasizer

Nano-ZS90 (Malvern Instruments, Westborough, MA, USA). Zeta potential (ζ; units: mV) was calculated using U_E by applying Henry's equation:

$$U_E = \frac{2\varepsilon \times \zeta \times f\,(k\alpha)}{3\eta} \qquad \text{(eq. 12.1)}$$

where, ε is the permittivity (units: F (Farad)/m), $f(\kappa\alpha)$ is a function related to the ratio of particle radius (α; units: nm) and the Debye length (κ; units: nm^{-1}), and η is the dispersion viscosity (units: mPa·s). The Smoluchowski approximation $f(\kappa\alpha)$ was set as 1.5. All measurements are reported as the mean ± one standard deviation (n = 3).

Average surface hydrophobicity using the fluorescent probe method

The average surface hydrophobicity of NPI as a function of pH and NaCl concentration was estimated using a FluoroMax-4 spectrofluorometer (Horiba Jobin Yvon Inc., Edison, NJ, USA) by the ANS (8-anilino-1-naphthalenesulfonic acid) fluorescent probe method based on the procedure of Kato and Nakai (1980) modified by Can Karaca and others (2011a,b). In brief, NPI solutions were diluted with water, containing the desired amount of NaCl, to obtain protein concentrations of 0.02%, 0.04%, 0.06%, 0.08% and 0.1% (w/w). For each diluted NPI concentration, two 15 mL test tubes containing 4 mL of NPI solution were prepared, with and without 20 µL of 8 mM ANS solution in water with NaCl concentration corresponding to sample NaCl concentration. Tubes were vortexed for 10 s then stored in the dark for 15 min at room temperature (21-23°C). Fluorescence intensity was measured using excitation and emission wavelengths of 390 and 470 nm, respectively, with both slit widths set at 1 nm. The fluorescence intensities of an ANS blank and a NPI blank (diluted protein solution without ANS probe) were subtracted from the fluorescence intensity of the sample to obtain the net fluorescence intensity which was then plotted against protein concentration. The initial slope (as determined by linear regression) was taken (arbitrarily divided by 10000) as an index of average protein surface hydrophobicity. All measurements are reported as the mean ± one standard deviation (n = 3).

Protein solubility

Protein solubility of NPI was investigated as a function of pH and NaCl content, according to Can Karaca and others (2011a,b). In brief, 20 mL protein solutions (0.25% w/w) were prepared

as previously described. For each solution, 12 mL was transferred into a 15 mL centrifuge tube and centrifuged (VWR clinical centrifuge 200, VWR International, Mississauga, ON, Canada) at 4,180 × *g* for 10 min at room temperature (21-23°C). Protein content was determined by measuring the total nitrogen levels in ~5 g of supernatant using a micro-Kjeldahl digestion and distillation unit (Labconco Corp., Kansas City, MO, USA) and a conversion factor of 6.25. Protein solubility (%) was determined by dividing the total amount of protein within the supernatant by the original amount in the sample, multiplied by 100%. All measurements are reported as the mean ± one standard deviation (n = 3).

Interfacial tension

The interfacial tension between canola oil and each NPI solution (as a function of pH and NaCl) was measured using a semi-automatic tensiometer (Lauda TD2, GmbH & Co., Lauda-Königshofen, Germany) according to the Du Noüy ring method. Interfacial tension for a water (without NPI) - canola oil system served as a control. Interfacial tension was calculated from the maximum force *(F_{max}; units: milli-Newtons; instrument measures mg x gravity)* using the following equation:

$$\gamma = \frac{F_{\max}}{4\pi R\beta} \qquad \text{(eq. 12.2)}$$

where, γ is the interfacial tension (mN/m), R is the radius of the ring (20 mm), β is a correction factor that depends on the dimensions of the ring and the density of the liquid involved (McClements, 2005). All measurements are reported as the mean ± one standard deviation (n = 3).

Emulsifying activity (EAI) and stability (ESI) indices

Emulsifying activity and stability indices were determined according to Pearce and Kinsella (1978). In brief, 5.0 g of the NPI solution (prepared as a function of pH and NaCl content) was homogenized with 5.0 g of canola oil using an Omni Macro Homogenizer (Omni International, Marietta, GA, USA) with a 20 mm saw tooth generating probe at speed 4 (~7,200 rpm) for 5 min. Fifty microliters of the emulsion was immediately taken from the bottom of the tube and diluted in 7.5 mL of 0.1% sodium dodecyl sulphate (SDS) dissolved in Milli-Q® water with NaCl concentration same as the samples tested, followed by vortexing for 10 s. A Genesys 10 UV-visible spectrophotometer (Thermo Scientific, Madison, WI, USA) was used to determine

the absorbance of the diluted emulsion samples at 500 nm using a plastic cuvette (1 cm path length). A second absorbance reading was taken from the dilution after 10 min. EAI and ESI were calculated by following equations:

$$EAI\ \left(\frac{m^2}{g}\right) = \frac{2\times 2.203\times A_0\times N}{c\times\varphi\times 10000} \quad \text{(eq. 12.3)}$$

$$ESI\ (\text{min}) = \frac{A_0}{\Delta A}\times t \quad \text{(eq. 12.4)}$$

where, A_0 is the absorbance of the diluted emulsion immediately after homogenization, N is the dilution factor, c is the weight of protein per volume (g/mL), φ is the oil volume fraction of the emulsion, and ΔA is the difference in absorbance between 0 and 10 min (A_0-A_{10}) and t is the time interval (10 min). All measurements are reported as the mean ± one standard deviation (n = 3).

Statistical analyses

All statistics were performed using SPSS Ver. 20.0 software (SPSS Inc., 2012, Chicago, IL, USA). A two-way analysis of variance (ANOVA) with Scheffe post–hoc test was used to test the significance of the main effects (pH and NaCl) and associated interaction on the physicochemical (surface charge and hydrophobicity, solubility and interfacial tension) and emulsifying (EAI and ESI) properties.

12.4 RESULTS AND DISCUSSION

Characterization of the NPI material

The NPI was determined to be comprised of 97.41% (w.b.). Figure 12.1 gives an SDS-PAGE polypeptide profile under non-reducing (lane 1) and reducing conditions (lane 2). Major bands under non-reducing conditions were found at ~24.5 kDa, ~14.4 kDa and ~12.3 kDa, representing ~12%, ~66% and ~20% of the total bands, respectively as determined by densitometry (lane 1, Figure 12.1). Under reducing conditions, major bands were found at ~24.5 kDa, ~21.7 kDa, ~16.5 kDa, ~11.2 kDa and ~ 9.1 kDa, accounting for ~6%, ~3%, ~11%, ~43% and 34% of the total bands, respectively (lane 2, Figure 12.1). The halo surrounding the 14.4 kDa and 11.2 kDa bands under non-reducing and reducing conditions, respectively, is thought to be associated with a high protein loading onto the gel. Based on the SDS-PAGE analysis, the NPI appears to be rich in napin, since predominant polypeptide bands have typical molecular weight of small and large chains of *Brassica napus* 2S proteins (Schwenke, 1990). The amino acid composition of NPI was found to be high in glutamine (+ glutamic acid) (22.50%), along with proline (8.25%), lysine (6.46%), leucine (5.97%) and arginine (5.91%) (Table 12.1). Chabanon and others (2007) also reported napin to be rich in glutamine (+ glutamic acid) and arginine, accounting for ~30 and 8.6% of the total amino acids.

Surface characteristics

Protein surface charge depends on both the amino acid composition and conformation of the protein molecules in solution (McClements, 2004). In general, highly charged proteins tend to have better solubility in aqueous systems due to the large amount of electrostatic repulsion (Can Karaca et al., 2011). Strong repulsion also fosters improved emulsifying properties of protein-stabilized emulsions, greater reactivity to cross linking formation during gelation and improved water hydration properties of the protein (McClements, 2005). Figure 12.2 shows the zeta potential (mV) for NPI solutions as a function of pH and salt concentration. A two-way analysis of variance found the medium pH (5.0) and NaCl concentration had a significant effect ($p<0.001$) on zeta potential of the protein so as the combination effect of these two factors. At acidic pH (i.e. pH 3.0), the addition of salt reduced the overall positive surface charge of the protein molecules. At medium pH (i.e. pH 5.0), the addition of salt shifted the overall surface charge from positive to negative and also greatly reduced the magnitude of the surface charge. At higher pH, which the native

protein exhibited negative surface charges, the addition of salt slightly increased the magnitude of the overall surface charge.

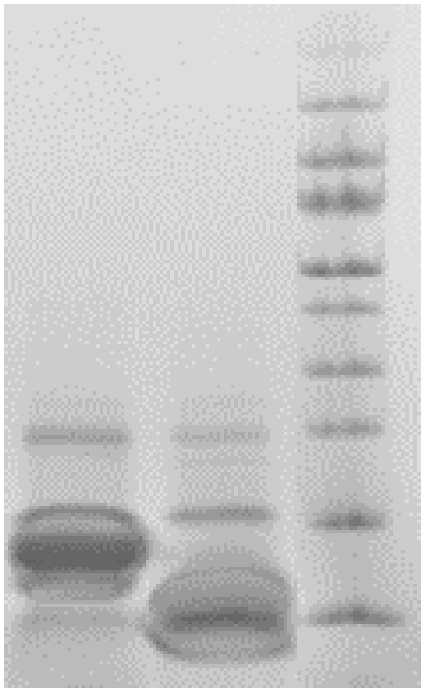

Figure 12.1 SDS-PAGE (reducing and non-reducing)(1 μL of 2 mg mL^{-1} NPI solution) applied to gradient 8-25% PhastGels. Lanes: (1) NPI (non-reducing); (2) NPI (reducing) and (3) Standard.

Table 12.1 Amino acid profile for the napin-rich protein isolate.

Amino acid	**Percent**
(Aspartic acid + Aspargine)	2.98
(Glutamic acid + Glutamine)	22.50
Alanine	3.63
Arginine	5.91
Cysteine	4.38
Glycine	4.21
Histidine	3.34
Isoleucine	3.09
Leucine	5.97
Lysine	6.46
Methionine	1.82
Phenylalanine	2.97
Proline	8.25
Serine	4.26
Threonine	3.33
Tryptophan	1.27
Tyrosine	1.58
Valine	3.82
Total:	**88.77**

For all materials, surface charge was low; having zeta potentials ranging between ~-5 mV to ~10 mV suggesting that the protein carried little net charge in the pH range of 2.0 to 8.0. NPI in the absence of added NaCl, showed a pI (zeta potential = 0 mV) at pH 6.6, where at pH > pI and pH < pI proteins assumed a net negative and positive charge, respectively. Figure 12.2, also showed that as pH declined from 8.0 to 4.0, zeta potential increased relatively linear up to pH 4.0, and then dropped to ~1 mV at pH 3.0, before rising again to ~3 mV at pH 2.0. It was suggested napin molecule structure remains stable at the pH range of 5.5 to 7.0 (Krzyzaniak et al., 1998).

The zeta potential behavior of NPI in the present study between pHs 3.0 and 4.0 is thus presumed to be due to structural changes in the NPI molecule. Jyothi and others (2007) showed that with the addition of 0.5 M NaCl, the napin became more compact indicating that there might be changes to the level of exposed amino acid groups on the surface that could lead to changes of surface charge.

The addition of NaCl to the NPI solutions resulted in a gradual and steady change in zeta potential as pH declined from pH 8.0 to pH 2.0. From pH 8 to 3.5, negative values were observed and between pH 3.5 and 4.0, NPI reached zero zeta potential. It is believed that NaCl at low concentration <0.5M, charge screening is prominent and may have shielded the charged sites of NPI molecule to reduce the thickness of its electric double layer. This effect was more pronounced at the 100 mM NaCl level, were the zeta potential values were closer to neutrality over the entire pH range, than at the 50 mM level (Figure 12.2). The addition of NaCl also acted to shift the pI of NPI from 6.6 to 3.5 and 3.9 when 50 mM and 100 mM NaCl was present, respectively. Wanasundara et al. (2012) reported at low ionic strength (<0.2 M NaCl), ions can non-specifically bind to the protein's surface to increase the thickness of the electric double layer. Consequently, molecules can adopt greater charge at its normal pI (i.e., without added NaCl) and a shift in the pH where net neutrality occurs. In the present study, the addition of 100 mM NaCl caused less of a shift in the pI value since its electric double layer was reduced more in size. In the literature, napin has been reported to have pI values >10.0 from *B. napus*, however this was typically based on theoretical values determined from its amino acid composition (Aider and Barbana, 2011). However, depending on the extent of various napin isoforms present, ionisable amino acid residues on protein surface may change. According to Yoshie-Stark et al. (2008), protein extraction conditions may affect the isoform composition in the final protein isolate. The present study used napin solubilized at low pH (3.0) leading to selectivity towards more basic isomers, however it seems all napin was extracted as no napin originated polypeptides were detected in the remaining meal residue (Wanasundara and McIntosh, 2008). However, further purification was not carried out for this NPI and the final protein product may contain some contaminants such as soluble fibre and non-napin protein (Figure 12.1 shows some other polypeptide bands) which can modify napin protein surface charges.

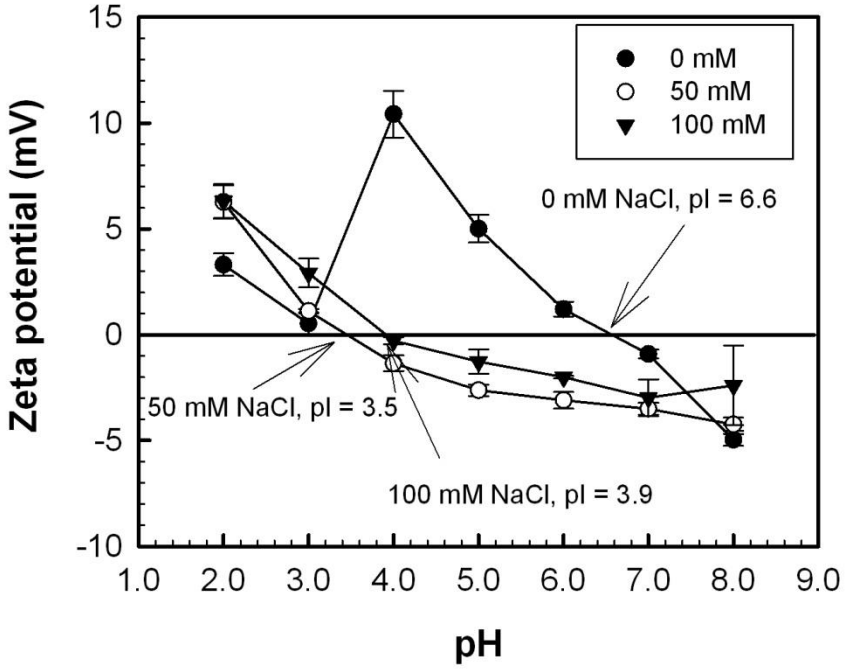

Figure 12.2 Zeta potential (mV) for NPI solutions as a function of pH and NaCl (mM) content. Data represent the mean ± one standard deviation (n = 3).

Surface hydrophobicity plays an important role in terms of protein solubility, protein-protein interactions (via hydrophobic interactions) and interfacial activity. The latter plays an active role in stabilizing the oil-water interface within emulsions by hydrophobic moieties orientating inwards towards the oil phase, and hydrophilic moieties towards the aqueous phase to lower interfacial tension (Stuart et al., 1991; Krause and Schwenke, 2001). In the present study, pH and NaCl concentration along with their combined effect were found highly significant ($p<0.001$) on changing surface hydrophobicity of napin. Figure 12.3 shows surface hydrophobicity for NPI solutions as a function of pH and salt concentration. Overall, surface hydrophobicity was found to be highest at low pH and 100 mM NaCl content. At pH 3.0 and 5.0, surface hydrophobicity increased with increasing NaCl content and the effect of NaCl was found greater under acidic conditions. Possibly as the screening of charge sites on the NPI increased, the protein molecule gained greater conformational entropy or freedom (i.e., chain flexibility); allowing for the partial unraveling and exposure of previously buried hydrophobic sites. It is presumed that the greater rate of change in hydrophobicity with salt content at pH 3.0 is due to the overall slightly

higher surface charge. At pH 7.0, surface hydrophobicity declined from 2.5 arbitrary units (A.U.) for NPI in the absence of added NaCl to 1.4 A.U. in the presence of 50 mM NaCl, and then increased to 3.5 A.U. with 100 mM NaCl present. At pH 7.0, surface charge on the native NPI is minimal since its close to its pI value (pH 6.6). It was presumed that the addition of NaCl content caused fluctuations to occur in the NPI conformation leading to slight changes in surface hydrophobicity. Jyothi et al. (2007) reported a low binding constant of various extrinsic fluorescence probes including ANS (~0.5 mol of probes binding to 1 mol of protein), which indicated napin is hydrophilic in nature. However in contrast to the present study, Jyothi et al. (2007) reported a decline in the hydrophobicity of napin with the addition of 500 mM NaCl. The authors proposed that the high concentration of NaCl lead to the stabilization of a more compacted NPI molecule in solution.

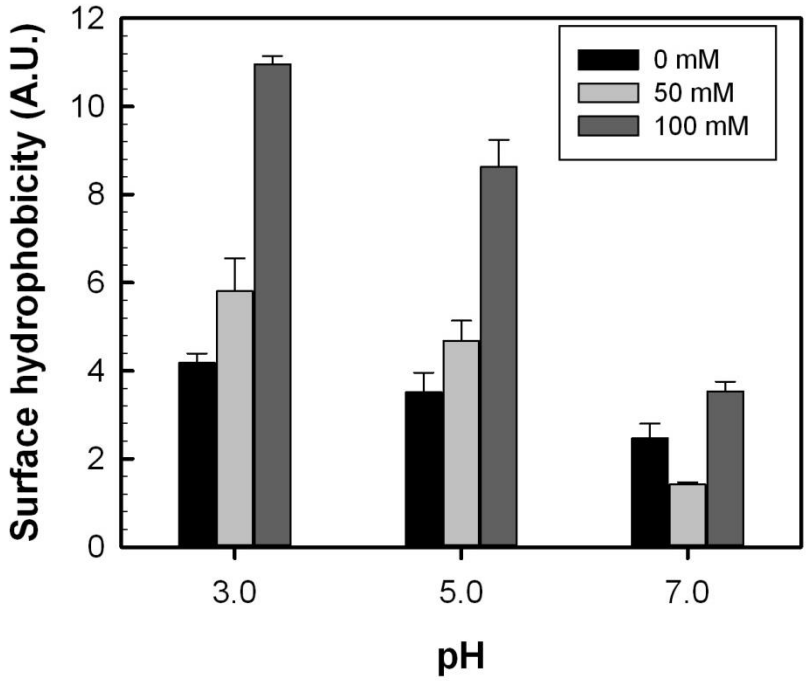

Figure 12.3 Surface hydrophobicity for NPI solutions as a function of pH and NaCl (mM) content. Data represent the mean ± one standard deviation (n = 3).

NPI solubility

A two-way analysis of variance found the main effects of pH ($p<0.001$) and NaCl concentration ($p<0.05$) to be statistically significant, whereas their associated interaction was not

($p>0.05$). Solubility was reported between 93.4% - 100% and only slight changes in values where observed due to the addition of NaCl. Overall solubility was found to be similar at pHs 3.0 (98.2%) and 5.0 (99.2%), however was slightly reduced at pH 7.0 (96.3%). Solubility of NPI was also found to be similar at NaCl levels of 0 mM (96.8%) and 100 mM (96.5%), however was found to be completely soluble with the addition of 50 mM NaCl. Although significant differences were found among the treatments, caution should be taken in terms of interpreting differences among treatments, as solubility for all NPI solutions remained high (>93.3%).

In a previous study conducted by Wanasundara et al. (2012) it was found that napin protein has high solubility at acidic pHs; when Brassica seed meals were extracted at pH between 3.0 and 4.0, low molecular weight proteins (<17 kDa) were found in the soluble fraction. Schwenke (1990) also showed that native napin isolate was completely soluble in the pH range of 1.0-10.0. Protein with good solubility is often associated with high surface charge and low hydrophobicity (McClements, 2004). Napin is known to have very basic pI (>10.0) and is hydrophilic in nature (Schwenke, 1990; Jyothi et al., 2007). Although the NPI in the present study exhibited low surface charge, NPI used in this study showed a relatively low hydrophobicity value, which may be the main factor for its excellent solubility across the tested pH levels. Having good solubility represents an important attribute for proteins to be used as an emulsifier, as the protein is required to diffuse to the oil-water interface from the bulk aqueous solution to reduce interfacial tension (Kinsella et al., 1985; McClements, 2005; Can Karaca et al., 2011). Proteins with lower surface charge or if salts are added to screen charged sites on the protein's surface, then protein- protein interaction dominates and proteins have a tendency to associate into larger aggregates and fall out of solution (McClements, 2004). Similarly, proteins with high surface hydrophobicity tend to aggregate via hydrophobic interactions to form larger aggregates, which then fall out of solution (Damodaran, 1989). In the present study, napin was found with relatively low surface hydrophobicity which reduced the chance of protein aggregation due to hydrophobic interaction between droplets.

Interfacial tension

The addition of NPI to the aqueous phase (regardless of the solvent conditions) was found to reduce the interfacial tension at an oil-water interface from 22.5 mN/m to 10-17 mN/m. Figure 12.4 shows interfacial tension for NPI solutions as a function of pH and salt concentration. A two-

way analysis of variance found pH, along with the combination effect of pH and salt, to have significant effect on the interfacial tension ($p<0.001$). Overall, interfacial tension declined from ~16.7 mN/m at pH 3.0, to 14.3 mN/m at pH 5.0 and further declined to 10.6 mN/m at pH 7.0, the major effect of salt was not significant and only caused slight changes of interfacial tension at each pH. At pH 3.0, interfacial tension declined slightly from 17.3 mN/m to 16.1 mN/m as NaCl levels increased from 0 mM to 100 mM; at pH 5.0, interfacial tension was relatively constant at ~14.3 mN/m as NaCl increased over the same range; and at pH 7.0, interfacial tension increased slightly with increased NaCl levels. When surface hydrophobicity and interfacial tension values are taken into consideration, the comparatively high surface hydrophobicity values of napin at pH 3.0 may have contributed to their reduced ability to lower interfacial tension at oil-water interface. It is hypothesized that at pH 7.0, NPI had low hydrophobicity and negative zeta potential which together have contributed to the lowest interfacial tension. As stated previously, the low hydrophobicity and surface charges allowed the NPI to become better solubilized and reduced the chance of protein- protein interaction before aligning at the interface, a protein's ability to reduce the interfacial free energy is essential for its use as an emulsifier and it is a good predictor of its emulsifying properties (Stuart et al., 1991).

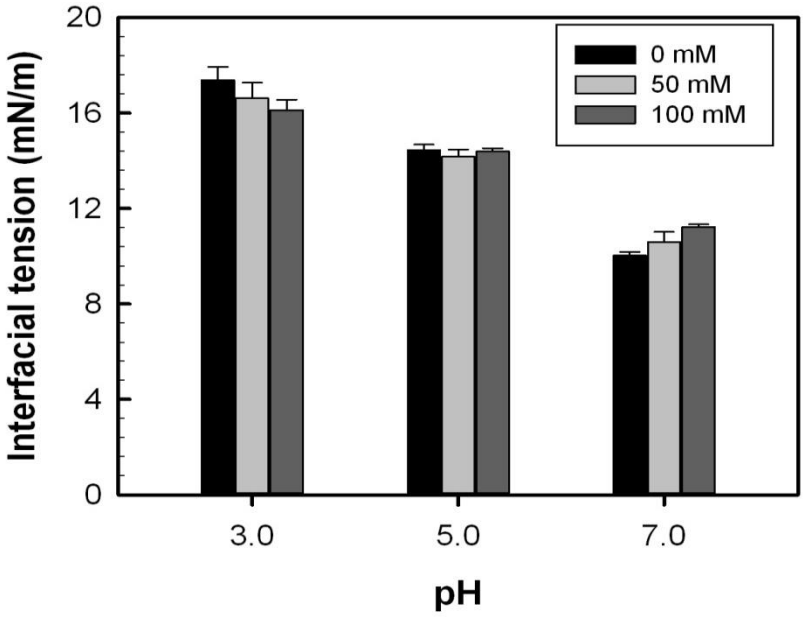

Figure 12.4 Interfacial tension (mN/m) for NPI solutions as a function of pH and NaCl (mM) content. Data represent the mean ± one standard deviation (n = 3).

Emulsifying properties

Emulsifying activity index (EAI) is the measure of interfacial area coated by a surfactant such as protein as explained by Pearce and Kinsella (1978). Figure 12.5A shows EAI for NPI solutions as a function of pH and salt concentration. A two-way analysis of variance found that the main effects of salt and pH to be significant ($p<0.001$), along with their associated interaction ($p<0.01$). Overall, EAI values were similar in magnitude at pH 3.0 (19.4 m^2/g) and pH 5.0 (18.7 m^2/g), and lower at pH 7.0 (12.8 m^2/g). The effect of NaCl on EAI was similar at pH 3.0 and 7.0. For instance, EAI at the 0 mM and 100 mM NaCl level were similar in magnitude, but increased significantly at the addition of 50 mM NaCl. However, the EAI values at pH 5.0 reduced as the level of NaCl increased. Proteins with good emulsifying properties are often found with high solubility and high surface charge (Dalgleish, 2004; Can Karaca et al., 2011). In the present study, solubility of NPI was excellent across the pH and NaCl levels tested which indicated there are other factors contributed to the variation of EAI values of NPI. For instance, similar trends were observed between the surface hydrophobicity and EAI of NPI where the values of NPI reduced as pH increased. It was hypothesized that surface hydrophobicity value alone was not a good predictor of emulsifying properties, but rather the overall distribution of hydrophobic and hydrophilic moieties on the protein molecule (Zayas, 1997). Kato and Nakai (1980) observed that a protein often has good emulsifying properties if the protein has more than 30% of nonpolar amino acid residue in its total amino acid profile. NPI in the present study show ~35.5% of total amino acid composition was composed of non-polar amino acid residues. Moreover, in this study, it is believed that the effects of pH and NaCl as well as their combined effects had greater impacts on the EAI values of NPI than the physicochemical properties of NPI. In fact, Krog and Sparsø (2004) stated that the emulsifying process and the final distribution of oil droplets are mainly affected by the energy input during homogenization and the influence of emulsifiers is limited. Krause and Schwenke (2001) reported ~4X higher surface coverage by napin isolate compared with cruciferin isolate indicated that napin is very surface active.

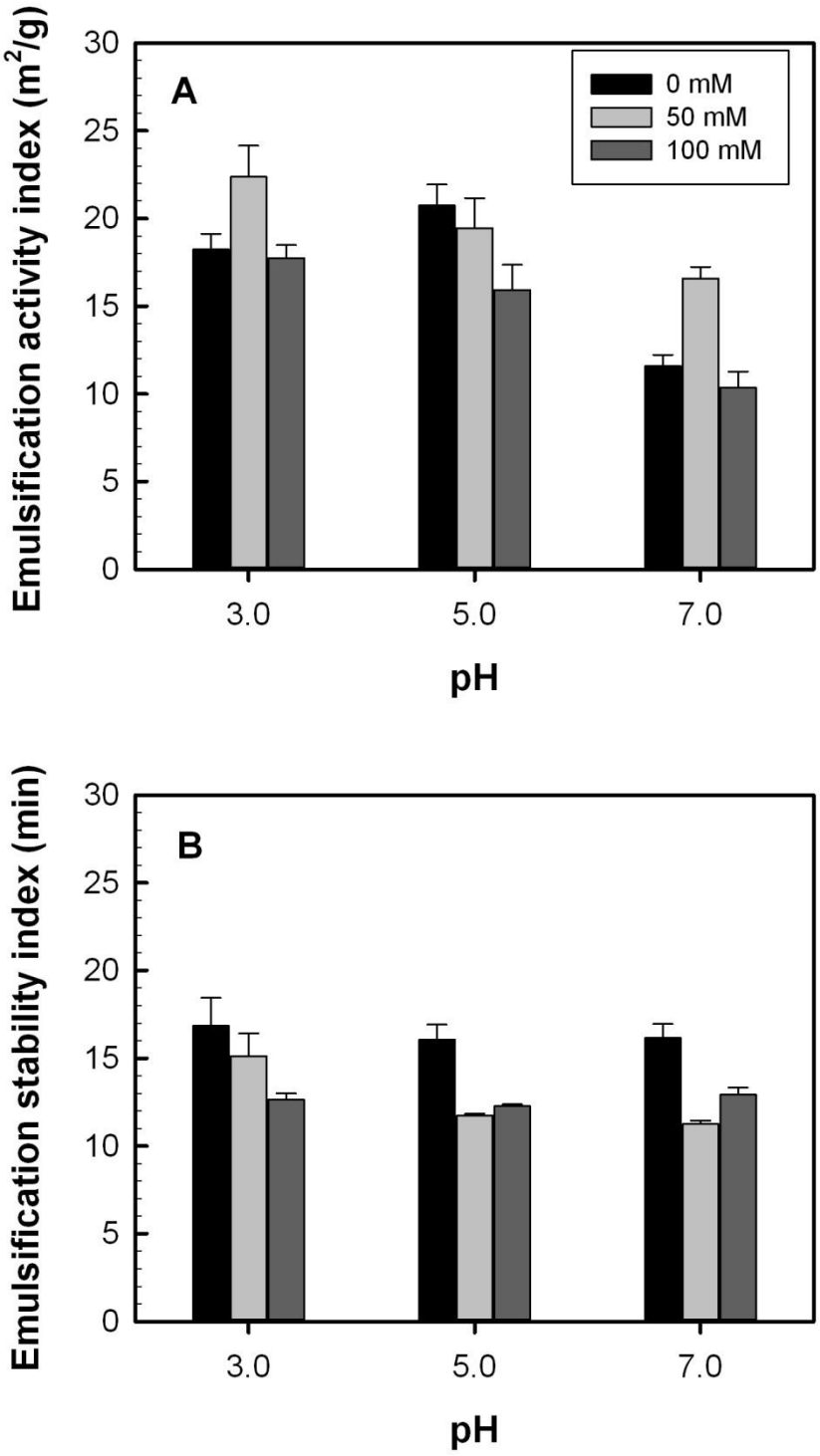

Figure 12.5 Emulsification activity (m^2/g) (A) and stability (min) (B) indices for NPI solutions as a function of pH and NaCl (mM) content. Data represent the mean ± one standard deviation (n = 3).

The emulsifying stability index (ESI) provides a measure of the stability of the diluted emulsion after homogenization (Can Karaca et al., 2011). Figure 12.5B shows ESI for NPI solutions as a function of pH and salt concentration. A two-way analysis of variance found that the main effects of pH ($p<0.01$) and salt ($p<0.001$), along with their interaction ($p<0.01$) were significant. According to ESI, NPI stabilized emulsion degraded rapidly and the addition of salt induced faster emulsion instability. At pH 3.0, ESI declined relatively linear from 16.8 to 12.6 min as NaCl content increased from 0 mM to 100 mM. In contrast, at pH 5.0, ESI declined from 16.1 min to 11.7 min as NaCl increased from 0 to 50 mM, and then increased slightly at 100 mM NaCl. A similar trend was also reported for pH 7.0. In all cases ESI was relatively the same in the absence of added NaCl, ranging between 16.0 to 16.8 min and then declined with the addition of NaCl. A charged viscoelastic surface can lead to increased electrostatic repulsion between droplets to help keep the emulsion stable (Damodaran, 1989). This is also verified by the statistic results of the present study which indicated higher surface charge lead to higher ESI values. This effect however can be reduced through the addition of salts, which act to screen charged sites and reduce the thickness of the electric double layer leading to droplet flocculation/aggregation (McClements, 2005). In this study, however the addition of salt only caused reduction of the overall surface charge at pH 5.0 and did not significantly reduced overall charges of NPI at pH 3.0 and 7.0, thus it is believed other factors might be affecting the reduced ESI value of NPI beside surface charge. Kulmyrzaeva and Schubertb (2004) studied the effect of potassium chloride and pH on whey protein induced emulsions and found the addition of KCl at more than 10 mM negatively affected the stability of the emulsion system due to the lowering of overall zeta potential from pH 2.5-7.0. Another study compared the effect of NaCl on flaxseed protein and soy protein induced emulsions and found that the addition of 50 mM NaCl and 100 mM effectively reduced oil droplet flocculation in flaxseed protein and soy protein induced emulsions, respectively, at isoelectric pH (4.2) (Wang et al., 2010). McClements (2004) also studied the effect of both monovalent salt (NaCl) and divalent salt ($CaCl_2$) on oil droplet size of soy protein stabilized emulsions and found oil droplet size remained < 1μm at 200 mM NaCl. However droplet size increased dramatically from 1.5 μm to 10 μm when $CaCl_2$ was added at levels > 4.0 mM.

12.5 SUMMARY

Surface charge and the isoelectric point for NPI was found to be much lower than expected. It was speculated that this could be due to the presence of impurity such as phenolic compounds and/ or phytic acids. It was found that NPI is hydrophilic in nature which could be associated with the high solubility across tested pHs. Overall, the emulsifying properties of NPI showed a relationship to the protein's surface characteristics (i.e., charge and surface hydrophobicity) which influenced their ability to lower interfacial tension. The medium factors such as pH and NaCl also had impacted NPI's emulsifying abilities. The emulsion forming properties of NPI appeared to be better at pH 3.0 and 5.0 than at a higher pH (7.0), with slight variations in response to NaCl. In contrast, the stability of these formed emulsions was less dependent on pH, and more influenced by the presence of NaCl where higher levels lead to greater instability.

-Chapter 13-

Summary

Canola proteins, because of their nutrition and functional properties could emerge as a potential alternative choice in the plant protein ingredient industry to soy, once launched into the marketplace. However, more information is needed to understand how the various protein fractions behave from a functional stand point in order to optimize breeding programs, extraction technology and ingredient performance in foods and/or in non-food industrial applications. Canola proteins are dominated by two main proteins, a salt soluble cruciferin protein and water-soluble napin protein. Each protein is different in terms of their structure, size and surface properties, all of which could lead to differences in their functional performance as ingredients, depending on the relative composition of commercially produced mixed isolates. The goal of this research was to examine similarities and differences in the surface properties of a cruciferin- and napin-rich protein isolate, and then relate this to their emulsifying properties under different pH (3.0, 5.0 and 7.0) and salt concentrations (0, 50 and 100 mM NaCl).

Both proteins differ considerably in size. The result of SDS-PAGE under reducing conditions shown cruciferin to have much larger sub-units, ranging in molecular mass from 17 to 150 kDa, whereas napin proteins were significantly smaller ranging between 12 and 17 kDa. Amino acid composition indicated that both proteins were high in glutamic acid and glutamine; however napin had slightly more (22.5 vs. 17.9%). Glutamine has pKa values of 2.17 and 9.13 for the α-carboxyl and α-amino sites, respectively, whereas glutamic acid has pKa values of 2.10, 9.47 and 4.07 for the α-carboxyl, α-amino and side chain groups, respectively. At the pKa values, 50% of the respective sites (i.e., α-carboxyl group) are protonated. In the present study, surface characteristics and functionality was measured at pH 3.0, 5.0 and 7.0. Since napin proteins contained higher levels of glutamine + glutamic acid than found in cruciferin, the overall charge should be less, especially at pH 3.0 and 5.0 where more sites would be protonated. Zeta potential values overall for napin protein isolates as a function of pH were substantial lower than that of cruciferin proteins. For instance, in the absence of NaCl, napin protein isolates showed zeta potential values ranging between -5 mV to +10 at pH 8.0 and 3.0, respectively, whereas cruciferin

protein isolates had values ranging between -30 mV to +35 mV at corresponding pHs. The addition of NaCl acted to shield the electric surface charge of both proteins through a counter-ion screening effect. As such the electric double layer was thought to decline in both cases. The isoelectric point of napin and cruciferin protein isolates (in the absence of salts) was found to occur at pHs 6.6 and 4.8, respectively. Values were lower than those reported in literature where pI of cruciferin and napin proteins have been reported at 7.2 and ~10.0-11.0 in the literature (Schwenke, 1988, 1994). Interaction of protein isolate with phenolic compounds and phytic acids might also have altered the chemical and physical properties of the protein isolate (Aider and Barbana, 2011; Wanasundara, 2011). However since cruciferin was extracted with a method reported to produce low phenolic and phytic acid (Krause et al., 2002), there is little concern of the presence of phenolic compounds and phytic acids for cruciferin-rich isolate. In the case of napin, at pHs<pI, proteins might interact with non-protein compounds such as phenolic compounds and/ or phytic acids to lead to variations in surface properties (Wanasundara, 2011).

Overall, the average hydrophobicity at the surface of cruciferin was also much higher that than that of napin, suggesting that more hydrophobic moieties (alanine, valine, isoleucine, leucine, methionine, phenylalanine, tyrosine and tryptophan) were present (~30% vs. 24%) and exposed at the surface. Furthermore, the effects of NaCl and pH on surface hydrophobicity were found also to be different between the two proteins. In the case of napin, hydrophobicity declined as the pH increased from pH 3.0 to 7.0 however, hydrophobicity was raised in the presence of NaCl. It is hypothesized that the screening of charged sites along the protein's surface lead to increased conformational entropy (flexibility) allowing for a higher amount of hydrophobic groups to become exposed. In contrast, for cruciferin, the effects of pH and salt on hydrophobicity were less clear. The highest hydrophobicity was found at pH 3.0 without NaCl, present, whereas the lowest was found at pH 7.0 in the presence of 100 mM NaCl. Overall, hydrophobicity declined as pH was raised from 3.0 to 7.0.

Napin protein isolate was almost completely soluble regardless of the pH and NaCl content. In contrast, the solubility of the cruciferin protein isolate ranged between ~80 and 90% under all solvent conditions with the exception of pH 5.0 and 7.0 in the absence of NaCl in which solubility was <20%. The presence of NaCl showed a 'salting-in' effect on the cruciferin where protein-water interactions were enhanced, resulting in greater structuring of the hydration layers surrounding the protein to lead to high solubility. This effect was presumed to be more dominant

than the screening effect of NaCl on the surface charge of the protein, which would have had an adverse effect on solubility, as was the case seen at pH 5.0 and pH 7.0.

During emulsion formation, soluble proteins migrate or diffuse towards the oil-water interface from the bulk aqueous phase where they then re-arrange and re-orient to position their hydrophobic moieties towards the oil phase and the hydrophilic moieties towards the bulk phase. The ability of napin and cruciferin proteins to reduce the interfacial tension was similar between the two proteins, despite minor differences seen in response to changes in pH and ionic conditions. Findings suggest that slight differences in protein solubility for both napin and cruciferin at the various solvent conditions did not impact its ability to reduce interfacial tension, nor did there appear to be a relationship with surface charge or average surface hydrophobicity.

The emulsifying properties of both cruciferin and napin proteins were both influenced by pH and ionic strength, however overall they had EAI and ESI values similar in magnitude indicating that they had similar emulsifying potential under the solvent conditions examined. For cruciferin proteins, no clear trend was evident with pH or NaCl level. EAI values were found to be similar at pH 3.0, regardless of the NaCl levels, whereas at pH 5.0, EAI values declined with increasing levels of NaCl. At pH 7.0, EAI values declined with the addition of 50 mM NaCl then remained constant. As for napin, the addition of 50 mM NaCl resulted in higher EAI values at pH 3.0 and 7.0 however at pH 5.0, the addition of NaCl reduced the EAI as NaCl increased. The ability for both cruciferin and napin proteins to stabilize the emulsion was reduced with the addition of NaCl. The stability of an emulsion is depended on the electrostatic repulsion between droplets in order to delay coalescence and flocculation (McClements, 2005). Addition of NaCl in this study resulted in reduced zeta potential for both protein isolates which lead to reduced emulsion stability.

Overall, this research found that despite cruciferin-rich and napin-rich protein isolates having quite different surface characteristics and solubility, the emulsifying forming and stabilizing effects were similar. Furthermore, separation of the two proteins from the isolate ingredient may not be necessary if emulsification is the only functional role the proteins are being used for, from a commercial stand point.

Part IV: Gelation properties of canola proteins

-Chapter 14-

Literature Review

14.1 Gelation

A gel is defined as a 3-dimensional network comprised of an 'infinitely branched polymer or aggregate' that spans the dimensions of the container. Gelation requires aggregation or association of protein particles, which is formed from the partial protein denaturation or change in conformation. Depending on the type of protein, solvent and gelling conditions various categories of gels can develop. Physical-type gels may be either weak or strong in nature. Strong physical gels involve protein junction zones in the form of lamellar microcrystals, glassy nodules, and double helices, and require elevated temperatures to induce melting of the gel network. In contrast, weak physical gels are more reversible in nature, and comprised of temporary linkages between proteins such as those from hydrogen or ionic bonding, or block copolymer micelles (Renard et al., 2006). Chemical-type gels are much stronger in nature due to the presence of point cross-links between protein molecules, such as from disulfide bridging or through the addition of fixatives (Renard et al., 2006). Globular proteins are typically considered to be heat-setting, meaning they require high temperatures to induce unfolding of the proteins and protein-protein association via hydrophobic interactions and disulfide bridging. As temperatures cool, hydrogen bonds develop to help strengthen the network structure (Renard et al., 2006). However, gel networks can vary considerably in strength, structure and opacity depending on the temperature used in the gelling process, the heating and cooling rates used, pH, protein concentration and the presence of salts resulting in a coagulate-type network comprised of random aggregates or a more fibrous type network resembling 'strings of beads' (Matsumura and Mori, 1996).

14.2 Gelation properties of canola proteins

The gelation properties of canola proteins have typically involved the addition of fixatives (e.g., transglutaminase), the use of chemically modified canola proteins and mixtures involving anionic polysaccharides. Léger and Arntfield (1993) studied gel formation involving 6% of 12S CPI that was extracted from modified protein micellar mass method. The study looked at CPI at different pH, addition of different concentration of salts, dithiothreitol, and guanidine hydrochloride. The pH range varied from pH 4.0 to 11.0, and found that stronger gels formed under

alkaline conditions relative to acidic ones. The authors reported that at pHs, close to isoelectric point of CPI, showed the highest dynamic storage moduli (G′; describes the elastic component of the gel). The addition of salt was found to contribute to the thermal denaturation properties of 6% 12S canola globulin. At pH 9.0, the 12S canola globulin thermal denaturation was 81˚C, however with 0.1M sodium salt such as sodium sulfate, sodium acetate, sodium chloride, and sodium thiocyanate increased the thermal denaturation to 85.75˚C~87.4˚C. Moreover, Léger and Arntfield (1993) reported that the addition of aforementioned sodium salts to the 12S canola globulin had similar cooling curves when temperature ramp was performed from 90˚C-25˚C at 2˚C/min. The authors indicated this could be due to similar gelation mechanism. Also, the study showed that addition of guanidine hydrochloride altered the protein conformation that interfered with the early stage of development of 12S canola globulin by disrupting the covalent bonds (Léger and Arntfield, 1993).

Rubino et al. (1996) also studied the gelation properties of canola proteins isolate that primarily consists of 12S canola protein. The study showed that 10% CPI did not form gel at pH 4.5 due to strong repulsive forces. Also, the addition of sinapic acid or thomasidioic acid caused weakening of canola protein gel. Interaction between CPI and phenolic compounds (sinapic acid and thomasidioic acid) varied depending on the pH ranges; at pH 4.5 sinapic acid interact electrostatically with CPI whereas at pH 7.0 and 8.5, hydrophobic interaction occurs between the canola proteins and thomasidioci acid. However, at pH 7.2, 10% CPI did from an opaque gel. Also, Rubino et al. (1996) reported that replacing the solvent from water to 0.1 M NaCl increased the elasticity and lowered the gel strength. Furthermore, the addition of sinapic acid or thomasidioic acid was found to reduce the G′ and elasticity of the canola protein network at pH 7.0. Schwenke et al. (1998) reported that gelation temperature of salt extracted CPI that was comprised of 70% cruciferin and 30% napin is 69˚C at pH 9.0 with 15% CPI. Also, the author reported that 12.5% purified cruciferin protein isolate-formed stronger gels with higher shear modulus than 12.5% canola proteins isolate between pH 6.0 and 8.0.

14.3 Gelation properties of soy proteins

The gelation properties of oilseed proteins found in the literature have primarily focused on soy (Gennadios et al., 1993; Ker and Chen, 1998; Renkema et al., 2000; Hu et al., 2013). Soy proteins are dominated by an 11S glycinin and 7S β-conglycinin protein. The former is a hexameric

protein comprised of acidic and basic polypeptide chains linked together by disulfide bonds. In contrast, the 7S protein is a trimer composed of three subunits (α′, α and β) with no disulfide linkages (Chen et al., 2013). Based on their structure, the thermal stability of the 7S protein is much less than the 11S protein allowing it to unravel at much lower temperatures. Salleh et al. (2002) produced heat set gel networks at pH 7.6 and 0.42 M NaCl using both soy glycinin and canola cruciferin to find that the soy gel was more transparent and elastic than the cruciferin network. The authors also reported that gel hardness increased with increasing in temperature, protein concentration, pH, and a decrease in ionic strength. Renkema et al. (2000) investigated the effect of pH on gel properties of purified glycinin and SPI (97% protein content) gels. Both glycinin and SPI gels formed find-stranded gels and had low G′ values at pH 7.6, however at pH 3.8 both soy proteins formed coarse gels and had higher G′ values. This also correlated with the solubility, where at pH 7.6 there was higher solubility compared to pH 3.8. The authors also stated the β-conglycinin role in SPI depends on the pH. At pH 7.6, β-conglycinin has minor role however at pH 3.8 the onsets of heat denaturation cause early formation of the gel of SPI.

The gelation properties of soy protein various depends on the soy major components. Renkema et al. (2001) researched glycinin, β-conglycinin and a 1:1 mixture of glycinin and β-conglycinin gels. The mixture of glycinin and β-conglycinin (1:1) had gels with fracture stress and strain values that are between glycinine and β-conglycinin gels at pH 3.8. The authors reported that glycinin had higher gelation temperature at the crossover point of G′ and G″ (G″; describes the viscous component of the gel) than β-conglycinin at pH 7.6. However, the concentration of the protein had more significant role in gelation temperature. Renkema and van Vliet (2002) investigated gelation temperature of 10% SPI at pH 7 using differential scanning calorimetry (DSC). DSC determines the degree of protein denaturation as a function of heating temperature. The author reported that denaturation peak temperature of glycinin was 88˚C and β-conglycinin was 68˚C. Furthermore, the small deformation rheological study indicated that after the heating stage, cooling of the soy protein gel increases G′ however it was thermoreversible. The authors reported that rearrangements and disulfide bonds do not form during cooling stage of soy protein. Utsumi and Kinsella (1985) reported major bonds involved with development of 11S gels are disulfide bonds and electrostatic interactions. In contrast, hydrogen bonds and hydrophobic interactions are major bonds that are involved in formation of 7S gels.

14.4 Rheological examination of proteins gels

The gelation properties of protein solutions are typically evaluated by small deformation oscillatory rheology involving temperature ramps and frequency sweeps. Temperature ramps during heating enables the monitoring of network development to occur as evident by a rise in the dynamic storage moduli (G′) with temperature as proteins aggregate after denaturation is induced (Renard et al., 2006; Lamsal et al., 2007). Aggregation is facilitated by hydrophobic interactions, leading to the formation of a 'string of beads' fibrous or coagulum structure (depending on solvent pH and salt concentrations). Gel temperature can be denoted by various methods, but typically it involves extrapolating the tangent associated with the steepest part of the rise of G′ to x-axis. At this temperature, the solution transitions from a sol to a gel (Lamsal et al., 2007). As the network cools, an increase in the amount of van der Waals forces and hydrogen bonding occurs leading to further strengthening of the gel network. A frequency sweep at a constant strain provides information on level of interactions within the system. For instance, is the dynamic loss moduli (G″) is greater than G′ that the system is behaving as a fluid under low frequency conditions, however, if G′>G″ then the material is more structured. A relative moduli-frequency independence may give an indication of a solid-like gel structure, whereas is the moduli are frequency dependent at relative low frequency the material may behaving like an entanglement polymer solution.

-Chapter 15-

The effect of protein concentration and the nature of interactions on the gelling properties of canola and soy protein isolates

Jae Hee Kim, Natallia Varankovich and Michael T. Nickerson

Department of Food and Bioproduct Sciences, University of Saskatchewan
51 Campus Drive, Saskatoon, SK, Canada, S7N 5A8

15.1 ABSTRACT

Gelation of canola (CPI) and soy (SPI) protein isolates were examined as a function of concentration, NaCl (0.1-0.5 M) and 2-mercaptoethanol (0.1-1 M) during a heating-cooling thermal scans, and as a function of time, frequency and strain. In the case of CPI, the magnitude of the storage modulus (G′) of the formed network was found to increase with increasing concentration at pH 7.0, whereas the gelling temperature (T_{gel}) remained constant at ~88^{o}C. The change in NaCl level from 0.1 to 0.5 M reduced the zeta potential form ~-20 to -4 mV, but had little effect on T_{gel} or network strength. In the presence of 2-mercaptoethanol, networks became weaker indicating the importance of disulfide bridging within the CPI network. Disulfide bridging, electrostatics and hydrogen bonding are all thought to have a role in CPI gelation. In the case of SPI, the magnitude of the storage modulus (G′) of the formed network, and T_{gel} was found to increase and decrease (~81→71^{o}C), respectively with increasing concentration at pH 7.0. Increases in NaCl from 0.1 to 0.5 M reduced the zeta potential from ~-44 to -13 mV and caused a shift in T_{gel} from ~81 to 67^{o}C, and increased G′. No gels were formed in the presence of 2-mercaptoethanol. Findings suggest that protein-protein aggregation induced either by increasing concentration along with disulfide bridging is important in network formation.

15.2 INTRODUCTION

Canola was originally bred in Canada from rapeseed varieties (*Brassica napus* L.*)* to have low levels of erucic acid (<2%) and glucosinolates (<30 μmol/g) for use mainly as an edible healthy oil, but also for use in margarines and biofuels (Newkirk, 2009). After oil extraction, the remaining meal tends to be rich in protein (36- 39%, wet basis) and fibre (~12%, wet basis); used mainly as a low cost feed for dairy and beef cattle, poultry, swine, sheep and farmed fish based on its nutritional value (Khattab and Arntfield, 2009; Newkirk, 2009). The proteins within the meal are considered to be highly nutritious, offering a well balance of essential amino acids for both animal and human nutrition (Ohlson and Anjou, 1979). Proteins arising from the meal are primarily comprised of the storage proteins napin and cruciferin, accounting for ~20% and ~60% of the total protein, respectively. Cruciferin (11S/12S, S is a Svedberg Unit) is a salt soluble globulin protein with a molecular mass of 300-310 kDa, has an isoelectric point (pI) of 7.25 (Zirwer et al. 1985; Wanasundara, 2011). The cruciferin molecule is a hexameric protein comprised of six subunits, each having an acidic α-chain (~30 kDa) and basic β-chain (~20 kDa)

held together by one disulfide linkage (Aluko and Mclntosh, 2000; Wanasundara, 2011). Wu and Muir (2008) reported non-covalent linkages such as hydrophobic interactions, hydrogen bonding and van der Waals interactions also played a signficant role in stabilizing the native conformation. In contrast, napin is a water-soluble albumin protein (2S) with a molecular mass of ~12-17 kDa. Napin is comprise of only 2 polypetides of ~4 and ~10 kDa linked together by a disulfide bond (Salleh et al., 2002) and has a calculated pI value of ~11 depending on its amino acid sequence (Wanasundara, 2011). Typically, the napin molecule is very hydrophilic, carries a positive net charge at neutral pH and displays low surface hydrophobicity (Wanasundara, 2011).

Although the functionality of canola protein isolate (CPI) has been previously studied, the gelation mechanism for canola has largely been left unexplored, especially as it relates to a direct comparison with soy proteins. Gelation studies involving canola proteins have typically involved the use of cross-linking agents (Pinterits and Arntfield, 2007; Sun and Arntfield, 2011) alone or in combination with polysaccharides (Uruakpa and Arntfield 2004, 2006a,b; Klassen et al., 2010), or involve the use of chemically modified canola proteins (Paulson and Tung, 1988; Schwenke et al. 1998). A gel is defined as a 3-dimensional network comprised of an 'infinitely branched polymer or aggregate' that spans the dimensions of the container. Globular proteins are typically considered to be heat-setting, meaning they require high temperatures (above the protein's denaturation temperature) to induce unfolding of the proteins and protein-protein association via hydrophobic interactions and disulfide bridging. As temperatures cool, hydrogen bonds develop to help strengthen the network structure (Renard et al., 2006). However, gel networks can vary considerably in strength, structure and opacity depending on the temperature used in the gelling process, the heating and cooling rates used, pH, protein concentration and the presence of salts. Léger and Arntfield (1993) studied gel formation involving 6% CPI to report that stronger gel networks formed under alkaline conditions relative to acidic ones. Whereas, Rubino et al. (1996) reported that a 10% canola protein solution was unable to gel at pHs <4.5 due to strong repulsive forces occurring within the material. To date, the gelation properties of oilseed proteins found in the literature have primarily focused on soy (Gennadios et al., 1993; Ker and Chen, 1998; Renkema et al., 2000; Hu et al., 2013). Soy proteins are dominated by an 11S glycinin and 7S β-conglycinin protein. The former is a hexameric protein comprised of acidic and basic polypeptide chains linked together by disulfide bonds. In contrast, the 7S protein is a trimer composed of three subunits (α′, α and β) with no disulfide linkages (Chen et al., 2013). Salleh et al. (2002) produced heat set gel

networks at pH 7.6 and 0.42 M NaCl using both soy glycinin and canola cruciferin to find that the soy gel was more transparent and elastic than the cruciferin network. The authors also reported that gel hardness increased with increasing in temperature, protein concentration, pH, and a decrease in ionic strength.

The overall goal of this research is to examine the mechanisms of gelation for canola proteins as a function of temperature and protein concentration, and in the presence of NaCl and destabilizing agents (e.g., urea and mercaptoethanol) using rheology and calorimetry, and compared with that of commercial soy protein isolate product.

15.3 MATERIALS AND METHODS

Materials

Defatted canola meal produced from *Brassica napus* (2012 crop year) was kindly donated by Agriculture and Agri-Food Canada (Saskatoon, SK, Canada) after being processed by POS BioSciences Corp. (Saskatoon, SK, Canada). The meal served as the starting material for protein extraction. A commercial soy protein isolate product was kindly donated by Archer Daniels Midland Company (PRO-FAM 974, Lot 13020412, Decatur, IL, USA) for this project. All chemicals used in this study, unless otherwise stated were purchased from Sigma-Aldrich (Oakville, ON, Canada). Water used in this study was Milli-Q^{TM} water (EMD Millipore, Billerica, MA, USA).

Preparation of canola protein isolates

Canola protein isolate (CPI) was prepared from defatted meal using slightly modified methods of Folawiyo and Apenten (1996), and Klassen et al. (2011). Initially, residual oil in the meal was removed by hexane extraction (x3) at a 1:3 meal to hexane ratio for 8 h. The meal was then air-dried for an additional 8 h to allow for residual hexane to evaporate. Protein extraction was as follows. In brief, 0.05 M Tris-NaCl buffer (Lot 103470, Fisher Scientific, Fair Lawn, New Jersey, USA) containing 0.1 M NaCl was prepared and adjusted to pH 7.0 using 1.0 N (HCl). The prepared buffer was then used to dissolve the defatted meal at a meal-to-buffer ratio of 1:10 for 2 h at room temperature (22-23˚C) under constant stirring (500 rpm) using a mechanical stir plate. The dispersion was then centrifuged (Sorvall RC Plus Superspeed Centrifuge, Thermo Fisher Scientific, Asheville NC, USA) at 3000 × *g* for 1 h to collect the supernatant, followed by a second

centrifuge step after removal of the pellet (3000 × *g* for 1 h) to further clarification. The supernatant was then vacuum filtered using #1 Whatman filter paper (Whatman International Ltd., Maidston, UK), dialyzed (Spectro/Por tubing, 6-8 kDa cut off, Spectrum Medical Industries, Inc, Rancho Dominguez, CA USA) at 4˚C where Milli-Q^{TM} water was changed 3 times a day for 72 h to remove the salt, and then freeze-dried (Labconco Corporation, Kansas City, MO, USA) to produce a dry CPI powder. The powder was stored at 4˚C for later usage.

Proximate composition

Chemical analyses on the CPI and SPI materials were performed according to the Association of Official Analytical Chemists (AOAC, 2003) Methods 925.10, 923.03, 920.87 and 920.85 for moisture, ash, crude protein and lipid (% dry weight basis), respectively.

Surface charge (zeta potential)

Overall surface charge of CPI and SPI was determined by measuring the electrophoretic mobility (U_E) of 0.05% (w/w) protein solutions at pH 7.0 in the absence and present of 0.1 M NaCl using a Zetasizer Nano-ZS90 (Malvern Instruments, Westborough, MA, USA). Zeta potential (ζ) is calculated by applying U_E to the Henry's equation:

$$U_E = \frac{2\varepsilon\zeta f(\kappa\alpha)}{3\eta} \qquad \text{(eq. 15.1)}$$

where ε is permittivity, f(κα) is a function related to the ratio of particle radius (α) and Debye length (κ), and η is the dispersion viscosity. A Smoluchowski approximation f(κα) of 1.5 was assumed for this study, as is convention when using a folded capillary cell, and with samples of particles sizes larger than 0.2 μm dispersed in a moderately electrolyte solution (> 1mM). The Smoluchowski approximation assumes that a) the concentration of particles (proteins) is sufficiently high such that such thickness of the electric double layer (Debye length) is small relative to the particle size (κα>>1); and b) ζ is linear related to U_E. All measurements were reported as the mean ± on standard deviation (n = 3).

Rheological properties of CPI and SPI solutions

The rheological properties of CPI and SPI solutions were examined under the following sample conditions. (a) Initially, the rheological properties of SPI solutions were examined as a function protein concentration (5.0, 6.0, 7.0, 8.0 and 9.0% w/w) at pH 7.0, followed by CPI at protein levels of 5.0, 7.0 and 9.0% (w/w) at the same pH. Canola and SPI was prepared by dispersing their respective powders (adjusted for protein levels) into 0.1 M NaCl prepared with Milli-Q water (Millipore Corporation, MA, USA), and was then allowed to stir using a mechanical stir plate at 500 rpm for 1 h at room temperature (22-23˚C). The pH of the solution was adjusted to 7.0 using 0.5 M NaOH or HCl, and periodically checked during stirring. (b) Secondly, the rheological properties for a 7% (w/w) CPI or SPI solution at pH 7.0 were examined as a function of NaCl (0.1 and 0.5 M NaCl), urea (0.1. 0.5, 1.0 and 5.0 M) and mercaptoethanol (0.1% and 1%) levels to test the nature of interactions within during gel formation.

All rheological measurements were made using an AR-1000 rheometer (TA Instrument, New Castle, DE, USA) equipped with a peltier plate temperature control, and a 40 mm diameter - 2˚ cone and plate geometry (with a gap of 51 μm). Each protein solution (~630 μL) was transferred onto the geometry, and allowed to equilibrate for 5 min prior to analysis. To prevent sample drying during heating, a light application of mineral oil was placed on the fringe of the geometry. The viscoelastic storage (G′) and loss (G″) moduli was initially followed during a heating-cooling cycle for each sample. Temperature was ramped upwards from 25˚C to 95˚C on a continuous basis at a rate of 1˚C/min, a frequency of 0.1 Hz and strain amplitude of 1%. The sample was then allowed to equilibrate at 95˚C for 5 min, and then ramped downwards from 95˚C to 25˚C at the same rate. The G′ was plotted vs. temperature on arithmetic coordinate to determine the heat setting temperature (or sol-gel transition temperature), taken by extending the tangent from the steepest part of the rise in G′ to the x-axis in the heating curve (Winter & Chambon, 1986; Rogers & Kim, 2011). Following the temperature cooling ramp, the sample was allowed to equilibrate at 25˚C for 1 min, followed by a time sweep measurement of G′ for 1 h at a frequency of 0.1 Hz to evaluate the level of structure formation over time. Once completed, both G′ and G″ was measured as a function of frequency over the range of 0.01 and 100 Hz, and plotted on log-log coordinates to give an indication of whether the sample is behaving as a viscous fluid, entangled solution or semi-solid gel. The magnitude of moduli was also given an indication of the relative strength of the structures being formed (or the level of order within the network. After the frequency scans, a

strain sweep was performed over a strain range of 0.014% to 500% at a frequency of 5 Hz. The strain sweep provided information relating to the relative strength of junction zones formed within the material, and their relative resistance to flow. The strain break was measured by extending the tangents for data before and after the break. The intersection point was taken as the % strain at break. All measurements were made within the linear viscoelastic regime. All samples were prepared in duplicate.

Differential scanning calorimetry

The thermodynamic properties of a 9.0% (w/w) CPI solution was investigated using differential scanning calorimetry (DSC). Ssamples of approximately 10 mg were weight into Tzero Alodined pans and hermetically sealed (TA Instruments, New Castle, DE, USA). Samples were heated at 5 °C/min from 25 to 110 °C using a Q2000 DSC (Ta Instruments, New Castle, DE, USA). The instrument was calibrated using indium. From the heating curve, the onset temperature and denaturation temperature were determined. Samples were measured in triplicate and reported as a mean ± one standard deviation. Exothermic events associated with soy proteins could not be detected by the instrument.

Confocal laser scanning microscopy

The morphology of CPI and SPI networks was examined using a Nikon Eclipse LV100 Confocal Laser Scanning Microscopy (Nikon, Tokyo, Japan). CPI and SPI gels were prepared as a function protein concentration (5.0, 7.0 and 9.0%, w/w) at pH 7.0. The gels were made by dispersing their respective powders (adjusted for protein levels) into 0.1 M NaCl prepared with Milli-Q water (Millipore Corporation, MA, USA), and then stirred using a mechanical stir plate at 500 rpm for 1 h at room temperature (22-23˚C). After 1 h of stirring, 10 μL of 1% Rhodamine B Isothyocyanate (RITC) in methanol solution was added to the CPI solutions, followed by stirring for an additional 1 h using a mechanical stirrer (500 rpm) at room temperature. The solution was then covered with aluminum foil to prevent light from reacting with the RITC dye. The solution was transferred to 0.5 mm-deep well concavity slide and was closed with a cover slip. The slides were carefully transferred to either an AR-1000 or AR-G2 rheometer (TA Instrument, New Castle, DE, USA), where they were placed on top of the peltier plate temperature control. The slides were also covered with aluminum foil. Temperature was ramped upwards from 25˚C to 95˚C at a rate

of 1˚C/min, allowed to equilibrate at 95˚C for 5 min, and then ramped downwards from 95˚C to 25˚C and then held at 25˚C for 1 h to mimic the rheological heating/cooling profile. Excitation and emission wavelengths were at 543 and 573 nm, respectively. Gel morphology images were captured from a depth close to the midpoint of the concave slide. All gels were prepared in triplicate and 3 images per slide were taken. A representative image from each slide was used for further analysis.

Image analysis

Fractal dimension and lacunarity was measured using Image J v1.48 (http://imagej.nih.gov/ij/) software. The FracLac V2.5 plug-in for Image J was used to convert the images from the confocal laser scanning microscopy to binary images. The white pixels represented the gel network whereas the dark areas represented aqueous solution. Furthermore, FracLac V2.5 was used for a box counting method to measure both the fractal dimension and lacunarity in power series. The box counting method places a series of grids of decreasing in size over an image and counting the boxes that contain foreground pixels (e.g., white pixels) for each grid size. Fractal dimension (d_f) was calculated as $d_f = -d+1$, where d is the slope of the line from a plot of log ($N\varepsilon$) versus log (ε) (Hagiwara et al., 1998). Where in FracLac, ε is the corresponding scale (ε = box size / image size) and $N\varepsilon$ is the number of boxes containing foreground pixels in the grid at a certain scale. Lacunarity ($A\varepsilon$) is the variation of the number of foreground pixels at each grid box. This indicates the heterogeneity or a gap in the gel network. FraLac calculated lacunarity by the equation:

$$A\varepsilon = (\sigma/\mu)^2 \qquad \text{(eq. 15.2)}$$

where σ is the standard deviation in pixel density within all box sizes ε and the average number μ of foreground pixels per box for the same grid size.

Statistics

A two-way analysis of variance (ANOVA) was used to test for statistical differences between protein type and concentration in terms of sol-gel transition temperatures, the magnitude of G′ and G″ (at the end of the time sweep) and % strain at break for both CPI and SPI. A paired

student T-test was used to test for differences among the aforementioned parameters for each of CPI and SPI as a function of concentration. A student T-test was also used to test for differences in the aforementioned parameters for gels in the absence and presence of urea, NaCl and mercaptoethanol. Finally, a one-way ANOVA with a Scheffe Post-Hoc test was used to test for significance for CPI (only) as a function of protein concentration for its thermal characteristics (e.g., onset and denaturation temperatures), fractal dimension and lacunarity. The latter was not tested in the case of SPI since data was not collected (*See Results and Discussion*). Data was analyzed by R program software (Version 2.15.2, R Foundation, Vienna, Austria).

15.4 RESULTS AND DISCUSSION

Characterization of the canola meal, CPI and the commercial SPI

The proximate composition of the defatted canola meal obtained from AAFC/POS BioSciences indicated that crude lipid levels were at ~ 3.1% (on a dry basis, d.b), which is typical for industrial processes after oil extraction. Protein and ash levels for the meal were reported at ~42.4% and ~9.4% (d.b.), respectively. Canola protein isolates were prepared using a salt extraction process to obtain protein levels of ~98.2% (d.b.) as measured by micro-Kjeldhal. Using a nitrogen conversion factor of 6.25 is presumed to lead to a slight overestimation of the true protein content. Kjeldhal measures the total nitrogen in the sample, which also includes nitrogen from protein, peptides, and free amino acids (McKenzie and Wallace, 1953). Crude lipid and ash contents within the CPI were found to be ~1.1% and ~4.2% (d.b.), respectively. The composition of the commercial SPI product sample showed protein levels of ~95.2% (d.b.) with low levels of ash (4.3% d.b.) and lipid (0.4% d.b.).

Surface charge or zeta potential for CPI and SPI was determined with and without 0.1 M NaCl at pH 7.0. In the absence of NaCl, CPI and SPI were found to both carry a net negative charge of -20.2 ± 0.98 mV and -43.9 ± 2.62 mV, respectively. The more highly charged SPI may result in increased electrostatic repulsion between neighboring proteins relative to CPI at the same protein concentration resulting in weaker networks once formed. For both proteins, the addition of 0.1 M NaCl resulted in a reduction in charge to -4.1 ± 0.21 mV and -13.2 ± 0.28 mV for CPI and SPI, respectively. The addition of NaCl acted to significantly reduce the magnitude of the protein's surface charge most likely due to a charge screening effect, where Na^+ and Cl^- ions acted to screen

the negatively and positively charged sites on the protein's surface, effectively reducing the thickness of the electric double layer in the process (Keowmaneechai and McClements, 2002).

A differential scanning calorimeter was used to measure the thermodynamic properties of CPI and SPI at pH 7.0 and at a 9.0% (w/w) concentration. The onset of denaturation and the denaturation temperature (point where maximal denaturation occurs) was determined to be 78.6 ± 0.4 ^{o}C and 87.1 ± 0.8 ^{o}C, respectively for CPI. Salleh et al. (2002) and, Wu and Muir (2008) reported denaturation temperatures of 86.6 ^{o}C and 83.9 ^{o}C associated with cruciferin-rich isolates. During denaturation, hydrogen bonding becomes disrupted causing the quaternary and tertiary structures of the proteins to disassociate and unravel into their secondary structures. Above these temperatures hydrophobic interactions can begin to dominate in part due to previously exposed hydrophobic sites and the formation of covalent disulfide bonds between neighboring cysteine residues (Doi, 1993). In contrast, denaturation could not be measured using the DSC in the case of the SPI most likely since the values were below the sensitivity limits of the instrument. Arntfield and Murray (1981) also reported that if denaturation has occurred previously, the no exothermic dips in the thermogram would be evident. It is possible that the commercial product may have undergone some level of denaturation during the production process. When comparing CPI and SPI, the lack of measurable values in SPI may indicate that the CPI proteins are more thermally stable.

Rheological properties of canola protein isolate during gelation

The rheological properties of CPI were followed first as a function of temperature, time, frequency and strain as a function of protein concentration. During the initial heating scan, little evidence of an elastic structure was evident until ~87-90^{o}C, after which a slight rise in G′ was evident (Figure 15.1A), becoming greater than G″ (not shown). Before this rise, CPI solutions behaved as a viscous liquid where G″ was found to be greater than G′ (data not shown). This rise in G′, corresponded to CPI denaturation temperature (87^{o}C) where proteins began to unravel to expose hydrophobic moieties, followed by protein aggregation driven by hydrophobic interactions and the formation of disulfide bonds between neighboring cysteine residues. The rise is also denoted as the gelation temperature (T_{gel}) and was found to be similar regardless of the protein concentration ($p>0.05$) (Table 15.1). G′ was greater at the 7.0% (w/w) concentration because due to higher protein packing and protein-protein association which lead to reduction of G″ and

increase in G′ (Figure 15.1A). Upon cooling, formed CPI-CPI aggregate further associated as hydrogen bonds began to reform and the gel network became stronger (Léger & Arntfield, 1993). As temperatures lowered from 95ºC to 25ºC, the elastic component saw an exponential increase in magnitude (Figure 15.1B). This similar pattern was also seen in Léger & Arntfield who evaluated CPI rheological properties during a temperature ramp (1993). In the present study, the G′ was found to be greatest for the 9.0 % (w/w) concentration, followed by the 7.0% (w/w) and 5.0% (w/w) at the start of the time sweep upon the completion of the heating/cooling ramps, and remained relatively constant over the 1 h period suggesting no further ordering within the network structure was occurring (Figure 15.1C; Table 15.1). Gaps in magnitude between the end of the heating run and start of the cooling rate (Figure 15.1A,B) and the end of the cooling run and the start of the time sweep (Figure 15.1B,C) reflect protein ordering during the short rest period within the experimental protocol.

At the end of the time sweep, networks were found to increase in magnitude from 211 Pa to 1222 Pa as the CPI concentrations increased from 5.0 to 9.0 % (w/w) (Table 15.1). In all cases, G′ was greater than G″ (Table 15.1). The rise in network strength was thought to be caused by increased protein aggregation, compaction and junction zone formation within the network as the void volume decreased. It is also thought that the rate of hydrogen bond formation and break down was similar over time as moduli remained constant.

Frequency sweeps of viscoelastic moduli on double logarithmic coordinates indicate characteristic gel-like material behavior where G′>G″ and the G′ is relatively independent of frequency (also known as the rubbery plateau of the viscoelastic spectrum (Ferry, 1980) (Figure 15.2). The crossover point of viscoelastic moduli at higher frequencies indicates that the material is entering the rubber-glass transition region of the viscoelastic spectrum. Within this region, mobility of proteins within the network is severely restricted to protein side chains or smaller molecules re-conforming to relieve stress by dissipating energy (Ferry, 1980). Frequency sweeps followed similar profiles, except the magnitude of moduli increased with increasing protein concentration as the material was presumed to have a greater amount of protein ordering and compaction (less free volume).

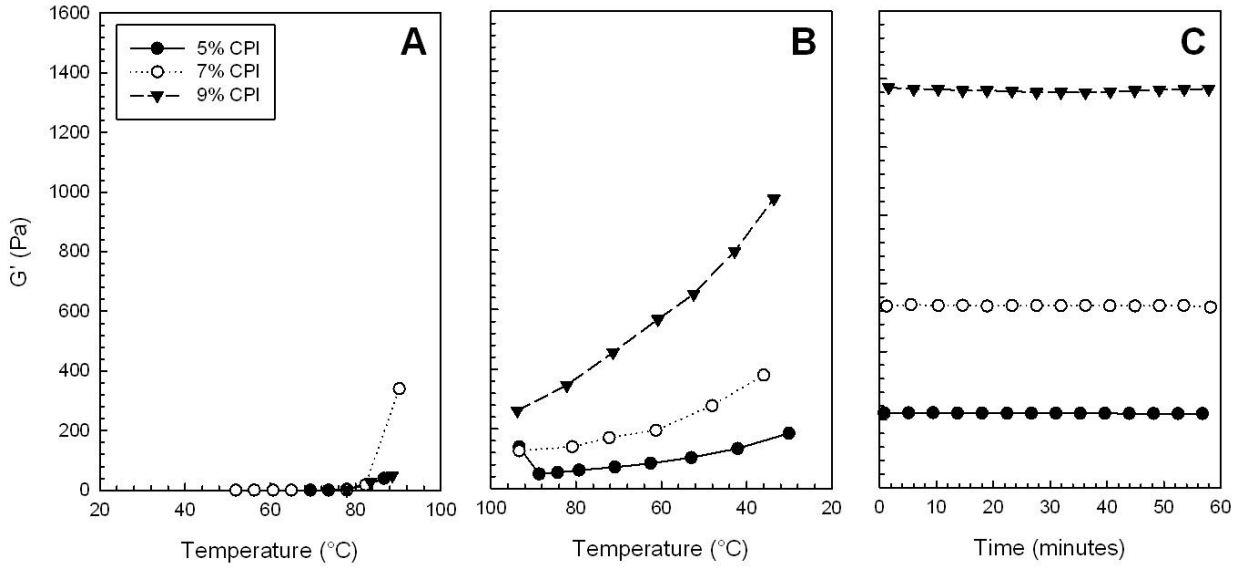

Figure 15.1. Dynamic storage (G′) modulus as a function of temperature and time for a canola protein isolate concentrations (5.0%, 7.0%, 9.0%) at 1% strain and 0.1 Hz. a) temperature ramp from 25ºC to 95ºC; b) temperature ramp from 95ºC to 25ºC; c) 1 hour time sweep at 25ºC.

Table 15.1 The gelation temperature during heating (T_{gel}), log viscoelastic storage (G′) and loss (G″) moduli after the 1 h time sweep at 25°C, and the log % strain at break for canola and soy protein isolates as a function of protein concentration. Data represent the mean and standard deviation of duplicate samples. The abbreviation of n.g. denotes a material that is non-gelling.

Concentration (%, w/w)	**T_{gel} (°C)**	**G' (Pa)**	**G″ (Pa)**	**log % Strain at break**
a) Canola protein isolate				
5.0	90.0 ± 0.0	210.8 ± 10.04	26.8 ± 1.10	1.7 ± 0.01
7.0	87.0 ± 3.5	508.4 ± 31.18	61.84 ± 5.48	1.8 ± 0.00
9.0	87.4 ± 0.8	1222 ± 69.30	191.45 ± 23.83	1.8 ± 0.01
b) Soy protein isolate				
5.0	n.g.	-	-	-
6.0	78.0 ± 2.8	8.60 ± 0.39	1.20 ± 0.03	1.6 ± 0.18
7.0	83.5 ± 4.9	29.1 ± 11.69	3.52 ± 1.27	1.6 ± 0.01
8.0	78.8 ± 2.3	43.5 ± 0.14	5.19 ± 1.29	1.5 ± 0.04
9.0	76.7 ± 6.6	48.6 ± 8.80	5.97 ± 1.02	1.5 ± 0.05

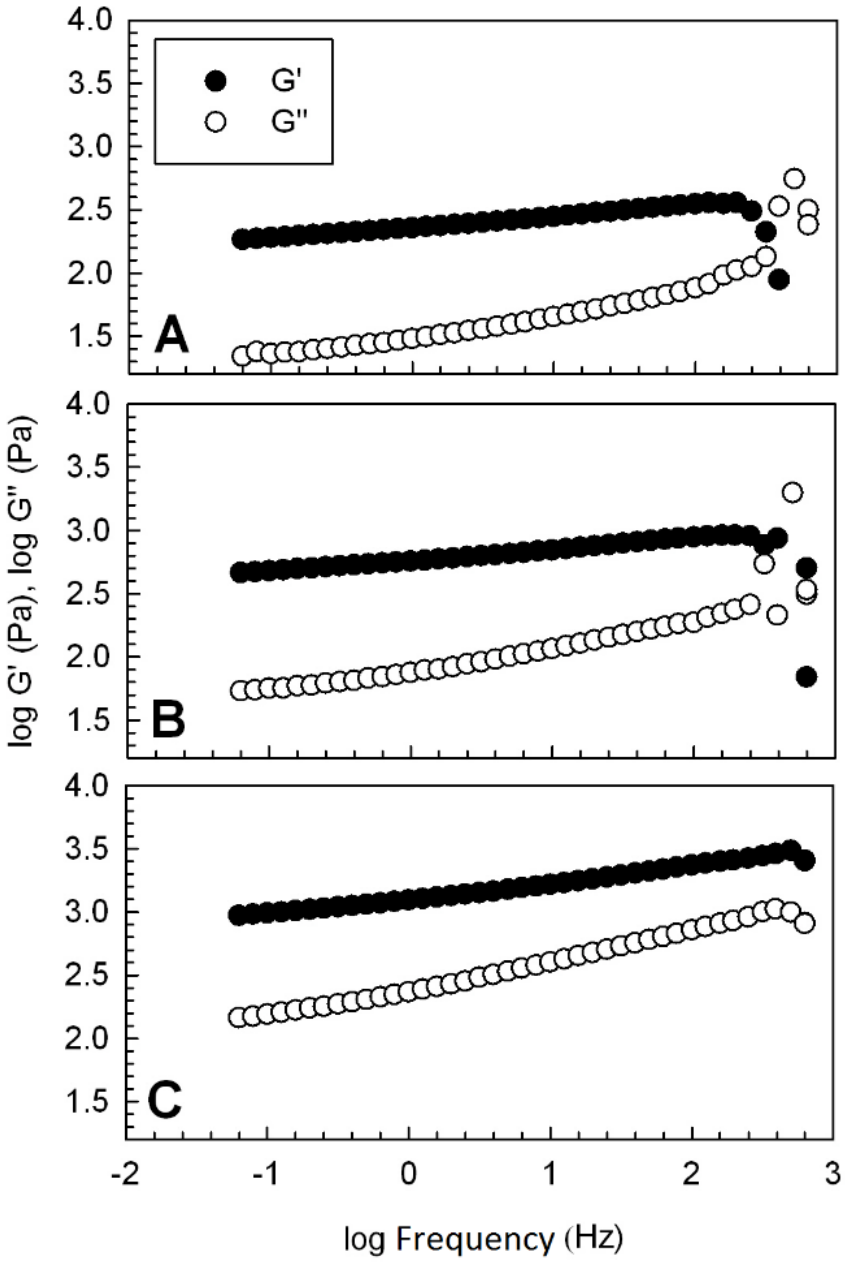

Figure 15.2. Dynamic storage (G′) and loss (G″) moduli as a function of frequency for a canola protein isolates at 5.0% (A), 7.0% (B) and 9.0% (C) protein concentrations.

A strain sweep was performed on all gels after to measure the relative strength of junction zones formed within the CPI and their resistance to flow. As shown in Figure 15.3, there was a sharp break in the log G′ versus log % strain suggesting the gel network was quite brittle in nature. For all CPI concentrations, G′ stay relatively constant until it rapidly decrease thither corresponded

to where the network starts to breakdown due to losses in hydrogen bonding (Eleya and Gunasekaran, 2004). The log % strain at break increased slightly from 1.7 to 1.8 (or 50 to 63 anti-logged) as CPI concentration increased from 5.0 to 7.0 % (w/w), then remained constant (Table 15.1, Figure 15.3). At the higher protein concentrations it was presumed that the network was stronger and capable of withstanding a higher amount of strain before a break in the network structure occurred, dissipating applied stress.

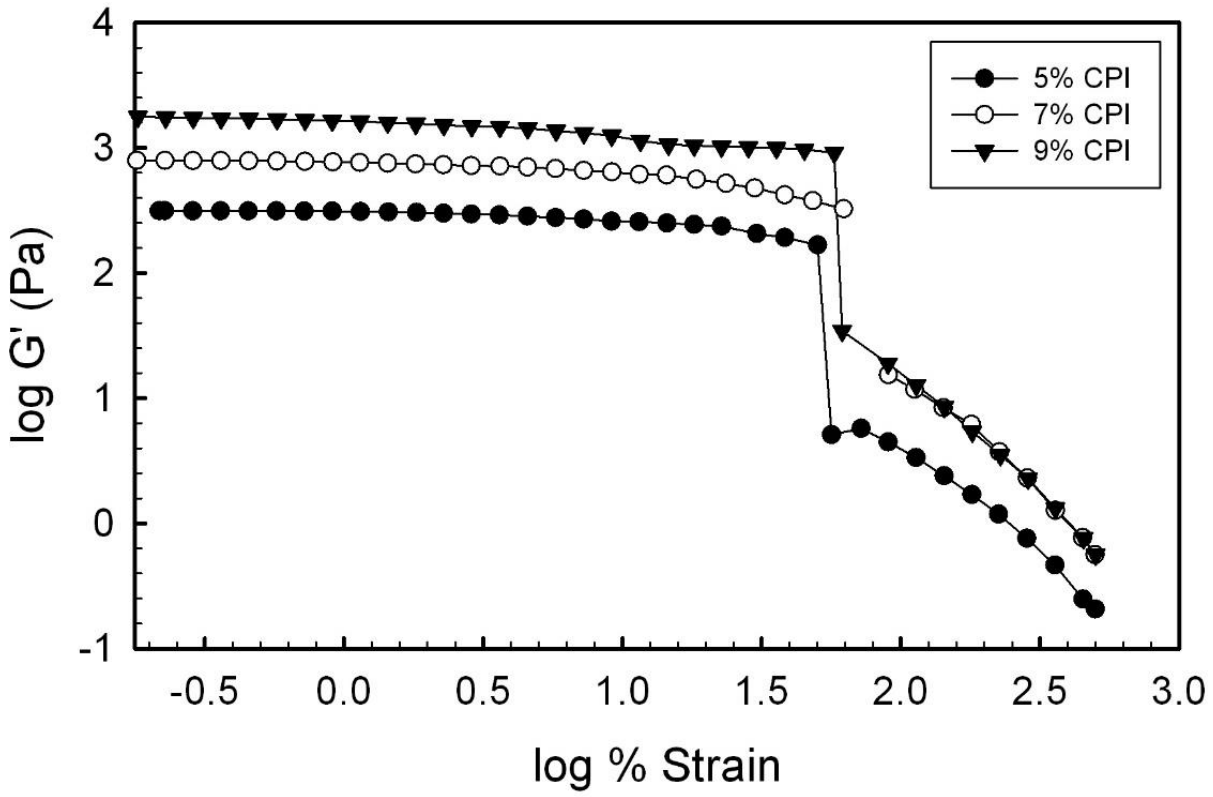

Figure 15.3. Dynamic storage (G′) modulus as a function of % strain for canola protein isolates at 5.0%, 7.0% and 9.0% (w/w) protein concentrations.

Rheological properties of soy protein isolate during gelation

The rheological properties of SPI were also followed first as a function of temperature, time, frequency and strain as a function of protein concentration. Similar to the CPI, elastic-like behavior was not seen until higher temperatures (> ~75^{o}C). The loss moduli were not shown,

however at T_{gel}, G′ was greater than G″. The gelling temperature for SPI was all found to be similar in magnitude ranging between ~77 and 83°C, which was typical for a heat setting protein network (Table 15.1). The 5.0% (w/w) SPI level did not result in network formation- due to insufficient protein concentration to form solid three dimensional network that could retain liquid and to act as elastic material. Although the denaturation temperatures of the commercial SPI could not be measured in this study due instrument sensitivity, others have reported the denaturation of pure soy glycinin and conglycinin to be near 88°C and 68°C, respectively using micro-DSC (Renkema et al., 2000; Renkema and Vliet, 2002). The denaturation of mixed soy protein isolates have been shown to have two endothermic transitions, representing soy glycinin and conglycinin (Renkema et al., 2000). Depending on the pH, denaturation temperatures shift to lower temperature as pH becomes acidic (Renkema et al., 2000). After T_{gel}, G′ continued to rise at similar rates (independent of protein concentration), as the soy proteins unravelled on heating and then aggregated via hydrophobic interaction and then the formation of disulfide bridges (Figure 15.4A). Contrast to CPI, SPI further aggregated as temperatures were above 80°C during the cooling scan (Figure 15.4B), showing greater structure formation (higher G′) than seen at the end of the heating scan. The greater magnitude possibly could be the result of a time delay to allow for proteins to re-orient being in a better orientation for form disulfide bridges. A similar profile was not found at higher temperatures during the cooling scan of CPI (Figure 15.1B) presumed to less covalent bonds being formed. During cooling a loss in strength occurred, followed by slight rise in G′ starting at temperatures <60°C due to the reformation of hydrogen bonds (Figure 15.4B). In contrast to CPI which saw significant increases in structure upon cooling, SPI remained relatively unchanged suggesting that the gel network formed was less dependent upon hydrogen bonding for stability. Similar to CPI, SPI gels remained relatively constant over the 1 h duration at 25°C suggesting the gel structures were not changing (Figure 15.4C). G′ at the end of the time sweep was found to increase from ~8.6 Pa to ~48.6 Pa as the concentration increased from 6.0% (w/w) to 9.0% (w/w) (Table 15.1). In all cases, G′ > G″ except for the 5.0% (w/w) protein concentration where G′ < G″ (Table 15.1). SPI networks were also found to have significantly reduced gel strength relative to the CPI networks (Table 15.1).

Frequency sweeps of viscoelastic moduli for a 5.0% and 9.0% (w/w) SPI material after the time sweep is shown in Figure 15.5. The 5.0% (w/w) plot indicates that the SPI is behaving as a liquid within the flow region of the viscoelastic spectrum where moduli change rapidly as a

function of frequency, and G′ < G″ (Figure 15.5A). Within this region, protein mobility is great, and protein-protein interactions are not sufficient for start forming network structures. Profiles were similar for concentrations between 6.0 and 9.0% (w/w) with only minor differences in magnitude. Therefore only the frequency sweep for the 9.0% (w/w) SPI concentration was given (Figure 15.5B). The profile suggest a gel network is formed, as evident by frequency independence of moduli within the rubber plateau region of the viscoelastic spectrum and G′ > G″ (Figure 15.5B). Similar to CPI, moduli entered the rubber-glass transition region at higher frequencies. Strain sweeps were also carried out at all SPI concentration to determine the % strain at break (Figure 15.6). In contrast, to CPI a more gradual break was evident suggesting the network was more rubbery in nature than brittle, and that junction zones within the SPI network were most likely weaker than the CPI gels. For all concentrations, the % strain at break was similar at 1.55 (35.5 anti-log) (Table 15.1).

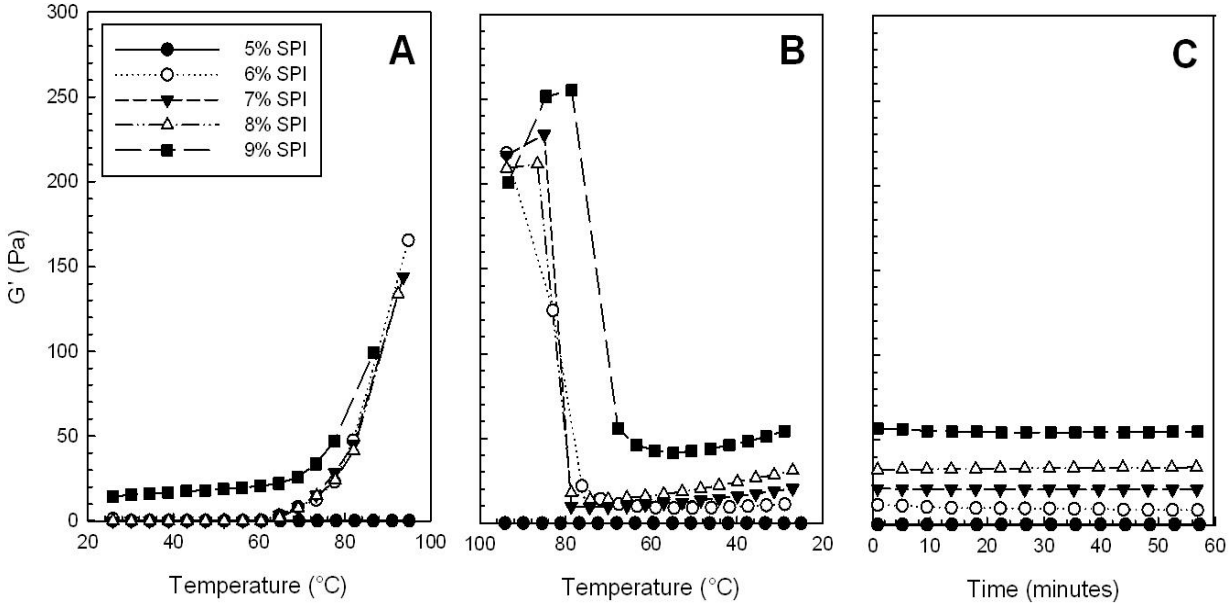

Figure 15.4. Dynamic storage (G′) modulus as a function of temperature and time for a soy protein isolate concentrations (5.0%, 6.0%, 7.0%, 8.0%, 9.0%) at 1% strain and 0.1 Hz. a) temperature ramp from 25˚C to 95˚C; b) temperature ramp from 95˚C to 25˚C; c) 1 hour time sweep at 25˚C.

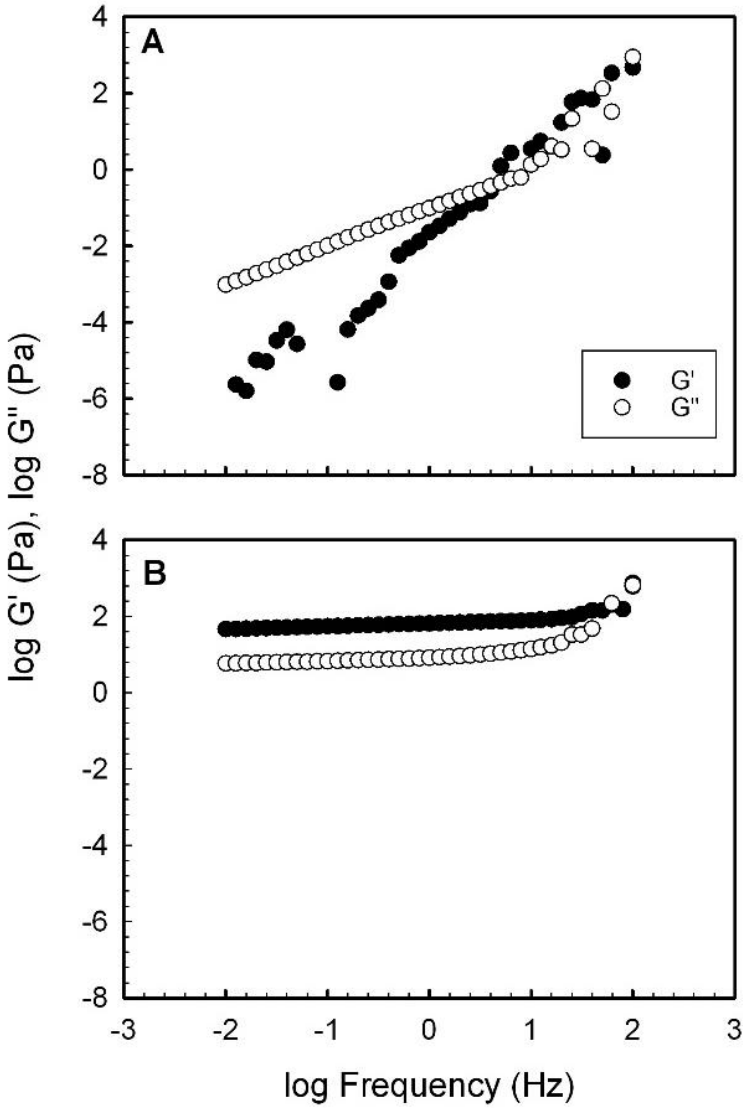

Figure 15.5. Dynamic storage (G′) and loss (G″) moduli as a function of frequency for soy protein isolates at 5.0% (A) and 9.0% (B) protein concentrations.

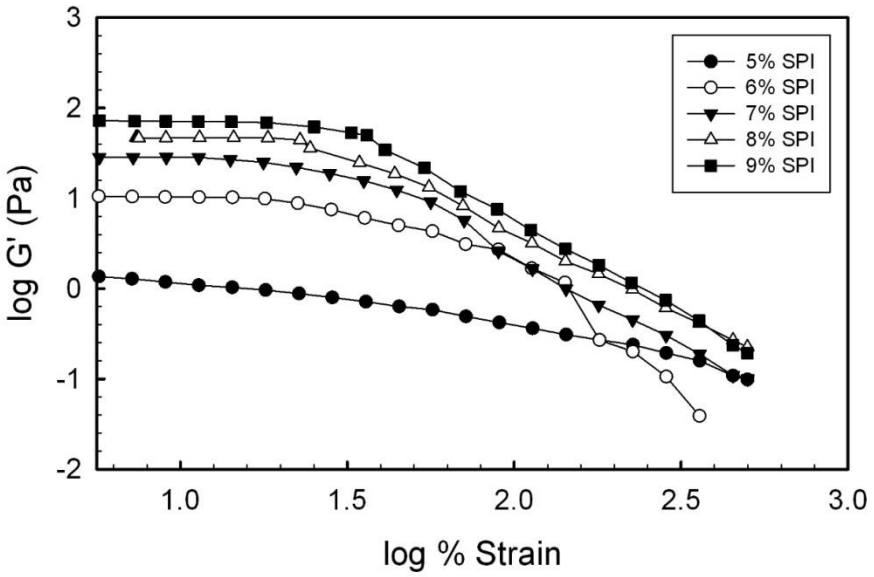

Figure 15.6. Dynamic storage (G′) modulus as a function of % strain for soy protein isolates at 5.0%, 6.0%, 7.0%, 8.0% and 9.0% (w/w) protein concentrations.

The nature of interactions within canola and soy protein gel networks

Rheological testing was done for CPI and SPI as a function of temperature, time, frequency and strain at a protein concentration of 7.0% (w/w) in the presence of NaCl (0.1 and 0.5 M), urea (0.1, 0.5, 1 and 5 M) and 2-mercaptoethanol (0.1 and 2%). In the case of CPI, similar temperature and frequency profiles were evident (not shown) as to Figure 15.1 for samples with NaCl and Urea (0.1 – 1 M), with some minor reduction in magnitude. T_{gel} values were also similar to those reported earlier (~86.0 - 90.2 ^{o}C). The addition of 5 M urea resulted in no gel formation, whereas the addition of 2-mercaptoethanol reduced the strength of formed networks considerably. Figure 15.7 gives the G′ values after the 1 h time sweep. The addition of NaCl at the levels used (<0.5 M) and little effect on network strength, despite its ability to reduce the electrostatic double layer and surface charge (zeta potential). The addition of increasing concentration of urea also had an impact as it disrupted primarily hydrogen bonding, but also hydrophobic interactions resulting in a progress reduction on G′ (Cho et al., 2006) (Figure 15.7). At the 5 M urea concentration, sufficient disruption of hydrogen bonding was evident to prevent network formation suggesting that hydrogen bonding plays a significant role in gelation. The addition of 2-mercaptoethanol resulted in a reduction in disulfide bonds between neighboring cysteine residues on the canola proteins,

however wasn't sufficient to prevent network formation. However, similar to Léger and Arntfield who added dithiothreitol to reduce disulphide crosslinks within CPI gels, the addition of 2-mercaptoethanol produced inferior gel (1993).

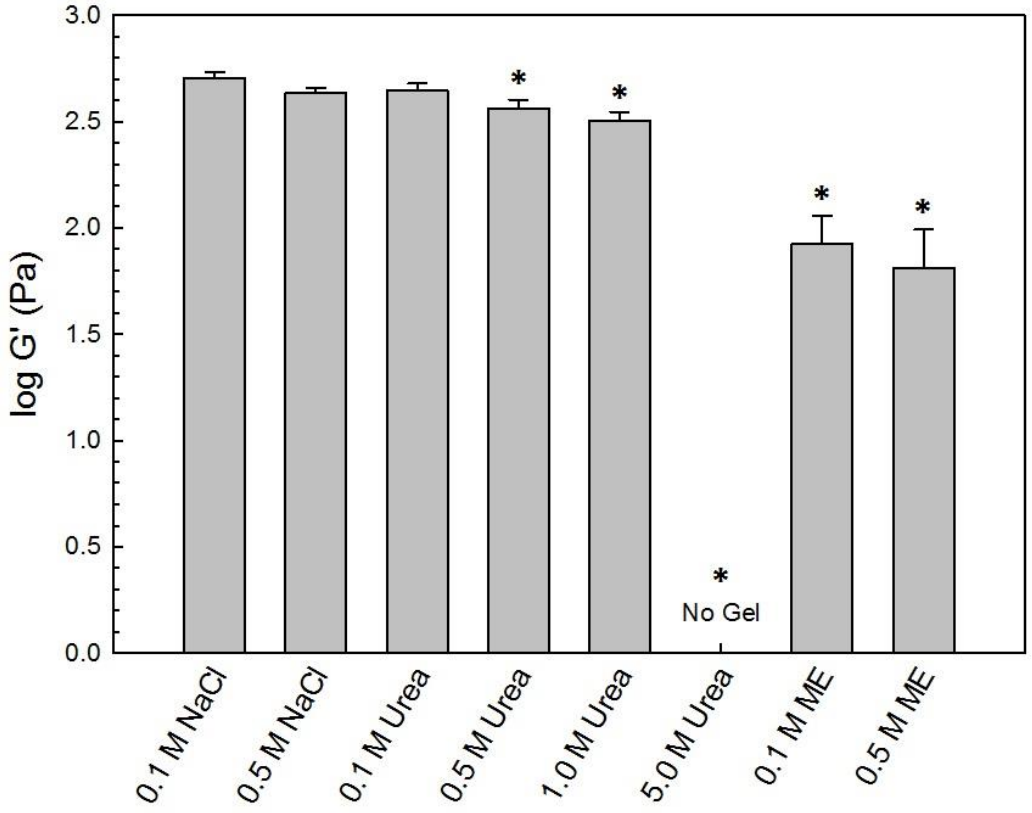

Figure 15.7 Dynamic storage (G′) modulus at the end of 1 h time sweep at 25°C for canola protein isolate networks (7.0% w/w) as a function of NaCl (0.1 and 0.5 M), urea (0.1, 0.5, 1 and 5 M) and 2-mercaptoethanol (0.1 and 1%) concentrations. The asterisk (*) symbol denote that they were significantly different than the control (0.1 M NaCl) ($p<0.05$).

Strain sweeps also were similar as those seen in Figure 15.3 for samples with NaCl and Urea (0.1 – 1 M) in which a rapid break point was evident. Findings suggest that these destabilizing salts had no major impact on the brittleness of the network (Figure 15.8A,B). However the addition of 5 M urea prevented gel formation, giving a strain profile characteristic of an entangled

protein solution (Figure 15.8B). The addition of 2-mercaptoethanol resulted in a switch from a more brittle gel to one with weaker junction zones as the disulfide bonds were reduced. The break point was more gradual in nature as the concentration of 2-mercaptoethanol increased (Figure 15.8C). Overall it is believed that CPI gels are stabilized primarily through hydrophobic interactions and hydrogen bonding with some stabilization and strength from disulfide bridging. The addition of 2-mercaptoethanol significantly ($p<0.001$) reduced the % strain at break compared to 0.1M NaCl CPI gel. In addition, higher percentage of 2-mercaptoethanol from 0.1% to 1%, there was significant ($p<0.001$) reduction in the % strain at break from 1.78 ± 0.04 to 1.34 ± 0.06.

Rheological measurements of SPI as a function of temperature and frequency in the presence of destabilizing additives were similar to those without for samples with NaCl (0.1 and 0.5 M) and urea (0.1, 0.5 and 1 M) with the exception of magnitude differences, whereas SPI solutions with urea (1 and 5 M) and 2-mercaptoethanol (0.1 and 1%) were all non-gelling (results not shown). Gelling temperatures for SPI with the addition of 0.5 M NaCl was found to significantly decrease from 83.5 ± 5.0 to 66.7 ± 1.0 ^{o}C indicating the structure formation was happening much earlier than when denaturation was expected ($p < 0.05$). The addition of excess NaCl is thought to promote protein-protein aggregation earlier. The addition of urea (0.1 and 0.5 M) has little effect on T_{gel}, which was 73.3 ± 2.1 and 80.0 ± 2.8 ^{o}C, respectively relative to the control (0.1 M NaCl) most likely since hydrogen bonds are mostly disrupted at higher temperatures.

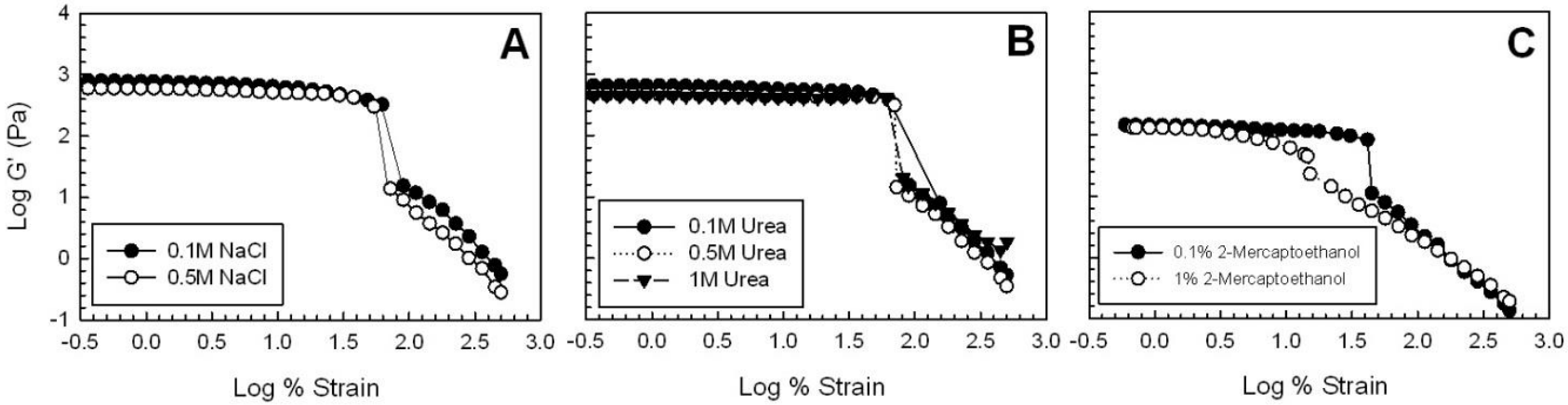

Figure 15.8. Dynamic storage (G′) modulus as a function of strain for a canola protein isolate as a function of NaCl (0.1 and 0.5 M) (A), Urea (0.1, 0.5 and 1 M) (B), and 2-mercaptoethanol (0.1 and 1 %) (C).

G′ at the end of the time sweep is given in Figure 15.9 for all materials. In contrast to CPI, the addition of 0.5 M NaCl to soy caused enhanced ordering of the protein structure resulting in significantly stronger gel networks forming. NaCl is thought to screen charges on the SPI to reduce the amount of electrostatic repulsion and the thickness of the electric double layer on proteins, to allow a greater amount of protein-protein interactions. SPI is thought to be more sensitive to the NaCl (0.5 M) than CPI, since the SPI carried a much stronger negative charge (-43.9 mV) than did CPI (-20.2 mV) at pH 7.0. Unlike CPI, the addition of 2-mercaptoethanol prevented network formation in SPI completely suggesting that disulfide bonding was essential for the formation of the network structure. Earlier it was hypothesized that a greater amount of disulfide bonds were forming based on differences in the heating-cooling profiles for both systems (Figure 15.1 and 15.4). Further, SPI were also more sensitive to hydrogen bonding than the CPI, where networks were unable to form at both the 1 and 5 M concentrations.

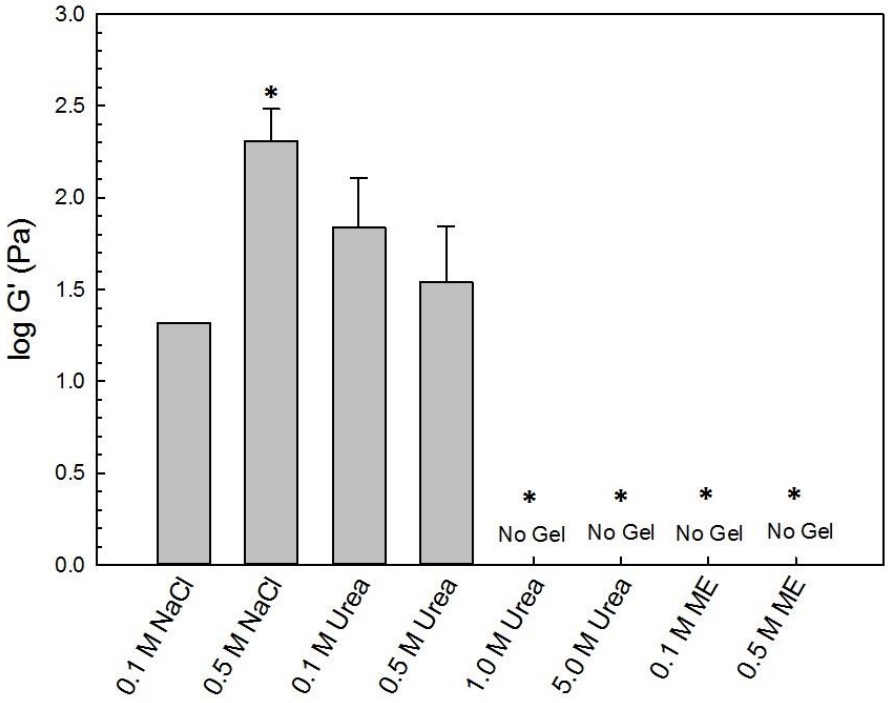

Figure 15.9. Dynamic storage (G′) modulus at the end of 1 h time sweep at 25ºC for soy protein isolate networks (7.0% w/w) as a function of NaCl (0.1 and 0.5 M), urea (0.1, 0.5, 1 and 5 M) and 2-mercaptoethanol (0.1 and 1%) concentrations. The asterisk (*) symbol denote that they were significantly different than the control ($p<0.05$).

Strain sweep data of the gel networks indicated that the 0.5 M NaCl SPI gel became more brittle, whereas the other gel networks containing (0.1 and 0.5 M) urea were similar. The % strain at break was similar in values for SPI gels that contained 0.1M and 0.5M urea (2.63 ± 0.04 and 2.70 ± 0.00). At low concentration of urea, SPI gels were able to form a gel without changing in gel structure. In contrast, CPI gels had significant decrease in % strain at break when 0.5M urea was added to the gel. This indicate that hydrogen bonding play more important role in CPI than SPI.

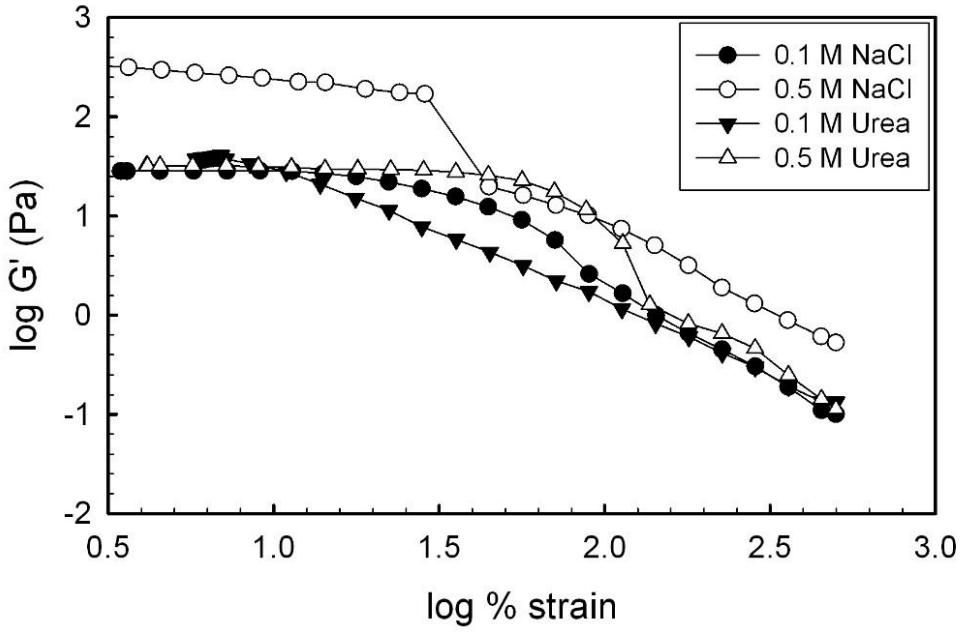

Figure 15.10. Dynamic storage (G′) modulus as a function of strain for a soy protein isolate as a function of NaCl (0.1 and 0.5 M) and urea (0.1 and 0.5 M) concentration.

Fractal analysis of the gel networks.

Confocal scanning laser microscopy was used to image the morphology of the CPI and SPI as a function of protein concentration, and then used to determine the fractal dimension and lacunarity of the gel network. Figure 12 gives CSLM images of CPI as a function of concentration, showing that the level of aggregation increases as the protein concentration was raised. After applying the box count method on CSLM images, data was fitted using a power-law model where the slope was used to calculate fractal dimensionality. The fractal dimension was found to be

similar for all concentrations ($p<0.05$), having values of 1.52 ± 0.08, 1.53 ± 0.03 and 1.59 ± 0.04 for the 5.0, 7.0 and 9.0% (w/w) concentrations, respectively. The CPI fractal dimension values fall within the range of other protein gels, which is between 1.5 and 2.8 (Eleya and Gunasekaran, 2003; Hagiwara et al., 1997; Ikeda et al., 1999; Wu and Morbidelli, 2001). The fractal dimension value stayed relatively constant as concentration increased, indicating that small aggregates grow into self-similar larger ones in a fractal manner, and close to value that is expected for the cluster-cluster aggregation model (Ikeda et al., 1999; Weitz and Lin, 1986). Fractal dimensions measured in this study were similar to that of pure soy glycinin ($d_f = 1.64$) and a mixed soy protein isolate ($d_f = 1.81$) which contained $MgCl_2$ (Nagano and Tokita, 2011).

Fractal dimension looks at the complexity of the gel structure, however better understanding of the gel network occurs when lacunarity is also evaluated (Dàvila and Parés, 2007). As the CPI concentration increased from 5.0% to 7.0%, then lacunarity of the gel decreased from 0.62 ± 0.06 to 0.41 ± 0.02 ($p<0.01$), where it then became constant as the concentrations were raised to 9.0% (w/w) (lacunarity of 0.40 ± 0.03) ($p>0.05$). The reduction of lacunarity value suggests there is less void space within the network (or a dense gel is formed). This suggests that at the 5.0% CPI concentration, cavities sizes are larger and less protein is available to occupy a given space. In Figure 15.11A, there is larger gap than Figure 11B and 11C, however the fractal dimension alone did not indicate a difference. High fractal dimension and lacunarity values indicates that there is noticeable heterogeneity in gel structure (Karperien, 2012). The lacunarity values furthered explain the morphology of the CPI as a function of protein concentration.

In the present study, clear images of the SPI could not be obtained using the CSLM. Several studies have reported issues with producing CSLM images of globular protein gels, suggested due to differences in solvents, protein-type, and gelation method used to prepare the samples. Hagiwara et al. (1997) was unable to obtain clear images of either soy glycinin or caseinate gels using CSLM, however was able to image β-Lactoglobulin. The gels were produced using varies methods depending on protein-types, and contained different levels of NaCl. There are several studies that were successful at imaging SPI and/or pure soy glycinin

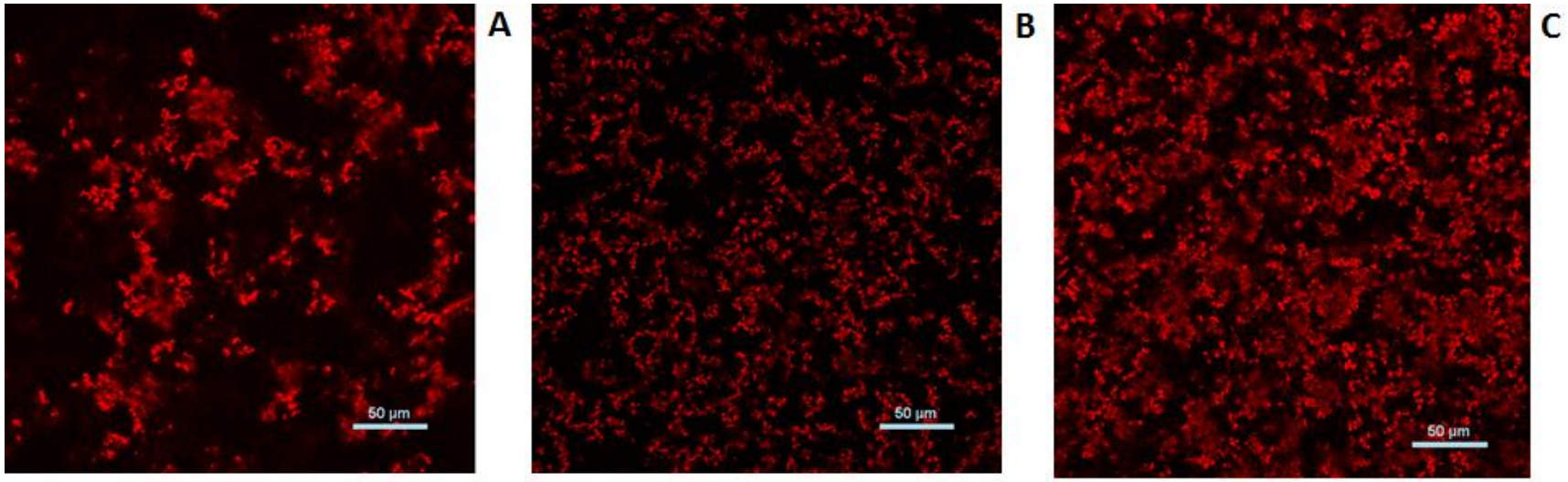

Figrue 15.11. Confocal micrographs of canola protein isolate gels (0.1M NaCl, pH = 7.0) as a function of concentration: A) 5.0%, B) 7.0% and C) 9.0% (w/w).

networks by CSLM (Nagano and Tokita, 2011; Renkema, 2004; Lakemond et al., 2003), however the proteins were prepared differently and contained some NaCl.

15.5 CONCLUSIONS

The present study examined the rheological properties and morphology of CPI and SPI gels as a function of concentration (5.0 – 9.0%), ionic strength (0.1 and 0.5 M NaCl) and in the presence of destabilizing agents such as urea (0.1, 0.5, 1.0 and 5.0 M) and 2-mercaptoethanol (0.1% and 1%). Small-deformation oscillatory measurements showed that the CPI formed stronger gels than SPI, with less dependence on disulfide and hydrogen bonds relative to SPI. For both proteins, there was no significant difference (~77°C - ~90°C) in gelling temperature as the protein concentration increased. Fractal dimension and lacunarity was analyzed using CLSM image to show the microstructure of CPI gels became denser as the concentration increase from 5.0% to 9.0% and followed a cluster-cluster aggregate growth model during the formation of the gel network.

Part V: Canola proteins as film forming agents

-Chapter 16-

Literature review

16.1 Biodegradable edible films

Biodegradable edible films are both economically and environmentally important to the food industry in terms of packaging and coating materials. Traditional petroleum-derived synthetic materials used in consumer packaging create tremendous demands in landfills, the environment and consumer health. As such, research activities surrounding biodegradable edible packaging have been increased substantially over the past decade as the food industry attempts to find an alternative to synthetic petroleum-based polymers using bio-based materials, such as proteins, polysaccharides, and lipids (Vargas et al., 2008; Gomez-Estaca et al., 2009; Janjarasskul and Krochta, 2010). In addition to the alleviated environmental impacts, depending on the materials selected, films may have the added advantages of being edible and/or being used as a controlled delivery system for bioactive (e.g., sodium alginate-gellan gum coating containing N-acetylcysteine and glutathione (Rojas-Grau et al., 2007)) or antimicrobial (e.g., hydroxyl propyl methyl cellulose-based film containing nisin (Sebti and Coma, 2002)) compounds to maintain product quality and extend shelf-life (Ou et al., 2004; Han and Gennadios, 2005). Typically, biodegradable edible films tend to be self-supporting and <250 microns thick, used to encase a product or to separate heterogeneous prepared food products to keep ingredients separate (e.g., to inhibit or control moisture transfer) (Krochta and De Mulder-Johnston, 1997; Janjarasskul and Krochta, 2010). Edible materials within films are classified more as additives than ingredients, as they have no significant nutritional value (Debeaufort et al., 1998). The films are required to be relatively tasteless to help prevent consumer detection (Contreras-Medellin & Labuza, 1981). Implementation of biodegradable edible packaging by the food industry will help offset demands on our landfills and the environment, and enhance consumers' health and wellness (e.g., due to reduced levels of potential chemicals that could leach into our foods), and improve product quality. Other advantages for using the biopolymer-based films may include: transparency, mechanical strength, barrier properties (moisture and gases) and their use in controlled delivery applications (Debeaufort et al., 1998; Janjarasskul and Krochta, 2010; Falguera et al., 2011). These characteristics can be tailored through material selection biopolymer characteristics (e.g., concentration), solvent (e.g., pH and the presence of salts), the environment (e.g., relative humidity

and temperature) and processing techniques. Film performance is typically assessed based on its mechanical properties, gas permeability, water vapor permeability, opacity, and moisture sorption property, based on common testing methods (Table 16.1).

16.1.1 Film materials

Biodegradable edible films are generally classified as being comprised of either lipids (e.g., solid fats, waxes, or resins) or biopolymers (e.g., proteins or polysaccharides); each has its own advantages and disadvantages (Table 16.2). Protein-based (e.g., gelatin, whey, soy and corn zein) and polysaccharide-based (e.g., alginate, carrageenan, chitosan and pectin) materials tend to form films with excellent mechanical properties and gas barrier properties, but have issues relating to moisture control due to the hydrophilic nature of the materials (Baldwin et al., 1995; Vargas et al., 2008; Janjarasskul and Krochta, 2010). In contrast, lipid-based (e.g., beeswax) films tend to display poor mechanical integrity and gas barrier properties, but provide excellent moisture control (Greener and Fennema, 1989; Janjarasskul and Krochta, 2010). In order to overcome deficiencies associated with lipid-based or biopolymer-based films, research is now primarily focused on composite films involving both. Optimization of film formulation is essential in order to balance the positive and negative attributes of each material.

Protein-based edible films developed from wheat gluten, casein, whey protein, and gelatin can be expensive, and as such, other plant protein materials have been explored for their potentialities to develop biodegradable edible films (Table 16.3). Of particular interest, is protein-rich meals left over from oil seed pressing (e.g., from soybean and canola) which tend to be low cost, abundant and have a high nutritional value.

Table 16.1 Functional properties of biodegradable edible films.

Functionalities	Definition and importance	Detection methods
Moisture sorption	Hydrophilic nature of edible films results in the absorption of water and hydrates under high RH environment, which decreases structural integrity, resistance to moisture transport, and mechanical strength.[1]	Swelling index (SI) = $(W_2–W_1)/W_1×100$ (W_1 = the weight of original film, W_2 = the weight of the film which is immersed into distilled water for 24 hours).[2] Moisture sorption isotherm (MSI): measures the water content of the films that are stored at different equilibrium RHs under a specific temperature.[3]
Water vapor permeability (WVP)	WVP is defined as water vapor transmission rate per unit area which is induced by the vapor pressure difference between the food and its surrounding environment under specified temperature and RH. Because many deteriorative chemical and enzymatic reactions, microbial growth, and textural properties of certain foods are governed by water activity and water content of foods, WVP of film is very important. [4]	WVP is determined by "cup method" (ASTM E96-93) based on the gravimetric technique. The film is sealed on a cup partially filled with the solution and stored in an air desiccators under controlled RH and temperature, and measuring the weight gain or loss of the film over time.[5, 6, 7, 8]
Optical property	Optical property of edible films refers to the transparency of films which depends on the formulation and fabrication procedures of films. It is crucial important for attractive ability of foods.[2]	A spectrophotometer is usually used to determine film opacity, and the adsorption spectrum is measured over a wavelength range of 400-800 nm.[9]

Table 16.1 Functional properties of biodegradable edible films (continued).

Functionalities	Definition and importance	Detection methods
Gas permeability	Gas permeability, the gas (O_2, CO_2, and aroma) transmission rate, is measured by unit gas pressure between food and the environment under specified temperature and humidity conditions. Due to lipid oxidation, enzymatic reaction, and respiration of postharvest fruits and vegetables, controlling O_2 and CO_2 permeabilities are very important; and aroma permeability is significant for the maintenance of flavor and aroma of foods.[4]	O_2 and CO_2 permeability is determined by ASTM D3985-02 method: the film is placed between two chambers under specific RH and constant temperature, one contains O_2 and CO_2 which can pass through the film and goes into another chamber which contains N_2; and O_2 permeability is measured by O_2 sensor, and CO_2 is determined by gas chromatography.[10]
Mechanical properties	The mechanical properties of film which include tensile and puncture strengths which reflect the ability of the film to resist external physical stress. Tensile strength (TS), tensile elongation (TE), elastic modulus (E) puncture strength (PS), and puncture deformation (PD) are mainly concerned. The improvement of mechanical properties of films can increase yield, facilitate handling, and protect foods from mechanical damage during food transportation.[4]	Tensile testing is performed using a TA.XT2 Texture Analyzer according to the ASTM D882-91 to determine TS, TE, and E; puncture testing is also measured using a TA.XT2 Texture Analyzer to determine PS and PD; and both of tests are operated in a specified RH (usually 54% RH at room temperature is applied).[2, 11]

References: adapted from: [1]Greener & Fennema (1989); [2]Gontard et al. (1992); [3]Gontard et al. (1993); [4]Janjarasskul & Krochta (2010); [5]Banker et al. (1966); [6]Kamper & Fennema (1985); [7]Kester & Fennema (1986); [8]Martin-Polo & Voilley (1990); [9]Gontard et al. (1994); [10]ASTM D3985-02 (2002); [11]ASTM D882-91 (1991).

Table 16.2 General overview of various biodegradable edible film materials.

Film materials	Formation mechanism	Advantages	Disadvantages	Examples
Polysaccharide – based films	Coacervation process disrupts interactions among long-chain polymer segments, and new intermolecular hydrophilic and hydrogen bonding are formed upon evaporation of the solvent to create a film matrix.[1, 2]	Materials are abundant, low cost, and easy to handle. Good gas and lipid barrier properties. Used in controlled delivery applications. Moderately good mechanical properties at low relative humidity (RH).[1, 2, 3]	Mechanical strength is weak at high RH. Poor moisture barrier property, highly water soluble.[1, 2]	Cellulose derivatives, starch, pectin, alginate, carrageenan, chitosan.[1, 2]
Protein – based films	Involves protein denaturation by heat and pH of solvents, followed by dehydration and cross linking. Casting or extrusion method are commonly used.[1, 2]	Used in controlled delivery applications. Good barrier property to against gases, aromas, and lipids.[4, 5]	The film is brittle and susceptible to cracking. High water vapor permeability.[1, 2]	Wheat gluten, corn zein, soy protein isolate, collagen and gelatin, milk proteins.[1, 2]
Lipid – based films	Involves dipping a supporting mold into a molten lipid, followed by cooling.[1, 2]	Low water vapor permeability. Induces a sheen on the surface of food product.[2, 6]	Poor mechanical properties, including being non-self-supporting. Waxy taste/texture. Greasy surface. Potential rancidity. Fragile and not cohesive.[1, 2]	Glycerol esters, waxes, resin, surfactants ($C_{16} – C_{18}$ fatty acids and fatty alcohols).[1, 2]

Table 16.2 General overview of various biodegradable edible film materials (continued).

Film materials	Formation mechanism	Advantages	Disadvantages	Examples
Composite films	Bi-layer film: Films are formed in two stages. 1st stage: the layer of polysaccharide or protein is casted and dried, 2nd stage: the lipid layer is combined.[7, 8]	Better water vapor barrier efficiency, and moderately good mechanical properties at low RH.[2, 4, 9]	The bi-layer structure has a tendency to crack and/or delaminate. Complicate processing steps.[2, 7]	Combining lipid compounds with a hydrocolloid-based structural matrix.[1, 2]
	Emulsion-film: Films are derived using a stable lipid-protein (or polysaccharide) emulsion. The lipid is dispersed in an hydrophilic phase (protein or polysaccharide) to form an emulsion.[5, 8]	Good mechanical strength. Simple process for manufacture, being applied on food at room temperature, adhesive.[1, 2, 9]	Less efficient due to non-homogeneous distribution. Stability issues relating to lipid melting temperature and solvent volatilization lead to loss in structure. Poor control over moisture transfer.[1, 2]	

References: adapted from: [1]Vargas et al. (2008); [2]Janjarasskul & Krochta (2010); [3]Baldwin et al. (1995); [4]Debeaufort & Voilley (1995); [5]Shellhammer & Krochta (1997); [6]Greener & Fennema (1989); [7]Krochta (1997); [8]Perez-Gago & Krochta (2005); [9]Gontard et al. (1994).

Table 16.3 Plant protein-based edible films found in the literature.

Film type	Formulation	Processing	Tests	Reference
Lentil protein	LPC (5%), Gly (50%)	Film forming solution (70ºC/20 min/pH 11.0); Setting conditions (25ºC/48h/50%RH)	Thickness, color, mechanical properties, WVP, TSM	Bamdad et al. (2006)
Faba bean protein	FPI (5%), Gly (40%, 50%, 60%)	Film forming solution (room temperature/pH 7.0, 9.0, and 12.0); Setting conditions (25ºC/48h/50%RH)	Thickness, color, mechanical properties, WVP, TSM, SEM analysis	Saremnezhad et al. (2011)
Soy protein	SPI (6%, 7%, 8%, 9%), Gly (40%, 50%, 60%, 70%)	Film forming solution (70ºC/20 min/pH 7.0); Setting conditions (25ºC/48h/30%RH)	Thickness, DSC, WVP	Kokoszka et al. (2010)
Soy protein	SPI (8.33%), Gly (50%), genipin (0%, 0.1%, 1%, 2.5%, 5%, 7.5%, 10%)	Film forming solution (70ºC/2 h/pH 9.0); Setting conditions (25ºC/48h/50%RH)	Thickness, opacity, TSM, mechanical properties, WVP, SEM analysis	Gonzalez et al. (2011)
Soy protein	SPI (5%), Gly (60%), Sor (60%), MTGase (4 units)	Film forming solution (70ºC/20 min/pH 8.0); Setting conditions (25ºC/48h/50%RH)	Thickness, tensile test, WVP, TSM, transparency, SEM analysis	Tang et al. (2005)
Pea protein	PPI (10%), Gly (20%, 30%, 40%, 50%)	Film forming solution (90ºC/25 min)	Tensile test, WVP, TSM	Choi & Han (2001)
Rapeseed protein	RP (4%), Sor/Sucrose (1.5%/0.5%, 1.5%/1.5%, 2.0%/0.5%, 2.0%/1.0%)	Film forming solution (room temperature); Setting conditions (25ºC/48h/50%RH)	Tensile test, WVP, SEM analysis	Jang et al., (2011)
Sunflower protein	ISFP (10%), Gly (50%), PEGs (40%, 50%, 60%)	Film forming solution (150ºC/3 min); Setting conditions (25ºC/48h/60%RH)	Mechanical properties, WVP	Orliac et al., (2003)

Abbreviations: lentil protein concentrate (LPC); faba bean protein isolate (FPI); soy protein isolate (SPI); pea protein isolate (PPI); rapeseed protein (RP); sunflower protein isolate (ISFP); glycerol (Gly); sorbitol (Sor); polyethylene glycols (PEGs); microbial transglutaminase (MTGase); relative humidity (RH); water vapor permeability (WVP), total soluble matter (TSM); scanning electron microscopy (SEM); differential scanning calorimetry (DSC)

16.1.2 Film preparation

Biopolymer-based films are traditionally formed either by casting or extrusion. In the casting method, biopolymer solutions are poured onto a mould, followed by gelation and drying. Cold-set biopolymers (e.g., gelatin, alginate, carrageenan, and gellan gum) are poured onto a mould as a hot sol typically in the presence of a polysaccharide-sensitive ion (e.g., alginate and calcium) to induce gelation as temperatures are cooled down. In contrast, heat-set biopolymers (e.g., soy protein, whey protein, and oval albumin) are poured onto the mould at room temperature. As temperatures are raised, proteins can be denatured and aggregated with neighboring proteins via hydrophobic interactions and covalent linkages to induce 'particulate-type' or 'fibrous-type' gel networks (Kester and Fennema, 1986; Debeaufort et al., 1998; Janjarasskul and Krochta, 2010). Proteins are quite sensitive to changes in temperature. Within the film formation processes, proteins may be disaggregated, dissociated and denatured by heating, which then promotes protein-protein aggregation as protein molecules re-align and associate with each other (Redl et al., 1999). The addition of cross linking agents and plasticizers are carefully balanced to ensure improve both film strength and flexibility once set (Pommet et al., 2003). Choi and Han (2002) prepared pea protein isolate (PPI)-based films through heating the film forming solution at 90 ºC for 5, 10, 20, 30, 40, and 50 min. The authors found that the heat treatment significantly improved the tensile strength and elongation of films, where the tensile strength and elongation of heat-denatured (20 min) PPI films were 7 and 13 times higher than non-denatured PPI films, respectively. Degassing of the film forming solution is essential to reduce the chance of air bubbles, as the material dries (Yang et al., 2010). During drying, the aqueous solvent is removed leading to significant increases in biopolymer concentration, aggregation and chain entanglement to form a self-supporting film. The film is then conditioned to a desired relative humidity before testing.

In the extrusion method, thermally-induced phase transition (e.g., in soy protein) (Cunningham et al., 2000), glass transition (e.g., in gelatin) (Park et al., 2008), and gelatinization characteristics (e.g., in starches) (Pushpadass et al., 2009) are important considerations in the film production (Janjarasskul and Krochta, 2010). Processing typically involves heating the biopolymers above their glass transition temperature (T_g) under low moisture conditions, and eventually leading to a uniform melt which can be easily shaped into films/packages using heat and pressure upon cooling, or thermal compression or injection molding. The thermal extrusion is

more cost effective with higher output than the casting method for making films, and the formation, aggregation, and cross linking structures in the film are highly dependent on processing temperature, drying rate, and screwing speed in the thermal extrusion (Rhim and Ng, 2007; Hernandez-Izquierdo and Krochta, 2008; Hernandez-Izquierdo et al., 2008). Many carbohydrates and proteins, such as sodium alginate (Liu et al., 2006), corn zein (Wang and Padua, 2003), and soy protein (Cunningham et al., 2000) exhibit potential thermoplastic behaviors for the film formation by thermal extrusion.

Lipid-based films are typically prepared by: a) melting the lipid material, followed by re-solidification; b) solubilizing the lipid material within an organic solvent, followed by evaporation; or c) creating an oil-in-water emulsion, followed by evaporation of the aqueous phase (Greener and Fennema, 1989; Gontard and Guilbert, 1994; Janjarasskul and Krochta, 2010).

Composite materials involving two (or more) biopolymers (e.g., proteins and polysaccharides) are also used in film production (Janjarasskul and Krochta, 2010), where gelation is induced via a process known as complex coacervation whereby two biopolymers with opposite net charges interact via electrostatic attractive forces within a narrow pH range (Janjarasskul and Krochta, 2010). This range typically extends from pHs > pK_a of the reactive site on the polysaccharide backbone (e.g., alginate, -COO- pK_a of 1.88) and pHs < pI (isoelectric point of a protein, e.g., whey protein pI 4.6), where the polysaccharide and protein assumes a net negative and positive charge, respectively. In contrast, composite films involving proteins/polysaccharides and lipids can be produced using a layer-by-layer stacking technique to form a laminate-type film or through the creation of an emulsion-based gel (and then film matrix) whereby lipid-droplets are dispersed within the biopolymer matrix (Perez-Gago and Krochta, 2005).

16.2 Plasticizers

Plasticizers are typically added to biopolymer-based films to overcome brittleness issues to make films more malleable and allow the films to be easily removed from the moulds (Sothornvit and Krochta, 2005; Janjarasskul and Krochta, 2010). Plasticizers are small poly alcohol (-OH) molecules added to the film forming solution to disrupt intermolecular interactions between chains and to replace polymer-polymer interactions with polymer-plasticizer interactions (via hydrogen bonding); resulting in a heterogeneous distribution of junction zones and the increase of chain mobility within the film matrix to make the film more flexible (Hettiarachchy

and Eswaranandam, 2005; Sothornvit and Krochta, 2005; Janjarasskul and Krochta, 2010). In general, plasticizers situate themselves into the polymeric network to disrupt the hydrogen bonding between neighboring polymers, reduce the intermolecular attractive forces, and increase the intermolecular space, thereby, allowing for improved flexibility, extensibility, and toughness of the films (Hettiarachchy and Eswaranandam, 2005; Sothornvit and Krochta, 2005; Janjarasskul and Krochta, 2010). On the other hand, since plasticizers lessen the attractive forces and increase the free volume in the film matrix, the diffusion coefficient for gases and water vapors are increased (Banker, 1966; Guilbert, 1986; Hettiarachchy and Eswaranandam, 2005).

Plasticizers used in the production of biodegradable edible films can be divided into water soluble (e.g., glycerol) and insoluble (e.g., saturated fatty acids) plasticizers (Siepmann et al., 1998). Hydrophilic plasticizers dissolve in the aqueous medium to provide more space between polymer chains when they are added into film forming solution. Theoretically, due to the hydrophilic nature, water soluble plasticizers result in an increase of water diffusion within film structure. In contrast, water insoluble plasticizers lead to a decrease in the water uptake of films. However, phase separation or formation of discontinuity zones within the film structure may result from the addition of water insoluble plasticizers to further decrease film flexibility and water vapor barrier property. Therefore, the optimum stirring for the film forming solution is critical for the application of water insoluble plasticizers (Bodmeier and Paeratakul, 1997). Moreover, in polymer science, plasticizers can be defined as internal (e.g., sorbitol and sucrose) or external (e.g., linseed oil and castor oil) plasticizers depending on the interactions between plasticizers and polymers. In brief, external plasticizers are low volatile substances which cannot chemically react with polymers through primary bonds and will be eventually lost by evaporation. Internal plasticizers have bulky structures to co-polymerize or react with original polymers to inhibit polymer-polymer interactions from occurring, therefore, films will be softer as evident by reduced elastic modulus values (Frados, 1976; Sothornvit and Krochta, 2005).

Both type and amount of plasticizers affect the interactions between biopolymers and plasticizers. For instance, film extensibility and flexibility can be increased and the film strength can be decreased as the concentrations of plasticizers are raised. Plasticizers with lower molecular weight and higher surface charge can easily insert into the film matrix to increase the plasticizing effect (Sothornvit and Krochta, 2001; Hettiarachchy and Eswaranandam, 2005). The compatibility of plasticizers with biopolymers is related to the plasticizers' size, shape, space between oxygen

atoms, as well as their water-binding abilities. Plasticizers must be readily soluble in the film forming solution and miscible with all polymers present. Polyols (e.g., glycerol, sorbitol, and polyethylene glycols), mono-, di-, or oligosaccharides (e.g., glucose, fructose-glucose syrups, and sucrose), lipids and their derivatives (e.g., phospholipids and surfactants) are the most commonly used plasticizers in the films (Sothornvit and Krochta, 2005).

16.3 Cross linking agents

In order to withstand the external stress and moisture environment that would occur during processing and handling of products, biodegradable edible films should have proper strength, flexibility, and barrier properties to maintain the integrity of products (Yang and Paulson, 2000b). Therefore, many researchers have been focused on improving film properties by means of cross linking using physical, chemical and enzymatic treatments.

Ultraviolet and γ-irradiation can be used to produce cross links in protein-based films; however, the efficiency at improving film properties is highly dependent upon the properties of the protein being used, especially the amino acid composition and molecular structure/conformation. For instance, the tensile strength of soy protein films was increased by 65%, whereas the tensile elongation for the same film decreased by 31% with the application of UV irradiation (0.0104 J/cm^2). In this case, the aromatic amino groups (e.g., tyrosine and phenylalanine) in soy protein participated within the cross linking reaction. In contrast, wheat gluten and pea protein films were not affected by γ-irradiation (Tomihata et al., 1992; Gennadios et al., 1998; Micard et al., 2000). Protein cross links can also form upon heating the film forming solution, following a similar mechanism as heat set gelation of globular proteins. During this process, proteins are completely or partially unraveled to expose hydrophobic moieties that were previously buried within the interior of the protein, followed by protein interactions via hydrophobic interactions and possibly disulfide bridging (Damodaran, 2008).

Depending on the material and film strength, cross linking agents may be added to the material being casted (e.g., transglutaminase + protein/chitosan; genipin + gelatin/chitosan) (Yajima et al., 2010; Porta et al., 2011). Chemical cross linking agents, typically containing aldehyde groups, can react with the amino groups of lysine residues to form bridges between protein chains (Song et al., 2011). Glutaraldehyde is the most commonly used chemical cross linking agent. However, due to its high toxicity, its application in biodegradable edible films has

been limited from the consideration of safety issues. Recently, a new natural cross linker, genipin have been used in the production of films. It is about 10,000 times less cytotoxic than glutaraldehyde (Yuan et al., 2007; Song and Zhang, 2009). Gonzalez et al. (2011) evaluated the properties of soy protein isolate (SPI)-based films with the addition of varying levels of genipin. The authors reported that mechanical and water vapor barrier properties were significantly improved by adding only a small amount (< 2.5% w/w genipin relative to the SPI) to the film forming solutions.

In contrast, enzymatic cross-linking agents are more popular and beneficial in the production of films (Song et al., 2011). Enzymatic cross linking agents (e.g., peroxidase and transglutaminase) can produce polymers with high molecular weight by catalyzing covalent cross linking reactions between proteins (Song et al., 2011). Because of the reduction of tensile strength and elongation by the application of peroxidase in the films (Michon et al., 1999), transglutaminase is more commonly used in film production, such as in the case of soy protein films (Tang and Jiang, 2007) and wheat gluten films (Tang et al., 2005). Transglutaminase catalyzes the acyl transfer of the γ-carboxyamide group of glutamine into the ε-amino group of lysine to release ammonia and introduces the ε-(γ-glutamyl)-lysine cross links in the protein molecules (Folk, 1980).

In general, cross linking agents in the film act to reduce film solubility, improve film strength, reduce swelling and decrease gas/water vapor permeability by increasing macromolecular interactions within the film. For instance, Porta and co-workers (2011) reported the application of $CaCl_2$ to cross link casein-based films enhanced protein-protein interactions, and led to a 31% reduction in the film thickness and decreased solubility.

16.4 Other film additives

16.4.1 Emulsifiers

Emulsifiers may be added, especially to composite films involving both biopolymer and lipid materials. Emulsifiers are surface active molecules with both polar and non-polar ends that act to modify the lipid-water interface (e.g., reduced interfacial tension) to make the two immiscible phases more stable (Krochta, 2002; Janjarasskul and Krochta, 2010). They can be incorporated into the film formulations to improve the dispersion of lipid particles and reduce interfacial tension of the solution to achieve sufficient surface wettability and adhesion of films

(Krochta, 2002). Rhim and co-workers (1999) observed that soy protein isolate-based films became thicker, stronger, and less susceptible to shrinkage with the addition of fatty acids (e.g., lauric acid, palmitic acid, stearic acid, and oleic acid). Some common emulsifiers used in film production include: acetylated monoglyceride, lecithin, polysorbate 60, and glycerol monopalmitate. Furthermore, proteins themselves have some emulsifying properties owing to their amphiphilic nature (Janjarasskul and Krochta, 2010).

16.4.2 Waxes

In order to improve the barrier properties associated with biopolymer-based films, waxes are commonly used as additives in the film formulations. Wax is a type of lipid with a long-chain fatty acid and tends to be solid at room temperature, and has high hydrophobicity (Kester and Fennema, 1986). Natural waxes (e.g., carnauba wax, candelilla wax, and rice bran wax) can be extracted from plants and seeds by nonpolar solvents, therefore, waxes cannot be solubilized into the aqueous solutions (Baldwin, 2007; Song et al., 2011). Because of the hydrophobic long-chain ester and free fatty alcohol in the molecular structure, waxes behave as desirable additives to improve the water vapor permeability of films. The water vapor permeability and total soluble matter of soy protein isolate-based films were gradually decreased with an increase of sorghum wax from 5% to 20% (w/w of protein) (Kim et al., 2002). However, the addition of waxes in the film formulation can decrease the mechanical strength and make the film become fragile, because waxes have poor ability to form covalent bonds with biopolymers in the film structure (Janjarasskul and Krochta, 2010). Moreover, there are some other disadvantages associated with the application of waxes in the films, such as greasy appearance and waxy taste and texture (Janjarasskul and Krochta, 2010). Beeswax, petroleum wax, carnauba wax, and candelilla wax are commonly used with biopolymers in the film formulations (Baldwin, 2007).

-Chapter 17-

Effect of protein and glycerol concentration on the mechanical, optical and water vapor barrier properties of canola protein isolate-based edible films[7]

Chang Chang and Michael T. Nickerson

Department of Food and Bioproduct Sciences, University of Saskatchewan,
51 Campus Drive, Saskatoon SK, Canada S7N 5A8

[7]Food Science and Technology International, In print (2014)

17.1 ABSTRACT

Biodegradable edible films prepared using proteins are both economically and environmentally important to the food packaging industry relative to traditional petroleum-derived synthetic materials. In the present study, the mechanical and water vapor barrier properties of casted canola protein isolate (CPI) edible films were investigated as a function of protein (5.0% and 7.5%) and glycerol (30%, 35%, 40%, 45%, and 50%) content. Specifically, tensile strength (TS) and elongation (TE), elastic modulus (E), puncture strength (PS) and deformation (PD), opacity, and water vapor permeability (WVP) were measured. Results indicated that TS, PS, and E decreased, while TE and PD values increased as glycerol concentration increased for both 5.0% and 7.5% CPI films. Furthermore, TS, PS, and E values were found to increase at higher protein concentrations within the CPI films, whereas PD values decreased. TE was found to be similar for both CPI protein levels. CPI films became more transparent with increasing of glycerol concentration and decreasing of CPI concentration. WVP value was also found to increase with increasing glycerol and protein contents. Overall, results indicated that CPI films were less brittle, more malleable and transparent, and had greater water vapor permeability at higher glycerol levels. However, as protein level increased, CPI films were more brittle, less malleable and more opaque, and also had increased water vapor permeability.

17.2 INTRODUCTION

There is an increasing interest surrounding biodegradable edible packaging over the past decade as the food industry attempts to find an alternative to synthetic petroleum-based polymers. Traditional petroleum-derived synthetic materials used in food packaging do not only cause the environmental pollution, but also create tremendous demands in landfills (Gontard et al., 1993; Kowalczyk and Baraniak, 2011). As such, researchers have been investigating natural biopolymer-based materials (e.g., protein-, polysaccharide- and lipid-based) which are both economically and environmentally important in terms of food packaging to develop biodegradable edible films as alternatives to synthetic petroleum-based packaging. In addition, because of the material selected for the production of biodegradable films, films may also have the added advantage of being edible and/or being used as a controlled delivery platform to improve product quality and safety (e.g., release of bioactive compounds, such as antioxidants), or to extend shelf-life (e.g., release of antimicrobial compounds) (Han and Gennadios, 2005). Biopolymer-based films are originated

from naturally renewable resources, such as proteins (e.g., gelatin, whey, soy and corn zein), polysaccharides (e.g., alginate, carrageenan, chitosan, and pectin), and lipids (e.g., beeswax). Protein- and polysaccharide-based materials tend to form films with excellent mechanical properties and gas barrier properties, but poor moisture control (Kester and Fennema, 1986; Baldwin et al., 1995; Vargas et al., 2008; Janjarasskul and Krochta, 2010). In contrast, lipid-based films tend to have excellent moisture barrier properties, but have poor mechanical and gas barrier properties (Greener and Fennema, 1989; Janjarasskul and Krochta, 2010). The formation of edible films using proteins from plant sources has been limited, but may be advantageous to those from animal sources because of their low cost, and consumer perceived safety concerns (e.g., prions) or dietary restrictions over consuming animal-derived products (Uppstrom, 1995; Gennadios, 2002). Films have been prepared previously using proteins from plant sources, such as, soy (Cho and Rhee, 2004), sunflower (Orliac et al., 2002), lentil (Bamdad et al., 2006), faba bean (Saremnezhad et al., 2011), pea (Choi and Han, 2001; Kowalczyk and Baraniak, 2011) and rapeseed (Jang et al., 2011).

Canola proteins have received some interests over the past few decades in terms of their functional attributes (Aluko and McIntosh, 2001, Yoshie-Stark et al., 2008), however despite this, protein products haven't gained any traction as a new food ingredient until recently. A few companies (e.g., BioExx Specialty Proteins (Toronto, ON, Canada) and Burcon NutraSciences (Vancouver, BC, Canada)) are looking to start moving canola protein ingredients into the marketplace. Canola (*Brassicaceae spp*.) is primarily grown for its oil content used for cooking and biodiesel purposes (Wu and Muir, 2008). Once the oil pressed, the remaining meal (high in protein and fiber) is typically used in feed applications (Canola Council of Canada, 1990; Uruakpa and Arntfield, 2005). In order to improve the viability of the canola industry, proteins are now being extracted from the meal as a value-added by-product for both food and non-food applications. Canola proteins are dominated by a salt-soluble globulin protein (cruciferin, 11S, molecular weight of 300 kDa) and a water-soluble albumin protein (napin, 2S, molecular weight of 12.5-15 kDa), constituting ~60% and ~20% of the total proteins, respectively (Wanasundara, 2011).

The formation of films generally involves some levels of protein denaturation, followed by surface dehydration either at room temperature or within a drying oven. Protein denaturation is required in order to induce unfolding to give a more open structure and to expose a greater number

of reactive sites which partake in various intermolecular interactions (e.g., disulfide bridging, hydrogen and ionic bonding, and hydrophobic interactions) to form the films (Krochta, 1997). Plasticizers, such as glycerol (or another small poly alcohol (-OH) molecule), are often added to protein-based films to overcome brittleness issues; making them more malleable by disrupting hydrogen bonds between neighboring proteins to reduce intermolecular attractive forces (Guilbert, 1986; Kester and Fennema, 1986). Glycerol also acts to create a heterogeneous distribution of junction zones within the protein matrix to make the film more flexible (Sothornvit and Krochta, 2005; Janjarasskul and Krochta, 2010).

Generally, protein-based films should be able to maintain integrity and withstand external stress from processing, handling, and storage; meaning they should have adequate mechanical strength and extensibility, to be competitive with traditional petroleum-derived packaging (Yang and Paulson, 2000b). Films should also be able to provide some moisture barrier properties. The overall aim of the present study is to investigate the effect of protein and glycerol concentration on the mechanical, optical and water vapor barrier properties of an edible film casted using canola protein isolate (CPI).

17.3 MATERIALS AND METHODS

Materials

Canola seeds (B. napus /variety VI-500) were kindly donated by Viterra (Saskatoon, SK, Canada) for this study. All chemicals used in this study were reagent grade, and purchased from Sigma-Aldrich Canada Ltd. (Oakville, ON, Canada). Milli-Q water was produced from a Millipore Milli-Q^{TM} water purification system (Millipore Corporation, Milford, MA, USA).

Preparation of a canola protein isolate

Canola seeds (stored at 4^{o}C in a sealed container prior to use) were initially screened based on size using first a #8 (2.63 mm) Tyler mesh filter (Tyler, Mentor, OH, USA) and then a #12 (1.70 mm) filter. The screened seed was frozen at -40^{o}C overnight, and then were cracked using a stone mill (Morehouse-Cowles stone mill, Chino, CA, USA). The seed coat and cotyledons were then separated using an air classifier (Agriculex Inc., Guelph, ON, Canada). The cotyledons oil was removed up to ~13% mechanically using a continuous screw expeller (Komet, Type CA59 C; IBG Monforts Oekotec GmbH & Co., Mönchengladbach, Germany), which was operated at a

speed of 59 rpm using a 3.50 mm choke. The residual oil in the meal was removed by hexane extraction (x3) at a 1:3 meal to hexane ratio for 8 h. The meal was then air-dried for an additional 8 h to allow for residual hexane to evaporate. CPI was prepared from defatted canola meal according to the method described by Folawiyo and Apenten (1996) and Klassen et al. (2011). In brief, 100 g defatted canola meal was dissolved in 1000 g 0.05 M Tris-HCl buffer containing 0.1M NaCl (pH = 7.0) at room temperature (21-23ºC) for 2 h under constant mechanical stirring at 500 rpm (IKAMAG RET-G, Janke & Kunkel GMBH & Co. KG, IKA-Labortechnik, Germany). The solution was then centrifuged (Sorvall RC Plus Superspeed Centrifuge, Thermo Fisher Scientific, Asheville NC, USA) at 3000 × *g* for 1 h to collect the supernatant. This was then filtered using # 1 Whatman filter paper (Whatman International Ltd., Maidstone, England), dialyzed (Spectro/Por tubing, 6-8 kDa cut off, Spectrum Medical Industries, Inc, USA) at 4 ºC for 72 h with frequent changes of Milli-Q water (Millipore Corporation, MA, USA) to remove the salt, and then freeze-dried (Labconco Corporation, Kansas City, Missouri 64132) at temperature difference of 35 ºC for 24 h to yield the CPI powder for later use.

The crude protein composition of CPI powder was determined using the Association of Official Analytical Chemists Method 920.87 (AOAC, 2003). The CPI produced was found to be comprised of 90.45% protein (%N x 6.25). CPI concentration used in this study reflected the protein content rather than powder weight.

Preparation of canola protein films

Film forming solutions were prepared by slowly dissolving CPI (5.0% and 7.5% w/w) in Milli-Q water under constant mechanical stirring at 500 rpm (IKAMAG RET-G, Janke & Kunkel GMBH & Co. KG, IKA-Labortechnik, Germany), adjusted to pH 3.0 using 1 M HCl, and then allowed to stir for 1 h at room temperature (21-23ºC). Glycerol was then added at 30, 35, 40, 45, and 50% (w/w of CPI) into the film forming solutions, and then allowed to stir (500 rpm) for an additional 10 min. Table 17.1 gives the contents of each film formulation tested. The film forming solutions were then degassed for 10 min within an ultrasonic bath at a frequency of 40 kHz (Branson Ultrasonic Cleaner, Model 2510R-DTH, USA) at room temperature (21-23ºC). Afterwards, the film forming solutions were heated to 50 ºC under stirring at 500 rpm for 5 min, and then casted onto a polytetrafluoroethylene (PTFE) mould (10 cm length; 10 cm width; 0.10 mm depth). Excess film forming solutions were removed using a straight edge. CPI films were

formed after drying overnight at room temperature (21-23^{o}C). The thickness of film was controlled by the standard depth of the PTFE mould, the time of drying process, and the amount of film forming solution (~15 mL) poured on the mould. Films were then removed from the mould, and conditioned to 54% relative humidity (using a saturated magnesium nitrate solution) within a desiccator at room temperature (21-23^{o}C) for 2 d. All films were prepared in triplicate. The addition of glycerol was decided based on the preparation of pure CPI films. Because there were intra- and intermolecular interactions between side chains of partially denatured CPI, molecular mobility in the film structure was restricted which lead to very brittle pure CPI film. Therefore, glycerol was added to decrease the interactions between protein chains and improve the malleability of CPI films (Zhang et al., 2001; Kokoszka et al., 2010). Glycerol levels within the prepared films were restricted to the range between 30 and 50%, since at levels <30%, films became too brittle and experience cracking during the drying process, whereas at levels >50%, films were too soft and sticky to be removed from the moulds after drying (data not shown). CPI levels within the prepared films were restricted between 5.0% and 7.5%, since at levels <5.0%, films were too thin to be removed from the mould as a full piece of film, whereas at levels >7.5%, films with 50% glycerol experienced cracking during the drying process (data not shown).

Table 17.1 Composition of CPI film-forming solutions prior to film casting.

Film	CPI (g)	CPI (% db)	Gly (g)	Gly (%/CPI)	Water (g)	Thickness (mm)
5.0% CPI, 30% Gly	5	77	1.5	30	93.50	0.06
5.0% CPI, 35% Gly	5	74	1.75	35	93.25	0.07
5.0% CPI, 40% Gly	5	71	2	40	93.00	0.07
5.0% CPI, 45% Gly	5	69	2.25	45	92.75	0.07
5.0% CPI, 50% Gly	5	67	2.5	50	92.50	0.07
7.5% CPI, 30% Gly	7.5	77	2.25	30	90.25	0.12
7.5% CPI, 35% Gly	7.5	74	2.63	35	89.87	0.10
7.5% CPI, 40% Gly	7.5	71	3	40	89.50	0.13
7.5% CPI, 45% Gly	7.5	69	3.38	45	89.12	0.13
7.5% CPI, 50% Gly	7.5	67	3.75	50	88.75	0.13

Film thickness

Film thickness was measured by using a digital micrometer (Model 62379-531, Control Company, U.S.A.) having a precision of 0.01 mm. Ten thickness measurements were taken on each triplicate film prepared.

Mechanical properties

Puncture strength and deformation

Both puncture strength (PS, N) and deformation (PD, mm) of the film were determined using a Texture Analyzer (Texture Technologies Corp., New York) as described by Gontard and co-workers (1992). Each film was mounted on a 65.6 mm diameter puncture mould and placed under a smooth edged cylindrical probe (4 mm diameter), the probe then moved through the film at a cross-head speed of 1 mm/s. The force-deformation curve data were collected by a microcomputer. PS was the maximum force (N) which was loaded on the film to puncture the specimen. PD was expressed as the length changes at the rupture point of film.

Tensile strength, tensile elongation and elastic modulus

Tensile strength (TS, MPa), tensile elongation (TE, %), and elastic modulus (E, Pa) of the film were determined using a Texture Analyzer with a load cell of 25 kg (Texture Technologies Corp., New York) on film strips (8 × 2.5 cm) which were pre-conditioned at 54% relative humidity under room temperature based on the ASTM D882-91 (1991). The film strips were placed between grips, and set up the initial grip separation to 40 mm and cross-head speed to 5 mm/s. The stress-strain curve data were collected by a microcomputer. TS was calculated by dividing the maximum load of the film strip by the area of cross-section of that strip (width of the strip (2.5 cm) × thickness of the strip); TE was calculated as a percentage of the length change of the film strip at the breakpoint of the film; E was expressed as the slope of the trend line on the stress-strain curve. Three measurements were taken on each triplicate film prepared.

Opacity

Film opacity was determined by using a spectrophotometer (Genesys 10uv, Thermo Fisher Scientific) as described by Gontard and co-workers (1994). The pre-conditioned films were cut into small strips (4.5 x 0.9 cm) and placed on the inside wall of the plastic cuvette (1 cm path

length). The absorption spectrum will be measured over a wavelength range of 400–800 nm. The area under the absorbance-wavelength curve was determined as the film opacity with the unit of A.nm. All measurements were performed in triplicate, for each type of films.

Water vapor permeability

Water vapor permeability (WVP) of the CPI films was determined using the "cup method" modified from the gravimetric technique of ASTM E96-93 (1993). For this study, PVC (polyvinyl chloride) cups were prepared to the following dimensions: outer cup height (2.65 cm), outer cup radius (2.50 cm), inner cup height (2.00 cm) and inner cup radius (2.25 cm). Films were placed on the top of the cup, then held in place by a lid (with an open centre of same dimensions as the inner cup radius) tightened by six screws. The open surface area of the film was 15.90 cm^2. Within the cup, 10 mL of saturated $Mg(NO_3)_2$ solution (54% relative humidity) was added. The entire cup (with $Mg(NO_3)_2$ solution plus film) was then placed within a desiccator containing $CaSO_4$ desiccant (0% relative humidity) at room temperature. The water transferred through the film was determined from the weight loss of the system (cup plus $Mg(NO_3)_2$ solution) over a 5 h duration at 30 min intervals, and weigh to the nearest 0.1 mg using an analytical balance (CPA224S, Sartorius, U.S.A.). Preliminary experiments (not shown) showed that a steady state of weight loss was reached after 5 h. WVP of the film was calculated using the WVP Correction Method which was described as the flowing formulae (Gennadios et al., 1994).

$$WVP = (WVTR_m \times L) / \Delta P \quad \text{(eq. 17.1)}$$

$$\Delta P = (P_{w1} - P_{w2}) \quad \text{(eq. 17.2)}$$

$$P_{w1} = P_T - (P_T - P_{w0}) \exp(N_w h/cD) \quad \text{(eq. 17.3)}$$

$$N_w = (6.43 \times 10^{-11}) \times WVTR_m \quad \text{(eq. 17.4)}$$

where $WVTR_m$ (water vapor transmission rate, g/m^2s) was calculated by dividing the slope by the open area of the cup (15.90 cm^2); L was the thickness of the film (mm), and ΔP was the real water vapor partial pressure difference across the film (kPa). P_{w1} was water vapor partial pressure at the film inner surface (kPa), P_{w2} was the water vapor partial pressure at film outer surface (kPa). Since the cup was placed in the desiccator containing $CaSO_4$ desiccant (0% relative humidity), and P_{w2} was 0 kPa. P_T was the total atmospheric pressure (101.3 kPa); P_{w0} was the partial pressure of water

vapor at the air of the surface of the $Mg(NO_3)_2$ solution which was 1.34267 kPa; N_w (g.mol/s.cm^2) was the measured value of $WVTR_m$; h was the stagnant air gap height between the film and the surface of $Mg(NO_3)_2$ solution; c was the total molar concentration of the air and water vapor (4.15×10^{-5} g.mol/cm^3); D was the diffusivity of water vapor through the air at 25 ºC (0.25375 cm^2/s). All measurements were performed on triplicate films.

Statistical analyses

All experiments were performed on triplicate films and reported as the mean ± one standard deviation. A two-way analysis of variance (ANOVA) was used to measure statistical differences in thickness, mechanical properties (PS, PD, TS, TE and E), and opacity, and WVP of CPI films among the various treatments (i.e., effect of glycerol and CPI concentrations).

17.4 RESULTS AND DISCUSSION

Mechanical properties

Film strength

The effect of glycerol and protein concentrations on strength (PS, TS and E) of CPI films were examined and given in Figures 17.1A, C and E. An analysis of variance of PS data indicated that glycerol ($p<0.001$) and protein concentration ($p<0.001$), along with their interaction ($p<0.01$) were all significant. Overall, PS data was found to be higher at the 7.5% CPI films than the 5.0% CPI films, and declined as glycerol level increased from 30% to 50% (Figure 17.1A). However, the decline occurred at different rates depending on the protein concentration. This rate was slightly less at the 5.0% CPI films where PS value decreased from ~2.29 N to ~0.89 N as the glycerol content increased from 30 to 50%, respectively (Figure 17.1A). In contrast, PS value declined from ~3.87 N to ~2.05 N as glycerol levels increased at the 7.5% CPI films (Figure 17.1A). An analysis of variance on TS data indicated that both glycerol ($p<0.001$) and protein ($p<0.001$) concentration were highly significant, however the interaction term was not significant ($p>0.05$). Overall, TS decreased with increasing glycerol content where TS declined from ~4.31 MPa for films with 30% glycerol to ~1.19 MPa with 50% glycerol present in 5.0% CPI films (Figure 17.1C). TS also was found to increase with increasing protein

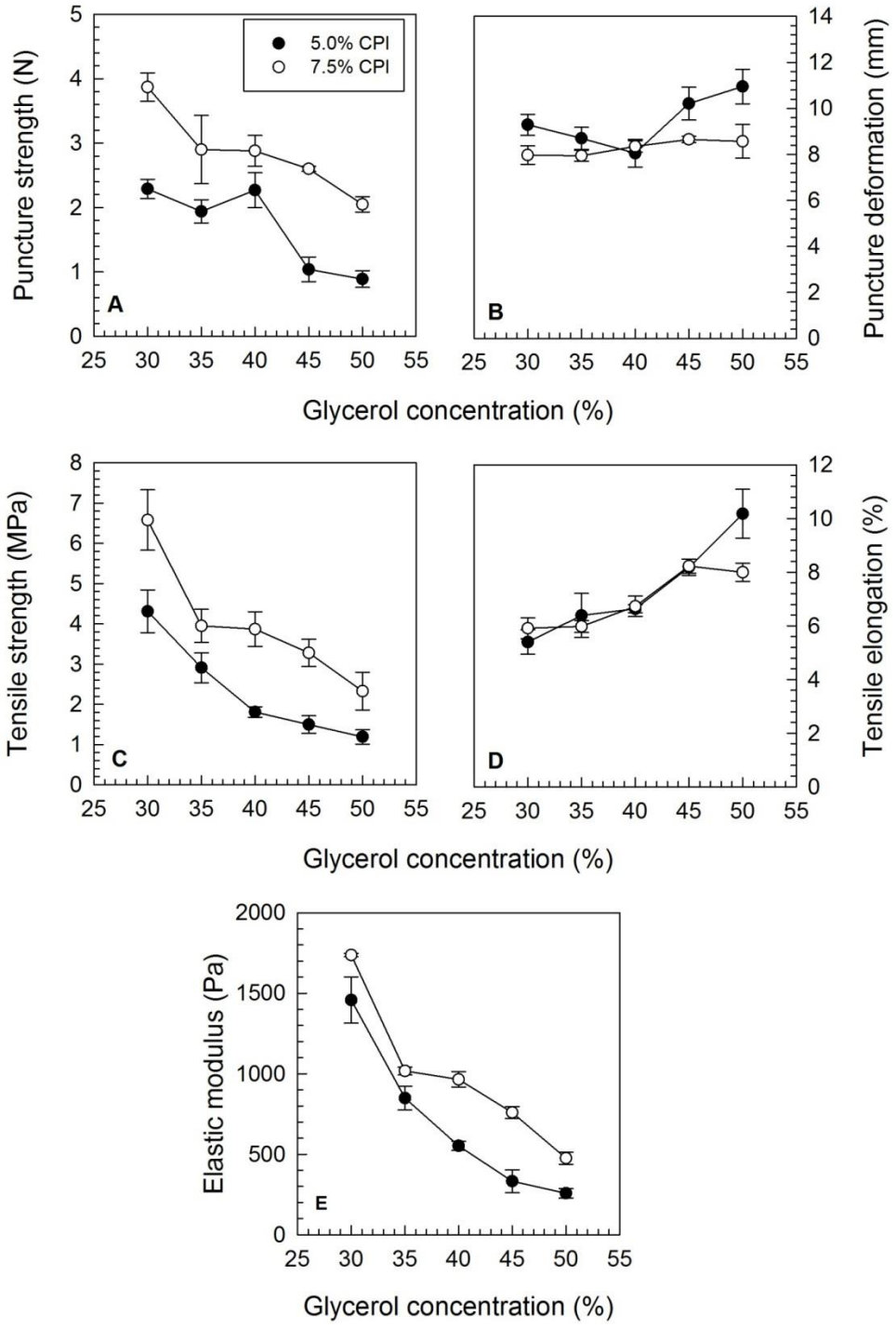

Figure 17.1. Puncture strength (A) and deformation (B), tensile strength (C) and elongation (D), and elastic modulus (E) of 5.0% and 7.5 % (w/w) canola protein isolate (CPI) films as a function of glycerol concentration. Data represent the mean ± one standard deviation (n = 3).

concentration from ~1.19 MPa to ~2.33 MPa when CPI concentration increased from 5.0% to 7.5% in films with 50% glycerol, respectively (Figure 17.1C). The lack of significant interaction suggested that the decline in TS with increasing glycerol content followed a similar trend at both protein concentrations. An analysis of variance of E data indicated that glycerol ($p<0.001$) and protein concentration ($p<0.001$), along with their interaction ($p<0.01$) were all significant. Overall, E was greater for the 7.5% CPI films than at the 5.0% CPI films, and declined with increasing glycerol concentration. At the 5% CPI level, E data declined from ~1,458 Pa at 30% glycerol to ~258 Pa at 50% glycerol in a curvilinear decline with reduced rates between 40 and 50% glycerol (Figure 17.1E). In contrast, at the 7.5% CPI level, the decline was more consistent from ~1,737 Pa at 30% glycerol to ~476 Pa at 50% glycerol (Figure 17.1E).

Overall, the strength of CPI films was thought to increase due to a rise in intermolecular CPI interactions within the film matrix as protein levels increased. Since CPI can contribute to the noncovalent interactions (e.g., hydrogen bonding, hydrophobic interactions), the film structure was strengthened by the higher CPI concentration (Cao et al., 2007). Furthermore, heating to 50^{o}C under acidic conditions (pH 3.0) was proposed to induce some unfolding and then subsequent hydrophobic interactions between CPI aggregates and sulfhydryl exchange reactions between cysteine moieties (Folawiyo and Apenten, 1996). As the film forming solution cooled, the CPI film was proposed to strengthen due to an increase in hydrogen bonding within the system (Fukshum and Vanburen, 1970). Film strength in the present study was also attributed to differences in film thickness, because film thickness greatly affects the film structure through the effect on the drying kinetics of the film forming solution. In fact, the thickness mainly depends on the solvent evaporation rate and the protein denaturation to affect cross links in film network organization (Debeaufort and Voilley, 1995). An analysis of variance of film thickness indicated that only protein concentration ($p<0.001$) was significant, and glycerol and their interaction ($p>0.05$) were not. Overall, films were ~0.12 mm thick at the 7.5% CPI level and ~0.07 mm thick at the 5.0% CPI level, regardless of the glycerol content (Table 17.1). Jang et al. (2011) also reported a similar rise in thickness of rapeseed protein films from ~47.4 μm to ~71.6 μm as protein levels increased from 2% to 5%, respectively. On the whey protein isolate-base films, although the increased glycerol concentration slightly increased film thickness, it didn't significantly affect the film thickness (Gounga et al., 2007). Furthermore, 7.5% CPI films had higher CPI concentration by area unit, which could enhance the intermolecular interactions and lead to the

formation of film matrix with higher cohesion (Cuq et al., 1996). This was demonstrated by Sobral (1999) on gelatin based films, in which PS value of films increased from 2.5 N to 30 N as the film thickness increased from 0.02 to 0.14 mm.

The strength of films reported in the present study using CPI was comparable to other plant protein films reported in literature (Table 17.2). Rhim et al. (1998) reported a soy protein film with 50% glycerol prepared at a 5.0% protein concentration had TS of ~6.34 MPa. Prepared under the same set of conditions, except at a lower soy protein concentration, Cho and Rhee (2004) reported 4.0% soy protein film to have TS of ~3.20 MPa. This trend in TS data with decreasing protein concentration was similar to that of the present study. The increased film strength at higher protein level is presumed to reflect greater biopolymer ordering within the film. Puncture strength values for CPI films with 50% glycerol (~0.9 or ~2.0 N for the 5.0 and 7.5% CPI level, respectively) also were within the similar range with 5.0% lentil protein-based films prepared with 50% glycerol (~1.6 N) (Bamdad et al., 2006) and the plastic sandwich wrap (~3.2 N) (Table 17.2). Liu and co-workers (2004) reported greater denaturation in protein-based films results in a more compact 3-diminsional microstructure with greater strength than those with less. According to Folawiyo and Apenten (1996), the film forming solution (5% CPI/50% Gly) were heated to 50ºC under acid condition (pH 3.0) for 5 min presumably allowing for partial denaturation of CPI; to give films with TS of ~1.19 MPa. In contrast, soy protein-based films (~6.34 MPa) (Rhim et al., 1998) and lentil protein-based films (~4.2 MPa) (Bamdad et al., 2006) were prepared through heating film forming solutions to 70 °C for 20 min (at comparable protein (5%) and glycerol (50%) concentrations) gave films with higher TS values than CPI films (Table 17.2), because of greater protein denaturation within the film matrix. Theoretically, protein denaturation can increase intra- and intermolecular cross links to tighten the film structure, so, further greatly affects the properties of edible films through the protein-protein interactions, and polymer morphology (Choi and Han, 2002). Choi and Han (2002) indicated that although 5 min heat treatment at 90 ºC was long enough to produce strong pea protein isolate (PPI) films, PPI films produced from the 20 min heat treatment were much stronger, due to the greater molecular rearrangement occurred during heating process. Although mechanical strength of 7.5% CPI films (PS of ~2.05 N) was considerably lower than the plastic sandwich wrap (PS of ~3.18 N) (Table 17.2), CPI films still could be considered as an acceptable packaging to replace

Table 17.2 Mechanical properties and water vapor permeability of various plant protein films found in the literature.

Film type	Formulation	Processing	TS (MPa)	TE (%)	PS (N)	WVP ($g.mm/m^2.h.kPa$)	Thickness (mm)
Soy protein[a]	5% SPI, 50% Gly	Film forming sol'n (70°C/20 min/pH 10.0); Setting conditions (25°C/48 h/50% RH)	6.34 ± 0.02	65.90 ± 25.30	-	5.40 ± 0.07	0.08±2.50
Lentil protein[b]	5% LPC, 50% Gly	Film forming sol'n (70°C/20 min/pH 11.0); Setting conditions (25°C/48 h/50% RH)	4.24 ± 1.26	58.22 ± 12.88	1.55 ± 0.20	0.10 ± 0.00	0.15±0.00
Pea protein[c]	10% PPI, 50% Gly	Film forming sol'n (90°C/25 min)	0.69 ± 0.07	92.00 ± 21.50	-	7.42 ± 0.69	5.83±0.85
Sunflower protein[d]	10% ISFP, 50% Gly	Film forming sol'n (155°C/2 min); Setting conditions (25°C/48 h/60% RH)	2.80	37.60	-	-	-
Canola protein[e]	5% CPI, 50% Gly	Film forming sol'n (50°C/5 min/pH 3.0); Setting conditions (21-23°C/48 h/54% RH)	1.19 ± 0.18	10.18 ± 0.91	0.89 ± 0.13	1.20 ± 0.17	0.07±0.01
Canola protein[e]	7.5% CPI, 50% Gly	Film forming sol'n (50°C/5 min/pH 3.0); Setting conditions (21-23°C/48 h/54% RH)	2.33 ± 0.47	8.00 ± 0.34	2.05 ± 0.12	1.50 ± 0.05	0.12±0.01
Plastic sandwich wrap	-	-	-	-	3.18 ± 0.12	0.03 ± 0.00	-

References: [a]Rhim et al. (1998), [b]Bamdad et al. (2006), [c]Choi and Han (2001), [d]Orliac et al. (2002)

Abbreviations: soy protein isolate (SPI); lentil protein concentrate (LPC); pea protein isolate (PPI); sunflower protein isolate (ISFP); glycerol (Gly); tensile strength (TS) and elongation (TE); puncture strength (PS); water vapor permeability (WVP); and relative humidity (RH)

synthetic petroleum-based packaging under moderate mechanical applications, such as separated packaging in a large box.

The decline in film strength in the present study with increasing glycerol concentration is presumed due to its plasticizing effect. Glycerol disrupts the order of CPI-CPI aggregates within the film matrix, results in a more heterogeneous spatial distribution of junction zones to increase free volume within the film matrix to improve the polymeric chains mobility (Donhowe and Fennema, 1992; Sothornvit and Krochta, 2005; Janjarasskul and Krochta, 2010). Glycerol also displaces some stabilizing hydrogen bonding between water molecules and the CPI, by interacting themselves (-OH groups) with the CPI through hydrogen bonding (Gontard et al., 1993). Some researchers reported that glycerol decreased hydrogen bonding to further increase free volume between protein molecules in pea protein and peanut protein films (Choi and Han, 2001; Liu et al., 2004), thus promoted an increase of deformation capacity of film structure to reduce the film mechanical resistance (Donhowe and Fennema, 1992). As a consequence, films were weaker and more flexible as levels of glycerol increased. Slight differences seen in the rate of decline in PS and E values with increasing glycerol concentration between both CPI levels is thought to be associated with the distribution of glycerol molecules. It is proposed that 7.5% CPI film has a more tightly ordered matrix resulting in a more heterogeneous distribution of glycerol molecules. In contrast, at the 5.0% CPI level, the less ordered film matrix allowed CPI to re-orient to accommodate the presence of glycerol. It could be summarized that glycerol has less ability to restrict the interaction between polymer chains under bulky protein content in the film matrix. Changes to molecular dynamics of CPI as a function of CPI and glycerol concentrations within the film matrix were also reflective in the PD and TE (Figures 17.1B and D) data, where slight differences in trends were seen, despite the overall rise in film flexibility with increasing glycerol content. Choi and Han (2001) reported a similar trend for TS data as a function of glycerol concentration, where TS decreased from ~4.9 MPa to ~0.7 MPa as the glycerol concentration increased from 20% to 50%.

Film deformability

The effect of glycerol and protein concentration on flexibility (PD and TE) of CPI films were examined and given in Figures 17.1B and D. An analysis of variance of PD data indicated that both glycerol ($p<0.001$) and protein ($p<0.001$) concentrations, and their interaction ($p<0.01$) to be significant. Overall, PD decreased from ~10.95 mm to ~8.57 mm as the protein concentration increased from 5.0% to 7.5% in films with 50% glycerol, respectively (Figure 17.1B). However the effect of increasing glycerol content was different depending on the

protein concentration. At the 5.0% CPI level, PD initially declined from ~9.29 mm to ~8.05 mm between 30% and 40% glycerol, and then increased from ~8.05 mm to ~10.95 mm between 40% and 50% glycerol level (Figure 17.1B). In contrast, the effect of glycerol at the 7.5% CPI level was less significant, increasing in a slow linear manner from ~7.97 mm to ~8.57 mm between 30% and 50% glycerol, respectively (Figure 17.1B). An analysis of variance of TE data found that both glycerol ($p<0.001$) and protein concentration ($p<0.05$), along with their interaction ($p<0.001$) were significant. Overall, TE was slightly greater in 5.0% CPI films than in 7.5% CPI films, and increased as the glycerol level increased. However the rate of increase was different depending on the protein concentration. For instance, at the 5.0% CPI level, TE data increased linearly from ~5.4% at 30% glycerol to ~10.2% at 50% glycerol (Figure 17.1D). In contrast, at the 7.5% CPI level, TE increased slowly between 30% and 40% glycerol from ~5.9% to ~6.7%, respectively, then jumped to ~8.2% at the 45% level before reaching a plateau (Figure 17.1D).

Comparison of TE data for CPI films with those reported for other plant protein-based films indicated significantly lower values, probably due to the low pH (pH 3.0) used to prepare the CPI film forming solution. Gennadios and co-workers (1993) found that soy protein films could be formed at both alkaline (pH 7.0 to 11.0) and acidic conditions (pH 1.0 to 3.0), where significantly higher TE values were reported under the former conditions (132.6-187.3%) than the latter (34.2-35.6%). The authors presumed that this was caused by poor protein dispersion nearer to its isoelectric point (pH 4.5). Moreover, the heating time could be an additional reason, since the hydroxyl groups of glycerol can replace protein-protein interactions in denatured protein by developing protein-glycerol hydrogen bonds to increase the chain mobility during the film formation, and finally leads to the increase of flexibility of films (Gontard et al., 1993). However, in the present study, CPI film forming solution was only heated for 5 min which was much shorter than 20 min for other films. This was demonstrated by Choi and Han (2002) on PPI films, in which the films produced from 20 min heat treatment had 2.0 to 3.5 times higher TE value than films produced from 5 min heat treatment.

Film opacity

Transparency (low opacity) of the prepared film is an important factor to consider in terms of designing food packages (depending on the product). In the present study, the color of films was slightly yellowish, and 7.5% CPI films were darker and more yellow than 5.0% CPI films. Film opacity of CPI films as a function of protein and glycerol concentrations was shown in Figure 17.2. An analysis of variance indicated that opacity of the films was affected

by both glycerol ($p<0.001$) and protein ($p<0.001$) concentration, along with their interaction ($p<0.05$). Overall, opacity of the film with 50% glycerol prepared at the 7.5% CPI level was greater than at the 5.0% CPI level, where values decreased from ~83.5 A.nm to ~76.4 A.nm, respectively (Figure 17.2). However, the rate of decline in opacity differed depending on the glycerol concentration. For instance, at the 5.0% CPI level, opacity value declined linearly from ~96.0 A.nm to ~76.4 A.nm as glycerol level increased from 30% to 50%, respectively (Figure 17.2). In contrast, at the 7.5% CPI level opacity value was relatively constant between 30% and 40% glycerol contents, with opacity values ranging between ~94.8 and ~96.6 A.nm, respectively, then declined sharply to ~84.5 A.nm at the 45% glycerol level where it remained constant (Figure 17.2). Gontard et al. (1994) reported that opacity value of films declined with increasing glycerol content, due to the transparent nature and increased dispersion of glycerol within the film matrix. Differences in trends between the two protein concentrations in the present study are thought to reflect the distribution of glycerol molecules within the film, where it is proposed that at the higher CPI level, a more heterogeneous distribution of glycerol occurs. The higher opacity value is presumed to be associated with the higher total solid contents in the 7.5% CPI film, the more tightly packed CPI network and the greater thickness relative to the 5.0% CPI film.

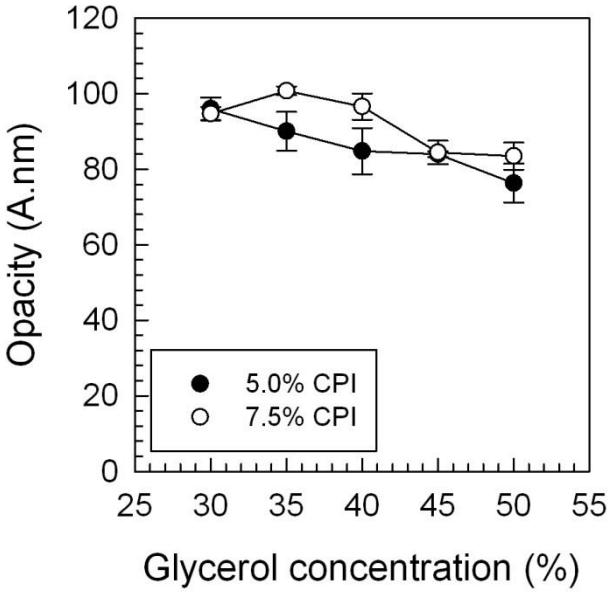

Figure 17.2. Opacity of 5.0% and 7.5% (w/w) canola protein isolate (CPI) films as a function of glycerol concentration. Data represent the mean ± one standard deviation (n = 3).

Water vapor barrier property

Water vapor permeability (WVP) of CPI films as a function of glycerol and protein concentrations was investigated, and shown in Figure 17.3. An analysis of variance of WVP data found that both glycerol ($p<0.001$) and protein ($p<0.001$) concentrations were significant, however their interaction ($p>0.05$) was not significant. Overall, WVP was found to increase from ~1.20 to ~1.50 g·mm/m^2·h·kPa as CPI concentration was raised from 5.0% to 7.5% in films with 50% glycerol, respectively (Figure 17.3). Additionally, WVP also increased from ~0.94 to ~1.50 g.mm/m^2.h.Pa as glycerol concentrations increased from 30% to 50% in a slightly curvilinear trend in 7.5% CPI films (Figure 17.3). Choi and Han (2001) also reported similar results on 10% pea protein films where the WVP increased from ~4.30 to ~7.42 g·mm/m^2·h·kPa as the glycerol concentration increased from 20% to 50%. The rise in WVP with increasing glycerol concentration is proposed to reflect an increase in inter-chain spacing and biopolymer mobility within the film matrix, and a decrease in internal hydrogen bonding within the film structure, leading to increased diffusion of water molecules (Gontard et al., 1993; Yang and Paulson, 2000a; Gounga et al., 2007). The rise in WVP with glycerol content may also be related to the rise in water absorption caused by the addition of hydrophilic material

in the films; enabling greater water diffusion through the matrix (Kamper and Fennema, 1984). Karbowiak and co-workers (2006) found that the moisture content of biopolymer films which mainly controlled the water molecular mobility, is greatly affected by the plasticizer. Therefore, since the plasticizing action of glycerol is favorable to adsorption and absorption of water molecules in the film structure (Coupland et al., 2000); the increased glycerol content can substantially increase WVP of films.

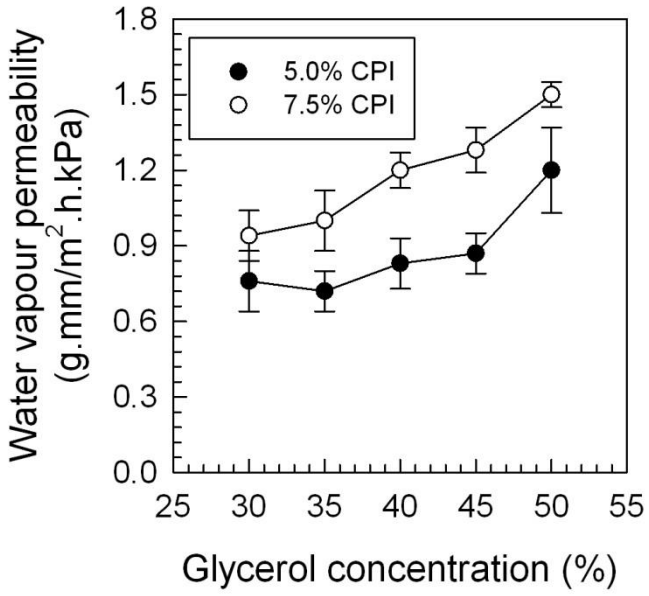

Figure 17.3 Water vapor permeability (WVP) of 5.0% and 7.5% (w/w) canola protein isolate (CPI) films as a function of glycerol concentration. Data represent the mean ± one standard deviation (n=3).

WVP of CPI films was much lower in comparison with other plant proteins films, but it was higher than WVP of plastic sandwich wrap (Table 17.2). This could be caused by a number of factors, such as film thickness, relative humidity (RH) for WVP measurement, and protein hydrophobicity. McHugh et al. (1993) stated that the thicker film had higher resistance to mass transfer across it, so, water vapor partial pressure at the film inner surface (P_{w1}) was increased to illustrate the much higher WVP of soy protein film and pea protein film than CPI films (Table 17.2). In the present study, film solubility was also tested during preliminary swelling experiments (not shown) to find complete dissolution of films almost immediately. Therefore, CPI films had much higher WVP than plastic sandwich wrap (Table 17.2). Do to the high solubility, CPI films could be appropriate for the application as hot water soluble

pouches (Bamdad et al., 2006). In Table 17.2, the inner cup RH for WVP measurement on soy protein, lentil protein, and pea protein films was ~75% (Rhim et al., 1998; Choi and Han, 2001; Bamdad, et al., 2006), however, WVP of CPI films was measured when the inner cup RH was 54%, so, P_{w1} for CPI films was lower than P_{w1} for soy protein, lentil protein, and pea protein films, which means soy protein, lentil protein, and pea protein films that are hydrophilic films exhibit higher WVP values, due to the water-film interaction (Banker et al., 1966). This theory was also demonstrated by Kokoszka and co-workers (2010) in soy protein-based films where the WVP of films at ~70% RH was much higher than the films at ~23% RH. In Table 17.2, it was found that CPI films had much lower WVP than soy protein films possibly as the result of greater hydrophobicity of the soy proteins than canola (Chabanon et al., 2007; Wang et al., 2008).

In the present study, WVP was also found to be greater for the films with 7.5% CPI content than with 5.0% CPI content. The trend is somewhat counterintuitive, more aggregated film structure with a denser protein matrix and larger pore size supposed to be formed with higher protein concentration (Gounga et al., 2007). Moreover, it was hypothesized that the higher amount of CPI allowed for a greater amount of CPI-water interactions than the lower amount of CPI, allowing for greater water mobility through the film matrix. It was demonstrated that WVP in rapeseed films increased from ~0.60 to ~0.88 $g \cdot mm/m^2 \cdot h \cdot kPa$ with the increase of rapeseed protein concentration from 2% to 5% (Jang, et al., 2011). Film thickness was also greater at the 7.5% CPI level than the 5.0% CPI level, suggesting that water molecules would take a longer pathway to go through the films with higher amount of CPI, so, more hydrophilic film (7.5% CPI film) would be able to keep more water molecules within the film matrix. Since the time period (5 h) for WVP measurement on CPI films was same in this study, 7.5% CPI films had higher WVP values than 5.0% CPI films. In addition, McHugh et al. (1993) observed that films with greater thickness had increased resistance to moisture transfer, so, a stagnant air layer formed on the inner film surface to characterize as a higher water vapor partial pressure for WVP measurement.

17.5 SUMMARY

The present study investigated the effect of glycerol and protein concentrations on the mechanical, optical and water vapor barrier properties of CPI films. In general, as the glycerol concentration was increased, films became weaker, more flexible and clearer. In contrast, as CPI concentration was raised, films became stronger, less flexible and more opaque. Water

vapor barrier property also became poorer as both glycerol and CPI concentrations increased. This study shows the potential of using CPI in the development of edible films/packaging.

-Chapter 18-

Effect of plasticizer-type and genipin on the mechanical, optical, and water vapor barrier properties of canola protein isolate-based edible films[8]

Chang Chang and Michael T. Nickerson

Department of Food and Bioproduct Sciences, University of Saskatchewan
51 Campus Drive, Saskatoon SK, Canada S7N 5A8

[8]European Food Research International, 238, 35-46 (2014)

18.1 ABSTRACT

The mechanical properties, opacity, and water vapor permeability of 5.0% (w/w) canola protein isolate (CPI) films were investigated in the presence and absence of 1% (w/w) genipin, and as a function of plasticizer-type (50% (w/w); glycerol, sorbitol, and polyethylene glycol 400). Findings indicated that tensile strength (TS), puncture strength (PS) and elastic modulus (E) values for CPI films prepared with sorbitol were the highest, followed by PEG-400 and then glycerol, whereas tensile elongation (TE) and puncture deformation (PD) values were greater for films prepared with glycerol, followed by PEG-400 and then sorbitol. In all cases, films prepared with genipin were stronger (greater TS, PS and E) and less flexible (lower TE and PD) than un-crosslinked films. Films also showed greater water vapor permeability (WVP) when prepared with glycerol, followed by PEG-400 and then sorbitol, however no differences were observed in the presence and absence of genipin.

18.2 INTRODUCTION

Edible films developed from biodegradable materials (e.g., proteins, polysaccharides, and lipids) have attracted much attention by the food industry, as consumers' demands for alternatives to traditional petroleum-based packaging which negatively impacts the environment and landfills (Gontard et al., 1993; Kowalczyk and Baraniak, 2011). Biodegradable edible films prepared from proteins (e.g., gelatin, wheat gluten, and peanut protein), polysaccharides (e.g., chitosan, pectin, and starch), and lipids (e.g., beeswax and resin) provide mechanical and barrier properties, as well as can be formulated to act as a delivery system for bioactive (e.g., sodium alginate-gellan gum contaning N-acetylcysteine and glutathione (Rojas-Grau et al., 2007)) or antimicrobial compounds (e.g., hydroxyl propyl methyl cellulose-based film containing nisin (Sebti and Coma, 2002)) to maintain product quality and extend shelf-life (Han amd Gennadios, 2005). Typically, proteins- and polysaccharides-based films tend to have good mechanical and gas barrier properties, but poor water vapor barrier property due to their hydrophilic nature (Janjarasskul and Krochta, 2010). In contrast, lipids-based films are poor at controlling gas diffusion and withstanding mechanical stresses, but good at controlling moisture migration due to their hydrophobic nature (Janjarasskul and Krochta, 2010). Because of perceived safety concerns (e.g., prion disease) and some dietary restrictions associated with using animal-derived proteins to prepare the films, plant proteins, such those from soy (Tang et al., 2005; Pruneda et al., 2008); sunflower (Orliac et al., 2003); faba bean (Saremnezhad et al., 2011); and rapeseed (Jang et al., 2011) represent an excellent alternative.

Canola (*Brassicaceae spp.*) is primarily grown today for its polyunsaturated fatty acid rich oil, used for cooking and biodiesel purposes (Wu and Muir, 2008). A by-product arising from the oil industry is a protein- and fiber-rich canola meal that is underutilized in the marketplace, sold traditionally for use as a livestock feed. The protein content within the meal can be up to 50% on a dry weight basis and has a well-balanced amino acid profile (Uppstrom, 1995). The majority of these proteins are a salt-soluble globulin protein, known as cruciferin (11S; molecular weight ~300 kDa; ~60% of the total proteins) and a water-soluble albumin protein, known as napin (2S; molecular weight ~12.5-15 kDa; ~20% of the total proteins) (Wanasundara, 2011). Although the functional attributes of canola protein concentrates or isolates produced from the meal, such as protein solubility, emulsion stability, and foaming capacity, have been investigated (Aluko and McIntosh, 2001), their applications for food industry, such as for packaging, still need to be explored.

In an effort to tailor the mechanical and barrier properties of protein-based films, various factors have been previously explored including protein concentration (Jang et al., 2011), plasticizer concentration/type (Gennadios et al., 1996; Cao et al., 2009; Mikkonen et al., 2009), film forming conditions (i.e., pH, temperature and the presence of salts) (Kowalczyk and Baraniak, 2011; Saremnezhad et al., 2011); and the addition of cross-linking agents (Tang et al., 2005; Tang and Jiang, 2007; Gonzalez et al., 2011). To improve the flexibility and to overcome brittleness of films, plasticizers (e.g., glycerol, sorbitol, and polyethylene glycol 400) are typically added to soften the structure (Gennadios et al., 1996; Cao et al., 2009; Mikkonen et al., 2009). The effectiveness is dependent on the composition, size, and shape of plasticizer used (Sothornvit and Krochta, 2001).

Moreover, the formation of cross-links by the addition of enzymatic or chemical fixatives has also been shown to influence film properties. For instance, genipin (GP), a natural chemical cross-linking agent extracted from *Gardenia Jasminoides Ellis* fruit has showed some promise, as it can result in cross-links of similar strengths as glutaraldehyde but is 10,000 times less cytotoxic (Song and Zhang, 2009). GP reacts with the primary amines (mainly lysine) within the protein for the formation of both inter- and intramolecular cross-links. Once reacted, a dark blue pigment develops (Touyama et al., 1994). Recently, genipin cross-linking was used to fix films derived from chitosan (Jin et al., 2004), silk fibroin and sericin (Motta et al., 2011), and soy protein (Gonzalez et al., 2011). Transglutaminase, a natural enzymatic cross-linking agent, has been widely used to improve the properties of edible films, such as soy protein-based films (Tang et al., 2005; Tang and Jiang, 2007), and wheat gluten-based film (Tang and Jiang, 2007).

The overall goal of the present research is to investigate the effect of plasticizer-type and genipin on the mechanical, optical, and water vapor barrier properties of canola protein isolates (CPI) films. Enhanced utilization of canola proteins may increase their integration into the vegetable protein ingredient market.

18.3 MATERIALS AND METHODS

Materials

Canola seeds (B. napus /variety VI-500) were kindly donated by Viterra (Saskatoon, SK, Canada) for this study. All chemicals used in this study were reagent grade, and purchased from Sigma-Aldrich Canada Ltd. (Oakville, ON, Canada) with the exception of genipin (GP) (CAS Number: 6902-77-8, Challenge Bioproducts Co., Ltd, Taiwan). Milli-Q water was produced from a Millipore Milli-Q^{TM} water purification system (Millipore Corporation, Milford, MA, USA).

Preparation of canola protein isolate

Canola seeds (stored at 4^{o}C in a sealed container prior to use) were initially screened based on size using first a #8 (2.63 mm) Tyler mesh filter (Tyler, Mentor, OH, USA) and then a #12 (1.7 mm). The screened seed was frozen at -40^{o}C overnight, and then were cracked using a stone mill (Morehouse-Cowles stone mill, Chino, CA, USA). The seed coat and cotyledons were then separated using an air classifier (Agriculex Inc., Guelph, ON, Canada). The cotyledons oil was removed up to ~13% mechanically using a continuous screw expeller (Komet, Type CA59 C; IBG Monforts Oekotec GmbH & Co., Mönchengladbach, Germany), which was operated at a speed of 59 rpm using a 3.5-mm choke. The residual oil in the meal was removed by hexane extraction (x3) at a 1:3 meal to hexane ratio for 8 h. The meal was then air-dried for an additional 8 h to allow for residual hexane to evaporate. CPI was prepared from defatted canola meal according to the method described by Folawiyo and Apenten (1996) and, Klassen et al. (2011). In brief, 100 g defatted canola meal was dissolved in 1000 g 0.05 M Tris-HCl buffer containing 0.1M NaCl (pH = 7.0) at room temperature (21-23^{o}C) for 2 h under constant mechanical stirring. The solution was then centrifuged (Sorvall RC Plus Superspeed Centrifuge, Thermo Fisher Scientific, Asheville NC, USA) at 3000 × *g* for 1 h to collect the supernatant. This was then filtered using # 1 Whatman filter paper (Whatman International Ltd., Maidstone, England), dialyzed (Spectro/Por tubing, 6-8 kDa cut off, Spectrum Medical Industries, Inc, USA) at 4 ºC for 72 h with frequent changes of Milli-Q water (Millipore Corporation, MA, USA) to remove the salt, and then freeze-dried (Labconco Corporation,

Kansas City, Missouri 64132) at temperature difference of 35 ºC (for 24 h to yield the CPI powder for later use.

The crude protein composition of CPI powder was determined using the Association of Official Analytical Chemists Method 920.87 (AOAC, 2003). The CPI produced was found to be comprised of 90.45% protein (%N x 6.25). CPI concentrations used in this study reflect the protein content rather than powder weight.

Preparation of canola protein films

Film forming solutions were prepared by slowly dissolving 5.0 % (w/w) CPI in Milli-Q water under constant mechanical stirring at 500 rpm (IKAMAG RET-G, Janke and Kunkel GMBH & CO. KG, IKA-Labortechnik, Germany), adjusted to pH 3.0 using 1 M HCl, and then allowed to stir for 1 h at room temperature. Glycerol, sorbitol and polyethylene glycol 400 (PEG-400) were then added at 50% (w/w of CPI) into the film forming solutions, and then allowed to stir (500 rpm) for an additional 10 min. A 0.4% (w/w) genipin solution was created by dissolving genipin (1% w/w of CPI) into Milli-Q water, and then added in the film forming solutions to stir (500 rpm) for 15 min. Table 18.1 gives the contents of each film formulation tested. The film forming solutions were then degassed for 10 min within an ultrasonic bath at a frequency of 40 kHz (Branson Ultrasonic Cleaner, Model 2510R-DTH, USA) at room temperature. Afterwards, the film forming solutions were heated to 50 ºC under stirring at 500 rpm for 5 min, and then casted onto a polytetrafluoroethylene (PTFE) mould (10 cm length; 10 cm width; 1 mm depth). Excess film forming solutions were removed using a straight edge. CPI films were formed after drying overnight at room temperature. Films were then removed from the mould, and conditioned to 54% relative humidity (using a saturated magnesium nitrate solution) within a desiccator at room temperature for 2 d. All films were prepared in triplicate.

Film thickness

Film thickness was measured by using a digital micrometer (Model 62379-531, Control Company, U.S.A.) having a precision of 0.01 mm. Ten thickness measurements were taken on each triplicate film prepared.

Table 18.1 Composition of CPI film-forming solutions prior to film casting.

Film	CPI (g)	CPI (% db)	Plasticizer (g)	Plasticizer (%/CPI)	GP (g)	GP (%/CPI)	Water (g)	Thickness (mm)
5.0% CPI, 50% Gly	5	67	2.5	50	0	0	92.50	0.07
5.0% CPI, 50% Sor	5	67	2.5	50	0	0	92.50	0.09
5.0% CPI, 50% PEG-400	5	67	2.5	50	0	0	92.50	0.10
5.0% CPI, 50% Gly, 1% GP	5	66	2.5	50	0.05	1	92.45	0.10
5.0% CPI, 50% Sor, 1% GP	5	66	2.5	50	0.05	1	92.45	0.09
5.0% CPI, 50% PEG-400, 1% GP	5	66	2.5	50	0.05	1	92.45	0.08

Opacity

Film opacity was determined by using a spectrophotometer (Genesys 10-UV, Thermo Fisher Scientific) as described by Gontard et al. (1994). The pre-conditioned films were cut into small strips (4.5 x 0.9 cm) and placed on the inside wall of the plastic cuvette (1 cm path length). The absorbance of film strips will be measured at wavelength of 400 nm, 500 nm, 600 nm, 700 nm, and 800 nm. The area under the absorbance-wavelength curve was determined as the film opacity with the unit of A.nm. All measurements were performed in triplicate, for each type of films.

Water vapor permeability

Water vapor permeability (WVP) of the CPI films was determined using the "cup method" modified from the gravimetric technique of ASTM E96-93 (1993). For this study, PVC (polyvinyl chloride) cups were prepared to the following dimensions: outer cup height (2.65 cm), outer cup radius (2.50 cm), inner cup height (2.00 cm) and inner cup radius (2.25 cm). Films were placed on the top of the cup, then held in place by a lid (with an open centre of similar dimensions as the inner cup radius) tightened by six screws. The open surface area of the film was 15.90 cm^2. Within the cup, 10 mL of saturated $Mg(NO_3)_2$ solution (54% relative humidity) was added. The entire cup (with $Mg(NO_3)_2$ solution plus film) was then placed within a desiccator containing $CaSO_4$ desiccant (0% relative humidity) at room temperature. The water transferred through the film was determined from the weight loss of the system (cup, $Mg(NO_3)_2$ solution) over a 5 h duration at 30 min intervals, and weigh to the nearest 0.1 mg using an analytical balance (CPA224S, Sartorius, U.S.A.). Preliminary experiments (not shown) showed that a steady state of weight loss was reached after 5 h. WVP of the film was calculated using the WVP Correction Method which was described as the following formulae (Gennadios et al., 1994).

$$WVP = (WVTR_m \times L) / \Delta P \quad \text{(eq. 18.1)}$$

$$\Delta P = (P_{w1} - P_{w2}) \quad \text{(eq. 18.2)}$$

$$P_{w1} = P_T - (P_T - P_{w0}) \exp(N_w h/cD) \quad \text{(eq. 18.3)}$$

$$N_w = (6.43 \times 10^{-11}) \times WVTR_m \quad \text{(eq. 18.4)}$$

where $WVTR_m$ (water vapor transmission rate, g/m^2s) was calculated by dividing the slope by the open area of the cup (15.90 cm^2); L was the thickness of the film (mm), and ΔP was the real water vapor partial pressure difference across the film (kPa). P_{w1} was water vapor partial

pressure at the film inner surface (kPa), P_{w2} was the water vapor partial pressure at film outer surface (kPa), since the cup was placed in the desiccator containing $CaSO_4$ desiccant (0% relative humidity), and P_{w2} was 0 kPa. P_T was the total atmospheric pressure (101.3 kPa); P_{w0} was the partial pressure of water vapor in air at the surface of the $Mg(NO_3)_2$ solution which was 1.34267 kPa; N_w (g.mol/s.cm^2) was the measured value of $WVTR_m$; h was the stagnant air gap height between the film and the surface of $Mg(NO_3)_2$ solution; c was the total molar concentration of air and water vapor (4.15×10^{-5} g.mol/cm^3); D was the diffusivity of water vapor through air at 25 ºC (0.25375 cm^2/s). All measurements were performed triplicate films.

Mechanical properties

Tensile strength, tensile elongation and elastic modulus

Tensile strength (TS, MPa), tensile elongation (TE, %), and elastic modulus (E, kPa) of the film were determined using a Texture Analyzer with a load cell of 25 kg (Texture Technologies Corp., New York) on film strips (8 × 2.5 cm) which were pre-conditioned at 54% relative humidity under room temperature based on the ASTM D882-91 (1991). The film strips were placed between grips, and set up the initial grip separation to 40 mm and cross-head speed to 5 mm/s. The stress-strain curve data were collected by a microcomputer. TS was calculated by dividing the maximum load of the film strip by the area of cross-section of that strip (width of the strip (2.5 cm) × thickness of the strip); TE was calculated as a percentage of the length change of the film strip at the breakpoint of the film; E was expressed as the slope of the trend line on the stress-strain curve. Three measurements were taken on each triplicate film prepared.

Puncture strength and deformation

Both puncture strength (PS, N) and deformation (PD, mm) of the film were determined using a Texture Analyzer (Texture Technologies Corp., New York) as described by Gontard et al. (1992). Each film was stabilized on the puncture mould (65.6 mm diameter), and the smooth edged cylindrical probe (4 mm diameter) was placed just above the center of film and moved through the film at a cross-head speed of 1 mm/s. The force-deformation curve data were collected by a microcomputer. PS was calculated as the maximum force (N) which was loaded on the film to puncture the specimen. PD was expressed as the length changes at the rupture point of film.

Scanning electron microscopy (SEM)

Cross-sectional images of all CPI films were taken using a scanning electron

microscope (Philips 505, Holland) operated at 30 kV. Specimens (0.5 cm × 0.5 cm) were cut and coated using a gold sputter coater (Edwards Sputter Coater S150B) in order to make samples conductive, and observed at 6000 × magnification.

Statistical analyses

All experiments were performed on triplicate films and reported as the mean ± one standard deviation. A two-way analysis of variance (ANOVA) was used to measure statistical differences in thickness, opacity, WVP and mechanical properties (TS, TE, E, PS and PD) of CPI films among the various treatments (i.e., effect of plasticizer-type (glycerol, sorbitol and PEG-400) and, fixative conditions (with and without GP)).

18.4 RESULTS AND DISCUSSION

Mechanical properties

Film strength

The effects of plasticizer-type and genipin (GP) on the strength (PS, TS and E) of CPI films were examined and shown in Figure 18.1A, 18.2A and 18.2C, respectively. An analysis of variance of PS data indicated that plasticizer-type ($p<0.001$) and fixative conditions ($p<0.001$), along with their interaction ($p<0.01$) were all significant. Overall, the PS of CPI films prepared with GP was higher than those without, however the magnitude and change in magnitude of PS differed slightly depending on which plasticizer was present. Increase ratios of PS values by the addition of GP were 1.88x, 1.82x, and 1.86x for CPI films with glycerol, sorbitol, and PEG-400, respectively (Figure 18.1A). Films with sorbitol or PEG-400 displayed similar PS ($p>0.05$), which were significantly higher than films prepared with glycerol (Figure 18.1A).

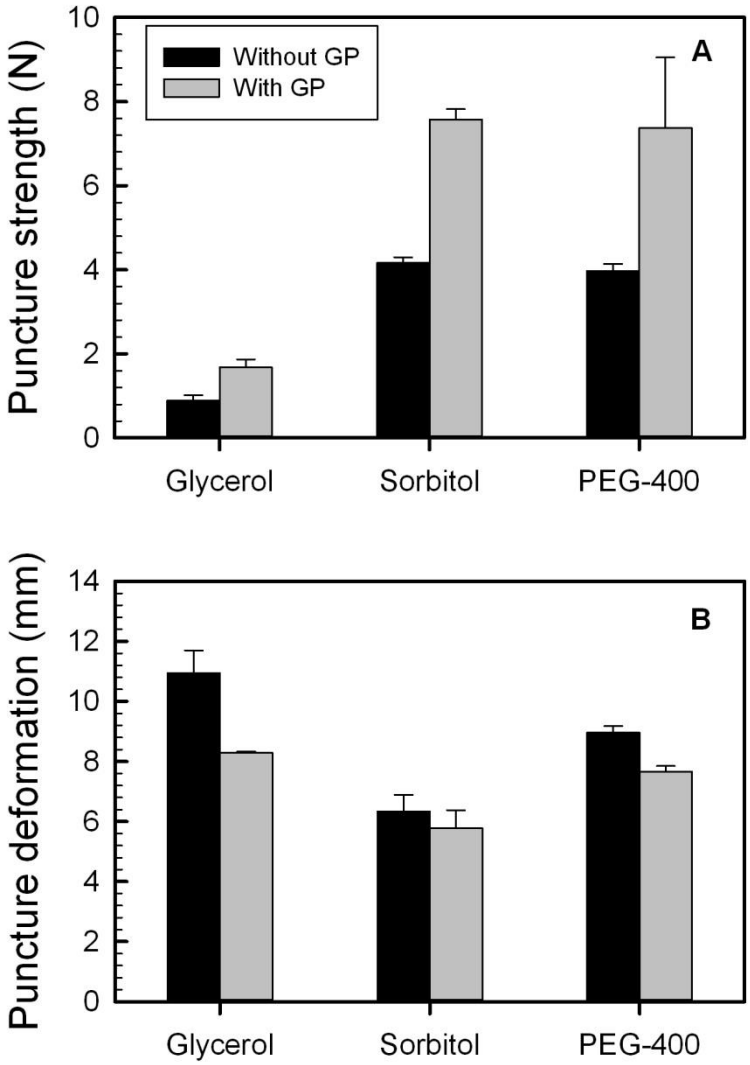

Figure 18.1 Puncture strength (A) and deformation (B) for 5% (w/w) canola protein isolates films in the presence of 50% (w/w) glycerol, sorbitol and PEG-400 prepared with and without 1% (w/w) genipin (GP). Data represent the mean ± one standard deviation (n =3).

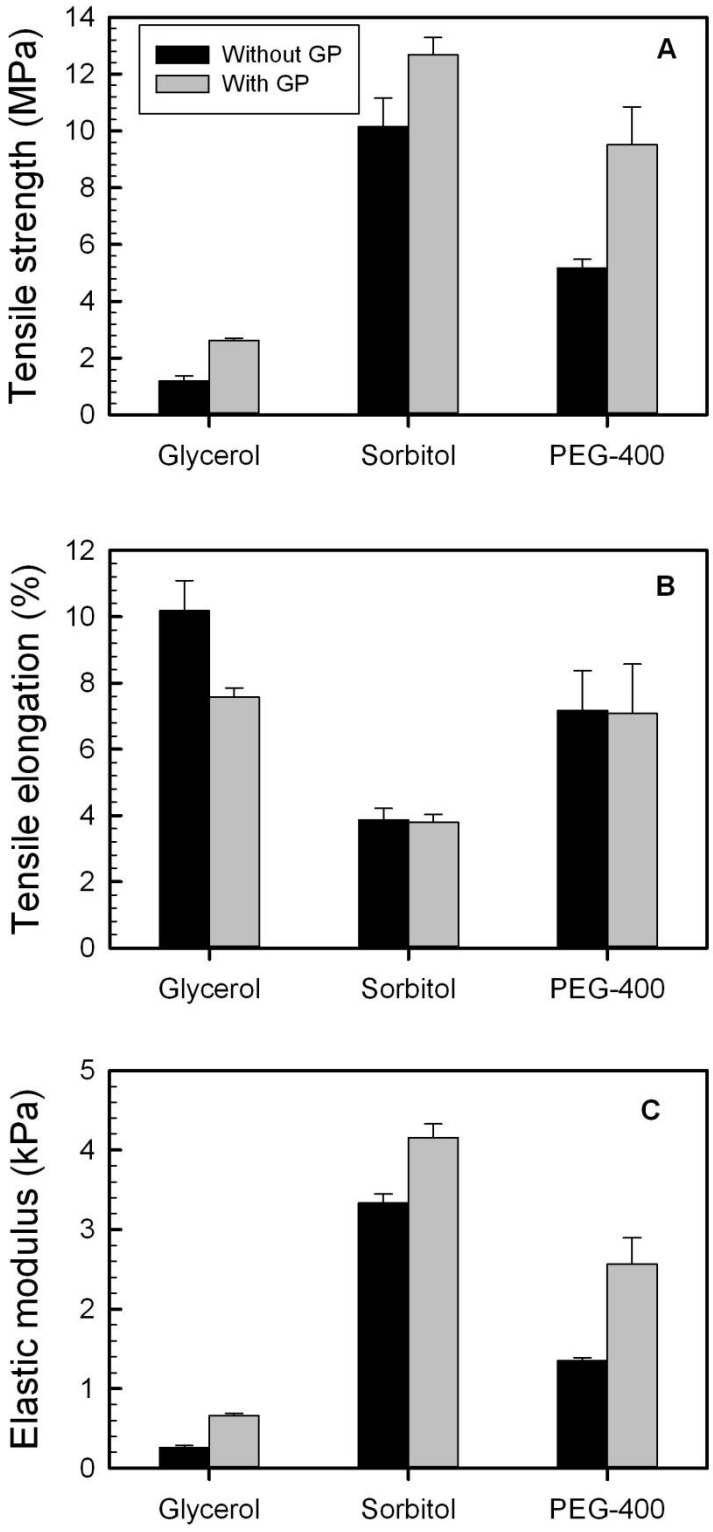

Figure 18.2 Tensile strength (A) and percent elongation (B) and, elastic modulus (C) for 5% (w/w) canola protein isolates films in the presence of 50% (w/w) glycerol, sorbitol and PEG-400 prepared with and without 1% (w/w) genipin (GP). Data represent the mean ± one standard deviation (n =3).

An analysis of variance on TS data indicated that both plasticizer type ($p<0.001$) and fixative condition ($p<0.001$) were highly significant, along with their interaction ($p<0.05$). Overall, TS of CPI films were greater in the presence of GP than without, however the magnitude and magnitude change was dependent upon the plasticizer-type. For instance, the addition of GP resulted in 1.94x, 1.25x, and 1.84x increase of TS on films with glycerol, sorbitol, or PEG-400, respectively (Figure 18.2A), and films with sorbitol were stronger than films with PEG-400, followed by the films with glycerol (Figure 18.2A). In contrast to the other formulations examined, the addition of GP only lead to an increase in TS of 1.25x suggesting sorbitol by itself was playing a more substantial role in enhancing film strength than the other plasticizer-types.

An analysis of variance of E data indicated that plasticizer-type ($p<0.001$) and fixative conditions ($p<0.001$), along with their interaction ($p<0.01$) were all significant. Elastic moduli data followed a similar trend as TS, where overall, E of CPI films was greater in the presence of GP than without, however the magnitude and magnitude change was dependent upon the plasticizer-type. Increase ratios of E values by the addition of GP were 2.54x, 1.25x, and 1.90x for CPI films prepared with glycerol, sorbitol, and PEG-400, respectively (Figure 18.2C). Films with glycerol were much weaker than films with sorbitol or PEG-400 (Figure 18.2C). Film thickness for all films ranged between 0.70 to 0.10 mm, however they were statistically similar.

In general, plasticizers are added to film forming solutions to overcome brittleness and increase flexibility associated with the protein film by modifying its structure. Some of the stabilizing protein-protein interactions within the film become replaced by plasticizer-protein interactions, leading to increases in void volume within the film and a rise in chain mobility in response to shear stress as the presence of the plasticizer disrupts the internal structure (Mangavel et al., 2003). Depending on the composition, size, and shape of the plasticizer added, varying abilities to modify structure can be observed (Sothornvit and Krochta, 2001). Theoretically, plasticizers containing more polar groups (-OH) should behave as better plasticizers due to the development of more protein-plasticizer interactions within the film, primarily via hydrogen bonding (Yang and Paulson, 2000). However, the complexity of protein-plasticizer interactions and structure modification is much more important. For instance, Ooi et al. (2012) reported polyvinyl alcohol/rambutan skin waste flour films prepared with glycerol led to lower TS than those prepared with sorbitol, since the glycerol was able to abide more water. Turhan et al. (2001) suggested that the higher molecular weight polymer-based plasticizers (e.g., PEG-4000 and PEG-8000) in methylcellulose-based films had reduced ability to form hydrogen bonds with the protein, leading to less of a plasticizing effect than

lower molecular weight ones (e.g., PEG-400). Furthermore, the compatibility of the plasticizer to the protein, in terms of phase separation or physical exclusion between plasticizer and protein, also can impact its structure modifying abilities. For instance, Orliac et al. (2003) and Cao et al. (2009) compared the effect of PEG-400 with glycerol and sorbitol on sunflower protein-based films and gelatin films, respectively, and found PEG-400 molecules had lower compatibility to both of protein-based films.

In the present study, CPI films were overall stronger in the presence to sorbitol, than glycerol or PEG-400. It is hypothesized that the size of the sorbitol was more compatible to the CPI network than the smaller glycerol molecule, allowing it to disrupt protein-protein interactions better than the glycerol. Furthermore, glycerol possibly was able to attract more water molecules into the film via glycerol-water interactions. In contrast, the PEG-400 polymer was proposed to not be as compatible as the sorbitol, and would be less effective at inserting itself in-between protein-protein interactions. Possibly forming phase-separated PEG-400 inclusions within the film matrix rather than be homogenously dispersed. However film strength was within similar ranges as others reported in literature.

Differences between strength (e.g., TS) among a selected few of protein-based films (e.g., soy, gelatin, and egg albumin) relative to those found in the present study, as a function of plasticizer-type are shown in Table 18.2. For instance, soy and egg albumin-based films prepared with sorbitol experienced a ~2 or ~3-fold increase, respectively relative to glycerol. In contrast, CPI films prepared in the present study were ~9-fold stronger in the presence of sorbitol than glycerol (without GP) (Table 18.2). Differences among the various proteins may also depend on the level of denaturation induced during preparation of the film forming solution. Liu et al. (2004) found that the three-dimensional structure of protein-based film is more compact with higher levels of denaturation; leading to a stronger film. Unfolding to the protein's tertiary structure exposed buried hydrophobic amino acids that partake in hydrophobic interactions within the film matrix, and buried cysteine residues which undergo disulfhydryl exchange reactions to form stabilizing disulfide bridges. Consequently, the plasticizing effects can be reduced if the network structure is stronger (Kowalczyk and Baraniak, 2011). For instance, soy protein isolate films (Tang et al., 2005; Pruneda et al., 2008) reported in Table 18.3 were heated up to 70 ºC for 20 min, relative to the current study where CPI was heated to 50ºC for 5 min. In contrast to work by Gennadios et al. (1996), in

Table 18.2 Comparison of mechanical properties and water vapor permeability of protein-based films with different types of plasticizer.

Film type	Formulation	TS (MPa)	TE (%)	WVP (g.mm/m^2.h.kPa)	References
Soy protein	5% SPI, 60% Gly	2.2 ± 0.25	159.9 ± 9.20	1.2 ± 0.01	Tang et al. (2005)
	5% SPI, 60% Sor	4.2 ± 0.04	101.8 ± 15.60	1.2 ± 0.05	
Soy protein	5% SPI, 60% Gly	1.2 ± 0.15	186.9 ± 19.08	8.9 ± 0.09	Pruneda et al. (2008)
	5% SPI, 60% Sor	2.4 ± 0.16	148.3 ± 9.65	5.3 ± 0.18	
Egg albumin	9% Egg albumin, 50% Gly	1.3 ± 0.14	32.2 ± 1.90	10.7 ± 0.25	Gennadios et al. (1996)
	9% Egg albumin, 50% Sor	3.7 ± 0.16	15.0 ± 1.40	4.9 ± 0.16	
	9% Egg albumin, 50% PEG-400	3.8 ± 0.15	59.7 ± 6.80	6.2 ± 0.22	
Canola protein	5% CPI, 50% Gly	1.2 ± 0.18	10.2 ± 0.91	1.2 ± 0.17	Present study
	5% CPI, 50% Sor	10.2 ± 1.00	3.9 ± 0.35	0.5 ± 0.14	
	5% CPI, 50% PEG-400	5.2 ± 0.30	7.2 ± 1.20	0.9 ± 0.08	

Abbreviations: soy protein isolate (SPI); canola protein isolate (CPI), glycerol (Gly); sorbitol (Sor); polyethylene glycol 400 (PEG-400); tensile strength (TS) and elongation (TE); water vapor permeability (WVP)

Table 18.3 Comparison of mechanical properties and water vapor permeability of protein films with and without cross-linking agents.

Film type	Formulation	TS (MPa)	TE (%)	WVP (g.mm/m^2.h.kPa)	References
(A) Genipin					
Soy protein	8.33% SPI, 50% Gly	3.2 ± 0.10	22.5 ± 5.02	0.8 ± 0.04	Gonzalez et al. (2011)
	8.33% SPI, 50% Gly, 1% GP	4.2 ± 0.38	45.8 ± 0.25	0.6 ± 0.10	
Canola protein	5% CPI, 50% Gly	1.2 ± 0.18	10.2 ± 0.91	1.2 ± 0.17	Present study
	5% CPI, 50% Gly, 1% GP	2.6 ± 0.08	7.6 ± 0.27	1.4 ± 0.15	
	5% CPI, 50% Sor	10.2 ± 1.00	3.9 ± 0.35	0.5 ± 0.14	
	5% CPI, 50% Sor, 1% GP	12.7 ± 0.61	3.8 ± 0.24	0.5 ± 0.04	
(B) Transglutaminase					
Soy protein	5% SPI, 60% Gly	2.2 ± 0.25	159.9 ± 9.20	1.2 ± 0.01	Tang et al. (2005)
	5% SPI, 60% Gly, 4 U MTGase	2.6 ± 0.28	105.9 ± 9.20	1.3 ± 0.05	
	5% SPI, 60% Sor	4.2 ± 0.04	101.8 ± 15.60	1.2 ± 0.05	
	5% SPI, 60% Sor, 4 U MTGase	4.5 ± 0.35	27.3 ± 3.61	1.3 ± 0.00	
Wheat gluten	5% WG, 40% Gly	1.1 ± 0.15	36.2 ± 5.22	-	Tang and Jiang (2007)
	5% WG, 40% Gly, 8 U MTGase	1.4 ± 0.16	20.8 ± 2.50	-	

Abbreviations: soy protein isolate (SPI); canola protein isolate (CPI); wheat gluten (WG); glycerol (Gly); sorbitol (Sor); genipin (GP); transglutaminase (MTGase); tensile strength (TS) and elongation (TE); water vapor permeability (WVP)

which TS data for egg albumin protein films prepared with sorbitol and PEG-400 were similar, the present study showed PEG-400 give CPI films reduced TS relative to those prepared with sorbitol. Similar results were reported by Orliac et al. (2003), Wan et al. (2005) and Cao et al. (2009) for sunflower proteins, soy proteins and gelatin, respectively, where authors argued that PEG-400 displayed lower compatibility to the proteins.

In the present study, the addition of GP is presumed to form both inter- and intra-molecular cross-links to strengthen all CPI films, regardless of the plasticizer-type used. Although the exact mechanism of GP cross linking is unknown, it is believed to occur between ε-amine groups (e.g., mainly lysine, and to a lesser extent hydroxylysine and arginine) and the GP molecule via a nucleophilic attack and a slower S_N2 nucleophilic substitution reaction. Butler et al. (2003) and Mi et al. (2003) proposed a mechanism involving GP attack on the amino containing cationic polysaccharide, chitosan. In brief, it involves a nucleophilic attack by a methylamine compound on the oleginic carbon at C-3 on deoxyloganin aglycone in the GP molecule causing the dihydropyran ring to open up. A second attack on the same amine group gives an aldehyde. The S_N2 nucleophilic substitution reaction between an amine group and the GP molecule leads to a replacement of the ester group on the GP molecule and release of a methanol molecule. Because of the two reactions, GP molecules can polymerize with each other to form chains up to 30-40 monomers in length, allowing it to partake in both short and long range crosslinking (Liang et al., 2004).

Film deformation

The effects of plasticizer-type and fixative condition on the deformability (i.e., PD and TE) of CPI films were shown in Figures 18.1B and 18.2B, respectively. An analysis of variance of PD data indicated that both plasticizer-type ($p<0.001$) and fixative condition ($p<0.001$), along with their interaction ($p<0.01$) were highly significant. Overall, PD was found to be less with the addition of GP (~7.2 mm) than without (~8.8 mm); and PD was found to be the lowest for sorbitol (~6.1 mm) followed by PEG-400 (~8.3 mm) and then glycerol (~9.6 mm) (Figure 18.1B). However, the effect of GP on each film differed depending on the plasticizer present. For instance, CPI-sorbitol films only experienced a 1.1-fold decrease in PD data from ~6.3 to ~5.8 mm with the addition of GP, whereas CPI-PEG-400 and CPI-glycerol films experienced a 1.2-fold (decreasing from ~9.0 to 7.7 mm) and 1.3-fold (decreasing from 11.0 to ~8.3 mm) decline,

respectively. An analysis of variance of TE data indicated that both plasticizer type ($p<0.001$) and fixative condition ($p<0.05$), along with their interaction ($p<0.05$) were significant. Plasticizer-type had a strong influence on the TE of the CPI films, more so than the presence of GP. TE values for CPI-Sorbitol (~3.9%) and CPI-PEG-400 (~7.2%) films were similar regardless of the presence of GP, whereas CPI-glycerol films significantly higher (~10.2%) in the absence of GP than with (~7.6%) (Figure 18.2B).

Overall, CPI films with different plasticizers prepared with and without genipin showed significantly reduced flexibility (i.e., % TE) relative to cross-linked and/or uncross-linked films prepared using soy protein (Tang et al., 2005; Pruneda et al., 2008), egg albumin (Gennadios et al., 1996) and wheat gluten (Tang and Jiang, 2007) (Tables 18.2 and 18.3). As previously described, plasticizers act to decrease intra- and intermolecular protein-protein interactions to increase void space in the film making it more flexible (Lieberma and Gilbert, 1973). Due to glycerol's hygroscopic nature, water molecules tend to be drawn into the film during its formation (Cheng et al., 2006). Glycerol containing films tend to be more flexible (higher %TE) than sorbitol, because glycerol can absorb more water molecule which is also a plasticizer (Gontard et al., 1993) into film structure. The addition of PEG-400 was found to be incompatible to the protein-based films, as previously described resulting in an intermediate %TE value between films with glycerol and those with sorbitol.

The addition of fixatives functions to counteract the effects of plasticizers by inducing intra- and intermolecular protein-protein cross-links to make the films stronger and less flexible. Tang et al. (2005) reported that soy protein-glycerol and soy protein-sorbitol formulations formed stronger (i.e., increased TS) and less flexible films (i.e., lower %TE) with the addition of microbial transglutaminase relative to those without (Table 18.3). A similar trend was also reported by Tang and Jiang (2007) for wheat gluten-glycerol films with and without transglutaminase (Table 18.3). In the present study, CPI-glycerol films also followed this trend in the presence and absence of GP. However, although the addition of GP significantly increased film strength in CPI-sorbitol and CPI-PEG-400 films (Figure 18.2A), it did not significantly affect TE values (Figure 18.2B). The similar result was also found on the chitosan film plasticized by polyethylene oxide (a molecular weight of 20,000 g/mol) with the addition of GP (Jin et al., 2004). The lower miscibility between plasticizer and biopolymer (e.g., CPI and chitosan) could be contributed to those results, so, the addition of GP is less effective to create the expansible networks in the films by breaking the

protein-protein and/or protein-plasticizer interactions (Gonzalez et al., 2011). Gonzalez and co-workers (2011) found the presence of GP increased both TS and TE values in soy protein-glycerol films (Table 18.3). Differences in film behavior in the presence of GP may reflect differences in the level of GP polymerization and intra- and inter-molecular cross-linking occurring with the protein network, heterogeneously distributed around the plasticizer inclusions.

Film opacity

Film opacity is an important attribute in terms of food packaging (Gontard et al., 1992; Orliac et al., 2003). In the present study, film opacity was investigated as a function of plasticizer-type and fixative condition and presented in Figures 18.3. An analysis of variance found only the main effects of plasticizer-type ($p<0.001$) and fixative condition ($p<0.001$) were significant, whereas their associative interaction was not ($p>0.05$). Overall, films prepared with glycerol were less opaque (~82.7 A.nm), followed by CPI-sorbitol (~94.3 A.nm) and CPI-PEG-400 (~102.6 A.nm) films (Figure 18.3). And the application of GP decreased transparency of films from ~100.1 A.nm to ~86.3 A.nm (Figure 18.3). Based on these findings, it was hypothesized that since the glycerol molecule was smaller than sorbitol and PEG-400, it was more homogenously dispersed. In contrast, both sorbitol and PEG-400 were more heterogeneously dispersed causing light to scatter more. A few of studies (Cao et al., 2009; Orliac et al., 2003) also reported a “blooming” and “blushing” phenomenon could also be happened on the surface of films plasticized by PEG-400, due to its lower compatibility with protein matrix, so, phase separation or physical exclusion could greatly increase the opacity of films. In contrast, cross-linking with GP causes opacity to rise due to an increase in protein-protein interactions, and as the result of the GP cross-linking reaction itself which induces a blue color once bound (Gonzalez et al., 2011; Song and Zhang, 2009), because of the spontaneous reaction of GP with amino acids in proteins (Touyama et al., 1994). A rise of opacity was also reported by Gonzalez et al. (2011) for soy protein films with GP, and by Tang et al. (2005) for soy protein films with transglutaminase.

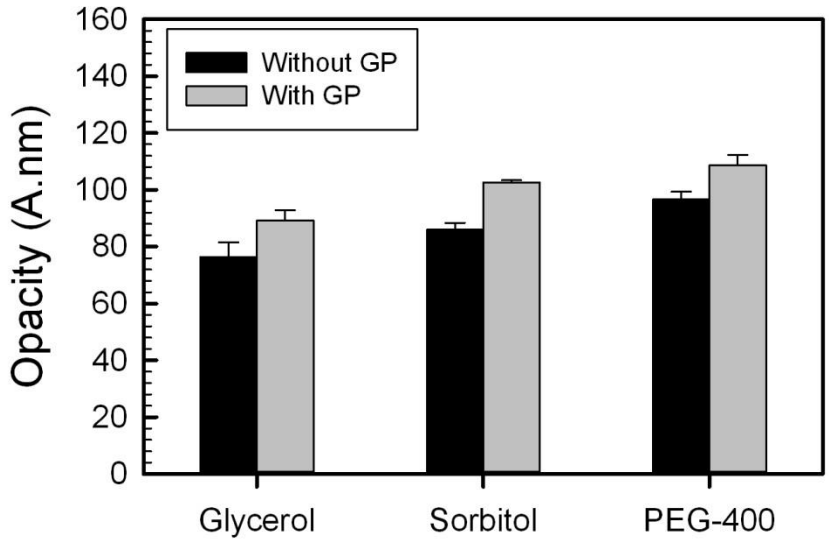

Figure 18.3. Opacity of 5% (w/w) canola protein isolates films in the presence of 50% (w/w) glycerol, sorbitol and PEG-400 prepared with and without 1% (w/w) genipin (GP). Data represent the mean ± one standard deviation (n = 3).

Water vapor barrier properties

The influence of plasticizer-type and fixative condition on WVP of CPI films was illustrated in Figure 18.4. An analysis of variance of WVP data found that only plasticizer-type was significant ($p<0.001$), whereas fixative condition ($p>0.05$) and their interaction term ($p>0.05$) were not. Overall, CPI-glycerol films showed the highest WVP (~1.3 g.mm/h.m^2.kPa), followed by CPI-PEG-400 (~0.9 g.mm/h.m^2.kPa) and CPI-sorbitol (~0.5 g.mm/h.m^2.kPa) films (Figure 18.4). The differences on WVP of films plasticized with glycerol, sorbitol, and PEG-400 could be caused by the different hygroscopic properties of the plasticizers. As reported in the study of water sorption equilibrium data by Rockland (1984), sorbitol exhibits lower absorptive properties than PEG-400, followed by glycerol. The hydrophilic nature of glycerol allows it to easily absorb more water molecules into films to increase the WVP. Furthermore, plasticizers of lower molecular weight can easily penetrate into the protein structure to disrupt the intermolecular interactions and increase the free volume of protein matrix; eventually increase the permeability of films (McHugh and Krochta, 1994; Sothornvit and Krochta, 2000). CPI-PEG-400 films are also presumed to have

higher WVP than CPI-sorbitol films, due to the presence of a large number of hydroxyl groups (-OH) which increases its affinity to water (Wan et al., 2005). Similar findings as a function of plasticizer-type were reported in soy protein (Wan et al., 2005) and oat spelt arabinoxylan (Mikkonen et al., 2009) films. Tables 18.2 and 18.3 gave WVP data for various protein-based films. CPI-based films prepared within the present study showed comparable WVP data to those reported by Tang et al. (2005) for soy protein films with and without transglutaminase (~1.2 g.mm/h.m^2.kPa), and by Gonzalez et al. (2011) for soy protein films with and without GP (~0.7 g.mm/h.m^2.kPa) (Tables 18.2 and 18.3). However the CPI-based films were significantly better than films prepared with egg albumin (~4.9-10.7 g.mm/h.m^2.kPa) by Gennadios et al. (1996) and soy protein films by Pruneda et al. (2008) (~5.3-8.9 g.mm/h.m^2.kPa) (Table 18.2).

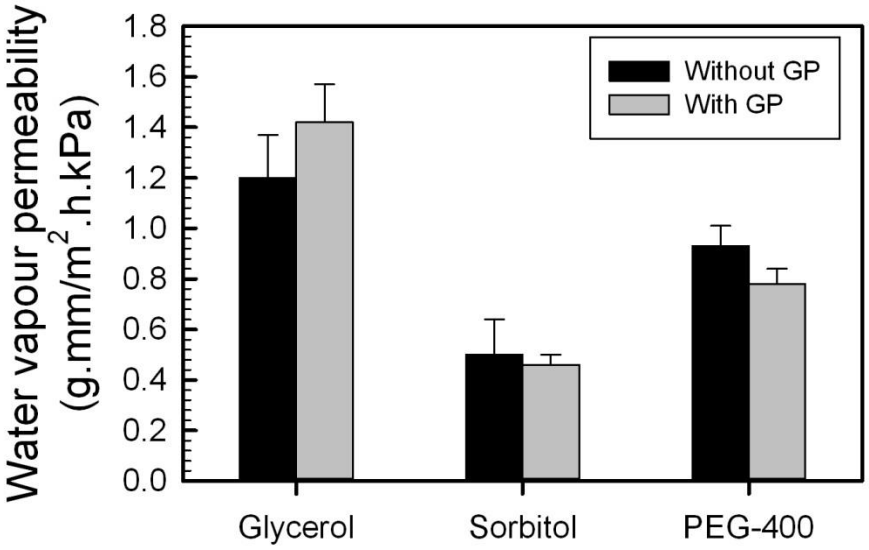

Figure 18.4. Water vapor permeability of 5% (w/w) canola protein isolates films in the presence of 50% (w/w) glycerol, sorbitol and PEG-400 prepared with and without 1% (w/w) genipin (GP). Data represent the mean ± one standard deviation (n = 3).

Film morphology

Cross-sectional images of CPI films with and without GP, plasticized by glycerol, sorbitol, and PEG-400 were visualized by SEM (Figure 18.5). Overall, CPI films with GP (Figure 18.5, B1-3) had more compact, homogenous, and less porous structure than films prepared without (Figure

18.5, A1-3). The latter appeared more heterogeneous in nature with much larger pores. The smaller pores sizes in the presence of GP is hypothesized the result of increased protein-protein interactions induced by intra- and intermolecular covalent cross-linking; resulting in films that have increased mechanical strength.

CPI-glycerol films (Figure 18.5, A1) showed a more organized structure with much larger pore size than CPI-sorbitol films (Figure 18.5, A2). The latter also showed a regular alignment of protein-protein aggregates with relatively smaller pores which may help explain its improved film strength and reduced flexibility. In contrast, CPI-PEG-400 films (Figure 18.5, A3) showed evidence of a more coagulated structure with large aggregates and different pore sizes. However the protein matrix looked less ordered that seen for CPI-sorbitol (Figure 18.5, A2) films and CPI-glycerol (Figure 18.5, A1) films; possibly reflecting the lower compatibility of PEG-400 with proteins in the film matrix.

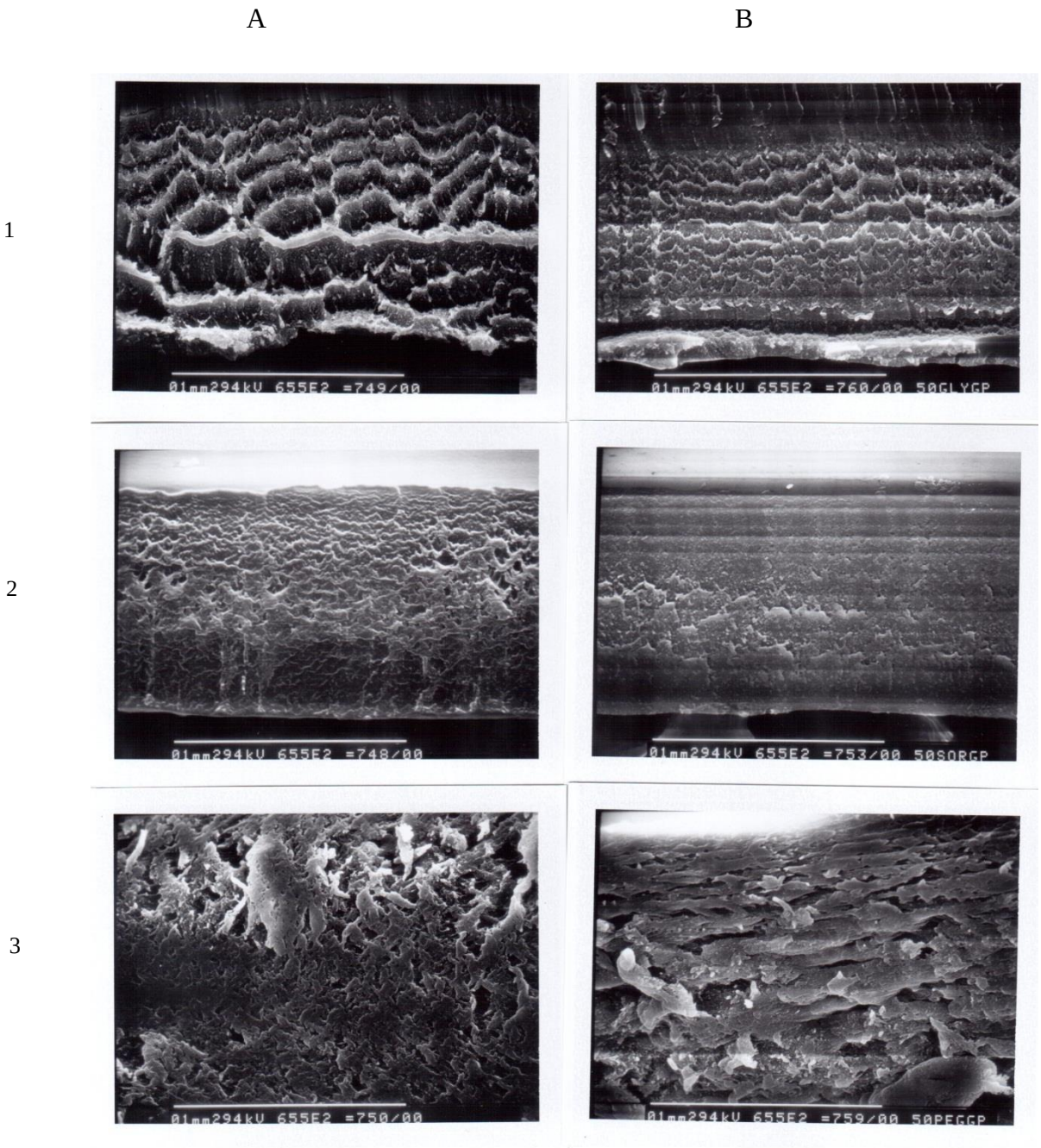

Figure 18.5. SEM cross-sectional images (at 6000 × magnification) of 5% (w/w) canola protein isolates films in the presence of 50% (w/w) glycerol (1), sorbitol (2) and PEG-400 (3) prepared in the absence (A) and presence of 1% (w/w) genipin (B).

18.5 SUMMARY

The present study evaluated the effect of plasticizer-type and fixative condition on the mechanical, optical and water vapor barrier properties, and morphology of CPI films. Generally, as the plasticizer changed from sorbitol to PEG-400, followed by glycerol, films became more flexible, and more permeable to water vapor. In contrast, when genipin was applied into films, films became stronger, less malleable, and more opaque. Based on these findings, CPI shows promise as a potential material for use in designing edible, biodegradable packaging in the future.

-Chapter 19-

Summary

Overall, this research investigated the influence of protein and glycerol concentration, plasticizer-type, and fixative condition on the mechanical, optical, and water vapor barrier properties of CPI films. In general, CPI films had higher mechanical strength as protein concentration increased due to the increased film thickness and a greater amount of intermolecular interactions occurring within the film structure. In contrast, as the glycerol concentration increased, CPI films became more flexible but weaker, presumably caused by protein-protein interactions being replaced by protein-glycerol interactions, and a more heterogeneous spatial distribution of junction zones within the film. Moreover, plasticizer-type is also an important factor to impact the mechanical properties of CPI films. CPI films were more flexible in the presence of glycerol, followed by sorbitol or PEG-400, since its smaller size was more compatible to the film matrix and its higher hydrophilic nature allowed it to attract water molecules which also performed as another plasticizer in the film structure; however, glycerol resulted in higher WVP of CPI films in comparison with sorbitol and PEG-400. Because of the formation of short and long range cross links in the film structure by the addition of genipin through the nucleophilic attack and S_N2 nucleophilic substitution reaction, CPI films became stronger but less malleable.

Film opacity was also studied as a function of protein and glycerol concentration, plasticizer-type and fixative condition in the film matrix. CPI films were more transparent as the glycerol concentration increased, because of the transparent nature and homogenous dispersion of glycerol in the film structure. However, films became more opaque at the higher CPI level presumed due to the higher solid contents, a more tightly packed structure, and greater thickness. Since glycerol (molecular weight of 92.09 g/mol) (Redl et al., 1999; Cunningham et al., 2000) is much smaller than sorbitol (molecular weight of 182.17 g/mol) (Barreto et al., 2003) and PEG-400 (molecular weight of 400 g/mol) molecules, it was presumed to be more homogeneously dispersed within the film forming solution, so, CPI films prepared with glycerol had lower opacity than films with sorbitol or PEG-400. In addition, due to the lower compatibility of PEG-400 with the protein matrix, CPI films with PEG-400 were more opaque than films with sorbitol.

Furthermore, the addition of genipin led to more opaque films than those without by the formation of cross links.

The effects of protein and glycerol concentration, plasticizer-type and the addition of genipin on WVP were also investigated in this research. WVP increased with the increase of both CPI and glycerol concentrations. In the case of glycerol, protein-protein interactions were replaced by the protein-glycerol interactions, leading to increases in free volume within the film to allow for a greater influx of water. In addition, higher levels of hydrophilic materials (e.g., glycerol and CPI) in the film formulation resulted in the increase of water mobility through the film matrix. Moreover, CPI films with sorbitol had lower WVP than films with PEG-400 or glycerol, because of the different water absorptive ability and molecular weight of plasticizers. CPI films with genipin were found to have lower WVP than without when sorbitol and PEG-400 were presented, however the same was not true when glycerol was present.

In this case of plasticizer-type and the addition of genipin in CPI films, film morphology was investigated by taking SEM images to explain the differences on the properties of CPI films. SEM images showed that CPI films with genipin had more compact and less porous structure than films without genipin to explain their better mechanical strength and water vapor barrier property. CPI-sorbitol films showed a more alignment structure with smaller pores than CPI-glycerol and CPI-PEG-400 films to explain their better mechanical resistance and lower moisture permeability. However, CPI-PEG-400 films had a more coagulated structure with larger aggregates to reflect the poor compatibility of PEG-400 with proteins.

In summary, although CPI film forming conditions (e.g., pH and temperature) were limited and the flexibility of CPI films were much lower, CPI films had much better water vapor barrier properties and comparable film strength relative to other plant protein-based films, therefore, CPI shows promise as a potential material for the development of edible films/packaging in the future.

Part VI: Other

-Chapter 20-

Acknowledgements

This research was funded through the Saskatchewan Ministry of Agriculture Development Fund, and the Saskatchewan Canola Development Commission.

-Chapter 21-

Literature cited

Agriculture and Agri-Food Canada (2010). *Lentils: Situation and Outlook*. Retrieved from http://www.agr.gc.ca.

Ahmed, J. (2010). Effect of high pressure on structural and rheological properties of cereals and legume proteins. In J. Ahmed, H. S. Ramaswamy, S. Kasapis, & J. I. Boye (Eds.), *Novel food processing: effects on rheological and functional properties* (pp. 225-255). Boca Raton, FL: CRC Press.

Aider, M., & Barbana, C. (2011). Canola proteins: composition, extraction, functional properties, bioactivity, applications as a food ingredient and allergenicity - a practical and critical review. *Trends in Food Science & Technology, 22,* 21-39.

Alizadeh- Pasdar, N., & Li-Chan, E. C. I. (2000). Comparison of protein surface hydrophobicity measured at various pH values using three different fluorescent probes. *Journal of Agricultural and Food Chemistry, 48,* 328-334.

Aluko, R. E., & McIntosh, T. (2001). Polypeptide profile and functional properties of defatted meals and protein isolates of canola seeds. *Journal of Science of Food and Agriculture, 81,* 391-396.

Aluko, R. E., & McIntosh, T. (2005). Limited enzymatic proteolysis increases the level of incorporation of canola proteins into mayonnaise. *Innovative Food Science and Emerging Technologies, 6,* 195-202.

Anker, M., Stading, M., & Hermansson, A. (1999). Effects of pH and the gel state on the mechanical properties, moisture contents, and glass transition temperatures of whey protein films. *Journal of Agricultural and Food Chemistry, 47,* 1878-1886.

Annunziata, O., Asherie, N., & Lomakin, A. (2002). Effect of polyethylene glycol on the liquid-liquid phase transition in aqueous protein solutions. *Proceedings of the National Academy of Sciences of the United States of America, 99,* 14165-14170.

Antonov, Y. A., & Goncalves, M. P. (1999). Phase separation in aqueous gelatin-κ-carrageenan mixture. *Food Hydrocolloids, 13,* 517-524.

Antonov, Y. A., & Soshinsky, A. (2000). Interactions and compatibility of ribuloso-1,5-bisphosphate carboxylase/oxygenase from alfalfa with pectin in aqueous medium. *International Journal of Biological Macromolecules, 27,* 279-285.

AOAC. (2003). *Official Method of Analysis*, 17th Edition. Association of Official Analytical Chemists. Washington, DC.

Arntfield, S.D. and Murray, E.D. (1981). The Influence of Processing Parameters on Food Protein Functionality I. Differential Scanning Calorimetry as an Indicator of Protein Denaturation. *Canadian Institute of Food Science and Technology Journal*. 14, 289-294.

Aryee, F. N. A., & Nickerson, M. T. (2012). Formation of electrostatic complexes involving mixtures of lentil protein isolates and gum Arabic polysaccharides. *Food Research International,* 48, 520-527.

ASTM D3935. (1981). *Annual book of ASTM standards*. Philadelphia, PA: American Society for Testing & Materials.

ASTM D3985-02. (2002). *Annual book of ASTM standards*. Philadelphia. PA: American Society for Testing & Materials.

ASTM D882-91. (1991). *Annual book of ASTM standards*. Philadelphia, PA: American Society for Testing & Materials.

ASTM E96-93. (1993). *Annual book of ASTM standards.* Philadelphia, PA: American Society for Testing & Materials.

Avramenko, N. A., Low, N. H., & Nickerson, M. T. (2013). The effects of limited enzymatic hydrolysis on the physicochemical and emulsifying properties of a lentil protein isolate. *Food Research International, 51,* 162-169.

Baeza, R. I., Carp, D. J., Pérez, O. E., & Pilosof, A. M. R. (2002). κ-Carrageenan-protein interactions: effect of proteins on polysaccharide gelling and textural properties. *LWT- Food Science and Technology, 35,* 741-747.

Baldwin, E. A. (2007). Surface treatments and edible coatings in food preservation. In M. S. Rahman (Ed.), *Handbook of Food Preservation* (pp. 478-508). Boca Raton, FL: CRC Press.

Baldwin, E. A., Nisperos, M., & Baker, R. A. (1995). Edible coatings for lightly processed fruits and vegetables. *Hortscience, 30,* 35-38.

Bamdad, F., Goli, A. H., & Kadivar, M. (2006). Preparation and characterization of proteinous film from lentil (*Lens culinaris*) – Edible film from lentil (*Lens culinaris*). *Food Research International, 39,* 106-111.

Bandyopadhyay, K., & Ghosh, S. (2002). Preparation and characterization of papain-modified sesame (*Sesamum indicum L*) protein isolates. *Journal of Agricultural and Food Chemistry, 50,* 6854-6857.

Banker, G. S., Gore, A. Y., & Swarbrick, J. (1966). Water vapor transmission properties of free polymer films. *Journal of Pharmacy and Pharmacology, 18,* 457-466.

Barreto, P. L. M., Pires, A. T. N., & Soldi, V. (2003). Thermal degradation of edible films based on milk proteins and gelatin in inert atmosphere. *Polymer Degradation and Stability, 79,* 147-152.

Bastos, D. S., Barreto, B. N., Souza, H. K. S., Bastos, M., Rocha-Leão, M. H. M., Andrade, T. C., & Gonçalves, M. P. (2010). Characterization of a chitosan sample extracted from Brazilian shrimps and its application to obtain insoluble complexes with a commercial whey protein isolate. *Food Hydrocolloids, 24,* 709-718.

Bérot, S., Compoint, J. P., Larré, C., Malabat, C., & Guéguen J. (2005) Large scale purification of rapeseed proteins (Brassica napus L.). *Journal of Chromatography B, 818,* 35-42.

Bhatty, R. S. (1988). Composition and quality of lentils (*Lens culinuris* Medik) - a review. *Canadian Institute of Food Science and Technology Journal, 21,* 144-160.

Bhatty, R. S., McKenzie, S. L., & Finlayson, A. J. (1968). The proteins of rapeseed (*Brassica napus L.*) soluble in salt solutions. *Canadian Journal of Biochemistry, 46,* 1191-1197.

Bidlingmeyer, B. A., Cohen, S. A, Tarvin, T. L., & Frost, B. (1987). A new, rapid, high-sensitivity analysis of amino acids in food type samples. *Association of Official Analytical Chemists Journal, 70,* 241-247.

Bodmeier, R., & Paeratakul, O. (1997). Plasticizers uptake by aqueous colloidal polymer dispersions used for the coating of solid dosage forms. *International Journal of Pharmaceutics, 152,* 17-26.

Bohidar, H., Dubin, P. L., Majhi, P. R., Tribet, C., & Jaeger, W. (2005). Effects of protein-polyelectrolyte affinity and polyelectrolyte molecular weight on dynamic properties of bovine serum albumin-poly(diallyldimethylammonium chloride) coacervates. *Biomacromolecules, 6,* 1573-1585.

Boral, S., & Bohidar, H. B. (2010). Effect of ionic strength on surface-selective patch binding-induced phase separation and coacervation in similarly charged gelatin-agar molecular systems. *Journal of Physical Chemistry B, 114*, 12027-12035.

Bourriot, S., Garnier, C., & Doublier, J-L. (1999). Micellar-casein–κ-carrageenan mixtures. I. Phase separation and ultrastructure. *Carbohydrate Polymers, 40*, 145-157.

Boye, J. I., Aksay, S., Roufik, S., Ribéreau, S., Mondor, M., Farnworth, E., & Rajamohamed, S. H. (2010a). Comparison of the functional properties of pea, chickpea and lentil protein concentrates processed using ultrafiltration and isoelectric precipitation techniques. *Food Research International, 43*, 537-546.

Boye, J., Zare, F., & Pletch, A. (2010b). Pulse proteins: processing, characterization, functional properties and applications in food and feed. *Food Research International, 43*, 414-431.

Bungenberg de Jong, H. G., & Kruyt, H. R. (1929). Coacervation (partial miscibility in colloid systems). *Proceedings of the Koninklijke Nederlandse Akademie van Wetenschappen, 32*, 849-856.

Burova, T. V., Grinberg, N. V., Grinberg, V. Y., Usov, A. I., Tolstoguzov, V. B., & de Kruif, C. G. (2007). Conformational changes in ι- and and κ-carrageenans induced by complex formation with bovine β-casein. *Biomacromolecules, 8*, 368-375.

Butler, M. F., Ng, Y. F., & Pudney, P. D. A. (2003). Mechanism and kinetics of the crosslinking reaction between biopolymers containing primary amine groups and genipin. *Journal of Polymer Science Part A-Polymer Chemistry, 41*, 3941-3953.

Can Karaca, A., Low, N., & Nickerson, M. (2011a). Emulsifying properties of canola and flaxseed protein isolates produced by isoelectric precipitation and salt extraction. *Food Research International, 44*, 2991-2998.

Can Karaca, A., Low, N., & Nickerson, M. (2011b). Emulsifying properties of chickpea, faba bean, lentil and pea proteins produced by isoelectric precipitation and salt extraction. *Food Research International, 44*, 2742-2750.

Canola Council of Canada. (1990). *Canola oil and meal: standards and regulations* (p. 4). Winnipeg, Manitoba: Canola Council of Canada Publication.

Canola Council of Canada. (2011). *What is Canola?* Retrieved from http://www.canolacouncil.org/oil-and-meal/what-is-canola/.

Cao, N., Fu, Y., & He, J. (2007). Preparation and physical properties of soy protein isolate and gelatin composite films. *Food Hydrocolloids*, *21*, 1153-1162.

Cao, N., Yang, X., & Fu, Y. (2009). Effects of various plasticizers on mechanical and water vapor barrier properties of gelatin films. *Food Hydrocolloids*, *23*, 729-735.

Chabanon, G., Chevalot, I., Framboisier, X., Chenu, S., & Marc, I. (2007). Hydrolysis of rapeseed protein isolates: kinetics, characterization and functional properties of hydrolysates. *Process Biochemistry*, *42*, 1419-1428.

Chandrasekaran, R., & Radha, A. (1995). Molecular architectures and functional properties of gellan gum and related polysaccharides. *Trends in Food Science and Technology, 6*, 143-147.

Chen, J., Chen, X., Zhu., Q., Chen, F., Zhao, X., and Ao, Q. (2013). Determination of the domain structure of the 7S and 11S globulins from soy proteins by XRD and FTIR. *Journal of the Science of Food and Agriculture*. 93, 1687-1691.

Cheng, L. H., Abd Karim, A., & Seow, C. C. (2006). Effects of water-glycerol and water sorbitol interactions on the physical properties of konjac glucomannan films. *Journal of Food Science, 71*, E62-E67.

Cho, S. Y., & Rhee, C. (2004). Mechanical properties and water vapor permeability of edible films made from fractionated soy proteins with ultrafiltration. *Lebensmittel-Wissenschaft Und-Technologies-Food Science and Technology*, *37*, 833-839.

Cho, Y.-H., & Park, J. (2003). Evaluation of process parameters in the O/W/O multiple emulsion method for flavor encapsulation. *Journal of Food Science, 68*, 534-538.

Choi, W. S., & Han, J. H. (2001). Physical and mechanical properties of pea-protein-based edible films. *Journal of Food Science*, *66*, 319-322.

Choi, W. S., & Han, J. H. (2002). Film-forming mechanism and heat denaturation effects on the physical and chemical properties of pea-protein-isolate edible films. *Journal of Food Science*, *67*, 1399-1406.

Chourpa, I., Ducel, V., Richard, J., Dubois, O., & Boury, F. (2006). Conformational modifications of α-gliadin and globulin proteins upon complex coacervates formation with gum Arabic as studied by Raman microspectroscopy. *Biomacromolecules*, *7*, 2616-2623.

Clark, A. H., & Ross-Murphy, S. B. (1987). Structural and mechanical properties of biopolymer gels. *Advances in Polymer Science, 83*, 57-192.

Contreras-Medellin, R., & Labuza, T. P. (1981). Prediction of moisture protection requirements for foods. *Cereal Food World, 26,* 335-343.

Coupland, J. N., Shaw, N. B., Monahan, F. J., O'Riordan, E. D., & O'Sullivan, M. (2000). Modeling the effect of glycerol on the moisture sorption behavior of whey protein edible films. *Journal of Food Engineering, 43,* 25-30.

Crenwelge, D. D., Dill, C. W., Tybor, T. B., & Landmann, W. A. (1974). A comparison of the emulsification capacities of some protein concentrates. *Journal of Food Science, 39,* 175-177.

Crouch, M. L., Tenbarge, K. M., Simon, A. E., & Ferl, R. (1983). cDNA clones for *Brassica napus* seed storage proteins: evidence from nucleotide analysis that both its napin are cleaved from a precursor polypeptide. *Journal of Molecular and Applied Genetics, 2,* 273-278.

Cunninghan, P., Ogale, A. A., Dawson, P. L., & Acton, J. C. (2000). Tensile properties of soy protein isolate films produced by a thermal compaction technique. *Journal of Food Science, 65,* 668-671.

Cuq, B., Gontard, N., Cuq, J. L., & Guilbert, S. (1996). Functional properties of myofibrillar protein based biopackaging as affect by film thickness. *Journal of Food Science, 61,* 580-584.

D'Arcy, R. L., & Watt, I. C. (1981). Water vapor sorption isotherms on macromolecular substrate. In L. B. Rockland & G. F. Stewart (Eds.), *Water Activity: Influences on Food Quality* (pp. 111-142). New York, NY: Academic Press.

Dalgalarrondo, M., Robin, J. M., & Azanza, J. L. (1986). Subunit composition of the globulin fraction of rapeseed (*Brassica napus*). *Plant Science, 43,* 115-124.

Dalgleish, D. G. (1997). Adsorption of protein and the stability of emulsion. *Trends in Food Science and Technology, 8,* 1-6.

Dalgleish, D. G. (2004). Food emulsions: their structures and properties. In S. E. Friberg, K. Larsson & J. Sjöblom (Eds.), *Food Emulsions,* (4th ed.) (pp 1-44). New York, NY: Marcel Dekker, Inc.

Damodaran, S. (1989). Interrelationship of molecular and functional properties of food proteins. In J. E. Kinsella & W. G. Sousie (Eds.), *Food Proteins* (pp 21-51). Champagin, IL: American Oil Chemists' Society.

Damodaran, S. (2005). Protein stabilization of emulsions and foams. *Journal of Food Science, 70,* R54-R66.

Damodaran, S. (2008). Amino acids, peptides, and proteins. In S. Damodaran, K. I. Parkin, & O. R. Fennema (Eds.), *Fennema's Food Chemistry* (pp. 217-329). Boca Raton, FL: CRC Press.

Dàvila, E. and Parés, D. (2007). Structure of heat-induced plasma protein gels studied by fractal and lacunarity analysis. *Food Hydrocolloids*. 21, 147-153.

de Jong, S., & van de Velde, F. (2007). Charge density of polysaccharide controls microstructure and large deformation properties of mixed gels. *Food Hydrocolloids*, *21*, 1172-1187.

de Kruif, C. G., & Tuinier, R. (2001). Polysaccharide protein interactions. *Food Hydrocolloids*, *15*, 555-563.

de Kruif, C. G., Weinbreck, F., & de Vries, R. (2004). Complex coacervation of proteins and anionic polysaccharides. *Current Opinion in Colloid & Interface Science, 9,* 340-349.

de Vries, R., Weinbreck, F., & de Kruif, C. G. (2003). Theory of polyelectrolyte adsorption on heterogeneously charged surfaces applied to soluble protein–polyelectrolyte complexes. *Journal of Chemical Physics, 118,* 4649-4659.

Debeaufort, F., & Voilley, A. (1995). Effect of surfactants and drying rate on barrier properties of emulsified edible films. *International Journal of Food Science and Technology, 30,* 183-190.

Debeaufort, F., Quezada-Gallo, J., & Voilley, A. (1998). Edible films and coatings: tomorrow's packagings: a review. *Critical Reviews in Food Science, 38,* 299-313.

Demetriades, K., Couplsnd, J. N., & McClements, D. J. (1997). Physical properties of whey protein stabilized emulsions as related to pH and NaCl. *Journal of Food Science, 62,* 342-347.

Dickinson, E. (1998). Stability and rheological implications of electrostatic milk protein-polysaccharide interactions. *Trends in Food Science and Technology, 9,* 347-354.

Dickinson, E., & Pawlowsky, K. (1998). Influence of κ-carrageenan on the properties of a protein-stabilized emulsion. *Food Hydrocolloids, 12,* 417-423.

Dickinson, E., & Stainsby, G. (1988). Emulsion stability. In E. Dickinson & G. Stainsby (Eds.), *Advances in Food Emulsions and Foams* (pp. 1-44). New York, NY: Elsevier applied science.

Dickinson, E., Ritzoulis, C., Yamamoto, Y., & Logan, H. (1999). Ostwald ripening of protein-stabilized emulsions: effect of transglutaminase crosslinking. *Colloids and Surfaces B: Biointerfaces, 12,* 139-146.

Doi, E. (1993). Gels and gelling of globular proteins. *Trends in Food Science & Technology*. 4, 1-5.

Dong, D., Hua, Y. F., Chem, Y. M., Kong, X. Z., Zhang, C. M., & Wang, Q. (2013). Charge

compensation, phase diagram, and protein aggregation in soy protein-gum Arabic complex formation. *Journal of Agricultural and Food Chemistry,* 61, 3934-3940.

Dong, X., Guo, L., Wei, F., Li, J., Jiang, M., Li, G., Zhao, Y., & Chen, H. (2011). Some characteristics and functional properties of rapeseed protein prepared by ultrasonication, ultrafiltration and isoelectric precipitation. *Journal of Science of Food and Agriculture, 91*, 1488-1498.

Donhowe, I. G., & Fennema, O. (1992). The effect of relative humidity on water vapor permeance of lipid-hydrocolloid bilayer films. *Journal of the American Oil Chemists Society, 69,* 1081-1087.

Doublier, J. L., Garnier, C., Renard, D., & Sanchez, C. (2000). Protein-polysaccharide interactions. *Current Opinion in Colloid & Interface Science*, *5*, 202-214.

Drelich, J., Fang, C., & White, C. L. (2002). Measurement of interfacial tension in fluid- fluid system. In A. T. Hubbard (Ed.), *Encyclopedia of Surface and Colloid Science* (pp. 3152-3166). New York, NY: Marcel Dekker Inc.

Drohan, O. D., Tziboula, A., McNulty, D., & Horne, D. S. (1997). Milk protein-carrageenan interactions. *Food Hydrocolloids*, *11*, 101-107.

Dror, Y., Cohen, Y., & Yerushalmi-Rozen, R. (2006). Structure of gum Arabic in aqueous solution. *Journal of Polymer Science Part B: Polymer Physics*, *44*, 3265-3271.

Ducel, V., Richard, J., Saulnier, P., Popineau, Y., & Boury, F. (2004). Evidence and characterization of complex coacervates containing plant proteins: application to the microencapsulation of oil droplets. *Colloids and Surfaces A: Physicochemical and Engineering Aspects*, *232*, 239-247.

Eleya, M.M.O., Ko, S., and Gunasekaran, S. (2004). Scaling and fractal analysis of viscoelastic properties of heat-induced protein gels. *Food Hydrocolloids*. 18, 315-323.

Elmer, C., Can Karaca, A., Low, N. H., & Nickerson, M. T. (2011). Complex coacervation in pea protein isolate-chitosan mixtures. *Food Research International*, *44*, 1441–1446.

Fahey, J. W., Zalcmann1, A. T., & Talalay, P. (2001). The chemical diversity and distribution of glucosinolates and isothiocyanates among plants. *Phytochemistry*, *56*, 5-51.

Falguera, V., Quintero, J. P., Jimenez, A., Munoz, J. A., & Ibarz, A. (2011). Edible films and coatings: structures, active functions and trends in their use. *Trends in Food Science & Technology*, *22,* 292-303.

Fang, Y. P., Li, L. B., Inoue, C., Lundin, L., & Appelqvist, I. (2006). Associative and segregative phase separations of gelatin/kappa-carrageenan aqueous mixtures. *Langmuir, 22*, 9532-9537.

Fenwick, G. R., & Heaney, R. K. (1983). Glucosinolates and their breakdown products in Cruciferous crops, foods and feeding stuffs. *Food Chemistry, 11,* 249-271.

Ferry, J.D. (1980). Viscoelastic properties of polymers. 3rd Edition. John Wiley & Sons, Inc. New York, NY.

Fñrgemand, M., Otte, J., & Qvist, K. B. (1998). Emulsifying properties of milk proteins crosslinked with microbial transglutaminase. *International Dairy Journal, 8,* 715-723.

Foegeding, E. A., & Davis J. P. (2011). Food protein functionality: A comprehensive approach. *Food Hydrocolloids, 25,* 1853-1864.

Folawiyo, Y. L., & Apenten, R. K. O. (1996). Effect of pH and ionic strength on the heat stability of rapeseed 12S (cruciferin) by the ANS fluorescence method. *Journal of the Science of Food and Agriculture, 70,* 241-246.

Folk, J. E. (1980). Transglutaminases. *Annual Review of Biochemistry, 49,* 517-531.

Food and Agriculture Organization of the United Nations. (2012). *Food outlook: Oil seeds market summary.* Retrieved from http://www.fao.org/fileadmin/templates/est/COMM_MARKETS_MONITORING/Oilcrops/Documents/Food_outlook_oilseeds/Food_outlook_Nov_12.pdf

Frados, J. (1976). *Plastics engineering handbook.* New York: Van Nostrand Reinhold.

Freer, E .M., Yim, K. S., Fuller, C. G., & Radke, C. J. (2004). Interfacial rheology of globular and flexible proteins at the hexadecane/water interface: comparison of shear and dilatation deformation. *The Journal of Physical Chemistry B, 108,* 3835-3844.

Friberg, S. E., Larsson, K., & Sjobolom, J.(2004). *Food Emulsions* (4th ed). New York, NY: Marcel Dekker.

Frinault, A., Gallant, D. J., Bouchet, B., & Dumont, J. P. (1997). Preparation of casein films by a modified wet spinning process. *Journal of Food Science, 62,* 744-747.

Fujikawa, S., Yokota, T., Koga, K., & Kumada, J. (1987). The continuous hydrolysis of geniposide to genipin using immobilized β-glucosidase on calcium alginate gel. *Biotechnology Letters, 9,* 697-702.

Fukushim, D., & Vanburen, J. P. (1970). Effect of physical and chemical processing factors on redispersibility of dried soy milk proteins. *Cereal Chemistry, 47,* 571-578.

Galazka, V. B., Smith, D., Ledward, D. A., & Dickinson, E. (1999). Interactions of ovalbumin with sulphated polysaccharides: effects of pH, ionic strength, heat and high pressure treatment. *Food Hydrocolloids, 13,* 81-88.

Ganzevles, R. A., Stuart, C. M. A., van Vliet, T., & de Jongh, H. H. K. (2006). Use of polysaccharides to control protein adsorption to the air-water interface. *Food Hydrocolloids, 20,* 872-878.

Garti, N., & Bisperink, C. (1998). Double emulsions: progress and applications. *Current Opinion in Colloid and Interface Science, 3,* 657-667.

Gehrig, P. M., Kryzaniak, A., Barciszewski, J., & Biemann, K. (1998). Mass spectrometric amino acid sequencing of a mixture of seed storage proteins (napin) from *Brassica napus* products of a multigene family. *Biochemistry, 93,* 3647-3652.

Gennadios, A. (2002). *Protein-based edible films and coatings* (pp. 1-672). Boca Raton: CRC Press.

Gennadios, A., Brandenburg, A. H., & Weller, C. L. (1993). Effect of pH on properties of wheat gluten and soy protein isolate films. *Journal of Agricultural and Food Chemistry, 41,* 1835-1839.

Gennadios, A., Brandenburg, A.H., Weller, C.L., and Testin, R.F. (1993). Effect of pH on properties of wheat gluten and soy protein isolate films. *Journal of Agricultural and Food Chemistry*. 41, 1835-1839.

Gennadios, A., Rhim, J. W., Handa, A., Weller, C. L., & Hanna, M. A. (1998). Ultraviolet radiation affects physical and molecular properties of soy protein films. *Journal of Food Science, 63,* 225-228.

Gennadios, A., Weller, C. L., & Gooding, C. H. (1994). Measurement errors in water vapor permeability of highly permeable, hydrophilic edible films. *Journal of Food Engineering, 21,* 395-409.

Gennadios, A., Weller, C. L., Hanna, M. A., & Froning, G. W. (1996). Mechanical and barrier properties and egg albumen films. *Journal of Food Science, 61,* 585-589.

Gerbanowskia, A., Rabillerb, C., & Guéguen, J. (2003). Behaviors of bovine serum albumin and rapeseed proteins at the air/water interface after grafting aliphatic or aromatic chains. *Journal of Colloid and Interface Science, 262,* 391-399.

Gharsallaoui, A., Yamauchi, K., Chambin, O., Cases, E., & Saurel, R. (2010). Effect of high methoxyl pectin on pea protein in aqueous solution and at oil/water interface. *Carbohydrate Polymers*, *80,* 817-27.

Ghodsvali, A., Khodaparast, M. H. H., Vosoughi, M., & Diosady, L. L. (2005). Preparation of canola protein materials using membrane technology and evaluation of meals functional peoperties. *Food Research International, 38,* 223-231.

Girard, M., Sanchez, C., Laneuville, S. I., Turgeon, S. L., & Gauthier, S. F. (2004). Associative phase separation of β-lactoglobulin/pectin solutions: a kinetic study by small angle static light scattering. *Colloids and Surface B: Biointerfaces*, *35*, 15-22.

Girard, M., Turgeon, S. L., & Gauthier, S. F. (2002). Interbiopolymer complexing between β-lactoglobulin and low- and high-methylated pectin measured by potentiometric titration and ultrafiltration. *Food Hydrocolloids, 16,* 585–591.

Gomez-Estaca, J., Montero, P., Fernandez-Matin, F., Alman, A., & Gomez-Guillen, M. C. (2009). Physical and chemical properties of tuna-skin and bovine-hide gelatin films with added aqueous oregano and rosemary extracts. *Food Hydrocolloids*, *23,* 1334-1341.

Gontard, N., & Guilbert, S. (1994). Biopackaging technology and properties of edible and/or biodegradable material of agricultural origin. *International Journal of Food Science and Technology*, *29,* 39-50.

Gontard, N., Duchez, C., Cuq, J. L., & Guilbert, S. (1994). Edible composite films of wheat gluten and lipids: water vapor permeability and other physical properties. *International Journal of Food Science and Technology*, *29,* 39-50.

Gontard, N., Guilbert, S., & Cuq, J. L. (1992). Edible wheat gluten films: influence of the main process variables on film properties using response surface methodology. *Journal of Food Science, 57,* 190-199.

Gontard, N., Guilbert, S., & Cuq, J. L. (1993). Water and glycerol as plasticizers affect mechanical and water vapor barrier properties of an edible wheat gluten film. *Journal of Food Science, 58,* 206-211.

Gonzalez, A., Strumia, M. C., & Igarzabal, C. I. A. (2011). Cross-linked soy protein as material for biodegradable films: synthesis, characterization and biodegradation. *Journal of Food Engineering, 106,* 331-338.

Gounga, M. E., Xu, S., & Wang, Z. (2007). Whey protein isolate-based edible films as affected by protein concentration, glycerol ratio and pullulan addition in film formation. *Journal of Food Engineering, 83*, 521-530.

Greener, I. K., & Fennema, O. (1989). Barrier properties and surface characteristics of edible, bilayer films. *Journal of Food Science, 54*, 1393-1399.

Gruener, L., & Ismond, M. A. H. (1997a). Effects of acetylation and succinylation on the functional properties of the canola 12S globulin. *Food Chemistry, 60,* 513-520.

Gruener, L., & Ismond, M. A. H. (1997b). Effects of acetylation and succinylation on the physicochemical properties of the canola 12S globulin. *Food Chemistry, 60,* 357-363.

Gu, Y. S., Decker, E. A., & McClements, D. J. (2005). Influence of pH and carrageenan type on properties of β-lactoglobulin stabilized oil-in-water emulsions. *Food Hydrocolloids, 19,* 83-91.

Gueguen, J., Bollecker, S., Schwenke, K. D., & Raab, B. (1990). Effect of succinylation on some physicochemical and functional properties of the 12S storage protein from rapeseed (*Brassica napus L.*). *Journal of Agricultural and Food Chemistry, 38,* 61-69.

Guilbert, S. (1986). *Food packaging and preservation* (pp. 371-394). London: Elsevier Applied Science.

Guo, X., Tian, S., & Small, D. M. (2010). Generation of meat-like flavourings from enzymatic hydrolysates of proteins from Brassica sp. *Food Chemistry, 119,* 167-172.

Gupta, A. N., Hohidar, H. B., & Aswal, V. K. (2007). Surface patch binding induced intermolecular complexation and phase separation in aqueous solutions of similarly charged gelatin-chitosan molecules. *Journal of Physical Chemistry B, 111,* 1137-10145.

Gupta, R., & Muralidhara, H. (2001). Interfacial challenges in the food industry: a review. *Trends in Food Science and Technology, 12,* 382-391.

Hagenmaier, R. D., & Shaw, P. E. (1992). Gas permeability of fruit coating waxes. *Journal of the American Society for Horticultural Science, 117,* 105-109.

Hagiwara, T., Kumagai, H., Matsunaga, T., and Nakamura, K. (1997). Analysis of Aggregate Structure in Food Protein Gels with the Concept of Fractal. *Bioscience, biotechnology, and biochemistry*. 61, 1663-1667.

Han, J. H., & Gennadios, A. (2005). Edible films and coatings: a review. In J. H. Han (Ed.), *Innovations in Food Packaging* (pp. 239-262). New York: Elsevier Academic.

Hansen, P. M. T., Hidalgo, J., & Gould, I. A. (1971). Reclamation of whey protein with carboxymethylcellulose. *Journal of Dairy Science, 54,* 830-834.

Harding, S. E., Day, K., Dhami, R., & Lowe, P. M. (1997). Further observations on the size, shape and hydration of kappa-carrageenan in dilute solution. *Carbohydrate Polymers, 32,* 81-87.

Harnsilawat, T., Pongsawatmanit, R., & McClements, D. J. (2006). Characterization of β-lactoglobulin-sodium alginate interactions in aqueous solutions: a calorimetry, light scattering, electrophoretic mobility and solubility study. *Food Hydrocolloids, 20,* 577-585.

Henry, D. C. (1931). The cataphoresis of suspended particles. Part I. The equation of cataphoresis. *Proceedings of the Royal Society London A, 133,* 106-129.

Hermansson, A., Eriksson, E., & Jordansson, E. (1991). Effects of potassium, sodium and calcium on the microstructure and rheological behaviour of kappa-carrageenan gels. *Carbohydrate Polymers, 16,* 297-320.

Hernandez-Izquierdo, V. M., & Krochta, J. M. (2008). Thermoplastic processing of proteins for film formation – a review. *Journal of Food Science, 73,* R30-R39.

Hernandez-Izquierdo, V. M., Reid, D. S., McHugh, T. H., Berrios, J. D., & Krochta, J. M. (2008). Thermal transitions and extrusion of glycerol-plasticized whey protein mixtures. *Journal of Food Science, 73,* E169-E175.

Hettiarachchy, N. S., & Eswaranandam, S. (2005). Edible films and coatings from soybean and other protein sources. In F. Shahidi (Ed.), *Bailey's Industrial Oil and Fat Products* (pp. 371-390). New York, NY: John Wiley & Sons, Inc.

Hettiarachchy, N. S., Kalapathy, U., & Myers, D. J. (1995). Alkali-modified soy protein with improved adhesive and hydrophobic properties. *Journal of the American Oil Chemists' Society, 72,* 1461-1464.

Hill, S.E. (1996). Emulsions. In G. M. Hall (Ed.) *Methods of Testing Protein Functionality* (pp. 153-158). New York, NY: Chapman and Hall.

Höglund, A. S., Rödin, J., Larsson, E., & Rask, L. (1992). Distribution of napin and cruciferin in developing rapeseed embryo. *Plant Physiology, 98,* 509-515.

Hu, F. B. (2003). Plant-based foods and prevention of cardiovascular disease: an overview. *American Journal of Clinical Nutrition, 78,* 544-551.

Hu, H., Fan, X., Zhou, Z., Xu., X., Fan, G., Wang, L., Huang, X., Pan, S., and Zhu, L. (2013). Acid-induced gelation behavior of soybean protein isolate with high intensity ultrasonic pre-treatments. *Ultrasonics Sonochemistry*. 20,187-195.

Hutchings, J. B. (1999). *Food color and appearance*. Gaithersburg: Chapman & Hall Foods Science Book, Aspen Publishers, Inc.

Ikeda, S., Foegeding, E.A., and Hagiwara, T. (1999). Rheological Study on the Fractal Nature of the Protein Gel Structure. *Langmuir*. 15, 8584-8589.

Islam, M., Phillips, G. O., Slijivo, A., Snowden, M. J., & Williams, P. A. (1997). Review of recent developments on regulatory, structural and functional aspects of gum Arabic. *Food Hydrocolloids, 11,* 493-505.

Ismond, M. A. H., & Welsh, W. D. (1992). Application of new methodology to canola protein isolation. *Food Chemistry, 45,* 125-127.

Jang, S. A., Lim, G. O., & Bin Song, K. (2011). Preparation and mechanical properties of edible rapeseed protein films. *Journal of Food Science, 76,* C218-C223.

Janjarasskul, T., & Krochta, J. M. (2010). Edible packaging materials. *Annual Review of Food Science and Technology, 1*, 415-448.

Jaramillo, D. P., Roberts, R. F., & Coupland, J. N. (2011). Effect of pH on the properties of soy protein–pectin complexes. *Food Research International, 44*, 911-916.

Jin, J., Song, M., & Hourston, D. J. (2004). Novel chitosan-based films cross-linked by genipin with improved physical properties. *Biomacromolecules, 5,* 162-168.

Jönsson, M., Skepö, M., Tjerneld, F., & Linse, P. (2003). Effect of spatially distributed hydrophobic surface residues on protein polymer association. *The Journal of Physical Chemistry B, 107*, 5511-5518.

Joshi, M., Adhikari, B., Aldred, P., Panozzo, J. F., Kasapis, S., & Barrow, C. J. (2012). Interfacial and emulsifying properties of lentil protein isolate. *Food Chemistry, 134,* 1343-1353.

Jourdain, L., Leser, M. E., Schmitt, C., Michel, M., & Dickinson, E. (2008). Stability of emulsions containing sodium caseinate and dextran sulfate: Relationship to complexation in solution. *Food Hydrocolloids, 22,* 647-659.

Jung, S., Murphy, P. A., & Johnson, L. A. (2005). Physicochemical and functional properties of soy protein substrates modified by low levels of protease hydrolysis. *Journal of Food Science C: Food Chemistry and Toxicology, 70,* C180-C187.

Jyothi, T. C., Singh, S. A., & Appu Rao, A. G. (2007). Conformation of napin (Brassica juncea) in salts and monohydric alcohols: Contribution of electrostatic and hydrophobic interactions. *Journal of Agricultural and Food Chemistry, 55,* 4229-4236.

Kaibara, K., Okazaki, T., Bohidar, H. B., & Dubin, P. L. (2000). pH-Induced coacervation in complexes of bovine serum albumin and cationic polyelectrolytes. *Biomacromolecules, 1,* 100-107.

Kamper, S. L., & Fennema, O. (1984). Water-vapor permeability of an edible, fatty-acid, bilayer film. *Journal of Food Science, 49,* 1482-1485.

Kamper, S. L., & Fennema, O. R. (1985). Use of an edible film to maintain water and vapor gradient in foods. *Journal of Food Science, 50,* 382-384.

Karbowiak, T., Hervet, H., Leger, L., Champion, D., Debeaufort, F., & Voilley, A. (2006). Effect of plasticizers (water and glycerol) on the diffusion of a small molecule in iota carrageenan biopolymer films for edible coating application. *Biomacromolecules, 7,* 2011-2019.

Karimi, F., Qazvini, N. T., & Namivandi-Zangeneh, R. (2013). Fish gelatin/Laponite biohybrid elastic coacervates: A complexation kinetics-structure relationship study. *International Journal of Biological Macromolecules, 62,* 102-113.

Karperien, A. (2012). What is Lacunarity?. http://rsb.info.nih.gov/ij/plugins/ fraclac /FLHelp/Lacunarity.htm. Retrieved on August 1, 2014.

Kato, A., & Nakai, S. (1980). Hydrophobicity determined by fluorescence probe methods and its correlation with surface properties of proteins. *Biochimica et Biophysica Acta, 624,* 13-20.

Keowmaneechai, E. and McClements, D.J. (2002). Effect of $CaCl_2$ and KCl on Physicochemical Properties of Model Nutritional Beverages Based on Whey Protein Stabilized Oil-in-Water Emulsions. *Journal of Food Science*. 67, 665-671.

Keowmaneechai, E., & McClements, D. J. (2002). Effect of $CaCl_2$ and KCl on physicochemical properties of model nutritional beverages based on whey protein stabilized oil-in-water emulsions. *Journal of Food Science, 67,* 665-671.

Ker, Y.C. and Chen, R.H. (1998). Shear-induced conformational changes and gelation of soy protein isolate suspensions. *LWT-Food Science and Technology*. 31, 107–113.

Kester, J. J., & Fennema, O. R. (1986). Edible films and coatings – a review. *Food Technology, 40,* 47-59.

Khattab, R. Y., & Arntfield, S. D. (2009). Functional properties of raw and proessed canola meal.

Food Science and Technology-LEB, 42, 1119-1124.

Kim, H. –J., Decker, E. A., & McClements, D. J. (2003). Influence of sucrose on droplet flocculation in hexadecane oil-in-water emulsions stabilized by α-lactoglobulin. *Journal of Agricultural and Food Chemistry, 51,* 766-772.

Kim, K. M., Hwang, K. T., Weller, C. L., & Hanna, M. A. (2002). Preparation and characterization of soy protein isolate films modified with sorghum wax. *Journal of the American Oil Chemists Society, 79,* 615-619.

Kinsella, J. E. (1979). Functional properties of soy proteins. *Journal of American Oil Chemists' Society, 56,* 242-258.

Kinsella, J. E., Damodaran, S., & German, J. B. (1985). Physicochemical and functional properties of oilseed proteins with emphasis on soy proteins. In A. Altshul & H. Wilcke (Eds.), *New Protein Foods: Seed* (pp. 107-179). London, UK: Academic Press.

Kizilay E., Basak Kayitmazer, A., & Dubin, P. L. (2011). Complexation and coacervation of polyelectrolytes with oppositely charged colloids. *Advances in Colloid and Interface Science, 167,* 24-37.

Klassen, D. R., & Nickerson, M. T. (2012). Effect of pH on the formation of electrostatic complexes within admixtures of partially purified pea proteins (legumin and vicilin) and gum Arabic polysaccharides. *Food Research International, 46,* 167-176.

Klassen, D.R., Elmer, C.M., and Nickerson, M.T. (2010). Associative phase separation involving canola protein isolate with both sulphated and carboxylated polysaccharides. *Food Chemistry*. 126, 1094-1101.

Klemmer, K. J., Waldner, L. Stone, A., Low, N. H., & Nickerson, M. T. (2012). Complex coacervation of pea protein isolate and alginate polysaccharides. *Food Chemistry, 130,* 710-715.

Klockeman D. M., Toledo, R., & Sims, K. A. (1997). Isolation and characterization of defatted canola meal protein. *Journal of Agricultural and Food Chemistry, 45,* 3867-3870.

Kokoszka, S., Debeaufort, F., Hambleton, A., Lenart, A., & Voilley, A. (2010). Protein and glycerol contents affect physico-chemical properties of soy protein isolate-based edible films. *Innovative Food Science and Emerging Technologies, 11,* 503-510.

Kowalczyk, D., & Baraniak, B. (2011). Effects of plasticizers, pH and heating of film-forming solution on the properties of pea protein isolate films. *Journal of Food Engineering, 105,* 295-305.

Krause J. P., & Schwenke, K. D. (2001). Behaviour of a protein isolate from rapeseed (*Brassica napus*) and its main protein components — globulin and albumin — at air/solution and solid interfaces, and in emulsions. *Colloids and Surfaces B: Biointerfaces, 21,* 29–36.

Krause, J. P., Schultz, M., & Dudek, S. (2002). Effect of extraction conditions on composition, surface activity and rheological properties of protein isolates from flaxseed (*Linum usitativissimum L*). *Journal of the Science of Food and Agriculture, 82,* 970-976.

Krochta, J. M. (1997). *Food proteins and their applications* (pp. 529-550). New York: Marcel Dekker.

Krochta, J. M. (2002). Protein as raw materials for films and coatings: definition, current status, and opportunities. In A. Gennadios (Ed.), *Protein-based Films and Coatings* (pp. 1-40). New York: CRC Press.

Krochta, J. M., & De Mulder-Johnston, C. (1997). Edible and biodegradable polymer films: challenges and opportunities. *Food Technology, 51,* 61-73.

Krog, N. J., & Sparsø, F. V. (2004). Food emulsifiers: their chemical and physical properties. In S. E. Friberg, K. Larsson & J. Sjöblom (Eds.), *Food Emulsions* (4th ed.) (pp. 86-87). New York, NY: Marcel Dekker, Inc.

Krzyzaniak, A., Burova, T., Haertle, T., & Barciszewski, J. (1998). The structure and properties of napin seed storage protein. *Die Nahrung, 42,* 201-204.

Kulmyrzaev, A. A., & Schubert, H. (2004). Influence of KCl on the physicochemical properties of whey protein stabilized emulsions. *Food Hydrocolloids, 18,* 13-19.

Kulmyrzaev, A., Chanamai, R., & McClements, D. J. (2000). Influence of pH and $CaCl_2$ on the stability of dilute whey protein stabilized emulsions. *Food Research International, 33,* 15-20.

Laemmli, U. K. (1970). Cleavage of structural proteins during the assembly of the head of bacteriophage T4. *Nature, 227,* 680–685.

Lakemond, C.M.M., de Jongh, H.H.J., Paques, M., van Vliet, T., Gruppen, H., and Voragen, A.G.J. (2003). Gelation of soy glycinin; influence of pH and ionic strength on network structure in relation to protein conformation. *Food Hydrocolloids*. 17, 365-377.

Lampart-Szczapa, E. (2001). Legumin and oilseed protein. In Z. E. Sikorski, editor. *Chemical and functional properties of food proteins*. (pp. 407-436). New York: CRC Press.

Lamsal, B.P., Jung, S., and Johnson, L.A. (2007). Rheological properties of soy protein hydrolysates obtained from limited enzymatic hydrolysis. *LWT-Food Science and Technology*. 40, 1215-1223.

Landry, J., & Delhaye, S. (1993). Determination of tryptophan in feedstuffs: comparison of sodium hydroxide and barium hydroxide as hydrolysing agents. *Food Chemistry, 49,* 95-97.

Lee, H. C., Htoon, A. K., Uthayakumaran, S., & Paterson J. L. (2007). Chemical and functional quality of protein isolated from alkaline extraction of Australian lentil cultivars: Matilda and Digger. *Food Chemistry, 102,* 1199-1207.

Léger, L.W. and Arntfield, S.D. (1993). Thermal gelation of the 12S canola globulin. *Journal of the American Oil Chemists' Society*. 70, 853-861.

Li, X., Fang, Y., Al-Assaf, S., Phillips, G., & Jiang, F. (2012). Complexation of bovine serum albumin and sugar beet pectin: stabilising oil-in-water emulsions. *Journal of Colloid and Interface Science, 388,* 103-111.

Li, Y. J., Xia, J. L., & Dubin, P. L. (1994). Complex-formation between polyelectrolyte and oppositely charged mixed micelles - static and dynamic light-scattering study of the effect of polyelectrolyte molecular-weight and concentration. *Macromolecules, 27,* 7049-7055.

Liang, H. C., Chang, W. H., Liang, H. F., Lee, M. H., & Sung, H. W. (2004). Crosslinking structure of gelatin hydrogels crosslinked with genipin or a water-soluble carbodiimide. *Journal of Applied Polymer Science, 91,* 4017-4026.

Lieberma, E. R., & Gilbert, S. G. (1973). Gas permeation of collagen films as affected by crosslinkage, moisture, and plasticizer content. *Journal of Polymer Science Part C-Polymer Symposium, 41,* 33-43.

Liebermann, E. R., Gilbert, S. G., & Srivinasa, V. (1972). The use of gas permeability as a molecular probe for the study of cross-linked collagen structures. *Trans. NY Academy of Science II, 34*, 694-708.

Lii, C. Y., Liaw, S. C., Lai, V. M. F., & Tomasik, P. (2002). Xanthan gum–gelatin complexes. *European Polymer Journal, 38*, 1377-1381.

Liu, C., Tellez-Garay, A. M., & Castell-Perez, M. E. (2004). Physical and mechanical properties of peanut protein films. *Lebensmittel-Missenschaft Und-Technologies-Food Science and Technology, 37,* 731-738.

Liu, L., Kerry, J. F., & Kerry, J. P. (2006). Effect of food ingredients and selected lipids on the physical properties of extruded edible films/castings. *International Journal of Food Science and Technology, 41,* 295-302.

Liu, S., Cao, Y. L., Ghosh, S., Rousseau, D., Low, N. H., & Nickerson, M. T. (2010a). Intermolecular interactions during complex coacervation of pea protein isolate and gum Arabic. *Journal of Agricultural and Food Chemistry, 58,* 552-556.

Liu, S., Elmer, C., Low, N. H., & Nickerson, M. T. (2010b). Effect of pH on the functional behaviour of pea protein isolate-gum Arabic complexes. *Food Research International, 43,* 489-495.

Liu, S., Low, N. H., & Nickerson, M. T. (2009). Effect of pH, salt and biopolymer ratio on the formation of pea protein isolate-gum Arabic complexes. *Journal of Agricultural and Food Chemistry, 57,* 1521-1526.

Liu, Y., Chen, W., & Kim, H. (2012). Mechanical and antimicrobial properties of genipin crosslinked chitosan/poly(ethylene glycol) IPN. *Journal of Macromolecular Science, Part B-Physics, 51,* 1069-1079.

Lizarraga, M. S., Vicin, P. D., Gonzalez, R., Rubiolo, A., & Santiago, L. G. (2006). Rheological behaviour of whey protein concentrate and lambda-carrageenan aqueous mixtures. *Food Hydrocolloids, 20,* 740-748.

Lönnerdal, B., & Janson, J. C. (1972). Studies on *Brassica* seed proteins: I. The low molecular weight proteins in rapeseed. Isolation and characterization. *Biochimica et Biophysica Acta (BBA) - Protein Structure*, 278, 175-183.

Lutz, R., Aserin, A., Portnoy, Y., Gottlieb, M., & Garti, N. (2009). On the confocal images and the rheology of whey protein isolated and modified pectins associated complex. *Colloids and Surfaces B: Biointerfaces, 69,* 43-50.

Makri, E. A., & Doxastakis, G. I. (2007). Surface tension of *Phaseolus vulgaris* and *coccieus* proteins and effect of polysaccharides on their foaming properties. *Food Chemistry, 101,* 37-48.

Malabat, C., Nchez-Vioque, I. R. S., Rabiller, C., & Gu guen, J. (2001). Emulsifying and foaming properties of native and chemically modified peptides from the 2S and 12S proteins of rapeseed (*Brassica napus L.*). *Journal of the American Oil Chemists' Society*, *78,* 235-242.

Mangavel, C., Barbot, J., Gueguen, J., & Popineau, Y. (2003). Molecular determinants of the influence of hydrophilic plasticizers on the mechanical properties of cast wheat gluten. *Journal of Agricultural and Food Chemistry, 51,* 1447-1452.

Marambe, P. W. M. L. H. K., Shand, P. J., & Wanasundara, J. P. D. (2013). In vitro digestibility of flaxseed (*Linum usitatissimum L.*) protein: effect of seed mucilage, oil and thermal processing. *International Journal of Food Science and Technology, 48,* 628–635.

Marcone, M. F., Kakuda, Y., & Yada, R. Y. (1998). Salt-soluble seed globulins of various dicotyledonous and monocotyledonous plants. II. Structural characterization. *Food Chemistry, 63,* 265–274.

Martinez, K. D., Sanchez, C. C., Ruiz-Henestrosa, V. P., Rodriguez Patino, J. M., & Pilosof, A. M. R. (2007). Soy protein-polysaccharide interactions at the air-water interface. *Food Hydrocolloids, 21,* 804-812.

Martin-Polo, M. O., & Voilley, A. (1990). Comparative study of water vapor permeability of edible films composed of arabic gum and glycerol monostearate. *Sciences Des Aliments, 10,* 473-483.

Matsudomi, N., Sasaki, T., Kato, A., & Kobayashi, K. (1985). Conformational changes and functional properties of acid-modified soy protein. *Agricultural and Biological Chemistry*, *49,* 1251-1256.

McClements D. J. (2006). Non-covalent interactions between proteins and polysaccharides. *Biotechnology Advances, 24,* 621-625.

McClements, D. J. (2000). Comments on viscosity enhancement and depletion flocculation by polysaccharides. *Food Hydrocolliods, 14,* 173–177.

McClements, D. J. (2004). Protein-stabilized emulsions. *Current Opinion in Colloid & Interface Science, 9,* 305-313.

McClements, D. J. (2005). *Food Emulsions Principles, Practices, and Techniques.* Boca Raton, FL: CRC Press.

McClements, D. J. (2007). Critical review of techniques and methodologies for characterization of emulsion stability. *Critical Reviews in Food Science and Nutrition, 47,* 611-649.

McDanell, R., McLean, A. E. M., Hanley, A. B., Heaney, R. K., & Fenwick, G. R. (1988). Chemical and biological properties of indole glucosinolates (glucobrassicins): a review. *Food and Chemical Toxicology, 26,* 59-70.

McHugh, T. H., & Krochta, J. M. (1994). Permeability properties of edible films. In J. M. Krochta, E. A. Baldwin & M. Nisperos-Carriedo (Eds.), *Edible Films and Coatings to Improve Food Quality* (pp. 139-187). Lancaster, PA: Technomic Publishing Co.

McHugh, T. H., Avena-Bustillos, R. D., & Krochta, J. M. (1993). Hydrophilic edible films: modified procedure for water vapor permeability and explanation of thickness effect. *Journal of Food Science, 58,* 899-903.

McKenzie, H.A and Wallace, H.S. (1954). The Kjeldahl determination of nitrogen – A critical study of digestion conditions – Temperature, Catalyst, and Oxidizing agent. *Australian Journal of Chemistry*. 7, 55-70.

Menegalli, F. C., Sobral, P. J. A., Roques, M. A., & Laurent, S. (1999). Characteristics of gelatin biofilms in relation to drying process conditions near melting. *Drying Technology, 17,* 1697-1706.

Mengatto, L., Luna, J. A., & Cabrera, M. I. (2010). Influence of cross-linking density on swelling and estradiol permeation of chitosan membranes. *Journal of Material Science, 45,* 1046-1051.

Mi, F. L., Sung, H. W., Shyu, S. S., Su, C. C., & Peng, C. K. (2003). Synthesis and characterization of biodegradable TPP/genipin co-crosslinked chitosan gel beads. *Polymer, 44,* 6521-6530.

Micard, V., Belamri, R., Morel, M. H., & Guilbert, S. (2000). Properties of chemically and physically treated wheat gluten films. *Journal of Agricultural and Food Chemistry, 48,* 2948-2953.

Michon, T., Wang, W., Ferrasson, E., & Gueguen, J. (1999). Wheat prolamine cross-linking through dityrosine formation catalyzed by peroxidases: improvement in the modification of poorly assessable substrate by "indirect" catalysis. *Biotechnology and Bioengineering, 63,* 449-458.

Mieth, G., Bruckner, J., Kroll, J., & Pohl, J. (1983). Rapeseed: constituents and protein products part 2: preparation and properties of protein- enriched products. *Die Nahrung, 39,* 32-41.

Mikkonen, K. S., Heikkinen, S., Soovre, A., Peura, M., Serimaa, R., Talja, R. A., Helen, H., Hyvonen, L., & Tenkanen, M. (2009). Films from oat spelt arabinoxylan plasticized with glycerol and sorbitol. *Journal of Applied Polymer Science, 114,* 457-466.

Miller, K. S., & Krochta, J. M. (1997). Oxygen and aroma barrier properties of edible films: a review. *Trends in Food Science & Technology, 8,* 228-237.

Miquelim, J. N., Lannes, S. C. S., & Mezzenga, R. (2010). pH influence on the stability of foams with protein-polysaccharide complexes at their interfaces. *Food Hydrocolloids, 24,* 398-405.

Mithen, R. F., Dekker, M., Verkerk, R., Rabot, S., & Johnson, I. T. (2000). Review: The nutritional significance, biosynthesis and bioavailability of glucosinolates in human foods. *Journal of the Science of Food and Agriculture, 80,* 967-984.

Mleko, S., Li-Chan, E. C. Y., & Pikus, S. (1997). Interactions of κ-carrageenan with whey proteins in gels formed at different pH. *Food Research International, 30,* 427-433.

Monsalve, R. I., & Rodriguez, R. (1990). Purification and characterization of proteins from the 2S fraction from seeds of the Brassicaceae family. *Journal of Experimental Botany, 41,* 89-94.

Monsalve, R. I., Villalba, M., López-Otín, C. & Rodríguez, R. (1991). Structural analysis of the small chain of the 2S albumin, napin nIII, from rapeseed. Chemical and spectroscopic evidence of an intramolecular bond formation. *Biochimica et Biophysica Acta (BBA) - Protein Structure and Molecular Enzymology, 1078,* 265-272.

Moreno, F. J. & Clemente, A. (2008). 2S albumin storage proteins: what makes them food allergens. *Open Biochemistry Journal, 2,* 16-28.

Morr, C. V., German, B., Kinsella, J. E., Regenstein, J. M., Van Buren, J. P., Kilara, A., Lewis, B. A., & Manigo, M. E. (1985). A collaborative study to develop a standardized food protein solubility procedure. *Journal of Food Science, 50,* 1715-1718.

Morris, E. R., Rees, D. A., & Robinson, G. (1980). Cation-specific aggregation of carrageenan helices: domain model of polymer gel structure. *Journal of Molecular Biology, 138,* 349-362.

Motta, A., Barbato, B., Foss, C., Torricelli, P., & Migliaresi, C. (2011). Stabilization of *Bombyx mori* silk fibroin/sericin films by crosslinking with PEG-DE 600 and genipin. *Journal of Bioactive and Compatible Polymers, 26,* 130-143.

Mounsey, J. S., O'Kennedy, B. T., Fenelon, M. A., & Brodkorb, A. (2008). The effect of heating on β-lactoglobulin–chitosan mixtures as influenced by pH and ionic strength. *Food Hydrocolloids, 22,* 65-73.

Moure, A., Domínguez, H., & Parajó, J. C. (2005). Fractionation and enzymatic hydrolysis of soluble protein present in waste liquors from soy processing. *Journal of Agricultural and Food Chemistry, 53,* 7600-7608.

Moure, A., Sineirob, J., Domíngueza, H., & Parajóa, J. C. (2006). Functionality of oilseed protein products: A review. *Food Research International, 39,* 945–963.

Murillo-Martínez, M. M., Pedroza-Islas, R., Lobato-Calleros, C., Martínez-Ferez, A., & Vernon-Carter, E. J. (2011). Designing W1/O/W2 double emulsions stabilized by protein-polysaccharide complexes for producing edible films: Rheological, mechanical and water vapour properties. *Food Hydrocolloids, 25,* 577-585.

Murray, E. D., Maurice, T. J., Barker, L. D., & Myers, C. D. (1980). Process for isolation of proteins using food grade salt solutions at specified pH and ionic strength. US Patent: 4208323.

Muzzarelli, R. A. A. (2009). Genipin-crosslinked chitosan hydrogels as biomedical and pharmaceutical aids. *Carbohydrate Polymers, 77,* 1-9.

Naczk, M., Amarowicz, R., & Shahidi, F. (1998). Role of phenolics in flavor of rapeseed protein products. *Development in Food Science, 40,* 597-613.

Nagano, T. and Tokita, M. (2011). Viscoelastic properties and microstructures of 11S globulin and soybean protein isolate gels: Magnesium chloride-induced gels. *Food Hydrocolloids*. 25, 1647-1654.

Nakai, S., Ho, L., Helbig, N., Kato, A., & Tung, M. A. (1980). Relationship between hydrophobicity and emulsifying properties of some plant proteins. *Canadian Institute of Food Science and Technology Journal, 13,* 23-27.

Neves, V. A., & Lourenco, E. J. (1995). Isolation and *in vitro* hydrolysis of globulin G1 from Lentils (*Lens Culinars*, Medik). *Journal of Food Biochemistry, 19,* 109-120.

Newkirk, R. (2009). Canola meal feed industry guide 4th ed. http://cigi.ca/wp-content/uploads/2011/12/2009-Canola_Guide.pdf. Retrieved on January 17, 2013.

Newkirk, R. W. (2009). *Canola meal feed industry guide* (4th ed.) Canola Council of Canada, Winnipeg, M.B.

Nickerson, M. T., & Paulson, A. T. (2004). Rheological properties of gellan, κ-carrageenan and alginate polysaccharides: effect of potassium and calcium ions on macrostructure assemblages. *Carbohydrate Polymers, 58*, 15-24.

Nickerson, M. T., Paulson, A. T., & Hallett, F. R. (2004). Dilute solution properties of κ-carrageenan polysaccharides: effect of potassium and calcium ions on chain conformation. *Carbohydrate Polymers, 58,* 25-33.

Nickerson, M. T., Paulson, A. T., & Speers, R. A. (2003). Rheological properties of gellan solutions: effect of calcium ions and temperature on pre-gel formation. *Food Hydrocolloids, 17,* 577-583.

Nilsson, S., & Piculell, L. (1991). Helix-coil transitions of ionic polysaccharide analyzed within the Poisson-Boltzmann cell model. 4-Effects of site specific counterion binding. *Macromolecules, 24,* 3804-3811.

Nitecka, E., & Schwenke, K. D. (1986). Functional properties of plant proteins. Part 8. Effect of some succinylation on some functional properties of the main globulin fraction from rapeseed (*Brassica napus L.). Die Nahrung, 30,* 969-974.

Nordlee, J. A., Taylor, S. L., Townsend, J. A., Thomas, L. A., & Bush, R. K. (1996). Identification of a Brazil-nut allergen in transgenic soybeans. *The New England Journal of Medicine, 334,* 688-692.

Ohlson, R. and Anjou, K. (1979). Rapeseed protein products. *Journal of the American Oil Chemistry*. 56, 431-437.

Ohlson, R., & Anjou, K. (1979). Rapeseed protein products. *Journal of the American Oil Chemists' Society, 56,* 431-437.

Okamoto, S. (1978). Factors affecting protein film formation. *Cereal Foods World, 23,* 256-262.

Ooi, Z. X., Ismail, H., Baker, A. A., & Azizi, N. A. A. (2012). The comparison effect of sorbitol and glycerol as plasticizing agents on the properties of biodegradable polyvinyl alcohol/rambutan skin waste flour blends. *Polymer-Plastics Technology and Engineering, 51,* 432-437.

Orliac, O., Rouilly, A., Silvestre, F., & Rigal, L. (2002). Effects of additives on the mechanical properties, hydrophobicity and water uptake of thermo-moulded films produced from sunflower protein isolate. *Polymer, 43,* 5417-5425.

Orliac, O., Rouilly, A., Silvestre, F., & Rigal, L. (2003). Effects of various plasticizers on the mechanical properties, water resistance and aging of thermo-moulded films made from sunflower proteins. *Industrial Crops and Products, 18,* 91-100.

Ortiz, M. S., & Wagner, J. R. (2002). Hydrolysates of native and modified soy protein isolates: structural characteristics, solubility and foaming properties. *Food Research International, 35,* 511-518.

Ortiz, M. S.E., Puppo, M. C., & Wagner, J. R. (2004). Relationship between structural changes and functional properties of soy protein isolates–carrageenan systems. *Food Hydrocolloids, 18,* 1045-1053.

Ou, S. Y., Kwok, K. C., & Kang, Y. J. (2004). Changes in vitro digestibility and available lysine of soy protein isolate after formation of film. *Journal of Food Engineering, 64,* 301-305.

Ould, E. M. M., & Turgeon, S. L. (2000a). Rheology of κ-carrageenan and β-lactoglobulin mixed gels. *Food Hydrocolloids, 14,* 29-40.

Ould, E. M. M., & Turgeon, S. L. (2000b). The effects of pH on the rheology of β-lactoglobulin/κ-carrageenan mixed gels. *Food Hydrocolloids, 14,* 245-251.

Overbeek, J. T. J., & Voorn, M. J. (1957). Phase separation in polyelectrolyte solutions. Theory of complex coacervation. *Journal of Cellular and Comparative Physiology, 49,* 7-26.

Papalamprou, E. M., Doxastakis, G. I., Biliaderis, C. G., & Kiosseoglou, V. (2009). Influence of preparation methods on physicochemical and gelation properties of chickpea protein isolates. *Food Hydrocolloids, 23,* 337-343.

Papalamprou, E. M., Makri, E. A., Kiosseoglou, V. D., & Doxastakis, G. (2005). Effect of medium molecular weight xanthan gum in rheology and stability of oil-in-water emulsion stabilized with legume proteins. *Journal of the Science of Food and Agriculture, 85,* 1967-1973.

Park, S. K., Bae, D. H., & Rhee, K. C. (2000). Soy biopolymers cross-linked with glutaraldehyde. *Journal of the American Oil Chemists Society, 77,* 879-883.

Paulson, A. T., & Tung, M. A. (1987). Solubility, hydrophobicity and net charge of succinylated canola protein isolate. *Journal of Food Science, 52,* 1557-1561.

Pearce, K. N., & Kinsella, J. E. (1978). Emulsifying properties of proteins: evaluation of a turbidimetric technique. *Journal of Agriculture and Food Chemistry, 26,* 716–23.

Pearson, A. M. (1983). Soy proteins. In B. J. F. Hudson (Ed.), *Developments in food proteins*. (pp. 67-108). London: Applied Science Publishers.

Pedroche, J., Yust, M. M., Lqari, H., Giron-Calle, J., Alaiz, M., Vioque, J., & Millan, F. (2004). Brassica carinata protein isolates: chemical composition, protein characterization and improvement of functional properties by protein hydrolysis. *Food Chemistry, 88,* 337-346.

Perez-Gago, M. B., & Krochta, J. M. (2005). Emulsion and bi-layer edible films. In J. H. Han (Ed.), *Innovations in Food Packaging* (pp. 384-402). New York: Elsevier Academic.

Piculell, L. (2006). Gelling carrageenans. In A. M. Stephen, G. O. Philips & P. A. Williams (Eds.), *Food polysaccharides and their applications* (pp. 239-287). Boca Raton, FL: CRC Press.

Pinterits, A. and Arntfield, S.D. (2008). Improvement of canola protein gelation properties through enzymatic modification with transglutaminase. *LWT-Food Science and Technology*. 41, 128-138.

Pinterits, A., & Arntfield, S. D. (2008). Improvement of canola protein gelation properties through enzymatic modification with transglutaminase. *Food Science and Technology, 41,* 128-138.

Plashchina, I. G., Mrachkovskaya, T. A., Danilenko, A. N., Kozhevnikov, G. O., Starodubrovskaya, N. Y., Braudo, E. E., & Schwenke, K. D. (2001). Complex formation of faba bean legumin with chitosan: Activity and emulsion properties of complexes. In E. Dickinson & R. Miller (Eds.), *Food colloids: fundamentals of formulation* (pp. 293-303). Great Britain: Royal Society of Chemistry.

Pommet, M., Redl, A., Morel, M. H., Domenek, S., & Guilbert, S. (2003). Thermoplastic processing of protein-based bioplastics: chemical engineering aspects of mixing, extrusion and hot molding. *Macromolecular Symposia, 197,* 207-217.

Porta, R., Mariniello, L., Di Pierro, P., Sorrentino, A., & Giosaffatto, C. V. L. (2011). Transglutaminase crosslinked pectin- and chitosan-based edible films: a review. *Critical Reviews in Food Science and Nutrition, 51,* 223-238.

Pownall, T. L., Udenigwe, C. C., & Aluko, R. E. (2010). Amino acid composition and antioxidant properties of pea seed (*Pisum sativum* L.) enzymatic protein hydrolysate fractions. *Journal of Agricultural and Food Chemistry, 58,* 4712-4718.

Pruneda, E., Hernandez-Peralta, J. M., Esquivel, K., Lee, S. Y., Godinez, L. A., & Mendoza, S. (2008). Water vapor permeability, mechanical properties and antioxidant effect of Mexican oregano-soy based edible films. *Journal of Food Chemistry, 73,* C488-C493.

Psomiadou, E., Arvanitoyannis, I., & Yamamoto, N. (1996). Edible films made from natural resources: microcrystalline cellulose (MCC), methylcellulose (MC) and corn starch and polyols – Part 2. *Carbohydrate Polymers, 31,* 193-204.

Pushpadass, H. A., Marx, D. B., Wehling, R. L., & Hanna, M. (2009). Extrusion and characterization of starch films. *Cereal Chemistry, 86,* 44-51.

Qi, W., Fong, C., & Lamport, D. T. A. (1991). Gum arabic glycoprotein is a twisted hairy rope. *Plant Physiology, 96,* 848-855.

Raab, B., Leman, H., Schwenke, K. D., & Kozlowska, H. (1992). Comparative study of the protein patterns of some rapeseed (*Brassica napus L.*) varieties by means of polyacrylamide gel electrophoresis and high-performance liquid chromatography. *Die Nahrung, 36,* 239-247.

Randall, R. C., Phillips, G. O., & Williams, P. A. (1989). Fractionation and characterization of gum from *Acacia senegal*. *Food Hydrocolloids, 3,* 66-75.

Ray, M., & Rousseau, D. (2013). Stabilization of oil-in-water emulsions using mixtures of denatured soy whey proteins and soluble soybean polysaccharide. *Food Research International, 52,* 298-307.

Redl, A., Morel, M. H., Bonicel, J., Vergnes, B., & Guilbert, S. (1999). Extrusion of wheat gluten plasticized with glycerol: influence of process conditions on flow behavior, rheological properties, and molecular size distribution. *Cereal Chemistry, 76,* 361-370.

Rees, D. A., Steele, I. W., & Williamson, F. (1969). Conformationalanalysis of polysaccharides. III. The relation between stereochemistry and properties of some polysaccharide sulfates (1). Journal of Polymer Science: *Polymer Letters, 28,* 261-276.

Renard, D., van de Velde, F., and Visschers, R.W. (2006). The gap between food gel structure, texture and perception. *Food Hydrocolloid*. 20, 423-431.

Renkema, J.M.S. (2004). Relations between rheological properties and network structure of soy protein gels. *Food Hydrocolloids*. 18, 39-47.

Renkema, J.M.S. and van Vliet T. (2002). Heat-induced gel formation by soy proteins at neutral *Journal of Agricultural and Food Chemistry*. 50, 1569-1573.

Renkema, J.M.S., Knabben, J.H.M., and van Vliet T. (2001). Gel formation by β-conglycinin and glycinin and their mixtures. *Food Hydrocolloids*. 15, 407-414.

Rhim, J. W., & Ng, P. K. W. (2007). Natural biopolymer-based nanocomposite films for packaging applications. *Critical Review in Food Science and Nutrition, 47,* 411-433.

Rhim, J. W., Gennadios, A., Weller, C. L., Cazeirat, C., & Hanna, M. A. (1998). Soy protein isolate-dialdehyde starch films. *Industrial Crops and Products, 8,* 195-203.

Rhim, J. W., Wu, Y., Weller, C. L., & Schnepf, M. (1999). Physical characteristics of emulsified soy protein fatty acid composite films. *Science Des Aliments, 19,* 57-71.

Robins, M., & Wilde, P. (2003). Colloids and emulsion. In A. Caballero (Ed.), *Encyclopedia of Food Sciences and Nutrition* (2nd ed.) (pp. 1517-1524). Oxford, UK: Academic Press.

Rochas, C., & Rinaudo, M. (1980). Activity coefficients of counter-ions and conformation in kappa-carrageenan systems. *Biopolymers, 19,* 1675-1687.

Rockland, L. B. (1984). Moisture sorption-practical aspects of isotherm measurement and use – Labuza, TP. *Food Technology, 38,* 112-112.

Rodrigues, S., Rosa da Costa, A. M., & Grenha A. (2012). Chitosan/carrageenan nanoparticles: effect of cross-linking with tripolyphosphate and charge ratios. *Carbohydrate Polymers, 89,* 282-289.

Rogers, M.A. and Kim, J.H.J. (2011). Rheological assessment of the sol-gel transition for self-assembling low molecular weight gelators. *Food Research International*. 44, 1447-1451.

Rojas-Grau, M. A., Tapia, M. S., Rodriguez, F. J., Carmona, A. J., & Martin-Belloso, O. (2007). Alginate and gellan based edible coatings as carriers of antibrowning agents applied on fresh-cut Fuji apples. *Food Hydrocolloids, 21,* 118-127.

Roy, F., Boye, J. I., & Simpson B. K. (2010). Bioactive proteins and peptides in pulse crops: pea, chickpea and lentil. *Food Research International, 43,* 432-442.

Ru, Q., Wang, Y., Lee, J., Ding, Y., & Huang, Q. (2012). Turbidity and rheological properties of bovine serum albumin/pectin coacervates: Effect of salt concentration and initial protein/polysaccharide ratio. *Carbohydrate Polymers, 88,* 838– 846.

Rubino, M.I., Arntfield, S.D., Nadon, C.A., and Bernatsky, A. (1996). Phenolic protein interactions in relation to the gelation properties of canola protein. *Food Research International*. 29, 653-659.

Salleh, H.R.B.M., Maruyama, N., Adachi, M., Hontani, N., Saka, S., Kato, N., Ohkawa, Y., and Utsumi, S. (2002). Comparison of protein chemical and physicochemical properties of rapeseed cruciferin with those of soybean glycinin. *Journal of Agriculture Food Chemistry*. 50, 7380-7385.

Sanchez, A. C., Popineau, Y., Mangavel, C., Larre, C., & Gueguen, J. (1998). Effect of different plasticizers on the mechanical and surface properties of wheat gliadin films. *Journal of Agricultural and Food Chemistry, 46,* 4539-4544.

Sanchez, C., & Renard, D. (2002). Stability and structure of protein–polysaccharide coacervates in the presence of protein aggregates. *International Journal of Pharmaceutics, 242,* 319-324.

Sanchez, C., Mekhloufi, G., & Renard, D. (2006). Complex coacervation between β-lactoglobulin and acacia gum: a nucleation and growth mechanism. *Journal of Colloid and Interface Science, 299,* 867-873.

Saremnezhad, S., Azizi, M. H., Barzegar, M., Abbasi, S., & Ahmadi, E. (2011). Properties of a new edible film made of faba bean protein isolate. *Journal of Agricultural Science and Technology, 13,* 181-192.

Schmidt, I., Novales, B., Boue, F., & Axelos, M. A. V. (2010). Foaming properties of protein/pectin electrostatic complexes and foam structure at nanoscale. *Journal of Colloid and Interface Science, 345,* 316-324.

Schmidt, I., Renard, D., Rondeau, D., Richomme, P., Popineau, Y., & Axelos, M. A. V. (2004). Detailed physicochemical characterization of the 2S storage protein from rape (*Brassica napus L.*). *Journal of Agricultural and Food Chemistry, 52,* 5995-6001.

Schmitt, C., & Turgeon, S. L. (2011). Protein/polysaccharide complexes and coacervates in food systems. *Advances in Colloid and Interfacial Science, 167,* 63-70.

Schmitt, C., Sanchez C., Desobry-Banon, S., & Hardy, J. (1998). Structure and technofunctional properties of protein-polysaccharide. *Critical Review in Food Science and Nutrition, 38,* 689-753.

Schmitt, C., Sanchez, C., Despond, S., Renard, D., Thomas, F., & Hardy, J. (2000). Effect of protein aggregates on the complex coacervation between β-lactoglobulin and acacia gum at pH 4.2. *Food Hydrocolloids, 14,* 403-413.

Schmitt, C., Sanchez, C., Lamprecht, A., Renard, D., Lehr, C., de Kruif, C. G., & Hardy, J. (2001) Study of β-lactoglobulin/acacia gum complex coacervation by diffusing-wave spectroscopy and confocal scanning laser microscopy. *Colloids and Surfaces B: Biointerfaces, 20,* 267-280.

Schmitt, C., Sanchez, C., Thomas, F., & Hardy, J. (1999). Complex coacervation between β-lactoglobulin and acacia gum in aqueous medium. *Food Hydrocolloids, 13,* 483-496.

Schultz, S., Wagner, G., Urban, K., & Ulrich, J. (2004). High-pressure homogenization as a process for emulsion formation. *Chemical Engineering and Technology, 27,* 361-368.

Schwenke, K. (1990). Structural studies on native and chemically modified storage proteins from rapeseed (*Brassica napus L.*) and related plant proteins. *Die Nahrung, 34,* 225-240.

Schwenke, K. D. (1994). Rapeseed protein. In B. J. F. Hudson (Ed.), *New and Developing Sources of Food Proteins* (pp. 281-306). London, UK: Chapman and Hall.

Schwenke, K. D., & Linow, K. J. (1982). A reversible dissociation of the 12S globulin from rapeseed (Brassica napus L.) depending on ionic strength. *Die Nahrung, 26,* K5-K6.

Schwenke, K. D., Drescher, B., Zirwer, D., & Raab, B. (1988). Structural studies on the native and chemically modified low-molecular mass basic storage protein (napin) from rapeseed (Brassica napus L.). *Biochemie und Physiologie der Pflanzen, 183,* 219-224.

Schwenke, K. D., Raab, B., Plietz, P., & Damaschun, G. (1983). The structure of 12S globulin from rapeseed. *Die Nahrung, 27,* 165-175.

Schwenke, K.D., Dahme, A., and Wolter, T. (1998). Heat-Induced gelation of rapeseed Proteins: effect of protein interaction and acetylation. *Journal of the American Oil Chemists' Society*. 75, 83-87.

Sebi, I., & Coma, V. (2002). Active edible polysaccharide coating and interactions between solution coating compounds. *Carbohydrate Polymers, 49,* 139-144.

Semenova, M. G. (1996). Factor determining the character of biopolymer-biopolymer interactions in multicomponent aqueous solutions modeling food systems. In N. Parris, A. Kato, L. K. Creamer & J. Pearce (Eds.), *Macromolecular Interactions in Food Technology* (pp 37-49). Washington, DC: ACS Symposium Series.

Semenova, M. G., Pavlovskaya, G. E., & Tolstoguzov, V. B. (1991). Light scattering and thermodynamic phase behavior of the system 11S globulin-κ-carrageenan-water. *Food Hydrocolloids, 4,* 469-479.

Ser, W. Y., Arntfield, S. D., Hydamaka, A. W., & Slominski, B. A. (2008) Use of diabetic test kits to assess the recovery of glucosinolates during isolation of canola protein. *LWT - Food Science and Technology, 41,* 934-941.

Shellhammer, T. H., & Krochta, J. M. (1997). Whey protein emulsion film performance as affected by lipid type and amount. *Journal of Food Science, 62,* 390-394.

Shieh, J.-Y., & Glatz, C. E. (1994). Precipitation of proteins with polyelectrolytes: role of the polymer molecular weight. In P. Dubin, J. Bock, R. Davis, D. N. Schulz & C. Thies (Eds.), *Macromolecular Complexes in Chemistry and Biology* (pp 273–284). Berlin: Springer-Verlag.

Siepmann, J., Paeratakul, O., & Bodmeier, R. (1998). Modeling plasticizer uptake in aqueous polymer dispersions. *International Journal of Pharmaceutics, 165,* 191-200.

Singh, S. K., & Jacobsson, S. P. (1994). Kinetics of acid hydrolysis of κ-carrageenan as determined by molecular weight (SEC-MALLSRI), gel breaking strength, and viscosity measurements. *Carbohydrate Polymers*, *23*, 89-103.

Singh, S., Siddhanta, A. K., Meena, R., Prasad, K., Bandyopadhyay, S., & Bohidar, H. B. (2007). Intermolecular complexation and phase separation in aqueous solutions of oppositely charged biopolymers. *International Journal of Biological Macromolecules*, *41*, 158-192.

Sobral, P. J. A. (1999). Propriedades funcionais de biofilms de gelatin em funcao da espessura. *Ciencia Engenharia, 8,* 60.

Sobral, P. J. A., Menegalli, F. C., Hubinguer, M. D., & Roques, M. A. (2001). Mechanical, water vapor barrier and thermal properties of gelatin based edible films. *Food Hydrocolloids, 15,* 423-432.

Song, F., & Zhang, L. M. (2009). Gelation modification of soy protein isolate by a naturally occurring cross-linking agent and its potential biomedical application. *Industrial & Engineering Chemistry Research, 48,* 7077-7083.

Song, F., Tang, D. L., Wang, X. L., & Wang, Y. Z. (2011). Biodegradable soy protein isolate-based materials: a review. *Biomacromolecules, 12,* 3369-3380.

Sothornvit, R., & Krochta, J. M. (2000). Plasticizer effect on oxygen permeability of beta-lactoglobulin films. *Journal of Agricultural and Food Chemistry, 48,* 6298-6302.

Sothornvit, R., & Krochta, J. M. (2001). Plasticizer effect on mechanical properties of beta-lactoglobulin in films. *Journal of Food Engineering, 50,* 149-155.

Sothornvit, R., & Krochta, J. M. (2005). Plasticizers in edible films and coatings. In J. H. Han (Ed.), *Innovations in Food Packaging* (pp. 403-433). New York: Elsevier Academic.

Spencer, C. M., Cai, Y., Martin, R., Gaffiney, S. H., Goulding, P. N., Magnolato, D., Lilley, T. H., & Haslam, E. (1988). Polyphenol complexation-some thoughts and observations. *Phytochemistry, 27,* 2397–2409.

Sperber, B. L. H. M., Schols, H. A., Cohen Stuart, M. A., Norde, W. A., & Voragen, G. J. (2009). Influence of the overall charge and local charge density of pectin on the complex formation between pectin and beta-lactoglobulin. *Food Hydrocolloids, 23,* 765-772.

Stone, A. K., & Nickerson, M. T. (2012). Formation and functionality of whey protein isolate–(kappa-, iota-, and lambda-type) carrageenan electrostatic complexes. *Food Hydrocolloids*, *27*, 271-277.

Stone, A. K., Cheung, L., Chang, C., & Nickerson, M. T. (2013). Formation and functionality of soluble and insoluble electrostatic complexes within mixtures of canola protein isolate and (κ-, ι- and λ-) carrageenan. *Food Research International, 54*, 195-202.

Stuart, M. A. C., Fleer, G. J., Lyklema, J., Norde, W., & Scheutjens, J. M. H. M. (1991). Adsorption of ions, polyelectrolytes and proteins. *Advances in Colloid and Interface Science, 34*, 477-535.

Sun, X.D. and Arntfield, S.D. (2011). Gelation properties of salt-extracted pea protein isolate catalyzed by microbial transglutaminase cross-linking. *Food Hydrocolloids*. 25, 25-31.

Swanson, B. G. (1990). Pea and lentil protein extraction and functionality. *Journal of the American Oil Chemists' Society, 67*, 276-280.

Syrbe, A., Bauer, W. J., & Klostermeyer, H. (1998). Polymer science concepts in dairy systems-an overview of milk protein and food hydrocolloid interactions. *International Dairy Journal, 8,* 179-195.

Sze-Tao, K. W. C., & Sathe, S. K. (2000). Functional properties and in vitro digestibility of almond (*Prunus dulcis* L) protein isolate, *Food Chemistry, 69,* 153-160.

Tan, S. H., Mailer, R. J., Blanchard, C. L., & Agboola, S. O. (2011). Canola protein for human consumption: extraction, profile, and functional properties. *Journal of Food Science, 76,* R16-R28.

Tang, C. H., & Jiang, Y. (2007). Modulation of mechanical and surface hydrophobic properties of food protein films by transglutaminase treatment. *Food Research International, 40,* 504-509.

Tang, C. H., Jiang, Y., Wen, Q. B., & Yang, X. Q. (2005). Effect of transglutaminase treatment on the properties of cast films of soy protein isolates. *Journal of Biotechnology, 120,* 296-307.

Tcholakova, S., Denkov, N. D., Ivanov, I. B., & Campbell, B. (2002). Coalescence in β-lactoglobulin-stabilized emulsions: effects of protein adsorption and drop size. *Langmuir, 18,* 8960–8969.

te Nijenhuis, K. (1997). Thermoreversible networks: viscoelastic properties and structure of gels. *Advances in Polymer Science, 130,* 1-267.

Tharanathan, R. N., and Mahadevamma, S. (2003). Grain legumes - a boon to human nutrition. *Trends in Food Science and Technology, 14,* 507-518.

Thompson, L. U., Allum- Poon, P., & Procope, C. (1976). Isolation of rapeseed protein using sodium hexametaphosphate. *Canadian Institute of Food Science and Technology Journal, 9,* 15-19.

Tolstoguzov, V. (2003). Some thermodynamic considerations in food formulation. *Food Hydrocolloids, 17,* 1-23.

Tolstoguzov, V. B. (1991). Functional properties of food proteins and role of protein-polysaccharide interaction. *Food Hydrocolloids, 4,* 429-468.

Tolstoguzov, V. B. (2002). Thermodynamic aspects of biopolymer functionality in biological systems, foods, and beverages. *Critical Reviews in Biotechnology, 22,* 89-174.

Tomihata, K., Burezak, K., Shiraki, K., & Ikada, Y. (1992). Cross-linking and biodegradation of native and denatured collagen. *Abstracts of Papers of the American Chemical Society, 204,* 326-poly.

Touyama, R., Takeda, Y., Inoue, K., Kawamura, I., Yatsuzuka, M., Ikumoto, T., Shingu, T., Yokoi, T., & Inouye, H. (1994). Studies on the blue pigments produced from genipin and ethylamine. 1. Structures of the brownish-red pigments intermediates leading to the blue pigments. *Chemical & Pharmaceutical Bulletin, 42,* 668-673.

Townsend, A. A., & Nakai, S. (1983). Relationship between hydrophobicity and foaming characteristics of food proteins. *Journal of Food Science, 48,* 588-594.

Turgeon, S. L., Beaulieu M., Schmitt C., & Sanchez, C. (2003). Protein–polysaccharide interactions: phase-ordering kinetics, thermodynamic and structural aspects. *Current Opinion in Colloid & Interface Science, 8,* 401-414.

Turgeon, S. L., Schmitt, C., & Sanchez, C. (2007). Protein-polysaccharide complexes and coacervates. *Current Opinion in Colloid and Interface Science, 12,* 166-178.

Turhan, K. N., Sahbaz, F., & Guner, A. (2001). A spectrophotometric study of hydrogen bonding in methylcellulose-based edible films plasticized by polyethylene glycol. *Journal of Food Science, 66,* 59-62.

Tzeng, Y. M., Diosady, L. L., & Rubin, L. J. (1988). Preparation of rapeseed protein isolate by sodium hexametaphosphate extraction, ultrafiltration, diafiltration and ion-exchange. *Journal of Food Science, 53,* 1537-1541.

Ueda, K., Itoh M., Matsuzaki, Y., Ochiai, H., & Imamura, A. (1998). Observation of the molecular weight change during the helix coil transition of kappa-carrageenan measured by the SEC-LALLS method. *Macromolecules, 31,* 675-680.

Uppstrom, B. (1995). Seed Chemistry. In D. S. Kimber & D. I. McGregor (Eds.), *Brassica oilseeds: production and utilization* (pp. 217-242). England: Wallingford.

Uruakpa, F. O., & Arntfield, S. D. (2005a). Emulsifying characteristics of commercial canola protein–hydrocolloid systems. *Food Research International, 38,* 659-672.

Uruakpa, F. O., & Arntfield, S. D. (2005b). The physico-chemical properties of commercial canola protein isolate-guar gum gels. *International Journal of Food Science and Technology, 40,* 643-653.

Uruakpa, F. O., & Arntfield, S. D. (2006a). Impact of urea on the microstructure of commercial canola protein-carrageenan network: a research note. *International Journal of Biological Macromolecules, 38,* 115-119.

Uruakpa, F. O., & Arntfield, S. D. (2006b). Surface hydrophobicity of commercial canola proteins mixed with κ-carrageenan or guar gum. *Food Chemistry, 95,* 255-263.

Uruakpa, F.O. and Arntfield, S.D. (2004). Rheological characteristics of commercial canola protein isolate–k-carrageenan systems. *Food Hydrocolloids*. 18, 419-427.

Utsumi, S. and Kinsella, J.E. (1985). Forces involved in soy protein gelation: effects of various reagents on the formation, hardness, and solubility of heat-induced gels made from 7S, 11S, and soy isolate. *Journal of Food Science*. 50, 1278-1282.

Vargas, M., Pastor, C., Chiralt, A., McClements, D. J., & Gonzalez-Martinez, C. (2008). Recent advances in edible coatings for fresh and minimally processed fruits. *Critical Review in Food Science and Nutrition, 48,* 496-511.

Veis, A. (2011). A review of the early developments in thermodynamic of complex coacervation phase separation. *Advances in Colloid and Interface Science, 167,* 2-11.

Vikelouda, M., & Kiosseoglou, V. (2004). The use of carboxymethylcellulose to recover potato protein and control their functional properties. *Food Hydrocolloids, 18,* 21-27.

Voragen, A. G. J., Pilnik, W., Thibault, J. F., Axelos, M. A .V., & Renard, C.M.G.C. (1995). Pectins. In A. M. Stephen (Ed.), *Food polysaccharides and their applications* (pp. 287-339). New York, NY: Marcel Dekker Inc.

Walstra, P., & van Vliet, T. (2008). Dispersed systems: basic considerations. In S. Damordaran, K. L. Parkin & O. R. Fennema (Eds.), *Fennema's Food Chemistry*, 4th ed. (pp. 783-847). Boca Raton, FL: CRC Press.

Wan, V. C., Kim, M. S., & Lee, S. (2005). Water vapor permeability and mechanical properties of soy protein isolate edible films composed of difference plasticizer combinations. *Journal of Food Science, 70,* E387-E391.

Wanasundara, J. P. D. (2011). Proteins of Brassicaceae oilseeds and their potential as a plant protein source. *Critical Reviews in Food Science and Nutrition, 51,* 635-677.

Wanasundara, J. P. D., & McIntosh, T. C. (2008). A process of aqueous protein extraction from Brassicaceae oilseeds. WIPO PCT/CA 2008/001055.

Wanasundara, J. P. D., & Shahidi. F. (1997). Functional properties of acylated flax protein isolates. *Journal of Agricultural and Food Chemistry, 45,* 2431–2441.

Wanasundara, J. P. D., Abeysekara, S. J., McIntosh, T. C., & Falk, K. C. (2012). Solubility differences of major storage proteins of Brassicaceae oilseeds. *Journal of the American Oil Chemists' Society, 89,* 869-881.

Wang, B., Li, D., Wang, L. -J., Adhikari, B., & Shi, J. (2010). Ability of flaxseed and soybean protein concentrates to stabilize oil-in-water emulsions. *Journal of Food Engineering, 100,* 417-426.

Wang, J. M., Xia, N., Yang, X. -Q., Yin, S. -W., Qi, J. -R., He, X. -T., Yuan, D. -B., & Wang, L.-J. (2012). Adsorption and dilatational rheology of heat-treated soy protein at the oil–water interface: Relationship to structural properties. *Journal of Agricultural and Food Chemistry, 60,* 3302–3310.

Wang, N. (2005). Optimization of laboratory dehulling process for lentil (*Lens culinaris*). *Cereal Chemistry*, *82*, 671-676.

Wang, X. S., Tang, C. H., Yang, X. Q., & Gao, W. R. (2008). Characterization amino acid composition and in vitro digestibility of hemp (*Cannabis sativa L.*) proteins. *Food Chemistry, 107,* 11-18.

Wang, X. Y., Lee, J., Wang, Y-p., & Huang, Q. (2007) Composition and rheological properties of β-lactoglobulin/pectin coacervates: effects of salt concentration and initial protein/polysaccharide ratio. *Biomacromolecules, 8,* 992-997.

Wang, Y., & Padua, G. W. (2003). Tensile properties of extruded zein sheets and extrusion blown films. *Macromolecular Materials and Engineering, 288,* 886-893.

Wang, Y., Gao, J. Y., & Dubin, P. L. (1996). Protein separation via polyelectrolyte coacervation: selectivity and efficiency. *Biotechnology Progress, 12*, 356-362.

Watt, I. C. (1983). The theory of water sorption by biological materials. In R. Jowitt, F. Escher, B. Hallstrom, H. F. Meffert, W. E. Spiess, & G. Vos (Eds.), *Physical Properties of Foods* (pp. 27-41). London: Applied Science Publishers.

Weinbreck F., Nieuwenhuijse H., Robijn G. W., & de Kruif C. G. (2003b). Complex formation of whey proteins: exocellular polysaccharide EPS B40. *Langmuir, 19,* 9404-9410.

Weinbreck F., Nieuwenhuijse H., Robijn G. W., & de Kruif C. G. (2004a). Complexation of whey proteins with carrageenan. *Journal of Agricultural and Food Chemistry, 52,* 3550-3555.

Weinbreck F., Wientjes R. H. W., Nieuwenhuijse H., Robijn G. W., & de Kruif C. G. (2004c). Rheological properties of whey protein and gum arabic coacervates. *Journal of Rheology, 48,* 1215-1228.

Weinbreck, F., de Vries, R., Schrooyen, P., & de Kruif, C. G. (2003a). Complex coacervation of whey proteins and gum Arabic. *Biomacromolecules, 4*, 293-303.

Weinbreck, F., Tromp, R. H., & de Kruif, C. G. (2004b). Composition and structure of whey protein/gum Arabic coacervates. *Biomacromolecules, 5,* 1437-1445.

Weitz, D.A. and Lin, M.Y. (1986). Dynamic Scaling of Cluster-Mass Distributions in Kinetic Colloid Aggregation. *Physical Review Letters*. 57, 2037-2040.

Wen, Y., & Dubin, P. L. (1997). Potentiometric studies of the interaction of bovine serum albumin and poly (dimethyldiallylammonium chloride). *Macromolecules, 30,* 7856-7861.

White, J. A., Hart, R. J., & Fry, J. C. (1986). An evaluation of the waters pico-tag system for the amino-acid analysis of food materials. *Journal of Automatic Chemistry, 8,* 170-177.

Winter, H.H. and Chambon, F. (1986). Analysis of Liner Viscoelasticity of a Crosslinking Polymer at the Gel Point. *Journal of Rheology*. 30, 367-382.

Wu, H. and Morbidelli, M. (2001). A Model Relating Structure of Colloidal Gels to Their Elastic properties. *Langmuir*. 17, 1030-1036.

Wu, J. and Muir, A.D. (2008). Comparative Structural, emulsifying, and biological properties of 2 major canola proteins, cruciferin and napin. *Journal of Food Science*. 73, C210-C216.

Wu, J., & Muir, A. D. (2008). Comparative structural, emulsifying, and biological properties of 2 major canola proteins, cruciferin and napin. *Journal of Food Science, 73,* C210-C216.

Wu, M., Xiong, Y. L., & Chen, J. (2011). Role of disulfide linkages between protein-coated lipid droplets and the protein matrix in the rheological properties of porcine myofibrillar protein-peanut oil emulsion composite gels. *Meat Science, 88,* 384-390.

Xia, J., & Dubin, P. L. (1994). In P. L. Dubin, J. Bock, R. Davis, D. N. Shultz & C. Thies (Eds.), *Macromolecular complexes in chemistry and biology* (pp. 247-271). Berlin: Springer-Verlag.

Xie, Y. R., & Hettiarachchy, N. S. (2006). Xanthan gum effects on solubility and emulsification properties of soy protein isolate. *Journal of Food Science, 62,* 1101-1104.

Xu, W., Nikolov, A., & Wasan, D. T. (2005). Shear-induced fat particle structure variation and the stability of food emulsions: 1. effects of shear history, shear rate and temperature. *Journal of Food Engineering, 66,* 97-105.

Xu, Y., Mazzawi, M., Chen, K., Sun, L., & Dubin, P. L. (2011). Protein purification by polyelectrolyte coacervation: influence of protein charge anisotropy on selectivity. *Biomacromolecules, 12,* 1512-1522.

Yajima, E. M., Zanin, G. M., & Cavalcanti, O. A. (2010). Thermal characterization of gelatin-chitosan free films crosslinked with genipin. *Latin American Journal of Pharmacy, 29,* 436-442.

Yang, L., & Paulson, A. T. (2000a). Mechanical and water vapor barrier properties of edible gellan films. *Food Research International, 33,* 563-570.

Yang, L., & Paulson, A. T. (2000b). Effects of lipids on mechanical and moisture barrier properties of edible gellan film. *Food Research International, 33,* 571-578.

Yang, L., Paulson, A. T., & Nickerson, M. T. (2010). Mechanical and physical properties of calcium-treated gellan films. *Food Research International, 43,* 1439-1443.

Ye, A. (2008). Complexation between milk proteins and polysaccharides via electrostatic interaction: principles and applications - A review. *International Journal of Food Science and Technology, 43,* 406-415.

Ye, A. Q., Flanagan, J., & Singh, H. (2006). Formation of stable nanoparticles via electrostatic complexation between sodium caseinate and gum arabic. *Biopolymers, 82,* 121-133.

Yiu, S. H., Altosaar, I., & Fulcher, R. G. (1983). The effects of commercial processing on the structure and chemical organization of rapeseed and its products. *Food Microstructure, 2,* 165-173.

Yoshie-Stark, Y., Wada, Y., & Wasche, A. (2008). Chemical composition, functional properties, and bioactivities of rapeseed protein isolates. *Food Chemistry, 107,* 32-39.

Yoshie-Stark, Y., Wada, Y., Schott, M., & Wasche, A. (2006). Functional and bioactive properties of rapeseed protein concentrates and sensory analysis of food application with rapeseed protein concentrates. *Food Science and Technology-LEB, 39,* 503-512.

Yuan, Y., Chesnutt, B. M., Utturkar, G., Haggard, W. O., Yang, Y., Ong, J. L., & Bumgardner, J. D. (2007). The effect of cross-linking of chitosan microspheres with genipin on protein release. *Carbohydrate Polymers, 68,* 561-567.

Yuan, Y., Wan, Z-L., Yin, S-W., Yang, X-Q., Qi, J-R., Liu, G-Q., & Zhang, Y. (2013). Characterization of complexes of soy protein chitosan heated at low pH. *LWT – Food Science & Technology, 50,* 657-664.

Zayas, J. F. (1997). Emulsifying properties of proteins. In J. F. Zavas (Ed.), *Functionality of Proteins in Food* (pp. 134-227). Berlin, Germany: Springer, Berlin.

Zhang, C. Y., Parton, L. E., Ye, C. P., Krauss, S., Shen, R., Lin, C. T., Porco Jr, J. A., & Lowell, B. B. (2006). Genipin inhibits UCP2-mediated proton leak and acutely reverses obesity and high glucose-induced beta cell dysfunction in isolated pancreatic islets. *Cell Metabolism, 3,* 417-427.

Zhang, J., Mungara, P., & Jane, J. (2001). Mechanical and thermal properties of extruded soy protein sheets. *Polymer, 42,* 2569-2578.

Zhang, T., Jiang, B., Mu, W., & Zhang, W. (2009). Emulsifying properties of chickpea protein isolates: Influence of pH and NaCl. *Food Hydrocolloids, 23,* 146-152.

Zhao, G., Liu, Y., Zhao, M., Ren, J., & Yang, B. (2011). Enzymatic hydrolysis and their effects on conformational and functional properties of peanut protein isolate. *Food Chemistry, 127,* 1438–1443.

Zirbel, F., & Kinsella, J. E. (1988). Factors affecting the rheological properties of gels made from whey-protein isolated. *Milchwissenschaft – Milk Science International, 43,* 691-69.

Zirwer, D., Gast, K., & Welfle, H. (1985). Secondary structure of globulins from plant seeds: a re-evaluation from circular dichroism measurements. *International Journal of Biological Macromolecules*. 7, 105-108.

Zirwer, D., Gast, K., Welfle, H., & Schlesier, B. S. (1985). Secondary structure of globulins from plant seeds: a re-evaluation from circular dichroism measurements. *International Journal of Biological Macromolecules, 7,* 105-108.

-Chapter 23-

Outputs

Highly qualified personal trained

- Lamlam Cheung (M.Sc. student – Protein stabilized emulsions)
- Chang Chang (M.Sc. student – Edible films)
- Jae Hee Kim (M.Sc Student – Canola protein gelation)
- Natallia Varankovich (Technician. – Confocal microscopy)
- Qian Dang (UG student – Coacervation)
- Anna Karalash (UG student – Coacervation)
- Anzhelika Teymurova (Post-doctorate fellow – Coacervation)
- Andrea Stone (Technician – Coacervation)
- Sujeema Abeysekara (Technician – napin extraction)

Manuscripts

1. **Stone, A.K., Teymurova, A., Chang, C., Cheung, L.** and Nickerson, M.T. 2014). Formation and functionality of canola protein isolate with both high- and low-methoxyl pectin under associative conditions. (Submitted to Food Science and Biotechnology, August 2014)
2. **Cheung, L.,** Wanasundara, J. and Nickerson, M.T. 2014. The effect of pH and NaCl levels on the emulsifying properties of a napin protein isolate. Food Biophysics. (Accepted June 2014)
3. **Chang, C.** and Nickerson, M.T. 2014. Effect of protein and glycerol concentration on the mechanical, optical, and water vapor barrier properties of canola protein isolate-based edible films. Food Science and Technology international (Accepted Aug 2013)
4. **Stone, A.K., Teymurova, A.** and Nickerson, M.T. 2014. Formation and functional attributes of canola protein isolate – gum Arabic electrostatic complexes. Food Biophysics, 9, 203-212
5. **Cheung, L.,** Wanasundara, J. and Nickerson, M.T. 2014. The effect of pH and NaCl levels on the physicochemical and emulsifying properties of a cruciferin protein isolate. Food Biophysics. 9, 105-113.

6. **Stone, A.K., Teymurova, A., Dang, Q., Abeysekara, S., Karalash, A.** and Nickerson, M.T. 2014. Formation and functional attributes of electrostatic complexes involving napin protein isolate and anionic polysaccharides. European Food Research and Technology, 238, 773-780. .
7. **Chang, C.** and Nickerson, M.T. 2014. Effect of plasticizer-type and genipin on the mechanical, optical, and water vapor barrier properties of canola protein isolate-based edible films. European Food Research and Technology, 234:35-46
8. **Stone, A.K., Cheung, L., Chang, C.** and Nickerson, M.T. 2013. Formation and functionality of soluble and insoluble electrostatic complexes within mixtures of canola protein isolate and (κ-, ι- and λ-type) carrageenan. Food Research International, 54, 195-202.

Presentations at conferences

1. **Chang, C.** and Nickerson, M.T. 2013. Effect of protein and glycerol concentrations on the mechanical and water vapour barrier properties of canola protein-based edible films, American Oil Chemists Society Annual Meeting, May 1-4th, Montreal, PQ
2. **Chang, C.** and Nickerson, M.T. 2013. Effect of plasticizer-type on the mechanical and water vapour barrier properties of canola protein-based edible films crosslinked with and without genipin, American Oil Chemists Society Annual Meeting, May 1-4th, Montreal, PQ
3. **Cheung, L.,** Wanasundara, J. and Nickerson, M.T. 2013. Effect of pH and salts on the physicochemical and emulsifying properties of cruciferin- and napin-rich protein isolates, American Oil Chemists Society Annual Meeting, May 1-4th, Montreal, PQ.
4. **Stone, A.K., Dian, Q.** and Nickerson, M.T. (2013), Formation and functionality of napin protein isolate-gum Arabic electrostatic complexes, American Oil Chemists Society Annual Meeting, May 1-4th, Montreal, PQ
5. **Stone, A.** and Nickerson, M.T. 2012. Complex coacervation between canola protein isolate and gum Arabic polysaccharides, 243rd American Chemical Society Annual Meeting, March 25-29th, San Diego, CA. 2012

6. **Stone, A., Chang, C.** and Nickerson, M.T. 2012. Formation of soluble and insoluble complexes within admixtures of canola protein isolate and gellan gum 243rd American Chemical Society Annual Meeting, March 25-29th. San Diego, CA. 2012
7. **Stone, A., Cheung, L**. and Nickerson, M.T. 2012. Formation of electrostatic complexes within canola protein isolate – (κ-, ι-, and λ-type) carrageenan mixtures, American Oil Chemist's Society Annual Meeting, May 7-9, Long Beach, CA, 2012
8. **Stone, A., Cheung, L., Chang, C.** and Nickerson, M.T. 2012. Functional attributes of canola protein-polysaccharide electrostatic complexes, American Oil Chemist's Society Annual Meeting, May 7-9, Long Beach, CA, 2012.
9. **Stone, A., Chang, C.** and Nickerson, M.T. 2012. Coacervation in admixtures of canola protein isolate and (low and high methoxy)-pectin. 11th International Hydrocolloids Conference, May 14-16. *West Lafayette, IN.*

Part VII: Appendices

Appendix A: Protein functionality testing manual

Protein Functionality Testing Manual

Michael Nickerson, Ph.D., P.Ag.
University of Saskatchewan

2012

Special thanks to the Saskatchewan Agricultural Development Fund and the Saskatchewan Canola Development Commission for financially supporting this project, and to Andrea Stone for her technical assistance.

Contact information:

Michael Nickerson, Ph.D., P.Ag.

Saskatchewan Ministry of Agriculture Research Chair –
(Protein Quality & Utilization)
Department of Food and Bioproduct Sciences
University of Saskatchewan
51 Campus Drive, Saskatoon, SK, S7N 5A8, Canada
Tel: (306) 966-5030
Fax: (306) 966-8898
E-mail: Michael.Nickerson@usask.ca

TABLE OF CONTENTS

1. INTRODUCTION

Protein ingredients represent a multi-billion dollar industry, presently dominated by animal proteins, such as gelatin, ovalbumin, casein and whey. In 2011, the US protein ingredient market for food is estimated to be worth ~2.84 billion, with $1.17 (avg. annual growth rate, AAGR 6.4%) and ~1.67 (AAGR 1.7%) billion coming from plant and animal sources, respectively. The global protein market is expected to hit $24.5 billion by 2015.

With increased concerns over the safety of animal-derived products, rising costs of dairy-based ingredients; growing dietary preferences and consumer demand for healthier foods; market trends are shifting towards lower cost and abundant plant-based alternatives. Plant proteins derived from agricultural crops have the potential to fill these market gaps, providing competition to soy products already in the market place. Plant proteins also have a significant price advantage over animal-based ingredients; for instance, casein is sold for ~$4.90 (USD) a pound, compared to soy or other plant proteins, which range between $0.42 to $2.08 (USD) per pound. Despite experiencing greater market growth than animal-derived protein ingredients, the wide spread use of plant proteins in the food and biomaterial sectors is hindered by their reduced solubility and functionality relative to animal-based products, and in the case of soy, its beany flavour, allergencity and tendency to cause flatulence.

Development of innovative knowledge and technology relating to proteins derived from agricultural crops will help support the movement of these products into existing markets (e.g., as food/biomaterial ingredients) and open up new market niches (e.g., functional foods and feed/pet food additives) for agricultural-based processors and producers. This strategy should lead to higher economic returns to producers through increased market demand for their crops/varieties and improved price stability.

The functionality of protein ingredients refers to any property other than their nutritional composition that influences their utilization. With the exception of solubility, many of the common functionality tests to describe protein performance are not standardized by any professional body (e.g., American Oil Chemists Society). And as such, values found in literature are difficult to compare from one group to the next due to slight differences in methodologies and protein preparation. In the following manual common tests are outlined in detail, step-by-step, as a guide to industry as they work to develop in-house testing methodologies to evaluate their products and processes. The manual also provides results from commercial protein isolates prepared from whey, wheat, eggs, peas and soy to be used as a comparative baseline. Although company names are not identified in this manual, it is noteworthy to mention that obtained values are specific to those products (i.e., isolates prepared by another company could give slightly different values) and as such should be used only as a guide. The manual describes basic testing for the following functional attributes: solubility, emulsification, foaming and water hydration/oil holding properties.

This manual is intended to help guide employees, buyers and managers of food companies working directly or indirectly with protein-based ingredients; researchers in their experimental designs; and for educational purposes.

2. BASIC CONCEPTS

Structure

Proteins are comprised of four structural levels: linear *primary* sequences comprised of long chains of amino acids containing varying side groups, which undergoes folding into *secondary* structures such as alpha-helices, beta-sheets, beta-turns and random coils. These undergo additional folding with other secondary structures to form subunits or its *tertiary* conformation. Finally, a protein's *quaternary* conformation is comprised of associated tertiary subunits.

Surface chemistry

Depending on the nature of the amino acids (i.e., polar, non-polar, neutral, acidic, basic and aromatic) and the folded conformation, proteins can display different surface chemistries such as charge and hydrophobicity. The former fosters greater associations between the protein and water (or buffers) (protein- solvent interactions) enhancing their ability to remain in solution, migrate to an oil (or gas)-water interface in emulsions or foams, and abide water. In contrast, increased levels of hydrophobicity promote a greater amount of "protein-protein" interactions (or aggregation) and foster greater associations with non-polar mediums, such as air in the case of foams, and oil droplets in the case of emulsions. Depending on environmental (e.g., pH, temperature, and presence of salts) and processing conditions (e.g., time/temperature and shear), protein conformation and surface chemistry can be altered to an extent that could have a negative, neutral or positive impact on functionality. In most instances, proteins used by the food industry undergo some level of denaturation from their native state. Often a small amount is useful to induce partial unraveling of the protein structure to exposure reactive hydrophobic amino acids to the surface.

Protein functionality

a) Solubility

Protein solubility is often a perquisite to many other functional attributes; enabling them to be used as emulsifiers, foaming agents, gelling agents or thickeners in a wide range of applications. The solubility of a protein is related to its structure (charge and hydrophobicity, isoelectric point), along with solution pH, temperature and salts (type and concentration). At the protein's isoelectric point (pI), the structure has no net surface charge typically resulting in minimal solubility since neighboring proteins will have a tendency to aggregate into larger structures and sediment. In contrast, at solution pH away from its pI the protein will display either a positive (pH<pI) or negative (pH>pI) net surface charge and have maximum solubility. The presence of a surface charge acts to repel neighboring proteins away from each other to keep them in solution.

The effect of salt on protein solubility is dependent on both the type and concentration present; leading to either a salting in or out effect. In general, mono- and divalent ions such as sodium, potassium, magnesium and calcium act to screen charges on the protein's surface to facilitate aggregation and loss of protein solubility. Temperature can also have both a positive and negative influence on solubility. At temperatures below the protein's denaturation temperature solubility is typically enhanced with increasing temperature. However, once the protein reaches its denaturation temperature its conformation begins to unravel and expose buried hydrophobic amino acids. As a result, neighboring proteins begin to aggregate and facilitate loss of solubility.

b) Emulsions

Emulsions are defined as mixtures of two (or more) immiscible liquids with one liquid being dispersed in a continuous phase of the other. Emulsions require some sort of energy input (e.g., high speed mixing or homogenization) to form, followed by a means to induce stability over time. Emulsions are widely found in food products, ranging from water-in-oil (W/O) emulsions, such as margarines and butter, or oil-in-water (O/W) emulsion, such as milk and salad dressings.

Due to the immiscibility of oil and water, emulsions are inherently unstable and over time move to separate into two distinct phases. Depending on the system, instability in an O/W emulsion could take the form of: (1) *creaming*, where oil droplets float to the surface individually due to density differences between the two phases; (2) *flocculation*, where oil droplets reversibly aggregate into larger flocs (i.e., oil droplets remain separate entities within the larger cluster) before floating to the surface; and (3) *coalescence*, where individual oil droplets irreversibly merge into larger droplets before floating to the surface. Proteins act to stabilize emulsions by coating the surface of individual oil droplets to prevent coalescence or flocculation; ensuring good dispersion of the oil droplets within the water continuous phase.

The effectiveness of proteins as emulsifiers stems from both their surface chemistry and conformation; both of which influences their ability to align at the oil-water interface. Within the protein coating, hydrophilic amino acids tend to align more towards the water phase, whereas hydrophobic amino acids orient towards the oil phase. Proteins that are more unraveled (e.g., casein) tend to integrate better at the interface versus more globular-type proteins (e.g., soy) which require greater time to align at the interface but form a thicker more stable film. Depending on the emulsion pH and the protein-type, oil droplets can repel one another at pH<pI or pH>pI to maintain good dispersibility within the water phase. At pHs close to the pI, oil droplets take on more of a neutral net charge and tend to aggregate leading to emulsion instability. Furthermore, depending on the distribution of hydrophilic and hydrophobic amino acids on the protein, integration and alignment at the oil-water interface may lead to sections of the protein extending out into solution. This effect creates steric forces which physically excludes neighboring droplets from coming together. Emulsion stability is also highly dependent on the shear rate and duration in which the emulsion is prepared. A greater amount of homogenization leads to the production of smaller droplets with improved emulsion stability.

c) Foams

Similar to emulsions, foams are mixtures of two immiscible phases with gases and water representing the dispersed and continuous phases, respectively. Protein-based foams are used in the food industry in meringues, mousses, beer and in whipped desserts. Similar to emulsions, foams form after an energy input (i.e., whipping, sparging, pouring) as proteins: migrate to the gas-water interface, re-orient to position hydrophobic amino acids towards the gas phase and hydrophilic amino acids towards the water phase, and then form a stiff gel-like film surrounding the gas bubbles that resists against rupturing. This film also connects with adjacent proteins to create a cage-like network with entrapped gas to constitute the foam structure.

Foam formation is related to properties of the protein such as surface hydrophobicity, conformation/flexibility, size and level of denaturation. Foam stability is typically best at a pH near the pI of the protein, where repulsive electrostatic forces are minimum. More viscous protein solutions tend to produce more stable foams, as liquid drainage from the protein cage-like network is reduced. A thicker protein solution in-between the gas bubbles also reduces Oswald Ripening (i.e., diffusion of gas from smaller gas bubbles to larger ones).

d) Water and oil holding

Water and fat holding properties of proteins are important for maintaining product quality and acceptability to consumers. They contribute to textural attributes, mouthfeel, and restrict expelled water on products (e.g., meats). The attraction of water to proteins or within a protein matrix can be considered in two parts: 1) bound water, which is no longer available for further reactions; and 2) trapped or retained water, which is free to participate in reactions and be expelled from the protein matrix or product if pressed. Proteins that are more highly charged tend to hold more water through electrostatic attractive forces, hydrogen bonding, and thus are related to protein composition (amino acid content and distribution), solution pH, salts and temperature. The pore structure of the protein network or food product is also important, as it influences the amount of protein-water interactions occurring as trapped water is pressed out.

In contrast, oil holding properties of proteins or a protein matrix is related to protein composition (hydrophobic amino acid content and distribution); pore structure of the protein network or food product; and oil type and droplet size/distribution throughout the food.

3. TESTING PROTOCOLS

A. PROTEIN DETERMINATION (BY MICRO-KJELDAHL)

Defined as:

Kjeldahl analysis determines percent nitrogen within the material; then using a conversion factor converts it to percent protein (1). The method involves digestion, distillation and titration processes.

Method:

1. Weigh 10 – 100 mg of sample into a digestion flask containing 1.5 g of catalyst (10:0.3 potassium sulfate: copper sulfate) and 2.0 mL concentrated sulfuric acid.
2. Run a reagent only blank, and a glycine standard.
3. Heat the flasks on the Micro Digester heating block for 10 min (Level 5), then turn to high until the material turns a clear green color. Continue digestion for an additional 15 min.
4. Allow the flasks to cool for ~10 min once digestion is complete, and then add 3-4 mL of double distilled water to dissolve any caking that may occur in the flasks.
5. Prepare the rapid distillation apparatus by boiling water in the steam reservoir.
6. Place a 125 mL Erlenmeyer receiving flask containing 15 mL of 4% boric acid and ~3 drops of N-point indicator under the condenser outlet (with the tip of the condenser fully submersed within the solution).
7. Transfer the digested sample into the sample funnel, and open the stopcock slowly to transfer the material into the mixing chamber.
8. Rinse the empty Kjeldahl flask and sample funnel with 3-4 mL of double distilled water until the pH of the wash water is neutral.
9. Add 15 mL of 50% NaOH to the sample funnel, then open stopcock to slowly add the base to the mixing chamber. Distill for 3-5 min.
10. Lower the receiving flask and allow distillation to continue for additional ~1 min.
11. Titrate the sample within the receiving flask with 0.0200 N HCl until the colour changes from green to pink and record the amount of HCl used.

$$\%N = \frac{(V_{HCl} - V_{Blk}) \times N_{HCl} \times 14.007 \times 100}{W}$$

Where

$\%N$ = Percent nitrogen

V_{HCl} = Volume of HCl used during the titration of the sample (mL)

V_{Blk} = Volume of HCl used during the titration of the reagent only blank

N_{HCl} = Normality of the HCl solution

W = Sample weight (mg)

% Protein = % N x conversion factor

Table 1. Common conversion factors typically used in research literature for various proteins. *Please note, that the universal conversion factor is typically used by industry when determining protein levels, with the exception of the dairy industry.*

Protein	Factor
Glycine (control)	5.36
Whey, and other milk products	6.38
Meat, eggs	6.25
Peas, navy beans, lentils, chickpeas, faba beans	5.70
Barley, oats	5.83
Rice	5.95
Soy	5.71
Wheat	5.70
Oilseeds	6.25
Universal conversion factor	6.25

Table 2. Protein levels determined for commercial protein isolates.

Commercial ingredient	% Protein
Egg protein isolate	78.01
Whey protein isolate	89.60
Wheat protein isolate	82.46
Soy protein isolate	79.90
Pea protein isolate	80.02

Note: All commercial products used a 6.25 conversion factor, with the exception of whey protein isolate which used 6.38.

B. PROTEIN SOLUBILITY

Defined as:

The concentration of protein dissolved within the water (buffer) phase relative to the original protein concentration added (2).

Method:

1. Prepare a 1% (w/w) protein solution => disperse 0.2 g of protein isolates (corrected on a weight basis for protein content) in 18 g of 0.1 N NaCl. Adjust to the desired pH (using 0.1 M NaOH or 0.1 M HCl) then bring the weight of the solution up to 20 g with 0.1 N NaCl followed by stirring at 500 rpm for 1 h at room temperature.
2. Centrifuge solutions at 9,100 × g for 10 min at room temperature.
3. Determine the nitrogen content within the supernatant using a micro-Kjeldahl digestion and distillation unit (Labconco Corp., Kansas City, MO, USA).
4. Percent protein solubility is calculated by dividing the nitrogen content of the supernatant by the total nitrogen in the sample (×100%).

Example:

Pea protein isolate contains 80% protein.

To prepare 20 g of a 1% (or 0.2 g) protein solution you must add 0.25 g of the isolate material (0.2/0.80 = 0.25).

Protein levels in the supernatant were found to be 0.1318% in 20 g of total weight (sample + buffer).

Solubility = [20 x 0.1318] / [0.25 x 0.80] x 100%

= 13.18%

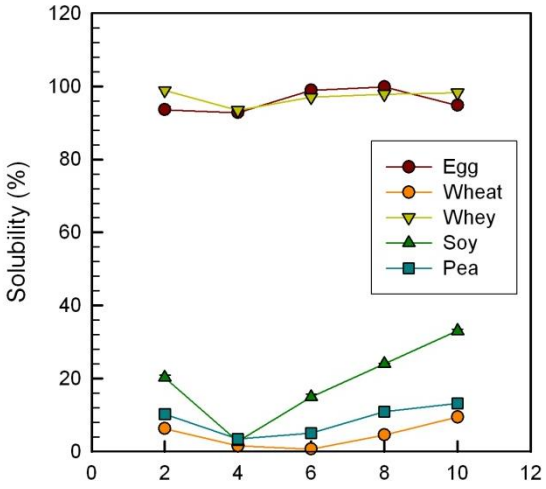

Figure 1. Percent protein solubility for commercial protein isolates at a 1.0% (w/w) protein concentration and as a function of pH.

Data represent the mean ± one standard deviation (n=3).

C. EMULSIFICATION CAPACITY

Defined as:

Emulsion capacity defines the amount of oil that can be emulsified by a standard amount of protein under a specific set of conditions; or the percent oil, relative to the total emulsion weight, required to invert an oil-in-water emulsion to a water-in-oil emulsion (inversion point) (3).

Method:

1. Prepare a 1% (w/w) protein solution => disperse protein isolates (corrected on a weight basis for protein content) in 10 mM sodium phosphate buffer (pH 7.00; adjusted with either 0.1 M NaOH or 0.1 M HCl) followed by stirring at 500 rpm overnight (~16 h) at 4°C.
2. Prepare a series of emulsions with different oil percentages by adding X grams of vegetable oil to 2 grams of the protein solution in a 50 mL screw capped centrifuge tube.
3. Homogenize at 8,000 rpm for 5 min using an Omni-mixer. Tip: Position the blade at the oil-water interface prior to homogenization.

4. Immediately measure emulsion conductivity using a conductivity meter.

5. Conductivity experiences a significant drop as the emulsion inverts from an oil-in-water emulsion to water-in-oil.
6. Emulsion capacity is expressed as grams of oil homogenized per gram of protein before the inversion was observed.

Example: Two grams of a 1% (w/w) whey protein isolate was used for testing (= 0.02 g protein). Add different amounts of oil, and identify the inversion point by the change in conductivity (e.g., 3.75 and 4 g). Take the avg. wt. of oil added before and after the inversion point to determine the emulsification capacity (e.g., [187.5 + 200] /2 = 193.75 g oil / g protein).

Improve sensitivity by adding smaller increments of oil closer to the inversion point.

Grams oil added	g Oil per g Protein	Conductivity (µS/cm)
2	100	20.73
3	150	48.10
3.5	175	27.96
3.75	187.5	34.50
4	200	0.55
5	250	0.14
6	300	0.23

Emulsion capacity is equivalent to g oil per g protein.

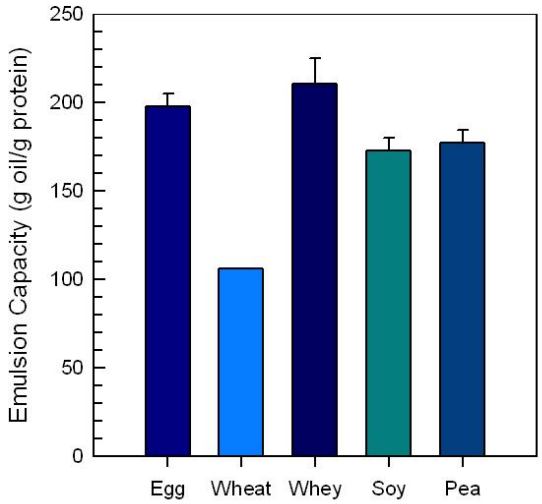

Figure 2. Emulsion capacity for commercial protein isolates at a 1.0% (w/w) protein concentration.

Data represent the mean ± one standard deviation (n=3).

D. EMULSIFICATION STABILITY

Defined as:

Emulsification stability by creaming refers to the ability of the protein-stabilized emulsion to resist creaming. Where creaming in the system arises from the density difference between oil and water. As an emulsion becomes unstable, oil droplets come together and migrate upwards to form a cream layer at the top of the emulsion and subsequently a serum layer is found at the bottom of the emulsion (4).

Method:

1. Prepare a 1% (w/w) protein solution => disperse protein isolates (corrected on a weight basis for protein content) in 10 mM sodium phosphate buffer (pH 7.00; adjusted with either 0.1 M NaOH or 0.1 M HCl) followed by stirring at 500 rpm overnight (~16 h) at 4°C.
2. Prepare an oil-in-water emulsion (10 mL total) by homogenizing 5 mL of 1.0% (w/w) protein solution and 5 mL of vegetable oil at 8,000 rpm for 5 min using an Omni-mixer.
3. Emulsions are then transferred into 10 mL graduated glass cylinders (inner diameter = 10.80 mm; height = 100.24 mm; as measured by a digital caliper) immediately after preparation.
4. The stability of the emulsion is monitored by observing the separation of a serum layer after 30 min of storage at room temperature. At this point, emulsions will separate into an aqueous layer (bottom), and a turbid layer at the top with a similar appearance to the original emulsion.
5. Emulsion stability (ES) is expressed as:

$$ES(\%) = \frac{V_B - V_A}{V_B} \cdot 100\%$$

where, V_B is the volume of the aqueous phase before emulsification (5 mL) and V_A is the volume of the aqueous (or serum) layer after 30 min of storage.

E.g., 0.5% (w/w)
Pea protein isolate – emulsion

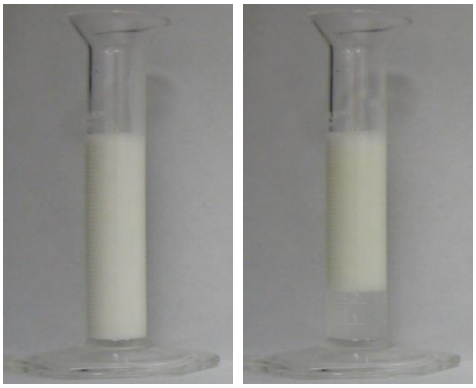

Time = 0 min Time = 30 min

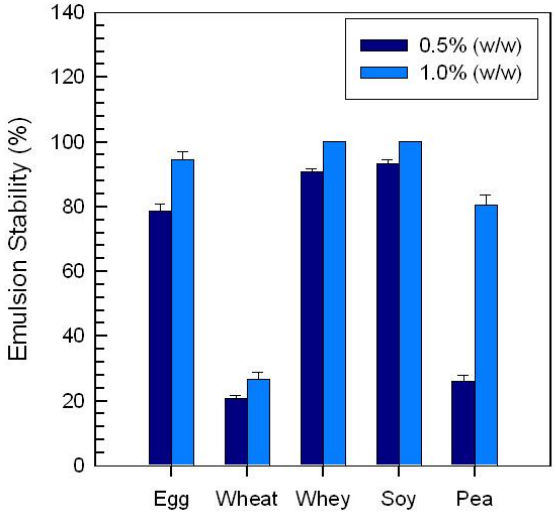

Figure 3. Emulsion stability for commercial protein isolates at a 0.5% and 1.0% (w/w) protein concentration.

Data represent the mean ± one standard deviation (n=3).

E. EMULSIFYING ACTIVITY AND STABILITY INDICES

Defined as:

Emulsifying activity index (EAI) describes the ability of a protein to form an emulsion; with the index providing an estimate of the interfacial area stabilized per unit weight of protein based on the turbidity of a diluted emulsion (5). The emulsifying stability index (ESI) provides a measure of the stability of the same diluted emulsion over a defined time period (5).

Method:

1. Prepare a 0.25% (w/w) protein solution => disperse protein isolates (corrected on a weight basis for protein content) in 10 mM sodium phosphate buffer (pH 7.00; adjusted with either 0.1 M NaOH or 0.1 M HCl) followed by stirring at 500 rpm overnight (~16 h) at 4°C.
2. Homogenize 5 g of protein solution with 5 g of vegetable oil at 8,000 rpm for 5 min using an Omni-mixer.
3. Transfer 50 µL of the emulsion immediately after homogenization (taken from the bottom of the tube) and dilute in 7.5 mL of 10 mM sodium phosphate buffer (pH 7.00) containing 0.1% sodium dodecyl sulphate (SDS); then vortex for 10 s.
4. An aliquot of this suspension is taken at time 0 and 10 min, and the absorbance of the diluted emulsion is measured at 500 nm using a UV spectrophotometer using plastic cuvettes (1 cm path length).
5. EAI and ESI are calculated by using the following equations:

$$EAI(m^2/g) = \frac{2 \cdot 2.303 \cdot A_0 \cdot N}{c \cdot \varphi \cdot 10000}$$

$$ESI(\text{min}) = \frac{A_0}{\Delta A} \cdot t$$

where, A_0 is the absorbance of the diluted emulsion post-homogenization, N is the dilution factor (×150), c is the weight of protein per volume (g/mL), φ is the oil volume fraction of the emulsion, ΔA is the change in absorbance between 0 and 10 min ($A_0 - A_{10}$) and t is the time interval, 10 min.

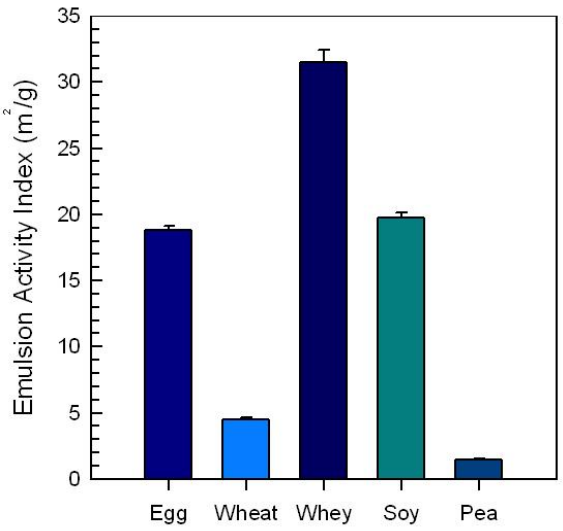

Figure 4. Emulsion activity index for commercial protein isolates at a 0.25% (w/w) protein concentration.

Data represent the mean ± one standard deviation (n=3).

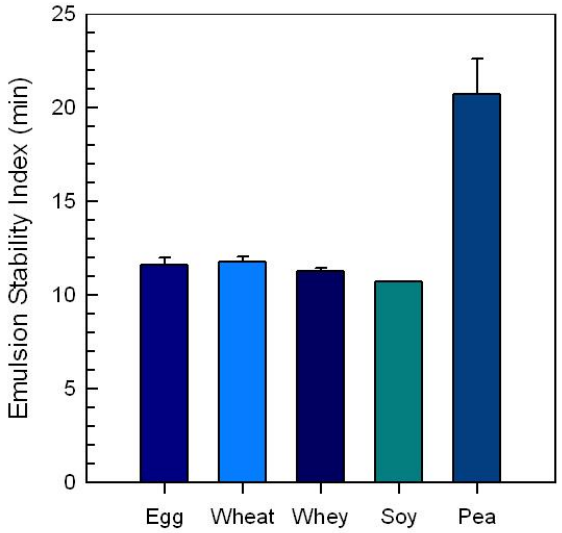

Figure 5. Emulsion stability index for commercial protein isolates at a 0.25% (w/w) protein concentration.

Data represent the mean ± one standard deviation (n=3).

F. WATER HYDRATION CAPACITY

Defined as:

The amount of water that can be absorbed by one gram of protein (1, 6).

Method:

1. Wet 1 g of protein (based on a wet basis) with 10 mL of 10 mM sodium phosphate buffer (pH 7.00; adjusted with either 0.1 M NaOH or 0.1 M HCl) in a weighted 30 mL centrifuge tube and mix thoroughly.
2. Vortex the sample every 5 min for a total of 30 min.
3. Centrifuge the sample at 1000 x g for 15 min.
4. Decant the supernatant and weigh the remaining sediment.
5. Water hydration capacity (WHC) is calculated by:

$$WHC = \frac{Wet\ sample\ \ wt. - Dry\ sample\ wt.}{Dry\ sample\ wt.}$$

Table 3. Water hydration capacities for commercial protein isolates.

Data represent the mean ± one standard deviation (n=3).

Commercial ingredient	WHC (g/g)
Egg protein isolate	CD[1]
Whey protein isolate	CD[1]
Wheat protein isolate	NM[2]
Soy protein isolate[3]	12.39 ± 0.32
Pea protein isolate	3.09 ± 0.11

Notes:
[1]CD = Completely dissolved.
[2]NM = Not measurable, remained suspended in water as particulates (not dissolved).
[3]For soy protein isolate, 20 g of water was used in the protocol rather than 10 g to ensure water was in excess.

G. OIL HOLDING CAPACITY

Defined as:

The amount of oil than can be absorbed by one gram of protein (1, 6).

Method:

1. Wet 1 g of protein (based on a wet basis) with 10 mL of vegetable oil in a weighted 30 mL centrifuge tube and mix thoroughly.
2. Vortex the sample every 5 min for a total of 30 min.
3. Centrifuge the sample at 1,000 x g for 15 min.
4. Decant the supernatant and weigh the remaining sediment.
5. Oil holding capacity (OHC) is calculated by:

$$OHC = \frac{Wet\ sample\ \ wt. - Dry\ sample\ wt.}{Dry\ sample\ wt.}$$

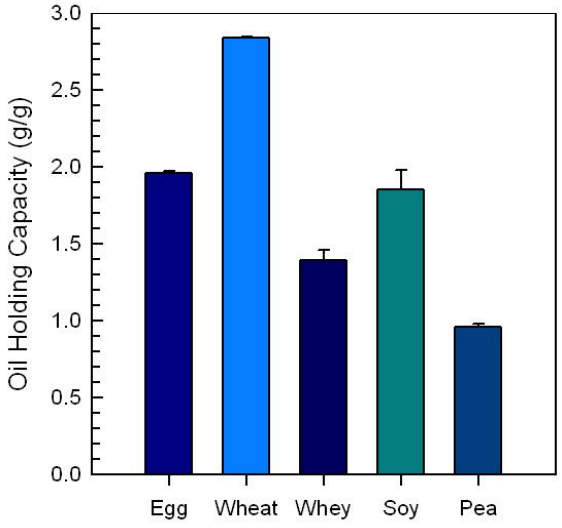

Figure 6. Oil holding capacities for commercial protein isolates.

Data represent the mean ± one standard deviation (n=3).

H. FOAM CAPACITY AND STABILITY

Defined as:

Foaming capacity (FC) is the ability for the protein at a given concentration to generate a foam, whereas foam stability (FS) is the ability of that protein to maintain its foam volume over a defined period of time (4, 7).

Method:

1. Prepare a 1% (w/w) protein solution => disperse protein isolates (corrected on a weight basis for protein content) in 10 mM sodium phosphate buffer (pH 7.00; adjusted with either 0.1 M NaOH or 0.1 M HCl) followed by stirring at 500 rpm overnight (~16 h) at 4°C.
2. Measure 15 mL of protein solution into a 400 mL beaker.
3. Homogenize for 5 min at 8,000 rpm using an Omni-mixer equipped with a saw tooth generating probe (positioned slightly below the air-water interface), then immediately pour the foam into a 100 mL graduated cylinder.

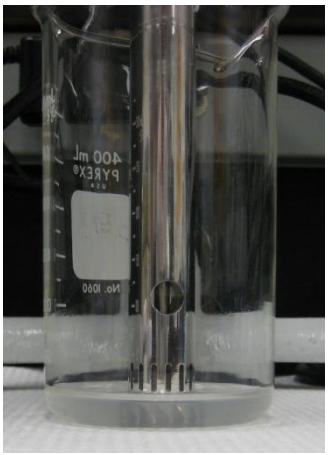

4. Record the foam volume within the graduated cylinder. Foam capacity is calculated from:

$$FC = \frac{Foam\ volume}{Initial\ sample\ volume\ (15\ mL)} \times 100\%$$

5. Measure the foam volume remaining in the graduate cylinder after time, t (30 min). Foam stability is calculated from:

$$FS = \frac{Foam\ volume\ after\ 30\ \text{min}}{Initial\ \ foam\ volume} \times 100\%$$

E.g., 1% (w/w) Whey Protein Isolate – Foam

Time = 0 min

Time = 30 min

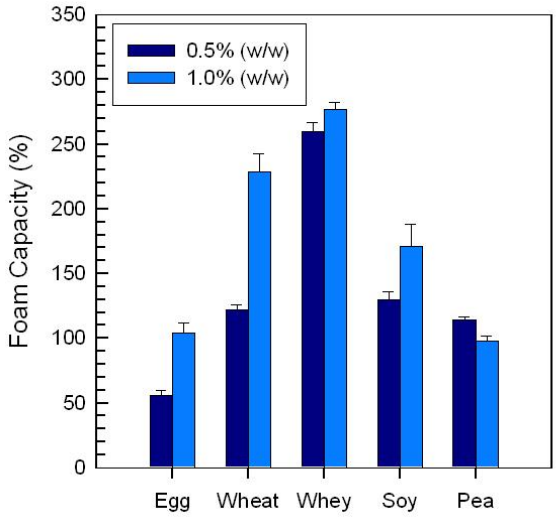

Figure 7. Foam capacity for commercial protein isolates at a 0.5% and 1.0% (w/w) protein concentration.

Data represent the mean ± one standard deviation (n=3).

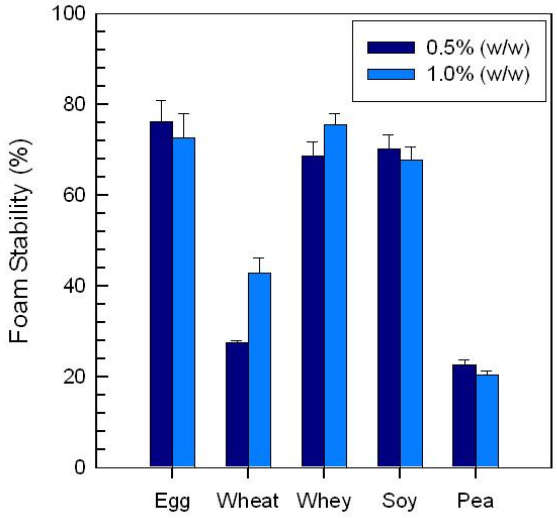

Figure 8. Foam stability for commercial protein isolates at a 0.5% and 1.0% (w/w) protein concentration.

Data represent the mean ± one standard deviation (n=3).

4. APPENDIX

Recipes:

10 mM Sodium Phosphate Buffer (pH 7.0)

- Dissolve 0.5836 g of monosodium phosphate (monohydrate) in 400 mL of distilled de-ionized water.
- Dissolve 1.5466 g of disodium phosphate (heptahydrate) in 400 mL of distilled de-ionized water.
- Mix solution, adjust to pH 7.0 and bring the total volume to 1 L. Store at 4°C.

0.1 M NaOH

- Dissolve 4 g of NaOH in 1 L of distilled de-ionized water (Molecular weight of NaOH is 40 g/mol x 0.1 mol/L = 4 g in 1 L).
- Store at room temperature

0.1 M NaCl

- Dissolve 5.844 g of NaCl in 1 L of distilled de-ionized water (Molecular weight of NaCl is 58.44 g/mol x 0.1 mol/L = 5.844 g in 1 L).
- Store at room temperature.

5. REFERENCES

1. AOAC. (2003). *Official methods of analysis* (17th ed.). Association of Official Analytical Chemists, Inc.VA, USA.

2. Morr, C. V., German, B., Kinsella, J. E., Regenstein, J. M., Van Buren, J. P., Kilara, A., Lewis, B. A., Mangino, M. E. (1985). A collaborative study to develop a standardized food protein solubility procedure. *Journal of Food Science, 50*(6), 1715-1718.

3. Crenwelge, D. D., Dill, C. W., Tybor, T. B., & Landmann, W. A. (1974). A comparison of the emulsification capacities of some protein concentrates. *Journal of Food Science, 39*(1), 175-177.

4. Liu, S., Elmer, C., Low, N. H., & Nickerson, M. T. (2010). Effect of pH on the functional behaviour of pea protein isolate-gum Arabic complexes. *Food Research International, 43*(2), 489-495.

5. Pearce, K. N., & Kinsella, J. E. (1978). Emulsifying properties of proteins: evaluation of a turbidimetric technique. *Journal of Agricultural and Food Chemistry, 26*(3), 716-723.

6. Ahmedna, M., Prinyawiwatkul, W., & Rao, R. M. (1999). Solubilized wheat protein isolate: functional properties and potential food applications. *Journal of Agricultural and Food Chemistry, 47*(4), 1340-1345.

7. Wilde, P. J., & Clark, D. C. (1996). Foam formation and stability. In G. M. Hall (Ed.). *Methods of testing protein functionality* (pp. 110-152). New York, NY: Chapman and Hall.

ADDITIONAL READING

Damodaran, S. (2006). Protein stabilization of emulsions and foams. *Journal of Food Science, 70*(3), 54-66.

Kinsella, J. E. (1979). Functional properties of soy proteins. *Journal of the American Oil Chemists' Society, 56*(3), 242-258.

McClements, D. J. (2007). Critical review of techniques and methodologies for characterization of emulsion stability. *Critical Reviews in Food Science and Nutrition, 47*(7), 611-649.

Appendix B: Marketing report on food proteins